CRANFIELD UNIVERSITY

BENJAMIN VENEDIGER

CIVIL AIRCRAFT TRAJECTORY ANALYSES - IMPACT OF ENGINE DEGRADATION ON FUEL BURN AND EMISSIONS

SCHOOL OF ENGINEERING
Thermal Power MSc by Research

MSc by Research
Academic Year: 2010 - 2013

Supervisor: Dr. Vishal Sethi
May 2013

CRANFIELD UNIVERSITY

SCHOOL OF ENGINEERING
Thermal Power MSc by Research

MSc by Research Thesis

Academic Year 2010 - 2013

BENJAMIN VENEDIGER

CIVIL AIRCRAFT TRAJECTORY ANALYSES - IMPACT OF ENGINE DEGRADATION ON FUEL BURN AND EMISSIONS

Supervisor: Dr. Vishal Sethi
May 2013

This thesis is submitted in partial fulfilment of the requirements for the degree of Master of Science

ABSTRACT

Commercial aviation and air traffic is still expected to grow by 4-5% annually in the future and thus the effect of aircraft operation on the environment and its consequences for the climate change is a major concern for all parties involved in the aviation industry. One important aspect of aircraft engine operation is the performance degradation of such engines over their lifetime while another aspect involves the aircraft flight trajectory itself. Therefore, the first aim of this work is to evaluate and quantify the effect of engine performance degradation on the overall aircraft flight mission and hence quantify the impact on the environment with regards to the following two objectives: fuel burned and NO_x emissions. The second part of this study then aims at identifying the potential for optimised aircraft flight trajectories with respect to those two objectives.

A typical two-spool high bypass ratio turbofan engine in three thrust variants (low, medium and high) and a typical narrow body single-aisle aircraft similar to the A320 series were modelled as a basis for this study. In addition, an existing emissions predictions model has been adapted for the three engine variants. Detailed parametric and off-design analyses were carried out to define and validate the performance of the aircraft, engine and emissions models. The obtained results from a short and medium range flight missions study showed that engine degradation and engine take-off thrust reduction significantly affect total mission fuel burn and total mission NO_x emissions (including take-off) generated. A 2% degradation of compressor, combustor and turbine component parameters caused an increase in total mission fuel burn of up to 5.3% and an increase in NO_x emissions of up to 5.9% depending on the particular mission and aircraft. However, take-off thrust reduction led to a decrease in NO_x emissions of up to 41% at the expense of an increase in take-off distance of up to 12%.

Subsequently, a basic multi-disciplinary aircraft trajectory optimisation framework was developed and employed to analyse short and medium range flight trajectories using one aircraft and engine configuration. Two different optimisation case studies were performed: (1) fuel burned vs. flight time and (2) fuel burned vs. NO_x emitted. The

results from a short range flight mission suggested a trade-off between fuel burned versus flight time and showed a fuel burn reduction of 3.0% or a reduction in flight time of 6.7% when compared to a “non-optimised” trajectory. Whereas the optimisation of fuel burn versus NO_x emissions revealed those objectives to be non-conflicting. The medium range mission showed similar results with fuel burn reductions of 1.8% or flight time reductions of 7.7% when compared to a “non-optimised” trajectory. Accordingly, non-conflicting solutions for fuel burn versus NO_x emissions have been achieved. Based on the assumptions introduced for the trajectory optimisation analyses, the identified optimised trajectories represent possible solutions with the potential to reduce the environmental impact.

In order to increase the simulation quality in the future and to provide more comprehensive results, a refinement and extension of the framework also with additional models taking into account engine life, noise, weather or operational procedures, is required. This will then also allow the assessment of the implications for airline operators in terms of Direct Operating Costs (DOC). In addition, the degree of optimisation could be improved by increasing the number and type of optimisation variables.

Keywords:

Aircraft Trajectory, Engine Degradation, Fuel Burn, Emissions, Optimisation

ACKNOWLEDGEMENTS

First of all, I would like to thank my supervisor Dr Vishal Sethi for his continuous support, valuable advice and guidance throughout the development of this work. I also would like to extend my thanks to Cranfield University PhD candidates Nqobile Khani and Hugo Pervier for their valuable support, suggestions and advice without which this work would not have been possible.

Furthermore, I would like to express my gratitude to all colleagues from the Engineering Department and the Flight Safety Department at Airberlin for their support, the fruitful discussions and their helpful comments.

I would also like to thank the School of Engineering and the Department of Power and Propulsion, who made it possible for me to pursue this MSc degree at Cranfield University.

Finally, I would like to thank all Cranfield University administrative staff for their prompt support regarding all administrative matters which enabled me to complete my work on time.

The research leading to the results presented herein has contributed to the European Union's Seventh Framework Program (FP7/2007-2013) for the Clean Sky Joint Technology Initiative under grant agreement n° CJSU-GAM-SGO-2008-001. Cranfield University also got valuable support from partners of Clean Sky, through the GSAF (Green Systems for Aircraft Foundation) group which include mainly the University of Malta, TU Delft and the Dutch Research Center (NLR).

TABLE OF CONTENTS

LIST OF FIGURES

LIST OF TABLES

LIST OF ABBREVIATIONS

ACARE	Advisory Council for Aeronautics Research in Europe
ATM	Air Traffic Management
CC	Combustion Chamber
CFD	Computational Fluid Dynamics
CO	Carbon monoxide
CP	Corner Point
CO_2	Carbon dioxide
CU	Cranfield University
CU2STF-HT	Cranfield University 2 Spool Turbofan-High thrust (Turbomatch)
CU2STF-LT	Cranfield University 2 Spool Turbofan-Low thrust (Turbomatch)
CU2STF-MT	Cranfield University 2 Spool Turbofan-Medium thrust (Turbomatch)
CUSA-L	Cranfield University Single Aisle-Long (Hermes)
CUSA-M	Cranfield University Single Aisle-Medium (Hermes)
CUSA-S	Cranfield University Single Aisle-Short (Hermes)
DOC	Direct Operating Costs
DP	Design Point
EGT	Exhaust Gas Temperature
EGTM	Exhaust Gas Temperature Margin
EHM	Engine Health Management/Engine Health Monitoring
FF	Fuel Flow
GA	Genetic Algorithm
GATAC	Green Aircraft Trajectories under ATM Constraints
GPHM	Gas Path Health Management
GWP	Global Warming Potential
H_2O	Water
HPC	High Pressure Compressor
HPT	High Pressure Turbine
ICAO	International Civil Aviation Organisation
ISA	International Standard Atmosphere
ITD	Integrated Technology Demonstrator
JTI	Joint Technology Initiative
LPC	Low Pressure Compressor
LPT	Low Pressure Turbine
LTO	Landing and Take-off cycle
MDO	Multi Disciplinary Optimisation

MTOW	Maximum Take-off Weight
N	Nitrogen
NO	Nitric oxide
NO_2	Nitrogen dioxide
NO_X	Oxides of nitrogen
NSGAMO	Non-dominated Sorting Genetic Algorithm Multi-Objective
O	Oxygen
OAT	Outside Air Temperature
O_2	Molecular oxygen
OD	Off-Design
OEW	Operating Empty Weight
PARTNER	Partnership for AiR Transportation Noise and Emissions Reduction
PCN	Shaft Speed (rpm/rpm(DP)
PEE	Payload Emissions Efficiency
PFEE	Payload Fuel Energy Efficiency
RPK	Revenue Passenger Kilometres
SBX	Simulated Binary Crossover
SESAR	Single European Sky ATM Research
SGO	System for Green Operations
SLS	Sea Level Static
SO_2	Sulphur dioxide
T/O	Take-Off
TBC	Thermal Barrier Coating
TERA	Techno-economic Environmental Risk Analysis
TOC	Top Of Climb
TOD	Top Of Descent
VBV	Variable Bleed Valve
VSV	Variable Stator Vanes

LIST OF SYMBOLS

Symbol	Definition	Unit
a	Speed of sound	m/s
A_0	Inlet flow area	m²
Alt	Altitude	m
AR	Wing aspect ratio	-
BPR	Bypass Ratio	-
c	Number of constraints	-
c_0	Inlet flow velocity	m/s
CAS	Calibrated Air Speed	m/s
C_D	Drag coefficient	-
C_{D0}	Zero lift drag coefficient	-
C_{DI}	Induced drag coefficient	-
C_{fc}	Skin friction coefficient	-
C_L	Lift coefficient	-
C_p	Specific heat (constant pressure)	J kg^{-1} K^{-1}
C_V	Specific heat (constant volume)	J kg^{-1} K^{-1}
C_1	Wing plan form geometry coefficient	-
C_2	Wing plan form geometry coefficient	-
C_3	Non-optimum wing twist coefficient	-
C_4	Viscous effects coefficient	-
CMF	Corrected Mass-Flow	kg/s
DAS	Density Air Spped	m/s
EAS	Equivalent Airspeed	m/s
EGT	Exhaust Gas Temperature	°C
EGTM	Exhaust Gas Temperature Margin	°C
EI	Emissions Index (Indices)	g(emissions)/kg(fuel)
f(X)	Objective function	-
$g_j(X)$	Inequality constraints (vector)	-
$h_l(X)$	Equality constraints (vector)	-
FAR	Fuel-Air-Ratio	kg(fuel)/kg(air)
FHV	Fuel Heating Value	J/kg
FN	Net thrust	kN
FPR	Fan Pressure Ratio	-
IAS	Indicated Air Speed	m/s

M	Mach number	-
Ma_0	Inlet Mach number	-
$\dot{m}$	Mass flow	kg/s
OPR	Overall Pressure Ratio	-
p_{inlet}	Component inlet pressure	Pa
p_{outlet}	Component outlet pressure	Pa
p_0	Ambient pressure	Pa
P	Power	J/s
P_{SLS}	Pressure (Sea Level Static)	Pa
Q_c	Component interference drag coefficient	-
r	Radius	m
R	Gas constant (dry air)	J kg^{-1} K^{-1}
SFC	Specific Fuel Consumption	mg/Ns
$S_{c,wetted}$	Component wetted surface area	m^2
S_{ref}	Plan form area	m^2
t	Temperature (static)	K
T	Temperature (total)	K
$T_{hot\ day}$	Temperature at Sea Level (ISA+30 conditions)	K
T_{inlet}	Component inlet temperature	K
T_{min}	Minimum temperature	K
T_{max}	Maximum temperature	K
T_{outlet}	Component outlet temperature	K
$T_{standard\ day}$	Temperature at Sea Level (ISA conditions)	K
T_{SLS}	Temperature (Sea Level Static)	K
$T;^{-}_{th}$	Thermodynamic average temperature	K
T_0	Ambient temperature	K
T_{t3}	Maximum compressor exit temperature	K
T_{t4}	Maximum turbine entry temperature	K
TAS	True Air Speed	m/s
TET	Turbine Entry Temperature	K
V_0	Flight velocity	m/s
V_j	Jet velocity	m/s
W	Mass flow	kg/s
W_l	Core mass flow	kg/s
w_f	Fuel flow	kg/s
X	Design vector (n-dimensional)	-

Greek Symbol	Definition	Unit
γ	Isentropic exponent	-
η	Efficiency	-
η_{comb}	Combustion efficiency	-
$\eta_{overall}$	Overall efficiency	-
η_{th}	Thermal efficiency	-
$\eta_{th,opt}$	Optimum thermal efficiency	-
η_{prop}	Propulsive efficiency	-
μ	Bypass Ratio	-
π	Pressure ratio	-
ρ	Density	kg/m^3
φ_c	Component form factor	-

1 Introduction

The first chapter provides a general introduction to the topic of this research project and specifies the context in which the subject research project was carried out. It furthermore describes the main objectives addressed in this work as well as the scope and a brief outline of the same.

1.1 Background

Today's need for reliable, fast global transportation is increasing and has set new standards for the aviation industry, and at the same time is creating new challenges in the field of science and technology. Commercial aviation is still expected to grow significantly in the future and thus the effect of aircraft operation on the environment and its consequences for climate change is a major concern and must be addressed at all levels in the aviation industry and beyond.

One key issue that must be addressed to contribute to a more sustainable environment is the reduction of aircraft engine CO_2 emissions and directly related to that a reduction in fuel burn as well as the reduction of aircraft engine NO_x emissions. The civil aero-engine market is highly competitive and engine manufacturers, engine maintenance providers and aircraft operators alike have to look for technological and economical improvements as well as determining environmental impacts of their products and operations. Those are two major requirements which are the basis for future gas turbine engine concepts and configurations powering next-generation aircraft. New engine designs or major alterations are high risk strategies for the engine manufacturers and operators due to the inherent cost of development and implementation. Many different novel or evolved gas turbine propulsion system solutions for commercial aircraft applications are being proposed by various engine manufacturers. These novel and evolved engine designs like geared fan designs have the potential to significantly improve environmental effects and to improve the economic impact of aircraft operations in the long term compared to the current state [1].

On the other side, there are existing aircraft and engine configurations in service today, which are expected to be operated for a considerable amount of time into the future. With a view to the commercial aviation sector and aircraft fleets being in operation today, there is a big potential to find solutions which can be proposed and applied to existing fleet operations in the short term. The analysis of existing aircraft and engine configurations and the identification of feasible solutions and strategies which yield the biggest efficiency improvements with regards to aircraft operations is one possible way to achieve a reduction in emissions. Due to the limitations in creating fundamental aircraft and engine design changes in the short term, those analyses must aim at operational aspects of air transportation. One major aspect is aircraft flight trajectories that allow for minimum pollutant emissions for a certain flight profile. The other important aspect of the analysis must deal with engine maintenance issues and its impact on the environment as well as its impact on the total engine life cycle.

1.2 Context

Global economic growth and a constant increase in worldwide air travel demand are directly associated with an increased public awareness of environmental issues such as air pollution, noise and climate change [2]. According to the 2011 ICAO (International Civil Aviation Organization) worldwide scheduled services forecast, passenger traffic is expected to grow by about 4-5 % annually till the year 2030. Figure 1-1 shows the historic growth in Revenue Passenger Kilometres (RPK) and passengers carried since the year 2000. It also shows the expected future development for these two figures till the year 2030. Several studies initiated by EUROCONTROL, dealing with the strategic research on air transport evolution present the future challenges for air traffic developments up to the year 2030, also in the light of global climate changes [3]. They stress the fact that adaptation is only one strategy to cope with climate change. Another important aspect is mitigation of factors that drive climate change to strongly reduce the effects on climate change [4]. Since aero-engines are largely contributing to the atmospheric pollution via emissions of CO_2, NO_x and other chemical compounds the aviation industry is investigating new solutions in order to address those environmental problems [5]. Detailed aero engine emission information is available in

references [6] and [7]. A comprehensive assessment of typical commercial aero engine combustors as listed in reference [6] and [7] has been conducted in reference [8] and the results underline the continuous reductions which have been achieved by engine manufacturers. An assessment of commercial aviation fuel efficiency on a fleet-wide basis, by means of the measure of Payload Fuel Energy Efficiency (PFEE), is presented in reference [9]. The study also suggests extending the assessment by including environmental performance metrics, which for example can account for NO_x emissions, to identify operational inefficiencies. The investigation of these aspects can be accomplished through collaborative international networks and projects that focus on the coordination of efforts in order to promote those improvements in commercial aviation.

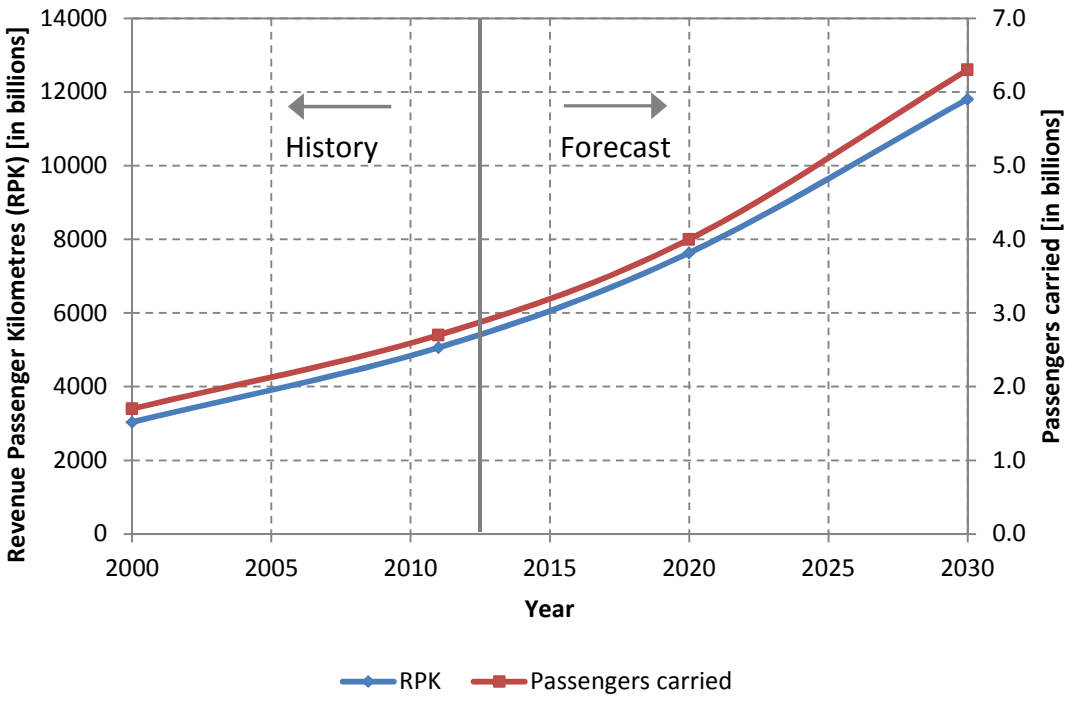

Figure 1-1: Worldwide passenger traffic history and forecast (ICAO)

The ICAO bundles its environmental activities through the Committee on Aviation Environmental Protection (CAEP) which is divided into several working and support groups covering a wide range of technical and operational aspects. The output provided by the different groups serves as basis for new standards on aircraft emissions set by ICAO. The current status, future goals and developments in mitigation

schemes to address environmental impacts are presented in dedicated reports released every three years [10], [11]. Several different programs and projects have been launched worldwide in the aeronautics field in order to address not only environmental issues created by aircraft operations but also to address overall challenges for global air transportation. They aim at providing solutions for the near term as well as for the longer future.

One project established in the U.S. in 2003 is called PARTNER - the Partnership for AiR Transportation Noise and Emissions Reduction [12]. It is a leading aviation cooperative research organization supported by governmental and academic institutions as well as industry collaboration partners. Amongst others, it seeks advances in the fields of technology and operational performance to improve air transport mobility and mitigate environmental concerns. Currently there are 41 projects under way which focus on five major topics, namely: Alternative fuels, emissions, noise, operations and tools and system-level/policy assessment [13]. One project report, for example, which evaluates specific CO_2 emissions metrics for a commercial aircraft certification requirement, can be found in reference [14]. One metric suggested in the report to define emissions performance is based on a full mission performance, id est the analysis of fuel burn over all flight phases of a representative mission.

At the same time, the PARTNER project is developing a comprehensive suite of software tools which will allow the facilitation of the before described topics considering their interdependencies and interactions. This suite comprises the following five functional components, each one addressing different fields: [15]

1. Aviation environmental Portfolio Management Tool for Impacts (APMT-Impacts)
2. Cost Benefit with the Aviation environmental Portfolio Management Tool (APMT-Cost Benefit)
3. Aviation environmental Portfolio Management Tool for Economics (APMT-Economics)
4. Aviation Environmental Design Tool (AEDT)

5. Environmental Design Space (EDS)

Similar projects to address environmental issues and others were initiated in Europe in 2001. They also focus on finding feasible solutions for the aviation sector in order to minimise emissions and improve aircraft operations. At the same time, a Group of Personalities composed a report that outlines a vision of the air transportation system in the year 2020. To put those visions into effect, an Advisory Council for Aeronautics Research in Europe -ACARE - was set up [16]. This council formed a foundation for the first European Technology Platform which formulated a suit of Strategic Research Agendas (SRA), namely SRA-1 created in 2002 and SRA-2 an updated edition created in 2004 [17].

These two agendas serve as a baseline to define research objectives for all stakeholders in the project in the various fields. Similar to the PARTNER project, 5 major challenge areas for technology development were identified in the first agenda SRA-1, namely: Noise and emissions, quality and affordability, safety, security and air transport system efficiency. Taken into account these challenge areas, five main objectives which result from the scope of the environmental challenge were set forth, two out of which are listed below: [18]

1. To reduce fuel consumption and CO_2 emissions by 50%
2. To reduce NO_x by 80%

In addition, the first agenda describes the allocation of efforts in order to meet those targets. The goal to reduce emissions by 50% requires the implementation of improvements in three arenas: Airframe, engine and air traffic management. Each arena contributing to the target emission reduction through the incorporation of evolved designs or improved conventional concepts for example. In case of the engine arena, a 15-20% reduction in engine fuel consumption is expected in order to meet the main targets. Those reductions being incorporated through increased thermal and propulsive efficiencies [19].

Furthermore, the updated Strategic Research Agenda SRA-2 which was released in 2004 extended the approach and contents of the first edition and added a number of development scenarios. Following the strategy of the first agenda and recalling its objectives, the second edition also refines existing targets and determines a series of 5 High Level Target Concepts (HLTC), each of them addressing a major concern of the air transportation system. In short they can be listed as follows:

1. Highly Customer Oriented HLTC
2. Highly Time Efficient HLTC
3. Highly Cost Efficient HLTC
4. Ultra Green HLTC
5. Ultra Secure HLTC

To keep pace with changing trends in the aviation sector worldwide and to implement already achieved goals into the concept of the major strategic agendas, an Addendum was released in 2008 to recall the main objectives and to update priorities with regards to newly arisen economic and environmental issues.

In alignment with the before described air transportation improvement objectives, the Clean Sky project was initiated to demonstrate and validate technology advances in order to meet the goals set by ACARE which will ensure the attainment of the aspired environmental improvements [20]. This research project being a public-private partnership, involves the support of industries, universities and research organizations alike. By its combined research activities, it will contribute towards meeting the objectives of ACARE HLT concept number 3 and 4 (see above), i.e. Highly Cost Efficient and Ultra Green air transportation systems.

The structure of the project is composed of 6 Integrated Technology Demonstrators (ITD), which focus on different technology improvement areas of the air transportation system. Those 6 ITDs are briefly described as follows: [20]

1. Green Regional Aircraft [GRA]
2. SMART Fixed-Wing Aircraft
3. Green Rotorcraft

4. Sustainable and Green Engines
5. Systems for Green Operation
6. Eco-Design

Those ITDs are linked through a simulation network to a Technology Evaluator which assesses the performance of the technologies developed within a certain Integrated Technology Demonstrator (ITD) and allows early appraisal of the results and comparison against the initial targets. This also means that necessary re-adjustments of particular technological advancements can be implemented and fed back into the on-going work. The fifth ITD (Systems for Green Operation) in particular deals primarily with the management of aircraft energy and the management of missions and trajectories. Especially the analysis of the different flight phases of an aircraft like cruise, take-off, approach and departure with respect to fuel consumption can deliver insight into the various environmental effects. Extensive research in mission and energy management can assist in reaching the higher level targets set by the Clean Sky project.

Cranfield University (CU) currently contributes to the above mentioned research topics through the development of advanced and optimised aircraft trajectories and consequent validation of their effectiveness. A concept called TERA (Techno-economic and Environmental Risk Assessment) was invented at Cranfield University [21]. The TERA concept incorporates several modules which allow modelling of gas turbine and aircraft performance, estimating noise and emissions, as well as environmental impact. An integrated optimiser enables detailed cycle studies taking into account a multi-disciplinary model scenario [22].

The importance of these integrated multi-disciplinary modelling tools becomes apparent when detailed and comprehensive analysis results are to be compiled. In order to effectively analyse the possibilities of more environmental friendly aircraft and engine operations it is necessary to create a framework which determines the boundaries for the analysis. This framework includes all modules which are considered

important for an accurate model, such as engines and airframes used or external conditions and restrictions, they could be technical or economical for example.

Those tools then allow the assessment of aircraft trajectories in terms of the key factors such as flight time, fuel consumption and emission of pollutants harmful to the environment. In order to identify an optimised aircraft trajectory it is necessary to create a working environment which contains all factors that can affect the aircraft trajectory. This includes engine performance models, aircraft performance models and models of the surrounding conditions. The so created framework can then be used for aircraft trajectory simulations and consequent optimisations. These optimisations can be carried out by different types of optimisers which are either generic or specific to the problem. Consequently, the application of different optimisation methods can yield varying results depending on the optimiser used. A basic optimisation framework approach for aircraft trajectory studies as described above has been setup and validated in the recent works by Zolata [23] and Marzal [24].

Since aircraft trajectory optimisation is a multi-objective problem, it is required to undertake trade-off analyses to be able to balance possible conflicting objectives. Many optimisation studies have been developed and carried out in the past with emphases on different objectives. For example, there are studies that focus to a greater extent on emissions reduction potential [25] or studies which emphasize on the economic aspects of trajectory optimisation [26]

1.3 Scope

The particular aircraft and engines investigated in this study only represent certain possible configurations based on publicly available data and assumptions supported by the applicable literature and thus may not necessarily be considered as feasible configurations per se. Furthermore, for all aircraft trajectory studies performed in this work only the flight mission itself has been considered and any other operational aspects such as air traffic management restrictions, airport procedures, or environmental aspects such as weather conditions or obstacles etc. have not been accounted for.

1.4 Objectives

The most important contributions to knowledge of the present work comprise five main aspects: (i) development of three aircraft engine models and subsequent comprehensive analysis of the engine performance in comparison to real engine data; (ii) implementation of an engine degradation scenario for the three developed engine models; (iii) combination of the created engine models with suitable aircraft models and execution of basic aircraft trajectory studies incorporating an engine emissions model; (iv) integration of the engine, aircraft and emissions models into a simple multi-disciplinary optimisation framework; (v) determination and assessment of optimum aircraft trajectories with respect to total flight time, total fuel burned and total pollutants emitted.

Based on those five aspects described above the main objectives of this work can be derived as follows:

- Model and adapt three different aircraft/engine configurations taking into account the effects of engine degradation.
- Evaluate basic aircraft trajectories and quantify their performance in terms of total flight time, total fuel burned and total pollutants (NO_x) emitted also considering engine degradation and engine derating.
- Adapt a multi-disciplinary optimisation framework for preliminary aircraft trajectory studies using Cranfield University simulation tools (Turbomatch, Hermes, Hephaestus/P3T3 and GATAC)
- Perform multi-objective aircraft trajectory studies focussing on total flight time, total fuel burned and total pollutants (NO_x) emitted to identify possible “greener” trajectories.
- Add basic quantitative results to the current trajectory analysis research and identify opportunities for future trajectory optimisation studies.

1.5 Outline

The present thesis is divided into seven main chapters with each chapter being subdivided into further sections and subsections.

Chapter 1 provided a general introduction to the research subject, the major objectives and scope of this work as well as this outline.

Chapter 2 provides an overview of basic aircraft and gas turbine engine technologies and their related implications for performance analyses. It also includes a review of gas turbine pollutants, their formation processes and impacts on the environment. Furthermore, chapter 2 discusses the concept of gas turbine engine degradation and the effects on engine components, engine performance and engine life. This chapter is concluded by the introduction of engineering optimisation processes, optimisation methods including optimisation techniques using genetic algorithms and their application to multi-objective trajectory problems.

Chapter 3 then outlines the problem definition for the research conducted in this work and it introduces some general considerations, assumptions and statements with regards to the basic aircraft trajectory analysis and the subsequent optimisation studies which are carried out. In addition, it comprises a brief overview of the past experience on trajectory optimisation.

Chapter 4 introduces the different simulation tools and models that have been used to conduct the aircraft trajectory studies. It covers the creation and verification of the individual models for engine performance (including degraded engine performance), aircraft performance, emissions predictions performance and their incorporation into the developed optimisation framework. The chapter finishes with a brief description of the optimisation framework briefly explaining the functions of the individual modules and how they interact with the overall framework.

Chapter 5 summarises and presents the results of the basic aircraft trajectory scenario studies. Results are shown for two different mission scenarios (short range flight and medium range flight) each one having been evaluated with a clean engine and a

degraded engine configuration. Furthermore, an engine derate scenario is included in this analysis as well. The results are assessed in terms of total flight time, total fuel burned and total pollutants (NO_x) emitted.

Chapter 6 summarises and presents the results of the preliminary aircraft trajectory optimisation studies. Similar to the approach used in chapter 5, the results are shown for two different mission scenarios (short range flight and medium range flight) for one aircraft variant.

Chapter 7 contains the discussion of the results, a summary of the achievements and the conclusions as well as a discussion of the existing limitations of this study. Based on these observations, recommendations for future work are discussed. Lastly, an outlook to future developments in aircraft and engine operation focussing on advancements in aircraft operational procedures and engine health monitoring techniques concludes this study.

2 Literature Review

This chapter forms the basis for the present study and aims to provide a basic overview of the current state commercial aircraft and engine technology. In addition, and to better understand the research approach of this work, it provides a detailed background of the relevant subjects which are addressed throughout this study. This includes discussions of gas turbine emissions, gas turbine degradation and their environmental effects as well as an introduction to engineering optimisation methodologies applicable to multi-objective trajectory optimisation.

2.1 Aircraft Technology

Conventional narrow-body twin-engine aircraft represent the major airframe configuration used in the short-to-medium range civil passenger transport market today. This aircraft type is, due to its initial design development and its long service history and thus the available previous experience, the standard aircraft design which is continuously being improved to increase airframe efficiency (best lift/drag ratio). These improvements arise from the use of new materials, advanced control systems and more effective lift devices. The propulsion systems of those aircraft are typically arranged in an under wing pylon mounted configuration which dictates certain aircraft features such as wing or landing gear design. This basic aircraft design is expected to remain in operation for a considerable amount of time into the future due to its large application base and its relatively low replacement rate in the worldwide fleet [27]. Current aircraft lifetimes can reach 25-35 years and may be extended even further in the future. At the same time, aggravated aviation legislations or increasing fuel prices may accelerate the replacement rate because more modern and efficient aircraft designs may have the potential to significantly reduce operating costs.

2.1.1 Aircraft Performance

Aircraft performance can be defined as an aircrafts' ability to accomplish a certain flight mission while considering all influencing factors. Two major influencing factors to be considered are the aircraft design and the propulsion system. They will have a

significant effect on the whole aircraft performance characteristics, since parameters such as flight speed or maximum capacity are directly linked to those factors. The environmental envelope, in which the aircraft's performance has been established, on the other hand, features the pressure altitude and temperature limitations. For civil passenger transportation aircraft three different aspects of aircraft performance can be addressed which mainly define the overall operational performance [28].

1. The physical aspect: Flight mechanics, aerodynamics, altimetry, external parameters influencing aircraft performance
2. The operational aspect: Operational methods, aircraft computer logics, operational procedures, pilot's actions
3. The regulatory aspect: Aviation regulations certification and operating rules, establishment of limitations

In the following the major physical aspects and principals, which affect aircraft performance, are briefly discussed. The operational aspect of aircraft performance will be addressed in more detail in the next chapter, highlighting important aspects of current civil aircraft operation and its underlying procedures. The regulatory aspect, even though of equivalent importance for aircraft operation, will only be briefly addressed in the next chapter.

In order to assess the basic performance of an aircraft configuration its aerodynamic properties and the cruising performance have to be estimated. Considering the cruise performance is important since this is typically the flight phase where most of the fuel is consumed. In addition, other flight phases like take-off, climb and descent have to be considered to analyse the aircraft performance for a complete flight mission [29].

The relationship between aircraft lift and drag can be described by the use of a drag polar which accounts for the dependence of the lift coefficient on the drag coefficient. For a particular flight phase the aerodynamic performance can be expressed by the total drag coefficient C_D as follows:

$$C_D = C_{D0} + C_{DI} \quad \textbf{(2-1)}$$

This where C_{D0} is called the zero lift drag coefficient (dependent on lift) and C_{DI} is called the induced drag coefficient (independent on lift).

The explicit equation of the zero lift drag coefficient can be estimated as described below:

$$C_{DI} = \left[\left(\frac{C_1}{C_2 \times \pi \times AR}\right) + C_3 + C_4 \times C_{D0}\right] \times C_L^2 \quad \textbf{(2-2)}$$

C_1 and C_2 are coefficients that account for the wing plan form geometry and C_3 and C_4 are coefficients that take into account the non-optimum wing twist and viscous effects. AR represents the wing aspect ratio and C_L is the lift coefficient.

The zero lift drag coefficient for an aircraft component such as the fuselage or wing can be expressed using the following equation:

$$C_{D0} = \frac{\sum\left(Cf_c, \varphi_c, Q_c, S_{c,wetted}\right)}{S_{ref}} \quad \textbf{(2-3)}$$

The overall zero lift drag coefficient of the aircraft is the sum of the C_{D0} of all individual components and factors. C_{fc} is the skin friction coefficient and φ_c is the form factor both necessary to estimate the subsonic profile drag of the particular component. Q_c accounts for the interference drag of the component and $S_{c,wetted}$ represents the wetted surface area of the component. The total drag is then divided by S_{ref} which is the plan form area.

During horizontal cruise flight with constant speed, where the engine thrust equals the aerodynamic drag, the aerodynamic efficiency E (lift to drag ratio) can be written as follows:

$$E = \frac{\frac{1}{2} \times \rho \times C_L \times V^2 \times S_{ref}}{\frac{1}{2} \times \rho \times C_D \times V^2 \times S_{ref}} = \frac{C_L}{C_D} \quad \textbf{(2-4)}$$

This is where ρ is the density of the air, C_L is the lift coefficient, C_D the drag coefficient, V the aircraft speed and S_{ref} the plan form area.

2.1.2 Aircraft Operation and Procedures

As described in the previous chapter, efficient aircraft usage depends not only on the physical aspects but also on operational and regulatory aspects. In the following section a brief outline of the operational aspects will be provided. Aircraft operation and operational procedures are continuously revised in order to accommodate changes which become necessary due to aircraft design modifications, airworthiness regulatory changes or the evolution of aviation policies. The latter being an important factor when environmental effects such as gaseous or noise emissions in aircraft operation are concerned. The Committee on Aviation Environmental Protection (CAEP) regularly updates policies and standards on aircraft engine emissions which, for example, address the engine certification requirements in terms of pollutants emitted at specified operational conditions. Currently, these conditions are consolidated in the specific Landing and Take-off (LTO) cycle shown in figure 2-1, which accounts for emissions at typical operation modes. It makes allowance for engine power settings at idle, take-off, climb and approach conditions but omits cruise conditions.

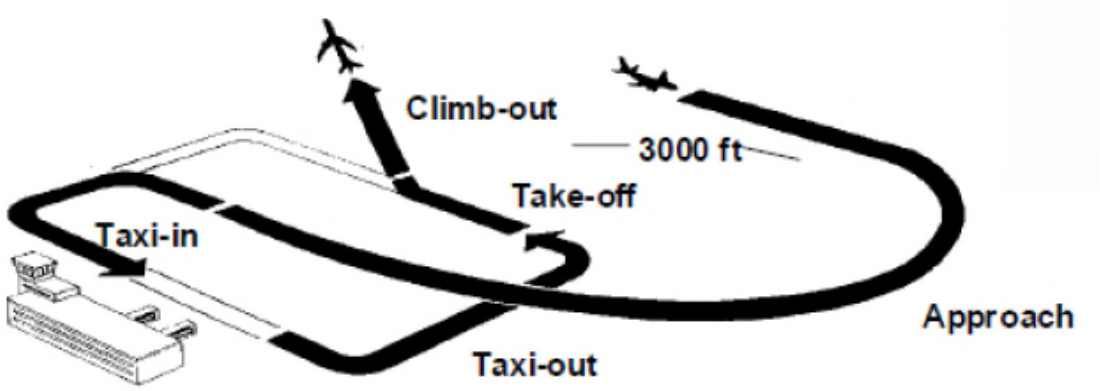

Figure 2-1: Landing and Take-off (LTO) cycle [30]

For example, countries like Switzerland and Sweden have enacted legislations which allow airports to introduce emission-based landing fees, based on the amount of nitrogen oxides emitted, to reduce pollutant emissions [31]. The resulting airspace concepts are prevalently driven by one or more of the following strategic objectives: (1) Safety, (2) capacity, (3) efficiency, (4) access and (5) environment [32]. The

International Civil Aviation Organization (ICAO) has published comprehensive material including descriptions of guidelines to construct visual and instrument flight procedures while maintaining acceptable levels of safety [33], [34]. These guidelines cover standard operating procedures such as regular departure, en-route or approach profiles as well as more specific procedures such as noise abatement flight profiles for take-off and approach. Reference [35] summarises and reviews numerous operational opportunities for civil aircraft operators to minimise fuel consumption and consequently emissions. The document not only addresses aircraft and engine specific opportunities, such as maintenance techniques and flight profile optimisation, but also covers airport operations, air traffic management or route planning. Several primary considerations are examined related to operational opportunities and the associated advantages and technical limitations are reviewed. Since environmental issues become more and more important for all parties involved in the aviation sector, a continuous adaption of new procedures is necessary to address changes imposed by those issues.

Aircraft operators also play a major role when it comes to the implementation of new, more environmental friendly operating procedures. A high level of preparedness and the availability of highly developed computer and network systems and its dense global interconnection can allow aircraft operators to enhance their operational procedures and launch significant operational initiatives [36]. These initiatives can include improvements of single aircraft flight trajectories as well as more encompassing alterations. Such improvements can be derived from the ITDs described in section 1.2 and can focus, for example, on the overall flight and fleet management.

Another factor which influences aircraft operations is air traffic management and air traffic control. As outlined in the introductory chapter of this work air traffic has significantly grown in the past and is expected to continue this trend in the future and associated with this there will be an increasing demand for innovations in air traffic management. Not only will the traffic on existing routes increase due to the increase in passengers but also new routes have to be implemented into the existing network structure. Again, improvements in this field require a multi-disciplinary approach as set forth by the Clean Sky project.

2.2 Engine Technology

Gas turbine engines are the major propulsion system for civil aircraft in service today with turbofan engines being the most widely used engine variant for short-to-medium as well as for long range applications. This engine type offers the greatest advantages in terms of fuel burn efficiency and noise levels over conventional turbojet engines. In terms of flight velocity, which allows efficient operation up to Mach numbers of 0.85, turbofan engines also provide an advantage over turboprop engines. Medium to high bypass ratio direct drive turbofan engines with a two or three spool design represent the current state of technology. Those engines comprise a conventional architecture with a large single-stage fan, a multi-stage Low Pressure Compressor (LPC, Booster), a multi-stage high pressure compressor, an annular combustor, a single or multi-stage high pressure turbine and a multi-stage Low Pressure Turbine as shown in figure 2-2 [37].

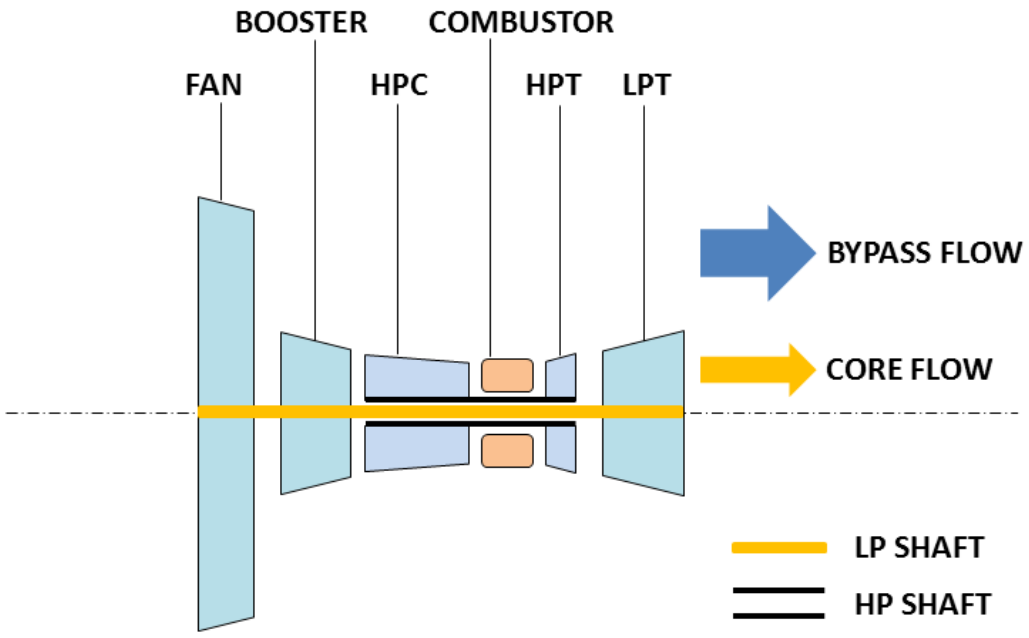

Figure 2-2: Typical two-shaft turbofan engine schematic

2.2.1 Turbofan Engine Performance

Engine performance encompasses the overall engine operability in terms of key parameters which are necessary to meet a given design specification. For aircraft gas turbine engines two key parameters which describe the engine performance are net thrust (FN) and specific fuel consumption (SFC). SFC is influenced by factors such as thermal efficiency, propulsive efficiency and combustion efficiency [38]. The three main design parameters of a turbofan engine are turbine entry temperature (TET), overall pressure ratio (OPR) and bypass ratio (BPR). A change in these three parameters will have an effect on the engine thermal and propulsive efficiency.

The maximum turbine entry temperature (TET) in aero engine combustors is limited by the mechanical integrity of the combustion chamber and turbine parts which are exposed to the highest gas temperatures in the engine. The material used for conventional combustor parts such as liners and domes and turbine parts such as blades, shrouds and vanes have a detrimental effect on the achievable maximum engine performance. Apart from the materials used for manufacturing, active cooling of these highly stressed engine parts is vital to ensure efficient operation. Thus, an engine design allowing higher turbine entry temperatures will normally yield an improved thermal efficiency.

The overall pressure ratio (OPR) of a gas turbine represents the total pressure at compressor exit in relation to the total pressure at engine inlet and thus depends on the number of compressors and the individual compressor design in a particular engine configuration. Maximum overall pressure ratios in aero engines are limited by the maximum permissible engine weight and the operating ranges of the combustor and the turbines. Aero engines typically feature an axial compressor arrangement which delivers the highest pressure rise per stage for a given compressor efficiency.

The engine bypass ratio (BPR) is defined as the ratio between the mass flow rate of air which bypasses the core engine, to the mass flow rate which is passing through the core engine which is involved in the combustion process. Maximum engine bypass ratios in aero engines are mainly limited by the increase in the size of the fan diameter

or by the decrease in size of the core engine diameter. Very large fan diameters will disproportionally increase aircraft total drag and increase the weight of the fan section which includes fan blades and the fan hub. In addition, a larger diameter will require additional Low Pressure Turbine stages to drive the fan at desired speed. On the other hand, decreasing the size of the core engine is limited by compressor stage pressure ratios and the size of the combustion chamber to achieve acceptable compressor and combustion efficiencies.

A much more detailed elaboration of the correlations between engine overall pressure ratio (OPR), bypass ratio (BPR) and fan pressure ratio (FPR) and detailed parametric analyses can be found in the works of Fletcher and Walsh [38] and in the work of Bräunling [39]. In addition, reference [40] specifically addresses flow characteristics in turbine engine components, such as inlets and nozzles and their related gas dynamic problems.

2.2.2 Thermal Efficiency

The thermal efficiency of an aero-engine is described as follows (equation 2-1):

$$\eta_{th} = \frac{{V_j}^2 - {V_0}^2}{FAR \times FHV} \quad \textbf{(2-5)}$$

V_0 is the flight velocity, V_j is the jet velocity, FAR is the fuel-air ratio and FHV is the fuel heating value. The thermal efficiency provides information about the quality of the engine thermodynamic cycle which in this form means conclusions about how effectively thermal energy is converted into useful work [39]. Since the thermal efficiency is dependent on pressures, temperatures, component efficiencies and other associated losses an improvement of those cycle parameters and thus an improvement in thermal efficiency will result in an increase in jet velocity [41]. The optimum achievable thermal efficiency of a heat machine based on a reversible process which, for example, could be an ideal cycle gas turbine can be described as follows:

$$\eta_{th,opt} = 1 - \frac{T_{min}}{T_{max}} \quad \textbf{(2-6)}$$

T_{min} and T_{max} are the minimum and maximum temperatures of the thermodynamic cycle as derived from the theoretical ideal Carnot cycle. For the assessment of the thermal efficiency of the Joule cycle, where heat is added over a temperature range, T_{min} and T_{max} are replaced by the ambient temperature and the thermodynamic average temperature is designated as $\overline{T}_{th}$ according to reference [42]. The optimum thermal efficiency is then approximated as follows:

$$\eta_{th,opt} = 1 - \frac{T_0}{\overline{T}_{th}} \tag{2-7}$$

T_0 is the ambient temperature and $\overline{T}_{th}$ is described as follows:

$$\overline{T}_{th} = \frac{T_{t4} - T_{t3}}{ln\frac{T_{t4}}{T_{t3}}} \tag{2-8}$$

T_{t4} is the maximum combustion chamber exit temperature and T_{t3} is the maximum Compressor exit temperature of a gas turbine engine. A more detailed elaboration of the effects of cycle parameters on thermal efficiency can be found in reference [39].

2.2.3 Propulsive Efficiency

The propulsive efficiency of an aero-engine is described with the following equation:

$$\eta_{prop} = \frac{2}{1 + \frac{V_j}{V_0}} \tag{2-9}$$

V_0 and V_j are again flight velocity and jet velocity respectively. The propulsive efficiency provides information about how the actual useful work is converted into propulsive power, id est the relationship between thrust power and the increase in kinetic energy in the engine. Since the propulsive efficiency is dependent on the engine bypass ratio and fan pressure ratio, an increase in engine bypass ratio and a reduction in fan pressure ratio will result in an improved propulsive efficiency through a decrease in jet velocity. This in turn will lead to a decrease in specific engine thrust. From the literature in references [39] and [41] it can be seen that there is an optimum value for fan pressure ratio when a fixed engine bypass ratio is assumed.

2.2.4 Overall Efficiency

Based on the considerations of sections 2.2.2 and 2.2.3 the overall engine efficiency is described as follows:

$$\eta_{overall} = \eta_{th} \times \eta_{prop} \quad \textbf{(2-10)}$$

The overall engine efficiency is the product of thermal efficiency and propulsive efficiency and represents the relationship between specific thrust performance and specific heat energy of the fuel. If the fuel heating value (FHV) is assumed constant, the overall efficiency can be expressed as the inverse of the specific fuel consumption (SFC) for a given flight velocity:

$$SFC \sim \frac{1}{\eta_{overall}} \quad \textbf{(2-11)}$$

An improvement in thermal and/or propulsive efficiency will result in improved overall engine efficiency.

2.3 Gas Turbine Engine Emissions

All gas turbine engines which burn fossil fuels emit pollutants that originate from the combustion products generated during engine operation. Many of the pollutants are hazardous to the environment and the human health while many of the harmful pollutants have been identified to cause measureable changes in the global atmosphere, local air quality and can be the cause for several diseases [43]. In a conventional gas turbine combustor a mixture of air and kerosene (hydrocarbon) is burned and the chemical energy contained in the fuel is converted into heat energy. Through the combustion process this hydrocarbon is converted to carbon dioxide (CO_2) and water vapour (H_2O), ideally in a Stoichiometric combustion that is described with the following reaction equation:

$$C_{12}H_{24} + 18\left(O_2 + \frac{79}{21}N_2\right) \rightarrow 12CO_2 + 12H_2O + 18\left(\frac{79}{21}\right)N_2 \quad \textbf{(2-12)}$$

One mole of kerosene requires the existence of eighteen mole of oxygen for the Stoichiometric combustion to be complete which will then release carbon dioxide (CO_2), water vapour (H_2O) and nitrogen (N_2) in the exhaust gas. In addition, a real combustion process will also release carbon monoxide (CO), oxides of nitrogen (NO_x), oxides of sulphur (SO_x) and unburned hydrocarbons (UHC). Most of the gas turbine pollutants and their concentrations can be directly related to the temperature in the combustor and the residence time in the combustor [44]. For example, NO_x emissions will decrease with lower residence times while higher combustion temperatures will cause NO_x emissions to rise. Higher temperatures will increase combustion efficiency but will increase NO_x emissions at the same time. On the other hand, a reduction in residence time and decrease in temperature will cause CO emissions to rise.

It can be differentiated between ground or near ground emissions designated as local air quality pollutants and emissions occurring at altitude which are considered as greenhouse gases. The ground or near ground emissions are controlled by an idealised standard LTO (Landing and Take-Off) cycle set forth by the International Civil Aviation Organization (ICAO) while cruise emissions are not regulated through specifications and thus are not considered by any policy instruments [45].The five main types of gas turbine emissions will be briefly described in the following chapters primarily focusing on their formation mechanisms and their effect on the atmospheric environment. Even though the release of water vapour can under given conditions cause the formation of vapour trails in the atmosphere and foster the formation of artificial cirrus clouds, which may contribute to changes of the atmosphere that abet the greenhouse effect, it will not be addressed further in this work. Table 2-1 exemplifies the typical exhaust gas composition of a conventional turbofan engine [39]. From this data one can also see that carbon monoxide concentrations and concentrations of unburned hydrocarbons are highest at low power conditions (idle power) and decrease with high power conditions (take-off). This is due to the fact that CO and UHC emissions will form as a result of incomplete combustion which occurs at lower power conditions in conventional combustors [39]. However it must also be kept in mind that engine

emission levels have a close relationship to basic cycle parameters such as pressure ratio and turbine inlet temperature.

Table 2-1: Typical turbofan exhaust gas composition (according to Bräunling [39])

	Idle power	Take-off power
Oxygen O_2	18.54 %	15.06 %
Carbon Dioxide CO_2	1.60 %	3.66 %
Nitrogen N_2, Inert Gases Ar, Ne and Water H_2O, Carbon Monoxide CO, Oxides of Nitrogen NO_x, Unburned Hydrocarbons UHC	79.86 %	81.28 %

2.3.1 Carbon Dioxide

The formation of carbon dioxide (CO_2) is a direct consequence of the complete combustion of the fuel in the combustor and its emission as such is inevitable. Due to its stability and the subsequent relatively long residence time in the atmosphere carbon dioxide is identified to be a significant contributor to global warming by boosting the greenhouse effect [44].

Since the amount of carbon dioxide emitted during the combustion process is directly linked to the amount of fuel burned, an emission reduction can only be achieved by increasing fuel efficiency and/or fuel savings.

2.3.2 Carbon Monoxide

Carbon monoxide (CO) is produced during the combustion process if there is not enough oxygen to form carbon dioxide, id est if no complete combustion takes place. Two preconditions which lead to formation of carbon monoxide are low combustion zone temperatures and/or insufficient time for combustion. These conditions can be caused by inadequate burning rates due to a low fuel/air ratio, inadequate mixing of fuel and air in the combustor with regions of weak or over-rich mixture strengths, or by quenching of combustion products which are entrained by the cooling air flow of the combustion chamber liners [44]. The fuel and air mixture strength in the

combustion zone will also have an effect on the CO concentration and mixtures being close to Stoichiometric cause high amounts of CO due to dissociation of carbon dioxide. An effective control of the fuel and air mixture in the combustor over a wide range of power settings will be beneficial for the overall combustion efficiency.

2.3.3 Oxides of Nitrogen (NO_x)

The formation of oxides of nitrogen results from the oxidation of atmospheric nitrogen in high-temperature regions of the flame in the combustor [44]. NO_x in this context refers to the sum of NO and NO_2 emissions. Nitric oxide represents one major pollutant compound of these oxides and it is formed in the high temperature regions of the combustor with temperatures above 1800K during high power conditions.

The NO formation follows the Zeldovich chain mechanism which can be described in three steps as shown below:

$$O_2 \rightleftharpoons 2O$$
$$O + N_2 \rightleftharpoons NO + N \quad \textbf{(2-13)}$$
$$N + O_2 \rightleftharpoons NO + O$$

Three different mechanisms, which are listed below, contribute to the NO formation:

1. “Thermal” NO: Thermal NO is characterised through its relatively high initiation temperatures which then lead to the formation reaction where atmospheric nitrogen is oxidised in the post-flame gases. In combustion engines NO_x formation starts with temperatures around 1200K.
2. “Prompt” NO: Prompt NO is generated through very fast formation reactions in low-temperature, fuel-rich flames. However, the formation mechanisms are very complex and have not been completely investigated and understood.
3. “Fuel” NO: The sources of fuel NO are the nitrogen portions bound in the fuel which transforms into NO_x during the combustion process. Thus the amount of generated fuel NO_x highly depends on the nitrogen content of the particular

fuel used. Kerosene fuels used in aero gas turbines typically contain low amounts of nitrogen.

There are two important factors that affect the formation of NO_x during the combustion process.

The first factor is the combustion flame temperature. An increase in flame temperature will cause an exponential rise in the NO_x formation rate. Conversely, a decrease in flame temperature with the same combustion effectivity will significantly reduce NO_x formation rates.

The second factor is the residence time of the fluid in the combustor. Low residence times will decrease the NO_x formation rate in a linear fashion. However, reduction of the residence time may have adverse effects on the generation of other pollutants such as CO and UHC [46].

The formation of NO_2 in particular is caused by oxidation of NO at relatively low temperatures:

$$2NO + O_2 \rightleftharpoons 2NO_2 \qquad \textbf{(2-14)}$$

This means at lower power conditions (idle power) the NO_2 formation rate is high and may be as much as 50 percent of the total NO_x (NO + NO_2) emissions. This is in line with the fact that NO_2 has a higher stability than NO at low temperatures [44].

NO_x emissions can have different undesirable effects on the environment depending on in which atmospheric layer they are generated and released. In the lower atmospheric layers of the troposphere and especially close to ground level, NO_x emissions will cause the formation of ozone O_3 while in the upper atmospheric layers of the stratosphere NO_x emissions will cause the stratospheric ozone to decrease (depletion of the ozone layer).

The ozone in the troposphere formed by photochemical reactions of NO_2 and its resulting molecular products can have a negative effect on health when the exposure is long enough while ozone concentrations are above 100 ppb (parts per billion).

Respiratory illnesses, impaired vision and other disorders can be the consequence of such exposure. Its relatively long residence time of about 10 month in the atmosphere amplifies its effect on the environment [47].

The NO_x emissions in the higher atmospheric layers of the stratosphere on the contrary cause a depletion of the existing ozone layer. The atmospheric ozone reacts with the nitric oxides and forms nitrous oxide and molecular oxygen. The newly formed nitrous oxide then again reacts with atomic oxygen to regenerate nitric oxides. Stable atmospheric conditions in the stratosphere foster this process since only very little mixing takes place and particles can remain in these layers for longer times. A reduction of the ozone layer causes an increase in ultra-violet radiation at ground level since there is less ozone available to absorb the radiation from the sun. An increased risk for skin cancer can be one consequence of this ozone layer depletion [47]. A detailed elaboration of the atmospheric effects initiated by the above described pollutants as well as their formation mechanism can be found in reference [5] while reference [27] provides a projection for future growth of aviation emissions and in particular NO_x emissions.

2.3.4 Oxides of Sulphur (SO_x)

Oxides of sulphur, and sulphur dioxide SO_2 in particular is generated during the reaction of the sulphur contained in the fuel with the oxygen in the air. Thus the amount of SO_2 generated during the combustion process mainly depends on the sulphur content of the fuel used. Since oxides of sulphur are toxic and corrosive high contents in the fuel will have a negative effect on the engine life and durability. However, minimum amounts of sulphur in the fuel are desired to maintain fuel lubricity and to prevent fuel system corrosion. The maximum permitted concentration for aviation kerosene is 0.3% by mass.

2.3.5 Unburned Hydrocarbons

Unburned hydrocarbons are formed during an incomplete combustion process mainly due to insufficient fuel atomization or inadequate burning rates. The amount of

generated unburned hydrocarbon products depends on the engine power conditions. Higher power conditions will reduce UHC emissions through an increased chemical reaction rate caused by higher combustor inlet temperatures and pressures [44].

2.3.6 Soot

Soot is produced during incomplete combustion of hydrocarbons in the fuel-rich regions of the combustor and where mixing is inadequate. Soot becomes visible as smoke when it is emitted through the engine exhaust nozzle in the atmosphere and consists of small particles of different size and form that make up aerosols [48]. Soot emissions in airport vicinities as well as soot emissions at altitude are of concern due to the effects of visible pollution on ground and the potential to affect contrails and cloud formation at altitude. A drastic reduction in soot emissions can be achieved by increasing the amount of air injected into the combustion zone which results in lower temperatures and more oxygen being available for combustion. Further strategies to reduce soot emissions focus on the improvement of fuel injection system to obtain adequate atomisation and better aeration of the fuel in the combustor [44].

2.4 Gas Turbine Engine Degradation

As outlined in the previous section 2.2, overall engine performance relies on many different matched component parameters such as compressor pressure ratios, combustion temperatures or turbine entry temperatures and thus changes of which will have a discernible effect on engine performance. Since a mechanical turbomachinery such as an aero-engine will exhibit substantial wear and tear over its service life it is essential to monitor and assess the condition of an engine continuously to ensure reliable operation within design and certification parameters. Engine degradation monitoring or Engine Health Monitoring (EHM) is an integral instrument for gas turbine operation and is necessary to determine engine performance at any given time and also to allow a prognosis for future performance trends. This trend monitoring is achieved through continuous recording of engine component data during the engine running envelope. Typically, the minimum essential data that is recorded for performance analysis consists of pressures and temperatures of the engine gas

path at discrete locations as well as shaft rotational speeds and engine fuel flow. In addition, engine oil temperature and oil pressure as well as engine vibration data (frequency and amplitude of shaft vibration) is recorded and analysed as part of the engine condition monitoring process [49]. Apart from those data based parameters which can be remotely analysed the actual visual inspections and gas path borescope inspections of the engine form another crucial element of an engine health monitoring concept [50]. One measure primarily used to determine the actual engine condition in terms of operational performance is the measurement of the engine Exhaust Gas Temperature (EGT). It is typically measured at locations after the High Pressure Turbine exit or at the first stages of the Low Pressure Turbine where gas path temperatures are relatively low to allow installation of appropriate sensors. From these exhaust gas temperature measurements one can infer the turbine entry temperature which in turn correlates with a certain engine thrust (shaft rotational speed). Two main categories can be established to classify engine degradation mechanisms:

1. A considerable amount of the overall engine degradation is caused by normal engine operation in different layers (altitudes) of atmospheric air. This includes deterioration of the engine due to natural ageing and constitutes a process which cannot be avoided ultimately.
2. Other significant drivers of engine degradation are either single random events such as foreign object damage (FOD) or material failures as well as engine operational procedures such as take-off derate, engine taxi policies and warm-up and cool down times. This also includes maintenance procedures to preserve the engine condition, id est engine washing or engine control system maintenance.

The analysis and quantification of engine degradation over time is an important factor for reliable and efficient engine operation. The prediction of engine performance degradation based on the change of characteristic engine parameters can offer valuable clues to expected engine operational life and its associated performance behaviour. The identification of the main influencing parameters is thus essential to

allow for accurate prediction results [51]. A probabilistic approach to engine degradation is presented in reference [52] where characteristic engine parameters such as temperatures, pressures etc., but also component tolerances and production data, are gathered to model the engine condition. A stochastic Monte-Carlo simulation is then applied to the pre-processed distribution functions of the characteristic parameters to generate plots that describe the change of global performance parameters, such as SFC, over time.

2.4.1 Typical Mechanisms of Engine Degradation

The two main categories of engine degradation described in the previous chapter are initiated and evoked by the alteration of several mechanical and/or chemical properties of the gas turbine engine parts. The degradation of aerodynamic components, such as the engine compressor, the combustor, and the turbine which all operate in harsh environments, is a major driver for engine performance deterioration. This is due to the fact that all of the below mentioned degradation modes will cause a change of the parts original shape, properties and condition [53]. A general overview of these mechanisms and their effects are presented in this chapter.

The selection of the degradation mechanisms examined in the present work is based on their effect on the gradual, long-term engine wear which is anticipated when a normal engine operation is taken as a basis. In turn this means degradation effects caused by single events such as foreign object damage (FOD), excessive flight loads, component malfunctions or sudden changes in environmental conditions (volcanic ash), all of which may lead to significant and rapid deterioration of the engine performance and/or integrity, are not reviewed as part of this study.

2.4.2 Thermal Distress

Mainly parts of the combustor and turbine are subjected to very high temperatures either directly by exposition to hot flow path gases or indirectly by their proximity to the engine hot section. This includes stationary mechanical parts such as combustion chamber liners, turbine vanes and structural turbine cases and frames as well as

rotating engine parts such as turbine disks, turbine blades and rotating seals. Even components like fuel nozzles and instrumentation devices for engine condition monitoring are affected by thermal distress.

Hot corrosion is one common mechanism which will cause a material loss of the affected component over time due to the chemical reaction between the base material and substances carried in the hot gas. These substances can originate from the fuel or from sources external to the engine such as sulphates or salts. This type of corrosion is designated as sulphidation. The integrity of hot section engine parts such as high alloy HPT blades and vanes will be impacted by this type of corrosion which is induced by a combination of sodium chloride from the inlet air and sulphur from the fuel. Another known distress mechanism is high temperature oxidation which is caused by a chemical reaction between the base material and free oxygen from the hot gaseous environment. This reaction will also lead to a removal of component material. In addition burn-off with significant material detachment due to excessive temperatures can occur in the combustion and turbine section [54]. Spalling and removal of the Thermal Barrier Coating (TBC) of the high pressure turbine blades will cause an immediate failure of the part due to the exposition of the base material to the high, beyond melting point temperatures.

2.4.3 Mechanical Wear

Engine air and oil seals in all parts of the engine are mostly affected by mechanical wear which causes an increase in leakage flow over time. But also engine bearings, gearboxes and other moving parts are subject to mechanical wear and many of the resulting effects are being researched in the domain of tribology. Continuous rubbing of the engine seals against each other during engine operation due to rotation or vibration leads to base material removal and consequently an increase in gaps. Cyclic operation (acceleration and deceleration) of the engine amplifies this abrasive wear effect and promotes leakages and mechanical wear.

2.4.4 Corrosion, Erosion and Abrasion

Corrosive distress arises on parts by chemical reaction of the base material with its environment. In most cases this is electrochemical oxidation of the exposed metal part reacting with oxygen from the surrounding air and/or moisture in the air. This type of corrosion can affect cold section engine parts such as steel alloy LPC blades and vanes where it can compromise their integrity.

Erosion of parts is caused by hard particles impinging a surface, thus rubbing away material and diminishing the parts' original thickness. It will mainly occur in airfoils which are in direct contact with the flow-path air. The ingested particles typically have to be larger than 10 µm in diameter to have an abrasive effect [54]. Dust, sand or other floating particles are common examples for these particles. Apart from airfoils, any other stationary or rotating part can be affected by erosion if it is exposed to an airflow which carries abrasive particles. Especially cooling air passages and cavities within the engine, where air circulates constantly, are prone to severe erosion.

In the context of this work abrasion is defined as material removal due to the rubbing of a moving blade tip against its stationary lining surface or due to the rubbing of a rotating interstage seal against its stationary counterpart. Those rubs can originate from flight loads and gyroscopic effects causing engine shafts and cases to deflect from their original positions and thus increasing or decreasing blade tip and seal clearances. In addition, rubbing can particularly occur in the engine turbines where material contractions are amplified due to the high temperature environment.

2.5 Effects of Engine Degradation

This chapter is focused on the effects of the previously described engine degradation mechanisms. The first subsection addresses the impact on the engine components or subsystems and their individual performances in terms of design and operational parameters. The second subsection will address the expected effect on the overall engine performance and the last section will deal with the implications on the life of the engine.

A degraded engine which has operated for a particular amount of time in service will show a higher fuel consumption compared to the initial fuel consumption values achieved right after engine production assuming the same amount of engine take-off thrust. This means over time the engine SFC will increase due to degradation of the engine component efficiencies, mainly of the compressor, the combustor and the turbine modules.

A parameter which is commonly used to describe the engine condition is called “EGT margin”. This value is calculated by subtracting the maximum allowable EGT provided by the engine manufacturer from the actual EGT measured during engine operation. As described in section 2.4, the TET is directly linked to the engine EGT. The maximum allowable EGT (EGT redline) represents the limit established by the engine manufacturer during certification tests and marks the maximum acceptable temperature at which the engine can operate without suffering rapid deterioration. Peak EGT values are usually reached at or shortly after take-off and thus depend on the OAT (Outside Air Temperature). One method utilised in modern turbofan engines to control the engine EGT is accomplished by flat-rating the engine at a certain ambient temperature. This means the engine will be able to provide maximum take-off thrust up to a specific ambient temperature, named “Corner Point” or CP (e.g. ISA+30°C) and beyond this point fuel flow will be limited to maintain a constant EGT and thus thrust will decrease. Figure 2-3 shows this effect on the EGT margin for a clean and degraded engine at corner point conditions. The degraded engine will have a lower EGT margin than the clean engine during a take-off at Corner Point conditions and thus operates with decreased performance margins.

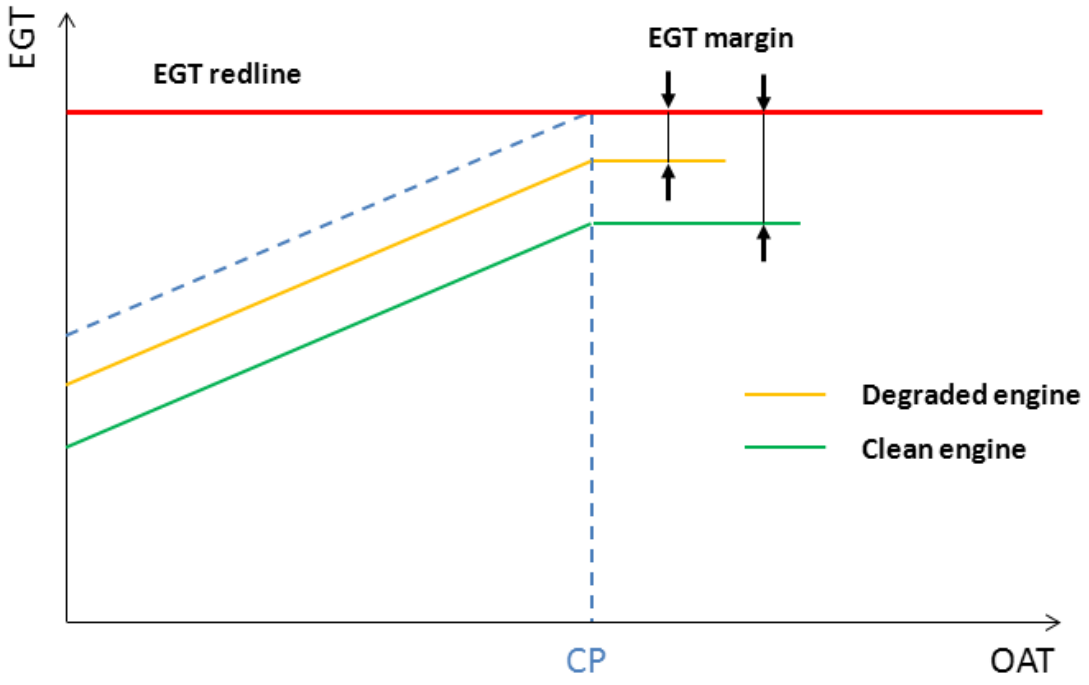

Figure 2-3: Effect of ambient temperature on engine EGT (flat-rated engine)

2.5.1 Effects on Engine Components

Engine component performance characteristics depend on their established design performance parameters. These parameters are determined during the matching of individual engine components in order to assemble a complete engine system. Five important performance parameters are listed below:

1. Compressor efficiency
2. Compressor flow capacity
3. Compressor pressure ratio
4. Combustion efficiency
5. Turbine efficiency

In the following, degradation effects of the two major engine components, the high pressure compressor and the high pressure turbine, will be briefly analysed. One main cause for compressor degradation is airfoil erosion which leads to an increase in surface roughness and a decrease in airfoil chord [55]. In the simplified form, the

power balance of the high pressure turbine and compressor in a turbofan engine with a certain bypass ratio μ can be given with the following equation:

$$W_I \times c_p \times (T_{Turb.inlet} - T_{Turb.exit}) = W_I \times c_p \times (T_{Compr.exit} - T_{Compr.inlet}) \quad \textbf{(2-15)}$$

This is where W_I is the core mass flow, c_p is the specific heat and T represents the inlet and exit temperatures of the associated component.

Based on the thermal ideal gas law the following general relationship between process temperatures and process pressures can be formulated:

$$\frac{T_{inlet}}{T_{outlet}} = \left(\frac{p_{outlet}}{p_{inlet}}\right)^{\frac{\gamma-1}{\gamma}} \quad \textbf{(2-16)}$$

This is where p represents the inlet and exit pressures of the associated component and γ is isentropic exponent for ideal gases.

In order to maintain this power balance between the turbine and the compressor for a given engine thrust level, a certain fuel flow to the combustor is required to provide the turbine with the necessary energy. Compressor degradation causes a decrease in the compressor exit pressure and flow capacity and thus the turbine work is decreased as well. The fuel flow and consequently the TET have to be increased in this case to recover the power output and to maintain the same engine thrust level. Due to the decline in compressor efficiency, the turbine has to generate more work to drive the compressor. Additional turbine efficiency degradation will aggravate this effect since the turbine then requires higher entry temperatures to compensate the lower power output [41].

Furthermore, combustor degradation can also be the cause for a drop in combustion efficiency. The combustion efficiency of a given combustor can be approximated by forming the quotient of theoretical fuel-to-air (FAR) ratio multiplied by the delta of the actual mean stagnation temperatures at combustor inlet ($T_{comb.inlet}$) and outlet ($T_{comb.outlet}$) and the actual fuel-to-air (FAR) ratio multiplied by the same actual mean stagnation temperatures:

$$\eta_{comb} = \frac{FAR_{theoretical} \times (T_{comb.outlet} - T_{comb.inlet})}{FAR_{actual} \times (T_{comb.outlet} - T_{comb.inlet})} < 1 \quad \textbf{(2-17)}$$

However, it must be noted that this definition is not in line with the fundamental definition based on the ratio of actual energy released to the theoretical quantity obtainable [46].

2.5.2 Effects on Engine Performance

From a bare engine stand point there are two important factors which determine the engine performance and which have an effect on the engine condition: (1) The first factor is the engine operational design scope with regards to maximum take-off thrust levels at a maximum ambient temperature representing the engine limitations. These limitations are directly linked to the maximum achievable combustion temperatures in the combustor, and thus directly linked to the turbine entry temperature TET. For example, continuous high power take-offs at high ambient temperatures will cause accelerated degradation of the engine. (2) The second factor is the engine utilisation rate in terms of hour to cycle ratio (stage length) and the engine operational envelope in terms of environmental and climatic conditions. For example, high daily aircraft utilisation in terms of cycles flown will increase the cyclic degradation of the engine. On the other hand, environmental conditions differ depending on the global region and the amount of erosive or anthropogenic pollutants in the air has a substantial effect on engine performance degradation [56]. Both factors combined will determine the overall engine degradation over time and thus are key elements to address for engine performance preservation strategies.

2.5.3 Effects on Engine Life

Aero engine life is on the one hand prescribed by the engine manufacturers who limit the life of certain parts based on load and stress calculations, engine thermal behaviour, material behaviour, engine long-time endurance testing and safety factors and requirements. For example, airworthiness standards prescribe part life limits in such way that cracks do not initiate. On the other hand engine life largely depends on

the operational conditions it is exposed to also in terms of maintenance and usage. This means for example that predetermined life limits of engine parts may change (increase/decrease) during the course of an engine model lifetime based on the operational experience. In the context of this work the definition of engine life is considered with respect to the fatigue life and thermal degradation of critical engine parts. In the following only two prevailing distress modes which affect gas turbine engine life will be briefly addressed in order to provide a context to the results of this work. In particular it is confined to the low-cycle fatigue (LCF) life and thermal fatigue which determine the maximum operational life of an engine component before it has to be removed for repair or retirement. In addition to cyclic fatigue, hot section parts such as turbine blades, turbine vanes, disks and combustor components are directly affected by thermal fatigue, hot corrosion and oxidation.

Low-cycle fatigue (LCF) life limitations are mainly determined by the number of cycles under high load conditions (high stresses). Particularly the amount of change in the material properties under a peak stress condition will have an effect on LCF. Particularly in short range applications low cycle fatigue becomes the limiting factor for the total life of rotating engine parts, whereas on longer range applications the creep life of the parts may become the limiter. Other factors which affect the fatigue behaviour are type and nature of loading, component size, surface finish and stress or strain concentrations [57]. In aero engines this condition is reached during take-off power settings imposing the highest stress on all engine parts. The reduction of take-off thrust can consequently lower the peak stresses and in turn positively affect LCF life.

This thrust reduction is also accompanied by a reduction in peak temperatures in the engine hot section. A lower turbine entry temperature (TET) will decrease the amount of thermal fatigue and the degree of engine degradation. On the opposite, engine degradation over time due to normal operation will increase the TET to maintain the same engine take-off thrust. Thus, over time, thermal stresses in the hot section will increase and both LCF life and thermal fatigue will be negatively influenced.

The above mentioned considerations only describe the basic aspects of two particular mechanisms which affect the engine life. Further detailed information about engine life assessments and lifing models can be found in reference [58].

2.6 Principles of Optimisation Processes

This section aims at providing a brief introduction into the major principles of optimisation processes and their application in practical engineering problems. This includes a general characterization of different optimisation problems as well as the assessment of appropriate and suitable optimisation methods.

2.6.1 Optimisation Problems

In general, an optimisation process represents the search for an optimal solution for a given problem while taking into account all known influencing factors. Using a mathematical approach it can be regarded as the process of finding the variables that lead to an optimal value of a given function which is to be optimised. Ultimately, the solution to an engineering optimisation problem will always involve the minimisation of the efforts required or the maximisation of the desired benefit [59].

According to Rao [59] optimisation problems can be classified in several ways depending on the particular problem to be addressed. An overview, as adapted from Rao, of the different optimisation problems is provided below:

- Classification based on the existence of constraints
- Classification based on the nature of the design variables
- Classification based on the physical structure of the problem
- Classification based on the nature of the equations involved
- Classification based on the permissible values of the design variables
- Classification based on the deterministic nature of the variables
- Classification based on the separability of the functions
- Classification based on the number of objective functions

For the purpose of this study and to put the above mentioned classifications into the research context, a generic optimisation problem can be defined in mathematical terms as follows:

$$X = \begin{Bmatrix} x_1 \\ x_2 \\ \vdots \\ x_n \end{Bmatrix} \text{ which minimises } f(X) \tag{2-18}$$

Subject to c constraints:

$$g_j(X) \leq 0, \quad j = 1,2,3,\dots,m$$
$$h_l(X) = 0, \quad l = m+1, m+2, \dots, c$$

This is where f(X) is the objective function, X is the design vector, $g_j(X)$ is the function defining the inequality constraints and $h_l(X)$ is the function defining the equality constraints. The design vector X contains all decision variables x_i, i=1,2,…n of the optimisation problem. The number of constraints c and/or m and the number of decision variables does not necessarily need to correlate and can be arbitrary.

For engineering problems such as aircraft trajectory optimisation problems, the objective functions can be regarded as surrogates for real goals which are to be approximated during the optimisation process and which will have to satisfy the requirements of the problem. These requirements then also impose limitations on the range of the specific values of the decision variables.

2.6.2 Optimisation Methods

There are different ways to address the optimisation problems defined in the previous chapter. Depending on the particular optimisation problem multiple methods may be suitable which may all be able to deliver satisfactory results. This means, the selection of an appropriate optimisation method requires the assessment of the particular problem in advance to ensure that the most feasible results can be obtained. For example, mathematical programming, also called mathematical optimisation, is one optimisation method that employs the search for an optimum solution from an available solution space. According to Rao [59] the field of mathematical programming

can be regarded as one of the branches in the field of operations research. In this context operations research is defined as a set of different problem-solving techniques applicable to various optimisation problems. Those methods are listed in table 2-2 with respect to their practical application. For the studies carried out in this work only the optimisation techniques of the first branch are considered and stochastic process techniques and statistical methods are not further explained.

Table 2-2: Methods of Operations Research (adapted from Rao [59])

Mathematical programming or optimization techniques	Stochastic process techniques	Statistical methods
Calculus methods	Statistical decision theory	Regression analysis
Calculus of variations	Markov processes	Cluster analysis, pattern recognition
Nonlinear programming	Queueing theory	Design of experiments
Geometric programming	Renewal theory	Discriminate analysis (factor analysis)
Quadratic programming	Simulation methods	
Linear programming	Reliability theory	
Dynamic programming		
Integer programming		
Stochastic programming		
Separable programming		
Multiobjective programming		
Network methods: CPM, PERT		
Game theory		
Modern or non-traditional optimization techniques		
Genetic algorithms		
Simulated annealing		
Ant colony optimization		
Particle swarm optimization		
Neural networks		
Fuzzy optimization		

2.7 Numerical Methods for Trajectory Optimisation

As outlined in table 2-2 mathematical programming techniques (nonlinear, geometric, etc.) are suitable to solve particular problems dependent on their complexity or classification. These techniques can be applied to optimisation problems where the minimum (or maximum) of a function of several variables including one or more defined constraints is desired. The group of modern or non-traditional methods listed

in table 2-2 represent more recent optimisation techniques, some of which are inspired by processes of nature (genetic algorithm) or by theories which are based on artificial models of uncertainties experienced in common processes (fuzzy logic). With regards to the requirements of solving an aircraft trajectory optimisation problem several techniques can be suitable due to their inherent solving mechanisms.

The following subsections discuss the three most important methods as grouped by Schwefel [60] and as used by Celis [61] and Zolata [23]. Those are hill climbing methods, random search methods and evolutionary methods. A schematic overview is presented in figure 2-4.

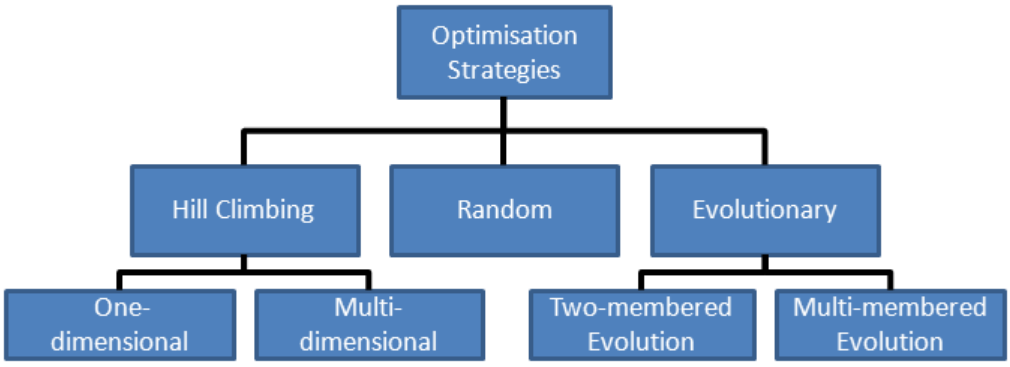

Figure 2-4: Overview of optimisation strategies (adapted from Schwefel [60])

2.7.1 Hill Climbing Methods

Hill climbing optimisation methods employ an iterative approach to finding a solution for a particular optimisation problem. It is characterised as a local search technique which means that, depending on if a maximum or minimum objective function value is sought after, the optimiser will incrementally change an element of the solution to find the best among a number of candidate solutions. Hill climbing methods can be used for one-dimensional and multi-dimensional optimisation problems. The solving techniques for multi-dimensional problems can be further divided into direct search methods, gradient methods and newton methods.

Direct search methods only use the value of the objective function without information about the gradient of the objective function to search for solutions superior to the current one. Thus it allows the application of this method to problems where the objective function is not differentiable or not continuous which in turn makes its use relatively simple. This simplicity on the other hand can have a negative impact on the optimisation performance as it may provide insufficient solutions for problems where numerous local maxima are present in the solution space.

Gradient methods also use the first partial derivative of the objective function assuming that it is differentiable. This means information inherent to the objective function, id est the gradient of the function, is necessary in order to approximate a numerical solution in the solution space while taking into account the search directions.

The first and second partial derivative is used in Newton methods which require a higher order of differentiability of the objective function. The optimisation process employs the second order partial derivatives of a quadratic function which are subsequently used in the inverted Hessian matrix to calculate the results.

2.7.2 Random Search Methods

Random search strategies for optimisation problems make use of probabilistic rather than deterministic rules to vary the parameters of the optimisation process. This means the parameters are subject to randomness which, however, does not necessarily imply arbitrariness [60]. The randomness of the optimisation parameters allows the process to explore solutions in many different directions independent of the structure of the objective function. On the other hand, due to the randomness the optimisation process does not take optimal steps towards the solution and hence may require a significant amount of computational resources. The relative simplicity of the random search method and its independence from the information about the objective function make them applicable to every case. Further information about random search methods and application examples can be found in reference [60].

2.7.3 Evolutionary Methods

Evolutionary optimisation methods imitate the biological process of evolution assuming that these natural mechanisms strive after optimal solutions. This means the basic concept of evolutionary optimisation methods relies on mechanisms such as reproduction, mutation or selection in order to find an optimal solution. Particular information about the problem to be analysed is not required to employ these methods. This provides the opportunity for a wide range of applications while maintaining reasonable complexity. Another advantage of this method is the ease by which problem constraints can be handled. These constraints normally occur in the form of inequalities which means that, if during the evolutionary progress there are descendants that do not satisfy the specific constraints, they are considered as unsuccessful candidates [62].

According to figure 2-4, evolutionary methods may be divided into two subcategories, two-membered and multi-membered optimisation strategies. The first strategy being the simplest form and consists of a population of two competing individuals which are changed during the evolution process through mutation and selection [62]. One problem of the two-membered strategy is the convergence rate and thus the possible inability to progress towards a global optimum. The multi-membered strategy tries to overcome this limitation by increasing the number of members in a population to imitate the natural processes more accurately.

2.8 Genetic Algorithms

Genetic algorithms (GA) represent an evolutionary optimisation method based on the principles of natural evolution. The underlying mechanisms of this method imitate techniques such as mutation, selection, inheritance and crossover to find useful solutions [63]. Genetic algorithms are used in many different fields and applications such as engineering design, economics or computational sciences. In order to define a genetic algorithm two elements are required. Firstly, a genetic representation of the solutions (individuals) to be assessed which means that the problem parameters have to be encoded in a chromosome-like data structure to form a candidate solution.

Secondly, a fitness function that allows evaluation of the progress of the solutions. In standard problems, the fitness function is the objective function to be optimised.

The methodology of genetic algorithms can be briefly described using the following steps:

1. Initialization: Form an initial population of randomly generated individuals.
2. Genetic operation: Select, recombine and mutate existing populations to generate a second generation population which is different from the first one. The genetic algorithm determines suitable solutions based on the requirements established in the fitness function.
3. Termination: Reach a predefined satisfactory stopping criteria or convergence of the solution.

The initial population is generally formed by a random generation of individuals which constitute the initial population for the optimisation process. If there are reliable, pre-existing solutions for a given problem, then those solutions can be utilised instead of a randomly generated population. This may improve the quality of the optimisation process and reduce computing time. The three main features or mechanisms of the genetic algorithm, named under point two, to advance a population towards a population consisting of individuals who represent the most suitable solutions are illustrated in figure 2-5. This iterative process forms one major element of the optimisation and has an influence on the performance of the genetic algorithm. The termination of the optimisation process can be based on different criteria and the most viable option depends on the particular optimisation problem. The process can be stopped by reaching, for example, a given fitness limit, a maximum number of generations or a maximum number of evaluations.

Two key parameters that define the optimisation performance are selection pressure and population diversity. A too high selection pressure may lead to premature convergence of the solution and low population diversity may limit the search space and the number of possible solutions.

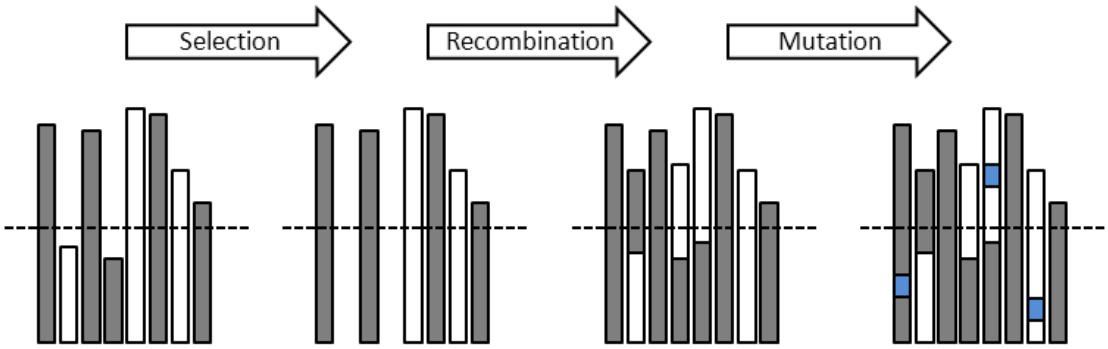

Figure 2-5: Main features of the genetic algorithm (adapted from Lipowsky [49])

According to Zitzler [64] genetic algorithms possess several desirable characteristics to address problems which involve multiple objectives and intractably large search spaces. Furthermore, Mitsuo in reference [65] states that genetic algorithms are able to maintain a population of potential solutions throughout the evolution generation process and thus are being useful when Pareto-solutions are evaluated. This evolutionary nature also becomes advantageous when solutions to complex problems are being searched because detailed information about the problem is not required.

2.9 Multi Objective Trajectory Optimisation

To define the aircraft trajectory optimisation problem addressed in this work and to highlight its main characteristics, the following list provides an overview of the most important classification elements. The aircraft trajectory optimisation problem can be described as:

- Constrained (one or more constraints)
- Dynamic (one or more function parameter(s))
- Optimal control (gradual progression)
- Non-linear (functions inputs and outputs)
- Real-valued (design variables)
- Deterministic (most parameters are deterministic)
- Multi-objective (two optimisation objectives)

Since the aircraft trajectory optimisation will involve the processing of multiple parameters the problem can be treated as multi-dimensional. The optimisation working space is not circumscribed in advance and thus the solutions are assumed to have several extreme points (local minima or maxima), id est the problem is considered to be multi-modal.

Furthermore the selection of the most suitable optimisation method depends on the characteristics of the objective function on the one side and the individual constraints defined on the other side. Considering the classification elements described above and taking into account the constraints of the problem, the objective function, even though being unknown, can be described as having the following properties:

- Highly non-linear (outputs and inputs are not directly proportional)
- Non-smooth/Non-differentiable (significant discontinuities)

An appropriate definition of the problem constraints will effectively narrow down the search space for the optimisation process.

If an optimisation problem consists of multiple objectives there will be not one optimal solution but instead there will be a set of solutions for the given problem [66]. These solutions are known as Pareto-optimal solutions. In relation to optimisation problems where sets of Pareto optimal solutions are obtained, those can be described in mathematical terms for a two-objective optimisation problem as follows: [67]

$$F = min\{f_1(X), f_2(X)\}$$
$$X \in S = \{X \in R^m : h(X) = 0, g(X) \geq 0\} \quad \textbf{(2-19)}$$

This is where $f_1(X)$ and $f_2(X)$ are scalar functions and S is the set of implicit constraints. The objective vector to be minimised is part of the objective space and the image of the search space under F can be denoted as follows:

$$C = \{y \in R^n : y = f(X), X \in S\} \quad \textbf{(2-20)}$$

The resulting Pareto front or Pareto curve as shown in figure 2-6 is made up of the image of all efficient solutions and the particular shape of the curve represents the

kind of trade-off between the two objective functions. All points between ($f_2(x;\hat{}),f_1(x;\hat{}$)) and ($f_2(x;\tilde{}),f_1(x;\tilde{})$) form the Pareto curve and each point of the curve stands for a non-dominated solution of the two-objective optimisation problem. This means an improvement of the objective represented by $f_1(X)$ will lead to a worsening of the objective represented by $f_2(X)$ [67].

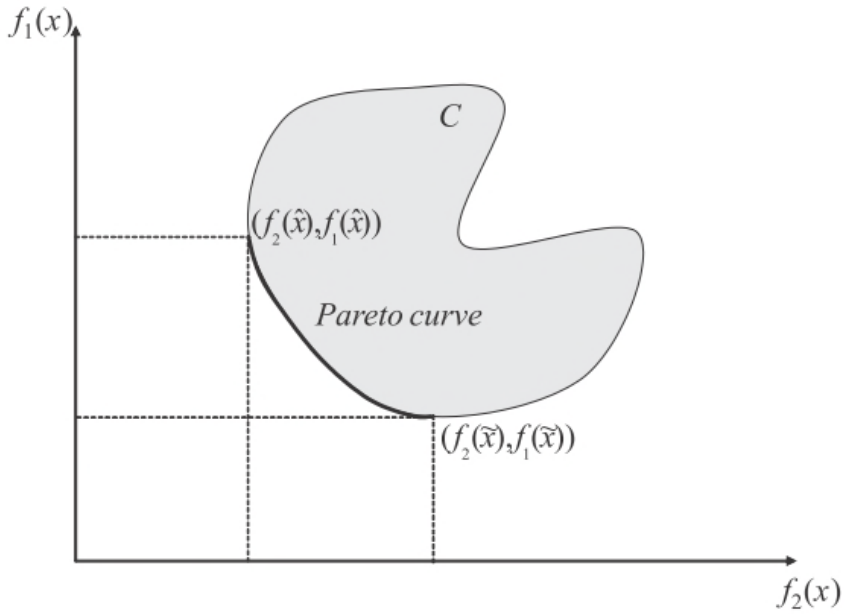

Figure 2-6: Example Pareto curve [67]

A comprehensive introduction to multi-objective evolutionary algorithms is presented in the paper in reference [68]. In this paper, evolutionary algorithms are classified based on the type of selection mechanism, which, for example, can be populations-based or Pareto-based. Reference [69] provides a detailed insight into solving multi-objective optimisation problems based on evolutionary algorithms. It presents and analyses in detail the research of contemporary multi-objective evolutionary algorithms and discusses associated multi-objective optimisation problems.

2.10 NSGAMO Genetic Optimiser

One particular genetic algorithm-based optimiser which has been proposed and developed by the authors in reference [66] and which is widely used for optimisation problems is called NSGA-II (Non-dominated Sorting Genetic Algorithm II). An updated

version of this algorithm, namely NSGAMO, is used in the GATAC (Green Aircraft Trajectories under ATM Constraints) optimisation suite. This suite is jointly used by Cranfield University and the University of Malta. The structure and application of the genetic operators of the GATAC optimiser differ in two ways from the original NSGA-II. Firstly, it uses a different selection process to form the mating pool and secondly, it uses a different sequence of genetic operators (SBX crossover and polynomial mutation) [70]. The basic optimisation flowchart of the NSGAMO optimiser is shown in figure 2-7.

The algorithm begins its calculation with an initial population which is randomly created. The population size multiplied by the initialisation ratio determines the number of cases to be sent to the optimisation framework for evaluation. Larger population sizes will increase the number of possible solutions on the one hand and on the other hand it will increase the number of evolutions and thus computing time to calculate the next generation. According to the defined fitness function for the specific case the algorithm will then reduce the population size to the specified value. Then the optimiser checks if the optimisation process is complete, which depends on if the maximum number of generations has been reached or the criteria of the fitness or objective function have been reached. At this point the optimiser enters an iterative loop to create new cases by applying genetic operators specific to the optimiser and sending these new cases to the framework for evaluation. The results are joined into the existing population and qualified based on their suitability. Another trimming of the population is carried out and the loop will continue until one of the final stopping criteria is met [71].

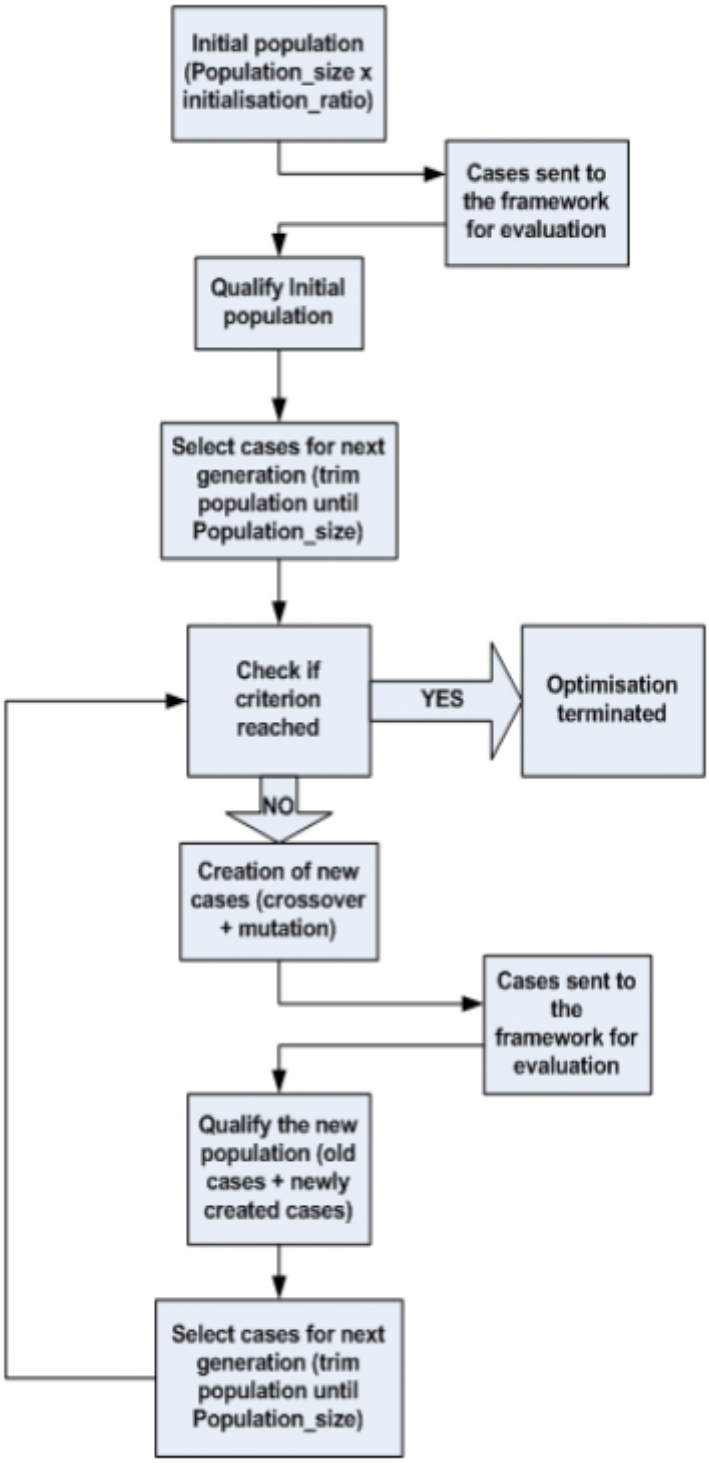

Figure 2-7: Optimisation flowchart [71]

3 Problem Definition

This chapter aims to define the problem statement of this work on the one hand and on the other hand aims to provide an interface between the fundamental information from the literature review and the specific requirements of the aircraft trajectory studies to be carried out and analysed in the following chapters. This involves a brief discussion of some general considerations with regards to the aircraft configurations and aircraft performance parameters as well as the flight trajectory itself. Furthermore, a definition of a simplified aircraft trajectory is provided and the requirements for the trajectory analyses and optimisations are discussed. This also includes the assumptions and statements made for models and frameworks developed in this study. The chapter concludes with a review of past works which have already addressed the subject of aircraft trajectory optimisation.

3.1 General Considerations

The analysis of aircraft trajectories makes it necessary to briefly introduce some general aspects of commercial aircraft operations. In a real environment there are many factors which influence an aircraft mission and consequently its performance from the beginning at the departure point till the arrival at the final destination. Figure 3-1 schematically illustrates a typical flight profile of a commercial passenger aircraft with its five particular flight phases namely (1) take-off, (2) climb, (3) cruise, (4) descent and (5) approach. Normally the cruise altitude and the range (travel distance) are interdependent in a way that shorter flight ranges will result in lower cruise altitudes and longer flight ranges will result in higher cruise altitudes. This is assuming that time spent in take-off and climb phases as well as the time spent in descent and approach phases are nearly constant. Since the cruise phase usually represents the flight phase where the engine and aircraft operate in their respective design points it is desirable to spend as much time of the whole flight in this condition.

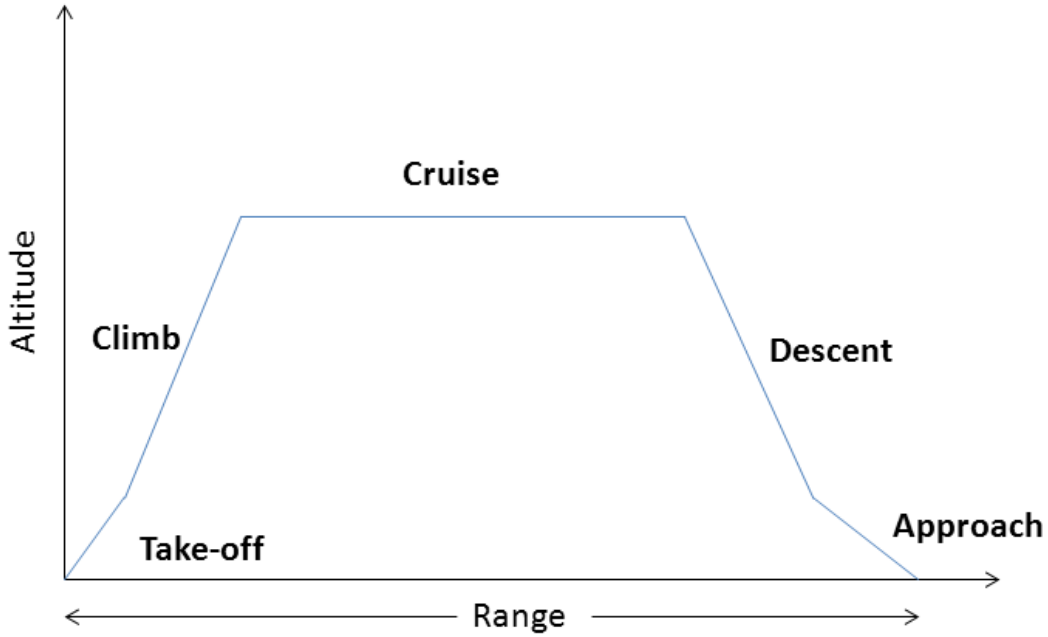

Figure 3-1: Typical flight mission profile and flight phases

3.1.1 Short-to-Medium Range Aircraft Configurations

The aircraft configurations considered in the following studies are based on publicly available information of the Airbus A320 family. This family represents a typical short to medium range, twin-engine commercial passenger aircraft that is widely used and also represents a significant share of the total worldwide fleet for this aircraft class. It comprises a narrow-body design with a retractable tricycle landing gear, low-wing cantilever monoplanes, a single vertical stabiliser and rudder mounted on a conventional tail unit. The passenger capacity for the different models ranges from 124 to 220 seats depending on class configuration and model.

3.1.2 Aircraft Speeds

One important characteristic performance value for aircraft trajectory analyses is the actual aircraft velocity. The setup of the aircraft trajectories in this study will require the definition of specific aircraft velocities in certain phases of the flight depending on the actual altitude. A brief overview of aircraft velocity definitions and their usages is given in the following.

Aircraft velocity can be expressed in different forms depending on the required application or the context it is used in. Some common forms are listed below: [72]

- Indicated Airspeed (IAS)
- Calibrated Airspeed (CAS)
- Density Airspeed (DAS)
- Equivalent Airspeed (EAS)
- True Airspeed (TAS)
- Mach Number (M)

The dependencies of these different forms of aircraft velocity are illustrated in figure 3-2 below. The Density Airspeed (DAS) is only shown for the sake of completeness and will not be explained in more detail.

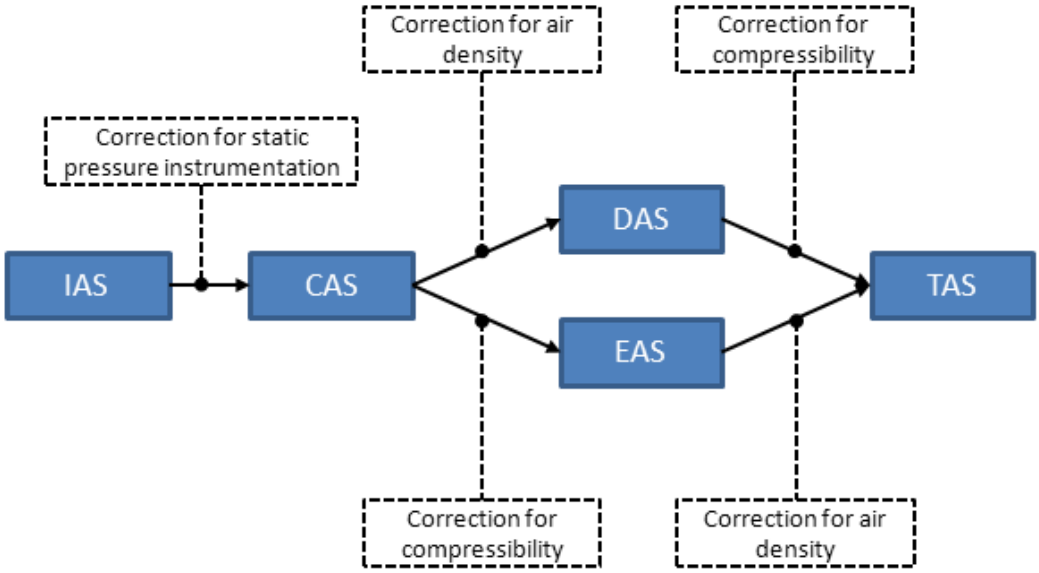

Figure 3-2: Aircraft velocity interdependencies (adapted from Scheiderer [72])

The Indicated Airspeed (IAS) is the aircraft velocity shown on an airspeed indicator which is calibrated for ISA conditions. IAS is commonly used in aircraft performance tables. The Calibrated Airspeed (CAS) results from the correction of the IAS to account for errors of the static pressure gauging system. In the subsonic region the CAS is defined as follows:

$$CAS = \sqrt{\frac{2\gamma}{\gamma - 1} \times \frac{p_0}{\rho_0}\left[\left(\frac{p_t - p_s}{p_0} + 1\right)^{\frac{\gamma-1}{\gamma}} - 1\right]} \quad \textbf{(3-1)}$$

As aircraft altitude and Mach number increase, the indication of the CAS will contain an error which is corrected by introducing the Equivalent Airspeed (EAS). The EAS accounts for these compressibility effects and a constant EAS corresponds to a constant dynamic pressure. It is defined as follows:

$$EAS = \sqrt{\frac{2\gamma}{\gamma - 1} \times \frac{p_s}{\rho_0}\left[\left(\frac{p_t - p_s}{p_0} + 1\right)^{\frac{\gamma-1}{\gamma}} - 1\right]} \quad \textbf{(3-2)}$$

Subsequently, the True Airspeed (TAS) is arrived at by allowing for air density corrections. The TAS is then defined as follows:

$$EAS = \sqrt{\frac{2\gamma}{\gamma - 1} \times \frac{p_s}{\rho_s}\left[\left(\frac{p_t - p_s}{p_s} + 1\right)^{\frac{\gamma-1}{\gamma}} - 1\right]} \quad \textbf{(3-3)}$$

The TAS can also be directly derived from the EAS by using the following equation:

$$TAS = \frac{EAS}{\sqrt{\rho}} \quad \textbf{(3-4)}$$

The Mach number M is often referred to in aircraft cruise conditions and is described as ratio of the True Airspeed (TAS) and the local speed of sound a:

$$M = \frac{TAS}{a} \quad \textbf{(3-5)}$$

The local speed of sound depends on the atmospheric temperature t_0, the isentropic exponent γ, and the gas constant R for dry air.

$$a = \sqrt{\gamma \times R \times t_0} \quad \textbf{(3-6)}$$

Since airspeed velocity measurements are based on the actual atmospheric conditions (temperature, pressure and density) the changes of these conditions with varying altitude must be taken into account as mentioned at the beginning of this section. To illustrate these changes, figures 3-3, 3-4 and 3-5 below depict the vertical distribution of temperature, pressure and density respectively in the International Standard Atmosphere (ISA) up to an altitude of 20 km [73]. The ambient temperature linearly decreases from sea level to an altitude of about 11 km after which it will remain constant up to an altitude of about 20 km. The ambient pressure and density decrease gradually from sea level to an altitude of 20 km. The referenced figures only cover the lowest layers of the atmosphere, namely the troposphere which reaches from sea level up to an altitude of about 11 km and the stratosphere which extends from there up to an altitude of 20 km. Both layers are commonly used for commercial aircraft operation.

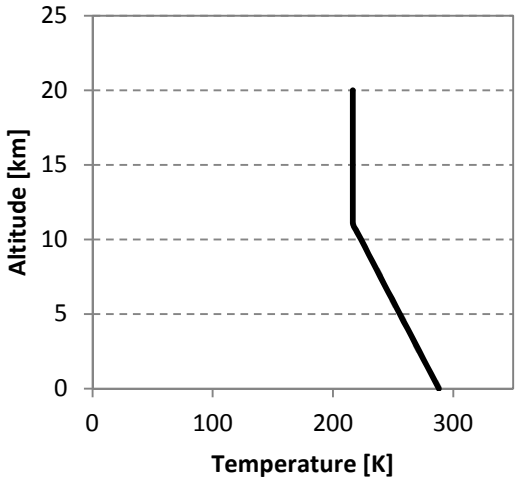

Figure 3-3: Ambient temperature vs. altitude

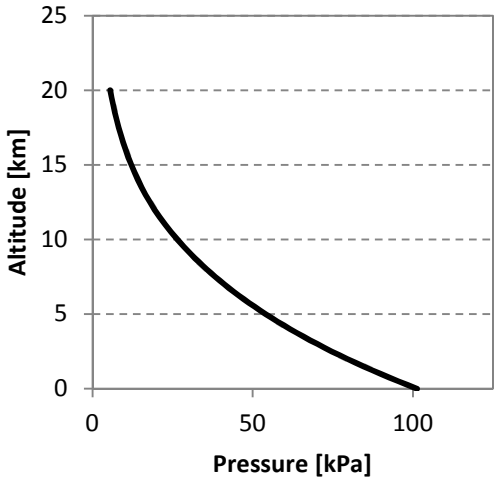

Figure 3-4: Ambient pressure vs. altitude

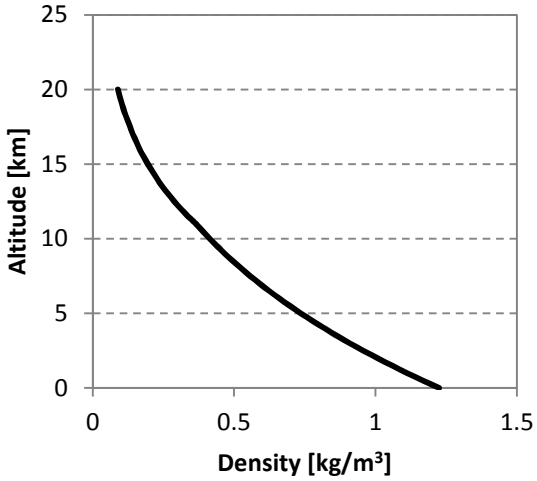

Figure 3-5: Air density vs. altitude

3.1.3 Aircraft Trajectory Definition

For the purpose of the scenario studies analysed in this work it is necessary to evaluate and analyse typical aircraft trajectories applied in current flight operation. In this study a typical flight trajectory, i.e. the mission profile, is comprised of the five previously mentioned flight phases. For each of the phases certain minimum and maximum operational limitations in terms of aircraft speed and rate of climb or descend exist. These limitations are imposed by influencing parameters such as the altitude effect, the temperature effect and the weight effect [28].

Since this study focuses on the first parts of the flight trajectory (take-off and climb) a brief review of those two flight phases will be provided in the following.

Even though the aircraft take-off phase depends on given external factors such as runway length or obstacles and variable conditions such as weather or airport restrictions, it can be broadly defined in two ways, namely take-off path (1) and take-off flight path (2). They can be described as follows: [28]

1. A standing start point to a point where the aircraft is at height (typically 1500 feet)
2. A point 35 feet above take-off surface at the end of the take-off distance

Since the aircraft take-off weight is in many cases below the maximum possible take-off weight due to the aircraft load condition it is possible to reduce the engine take-off thrust and thus reduce fuel burn and engine degradation.

According to reference [28] a climb is generally carried out at a constant Indicated Air Speed (IAS) and Mach number. The climb profile and technique can be divided into 3 phases which have a direct effect on fuel burn [74]:

1. Climb at constant IAS = 250 knots up to 10000 feet
2. Climb at constant IAS = 300 knots above 10000 feet
3. Climb at constant Mach number = 0.78 above crossover altitude

This is where the crossover altitude is the altitude where 300 knots IAS is equal to Mach 0.78.

For the sake of completeness the cruise and descent phase are briefly described in the following. The most important parameters which define the cruise phase are altitude (flight level) and aircraft cruise speed (Mach number) [74]. Depending on the aircraft weight, mission range, winds and atmospheric conditions different optimum speeds and altitudes with respect to fuel consumption and flight time can be identified. Similar to the climb phase the descent phase is generally carried out a constant IAS and Mach number. The descent is caused by a thrust reduction where the difference between engine thrust and aircraft aerodynamic drag becomes negative and thus the descent gradient and rate of descent becomes negative as well. Furthermore, to better understand typical aircraft flight profiles and to support the trajectory definitions mentioned above, a real flight trajectory for a typical single aisle aircraft configuration is referenced in figure 3-6 and 3-7. The flight distance of the mission is approximately 1400 km. Figure 3-6 shows the fuel flow trend over time and along the flight profile in percent of the take-off fuel flow. Correspondingly, figure 3-7 illustrates the engine EGT trend in percent of the applicable EGT redline of the number one engine for the same flight.

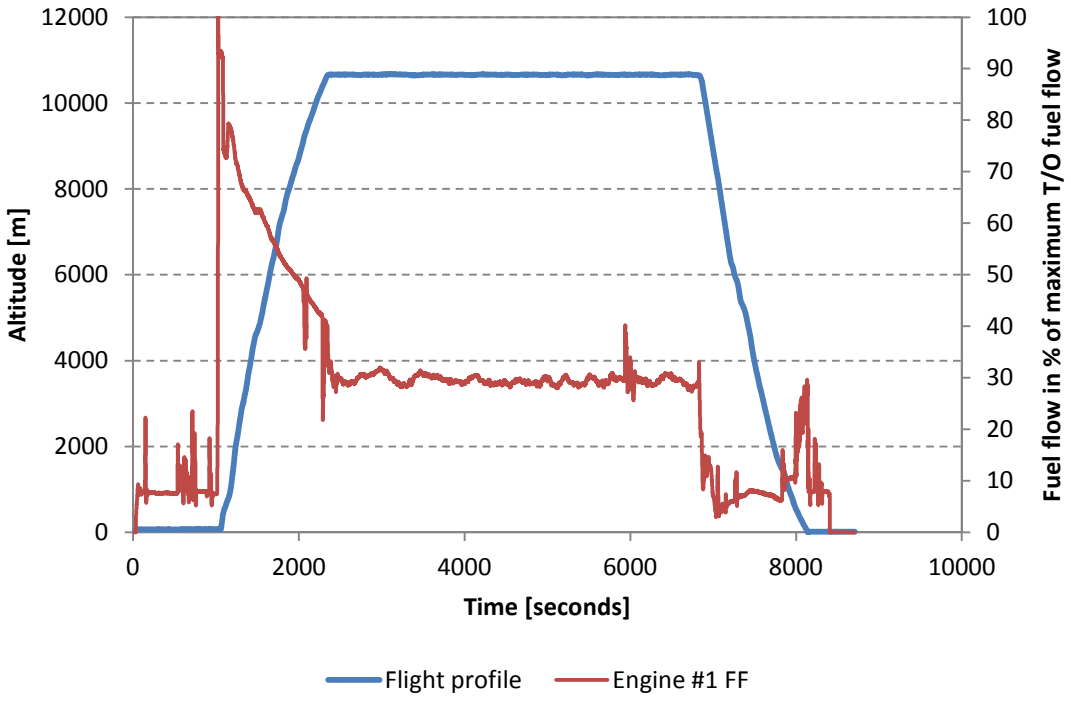

Figure 3-6: Flight profile with engine fuel flow (Airbus A321); courtesy of Airberlin

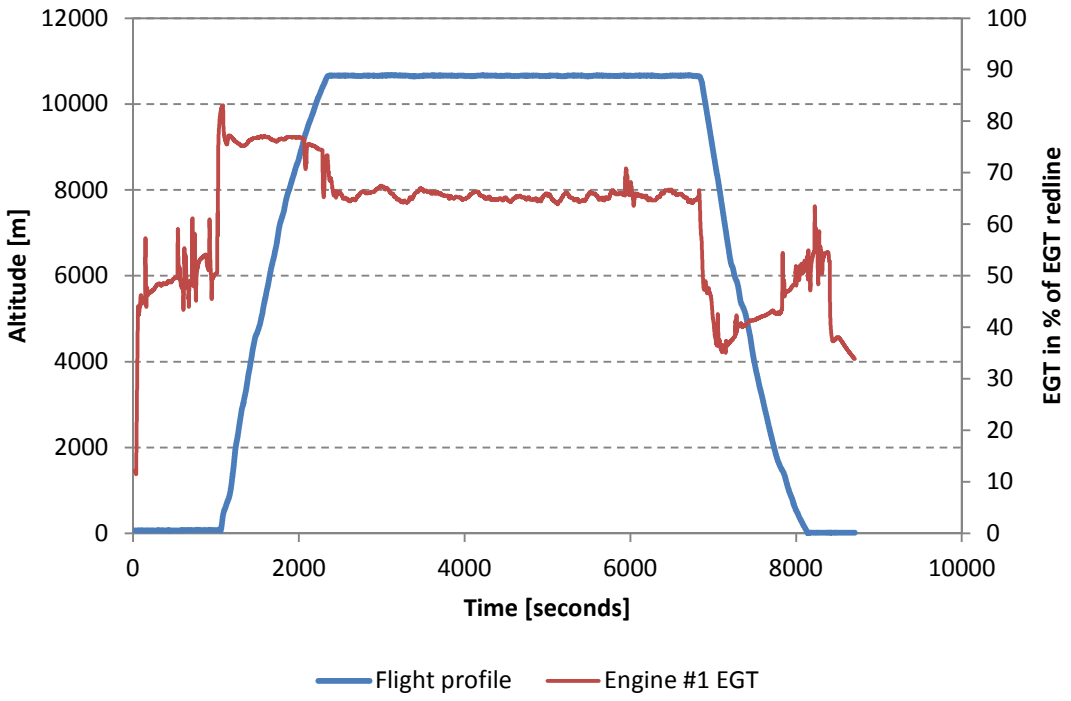

Figure 3-7: Flight profile with engine EGT (Airbus A321); courtesy of Airberlin

Based on the previously described information a baseline trajectory has been defined as a reference to allow a comparison of the different analysed scenarios. The basic points of the trajectory can be summarised as follows:

- 1 minute take-off phase to 457 m altitude (1500 feet)
- Climb from 457 m to 3048 m at constant EAS = 250 knots
- Accelerate from EAS = 250 knots to 300 knots at constant altitude (3048 m)
- Continue climb from 3048 m to cruise altitude 10668 m
- Cruise at constant Mach number = 0.785
- Descent slope is based on aircraft cruise altitude

In case of the engine derate scenario a 15% take-off thrust reduction has been assumed. This assumption represents a typical value derived from real engine flight data. These basic points have been used as inputs for the aircraft performance model Hermes which calculates the aircraft trajectory based on the defined parameters. The aircraft performance model will be explained in more detail in section 4.2.

3.1.4 Optimised Aircraft Trajectory

Optimised aircraft trajectories aim at providing the most suitable flight profile for a given mission in terms of flight time, fuel burned and emissions generated. It becomes clear that these three goals are not always complementing each other but rather represent conflicting objectives. This results in a search for a trade-off between these goals for the particular flight mission. Thus one major aim of this research work is to analyse aircraft trajectories with regards to the above mentioned objectives and in a second step to find optimised trajectories. These optimised trajectories or so called "greener" trajectories aim at a reduction in fuel burn and emissions by introducing a variation in the climb profile and cruise phase while maintaining feasible results in terms of flight time and operability. This means the trajectory optimisation cases addressed in this work focus on the climb profile and cruise phase.

Many existing studies on aircraft flight trajectory analysis and optimisation also focus only on particular flight phases and address these in detail due to the significant increase in complexity when dealing with complete flight trajectories. Clarke [75] analyses in his study the feasibility of an airport specific continuous descent approach (CDA) procedure mainly to achieve an arrival noise reduction but which also resulted in a substantial reduction in NO_x emissions below 3000 feet (915 m). Patterson [76] analysed real-time aircraft data for departure and arrival profiles with respect to engine fuel burn and emissions. Actual operational fuel flow data from several aircraft has been compared to ICAO standard cycle data. It was found that actual fuel burn data for these profiles significantly deviated from the ICAO data and was generally overestimated. Another study on CDA has been carried out by Alam et al. [77]. They propose a methodology to compute dynamic CDA aircraft routes which are laterally and vertically optimised on particular objectives such as noise, emissions and fuel burn. The results indicate that a reduction in noise, emissions and fuel burn can be accomplished at the same time when employing dynamic CDA routes. Environmentally friendly departure procedures for civil aircraft have been investigated by Torres et al. [78] using a multiobjective, constrained, nonlinear optimisation methodology. These results also indicate possible noise and emissions reductions achieved through

optimised departure profiles. A detailed descent analysis was carried out by Trani [79] and it is concluded that continuous descent approaches can save fuel and time when applied to real aircraft operations with existing constraints.

3.2 Assumptions and Statements

The adaptation of the aircraft, engine and emissions models as well as the optimisation framework used in this study requires the definition of several assumptions and statements which take into account the respective model limitations on the one hand and which allow for the restriction of the scope of application on the other hand. The consideration of these assumptions is of major importance in order to evaluate the achieved results. The assumptions and limitations for the aircraft trajectory studies are as follows:

1. For all trajectory studies ISA+5°C conditions have been assumed during all flight phases apart from take-off. Take-off was assumed at ISA conditions.
2. Only take-off, climb and cruise phases have been considered for analysis; descent, landing and taxi phases have not been considered. Although all above mentioned phases are included in the aircraft performance model when calculating the aircraft trajectory the results for these phases are only approximate and have thus been omitted.
3. There is no provision made for speed continuity between cruise and descent phases. This may cause large variations in aircraft speed at the transition between cruise and descent.
4. Mission ranges have been selected taking into account the payload-range limitations of the three different aircraft variants.
5. The maximum climb and descent angle was limited to 7.5°.
6. All climb segments and all descent segments are flown with adjusted engine power settings to match constant flight times for climb and descent phases.
7. The take-off phase duration is kept constant and equals one minute.
8. The derate scenario assumes a 15% take-off thrust reduction.

For the optimisation framework (GATAC) and the trajectory optimisation studies itself the following modified assumptions and limitations, differing from the previously mentioned, apply:

1. There is no limitation to the maximum climb and descent angle.
2. All climb segments are flown with maximum climb engine power settings.
3. Descent segments are flown with constant preset engine power settings.
4. There is no speed continuity during acceleration from one climb segment to the next.

3.3 Past Experience on Trajectory Analysis and Optimisation

This section is intended to provide a brief review of aircraft trajectory optimisation studies that have been carried out at Cranfield University in the past. The studies constitute the basis for the optimisation approach adapted in the present work utilising a similar optimisation framework and algorithm. Highlights from three past works undertaken by Cesar Celis, Hasan Zolata and Roman Marzal are further described to set up the context for the developments of the present study.

In his work [61], Cesar Celis investigates suitable methodologies for aircraft trajectory optimisation and subsequently develops simulation models which are then implemented into a multi-disciplinary optimisation framework to evaluate more environmentally friendly operational procedures. The framework contains models for aircraft performance, engine performance and emissions performance. Furthermore, his study also includes the optimisation of aircraft engine cycles and its inherent design trade-offs which originate from conflicting objectives such as low operating costs or low environmental impacts. To solve the aircraft trajectory optimisation problem, Celis employs evolutionary methods based on genetic algorithms (GA) due to their robustness, their simplicity and their suitability for problems involving a number of constraints and objectives and where the space of potential solutions is large. Several case studies are presented which focus on the minimisation of total flight time, total fuel burned and total NO_x emissions. The results of those case studies illustrate the interaction of the major influencing parameters that have to be considered for aircraft

trajectory analyses. Those parameters are aircraft speed, cruise altitude and the maximum thrust requirements during climb to reach this altitude.

A further multi-disciplinary approach to aircraft trajectory optimisation is presented by Hasan Zolata [23]. His work also addresses the trajectory optimisation problem through the implementation of a multi-disciplinary simulation framework and the use of a commercially available genetic optimisation algorithm. To identify more environmentally friendly flight trajectories, in terms of fuel burn and pollutant emissions, a number of case studies have been carried out. These studies include the optimisation of a whole flight as well as the optimisation of a particular flight phase, namely the climb segment. The results indicate that aircraft trajectories with minimum environmental impact can be identified by employing the developed multi-disciplinary simulation framework. It was also found that trajectories optimised for minimum fuel were generally in conflict with trajectories optimised for minimum pollutant emissions.

Similar to the two previously mentioned studies, Roman Marzal [24] investigates in his study the suitability of a particular genetic algorithm-based aircraft trajectory optimisation tool. In the initial part of the study two different commercial optimisers, namely Matlab NSGA-II and Matlab MOGA were benchmarked against the GATAC optimisation suite in order to validate its performance. The benchmarking studies included different standard test problems which aim at testing individual properties of the optimiser with regards to quality of the solutions achieved. After confirming the suitability of the GATAC optimisation suite for multi-objective optimisation problems a two-objective aircraft trajectory optimisation study has been performed to test its capabilities. The analysed scenarios also focused on fuel burn and emissions improvements through optimisation of the climb phase. The results indicate that more efficient trajectories can be found when taking into account that optimisation objectives can be opposing.

The above mentioned studies are three current examples of trajectory optimisation research approaches from Cranfield University and have been selected due to the influence on the present work. Further studies which dealt with the analysis and

assessment of aircraft trajectory optimisations, but which are not covered in detail here, have been carried out in the past.

Matthew Sammut [80] conducted in his study a multivariable parameter optimization of flight trajectories focusing on economical climb trajectories for different aircraft variants. Several characteristic trajectories have been modelled, evaluated and compared in terms of climb fuel consumption. Results of the optimised trajectories confirmed the suitability of the employed optimisation methodology.

A multidisciplinary aero-engine exhaust study has been carried out by Shakariyans et al. [81] investigating the effects of flight conditions, power settings and combustor parameters on the engine emissions. Multi-reactor combustor models were used to predict pollutant emissions and then benchmarked against certification data. On ground and in-flight emission profiles have successfully been simulated. In a subsequent study by Shakariyans et al. [82] an engine deterioration scenario was also included in the emissions prediction analysis.

Antonio Filippone [83] carried out a comprehensive analysis of transport aircraft flight performance by adapting a multidisciplinary approach including various models to simulate aircraft performance, engine performance and noise performance. The analyses indicated that an accurate engine performance model will be the most critical aspect with respect to aircraft performance calculations.

A study, which focusses on adaptive engine technologies, such as fan and compressor flow control, blade clearance control or combustion control to reduce engine emissions, has been conducted by Mercer et al [84]. Potential positive and negative impacts of these technologies have been quantified one at a time and the results show that fuel burn can be reduced through improved propulsive efficiency and/or drag reduction depending on the technology applied.

A comparison of open-rotor engine concepts and conventional turbofan engines used in short range aircraft applications has been presented by Adam Waldowski [85] in his work also focusing on mission fuel burn and pollutant emissions. The open-rotor

engine concept yields promising results which indicate an improvement in fuel burn and pollutant emissions in comparison to conventional turbofans for shorter missions ranges.

4 Framework Tools

This chapter provides an introduction to the simulation tools and models for the engine, the aircraft and the emissions assessment used to carry out the basic aircraft trajectory studies. It also includes a description of the adapted trajectory optimisation framework and its operating principles.

4.1 Engine Performance Model (Turbomatch)

The engine configuration that is used throughout this study represents a two-spool high bypass ratio turbofan with separate exhaust nozzles. The basic configuration is shown in figure 4-1 in the next section. The basic engine model was developed in Cranfield University based on publicly available information and was adapted for the work carried out in this study [86]. Three engine configurations were derived from the basic engine model, one representing a low thrust configuration shortly addressed as CU2STF-LT, another a medium thrust configuration addressed as CU2STF-MT and a high thrust configuration addressed as CU2STF-HT. All three configurations encompass the same fixed mechanical and dimensional engine design like fan diameter and two-spool architecture. The three engine models were used for steady state design point and off design point simulations and the results were compared with engine specifications of the CFM56-5B engine series [87]. The CFM56-5B series engine powers the Airbus A320 Family of aircraft and is available with different thrust ratings, for example CFM56-5B6 (low thrust) and CFM56-5B4 (medium thrust) and CFM56-5B3 (high thrust). The thrust rating relates to the maximum engine take-off thrust.

The below described engine model performance results were achieved by using the Cranfield University in-house simulation code Turbomatch [88]. This program is used for engine modelling and engine parametric studies. The code allows a high engine modelling accuracy and comprises all basic gas turbine performance simulation features as well as advanced simulation capabilities. It has a modular design to model various gas turbine components (e.g. Compressors, Burners, and Turbines) and to carry out performance calculations with subsequent result plotting including component maps. It allows analysis of degraded engine performance through alteration of certain

engine components providing the opportunity to simulate a wide range of engine operating conditions.

Other programs that provide similar functionality to perform gas turbine performance simulations are, for example, GasTurb developed by Joachim Kurzke [89] and GSP (Gas Turbine Simulation Program) developed by the Dutch aerospace knowledge enterprise NLR (Nationaal Lucht- en Ruimtevaartlaboratorium) [90].

4.1.1 Turbomatch Engine Model

The basic engine model structure of the CU2STF model is depicted in figure 4-1 while figure 4-2 shows the engine component structure as used in the Turbomatch simulation code. It is a two-shaft design where the Low Pressure Turbine (LPT) drives the fan and the Low Pressure Compressor (LPC; Booster) and the High Pressure Turbine (HPT) drives the High Pressure Compressor (HPC). After the intake the air propelled by the fan is split into the core flow and the bypass flow. The core flow provides air for the gas generator which is comprised of LPC, HPC, Combustor, HPT and LPT and is then discharged through the Core Nozzle. The bypass flow is ducted and discharged through the Bypass Nozzle. Air is bled from the LP Compressor (LPC exit air) and is discharged into the bypass flow to allow adjustment of the LP Compressor outlet flow and thus allows handling of the inlet conditions of the HP Compressor. Furthermore it ensures that the LPC will operate within its design limits. For normal operation, the handling bleed will be utilised during transient engine operation with lower engine power settings while no air is bled during take-off or cruise conditions. Also, air is bled from the HP Compressor (HPC exit air) to cool the HP Turbine. An additional 200KW of work is extracted from the HP Turbine to account for the drive of the engine auxiliary systems such as fuel and oil pumps and electrical generators.

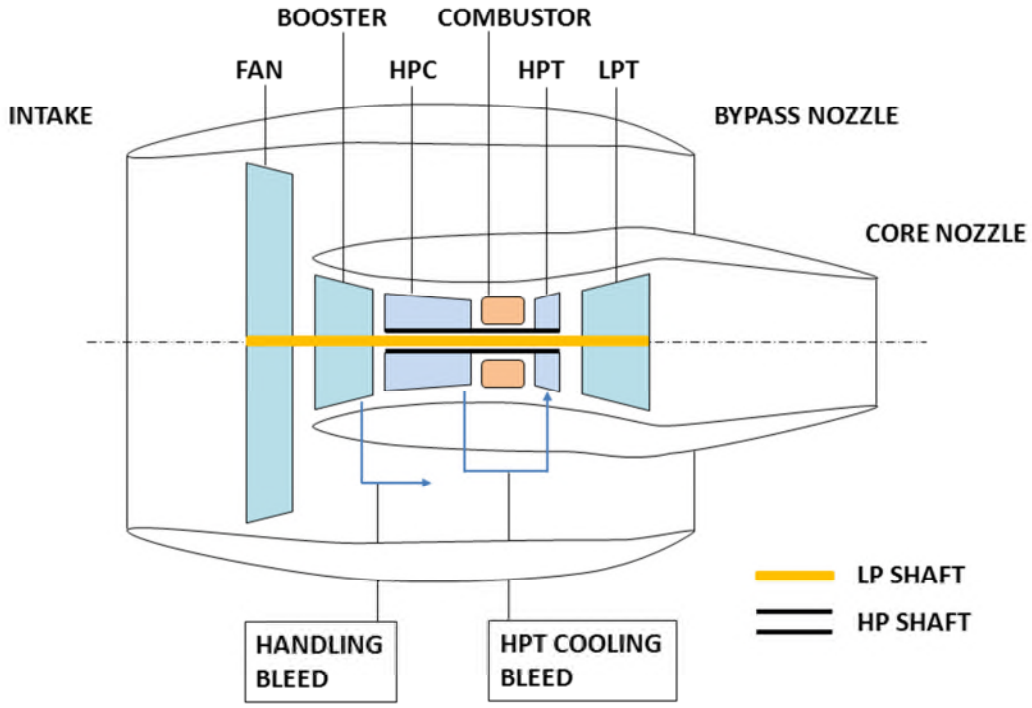

Figure 4-1: Typical two-spool high bypass turbofan engine configuration

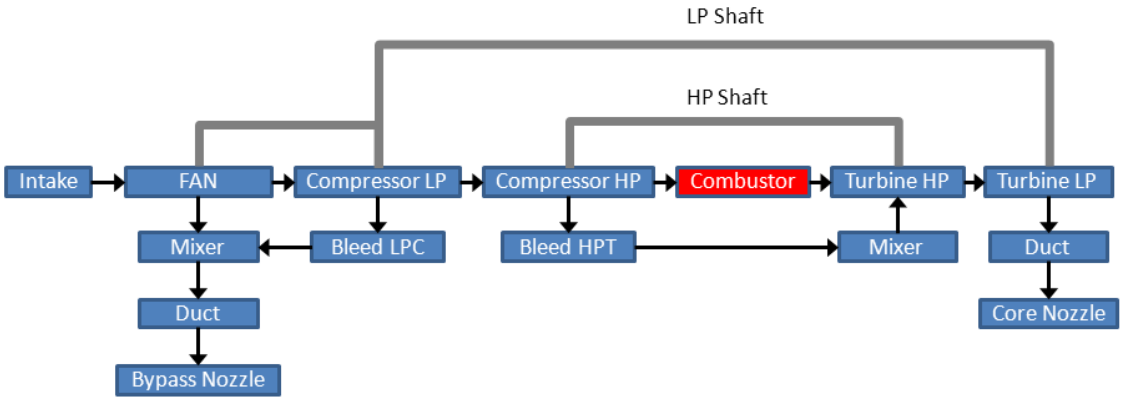

Figure 4-2: Basic engine component data (Turbomatch)

4.1.2 Engine Design Point Selection and Performance

As 'Design Point' one can define the particular point in the operating range of a gas turbine when the engine is running at the particular speed, pressure ratio and mass flow for which the engine components were designed [91]. The design point of the CU2STF-LT, CU2STF-MT and CU2STF-HT engine model was selected to be at the Top Of Climb (TOC) with International Standard Atmosphere (ISA) conditions, at an altitude of 10668 meters and a Flight Mach Number of 0.8. Table 4-1, table 4-2 and table 4-3 show the engine specifications from the public domain. In order to model the engines in Turbomatch, some additional conditions had to be determined prior to performing the design point matching calculations. The engine intake mass flow (TOC mass flow) was determined according to the equation of continuity and the ideal gas law considering an inlet air flow with a Mach number in the range of 0.6 – 0.7 and an inlet area based on the fixed fan diameter as listed in table 1, table 2 and table 3 respectively [92]. In this case the continuity equation for the engine inlet mass flow W can be formulated as follows:

$$W = \rho \times c_0 \times A_0 \quad \textbf{(4-1)}$$

This is where ρ is the air density defined as:

$$\rho = \frac{p_0}{R \times t_0} \quad \textbf{(4-2)}$$

With p_0 as the ambient pressure, R as gas constant for dry air and t_0 as ambient temperature at design point conditions. Furthermore c_0 is the inlet flow velocity defined as:

$$c_0 = Ma_0 \times \sqrt{\gamma \times R \times t_0} \quad \textbf{(4-3)}$$

This is with Ma_0 as the inlet Mach number, γ as isentropic exponent, R as gas constant for dry air and t_0 as ambient temperature. The inlet area A_0 is given as follows:

$$A_0 = \pi \times r^2 \quad \textbf{(4-4)}$$

This is where the radius r^2 is derived from the fixed fan diameter.

Using the described approach the inlet mass flow was calculated to W=179 kg/s. These assumptions and the listed engine specifications are also supported by the literature reference [39] and [93].

The design point TET was adjusted based on the overall pressure ratio (OPR) and the net thrust at the design point. In addition, for typical turbofan engines as depicted in figure 4-1 there are three main design parameters which affect the engine thrust and specific fuel consumption (SFC). Those are bypass ratio (BPR), overall pressure ratio (OPR) and turbine entry temperature (TET). The overall pressure ratio (OPR) and the thrust at the Top Of Climb were the basis for the determination of the engine design point parameters for turbine entry temperature (TET) and bypass ratio (BPR). The optimum fan pressure ratio (FPR) was determined according to the calculated TET, OPR and BPR at design point conditions with Flight Mach Number of 0,8 [94]. To avoid design and handling problems a FPR lower than the optimum was chosen.

In all below described characteristic maps the mass flow is given as Corrected Mass Flow which corresponds to a pressure and temperature correction to Sea Level Static (SLS) conditions. The Corrected Mass Flow (CMF) is given as follows:

$$Corrected\ Mass\ Flow = \frac{W\sqrt{\frac{T}{T_{SLS}}}}{\frac{P}{P_{SLS}}} \quad \textbf{(4-5)}$$

W is the actual mass flow, and T and P are the actual temperature and pressure respectively. Temperature and pressure are corrected to Sea Level Standard and ISA conditions as follows:

$$T_{SLS} = 288.15\ K \quad \textbf{(4-6)}$$

$$P_{SLS} = 101.325\ Pa \quad \textbf{(4-7)}$$

A tabular summary of the engine specifications at design point conditions (Top Of Climb) and take-off conditions for each engine variant is listed in the following tables 4-1, 4-2 and 4-3.

Table 4-1: Engine specification comparison CU2STF-LT (CFM56-5B6) [87]

Engine Model Take-off Performance Flight Mach Number: Ma 0,0 Altitude: 0 m ISA conditions + 30°C				
	Unit	**Engine specification**	**CU Turbomatch**	**Delta**
T/O thrust	N	104500	104510	0.01%
T/O mass flow	kg/s	382.8	377.9	-1.30%
T/O BPR	-	5.90	5.87	-0.51%
T/O TET	K	-	1500	-
T/O fuel flow	kg/s	-	0.920	-
Engine Model Design Point Performance (Top Of Climb) **Flight Mach Number: Ma 0,8 Altitude: 10670 m ISA conditions**				
	Unit	**Engine specification**	**CU Turbomatch**	**Delta**
TOC thrust	N	25040	25075	0.14%
TOC mass flow	kg/s	-	179.0	-
TOC SFC	g/kN s	-	16.65	-
TOC BPR	-	-	5.45	-
TOC TET	K	-	1345	-
TOC OPR	-	32.6	32.6	0.00%
Fan diameter	m	1.73	-	-

Table 4-2: Engine specification comparison CU2STF-MT (CFM56-5B4) [87]

Engine Model Take-off Performance Flight Mach Number: Ma 0,0 Altitude: 0 m ISA conditions + 30°C				
	Unit	**Engine specification**	**CU Turbomatch**	**Delta**
T/O thrust	N	120100	120550	0.37%
T/O mass flow	kg/s	406.8	404.3	-0.62%
T/O BPR	-	5.70	5.60	-1.79%
T/O TET	K	-	1575	-
T/O fuel flow	kg/s	-	1.101	-
Engine Model Design Point Performance (Top Of Climb) **Flight Mach Number: Ma 0,8 Altitude: 10670 m ISA conditions**				
	Unit	**Engine specification**	**CU Turbomatch**	**Delta**
TOC thrust	N	25040	25075	0.14%
TOC mass flow	kg/s	-	179.00	-
TOC SFC	g/kN s	-	16.65	-
TOC BPR	-	-	5.45	-
TOC TET	K	-	1345	-
TOC OPR	-	32.6	32.6	0.00%
Fan diameter	m	1.73	-	-

Table 4-3: Engine specification comparison CU2STF-HT (CFM56-5B3) [87]

Engine Model Take-off Performance Flight Mach Number: Ma 0,0 Altitude: 0 m ISA conditions + 30°C				
	Unit	**Engine specification**	**CU Turbomatch**	**Delta**
T/O thrust	N	146800	147570	0.52%
T/O mass flow	kg/s	439.1	431.4	-1.78%
T/O BPR	-	5.40	5.30	-1.89%
T/O TET	K	-	1760	-
T/O fuel flow	kg/s	-	1.486	-
Engine Model Design Point Performance (Top Of Climb) **Flight Mach Number: Ma 0,8 Altitude: 10670 m ISA conditions**				
	Unit	**Engine specification**	**CU Turbomatch**	**Delta**
TOC thrust	N	28560	28254	-1.08%
TOC mass flow	kg/s	-	179.00	-
TOC SFC	g/kN s	-	16.91	-
TOC BPR	-	-	5.45	-
TOC TET	K	-	1440	-
TOC OPR	-	35.5	35.5	0.00%
Fan diameter	m	1.73	-	-

Table 4-4 below lists the most important engine model design point parameters of the major components and the respective efficiencies as used in the Turbomatch simulation code for the three different engine variants.

Table 4-4: Engine model design point parameter

Engine Design Point Parameter			
Parameter	**CU2STF-HT**	**CU2STF-MT**	**CU2STF-LT**
Fan Pressure Ratio	1.665	1.685	1.685
LPC Pressure Ratio	1.850	1.828	1.828
HPC Pressure Ratio	11.53	10.59	10.59
Fan Efficiency	0.900	0.895	0.895
LPC Efficiency	0.880	0.880	0.880
HPT Cooling Air Flow [%]	14.0	14.0	14.0
Combustion Efficiency	0.999	0.999	0.999
Combustion Pressure Loss	0.06	0.06	0.06
HPT Efficiency	0.90	0.90	0.90
LPT Efficiency	0.92	0.92	0.92
HPC Surge Margin	0.85	0.85	0.85
HPC Efficiency	0.875	0.875	0.875

4.1.3 Engine Off-Design Performance

The engine off-design performance refers to the operation of the engine at varying conditions such as different altitudes, different ambient temperatures and different Mach numbers. In order to investigate the influence of these parameters on the engine model performance, two series of parametric analyses have been carried out, where the first analysis uses the altitude as variable parameter and the second analysis uses the ambient temperature (ISA deviation) as variable parameter. In order to exemplify the effects of the off-design performance analysis, figure 4-3 illustrates an ideal gas turbine cycle that comprises a compression process, a heat addition process and an expansion process.

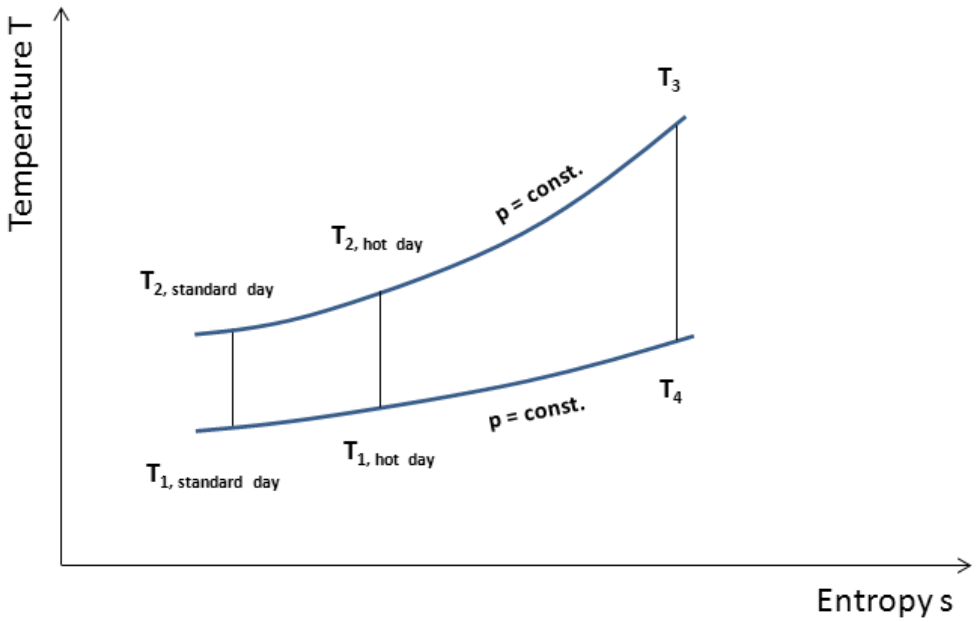

Figure 4-3: Ideal cycle and ambient temperature effects

Figure 4-4 shows the set of curves obtained for the SFC versus Mach number at different altitudes ranging from 0 m to 11000 m and figure 4-5 shows the curves for the net thrust versus Mach number at the same altitudes. For both analyses engine TET was kept constant at the take-off point value of 1500K and Mach numbers at sea level range from 0.4 to 0.8 while for the 0 m altitude scenario, Mach numbers from 0.0

to 0.8 are plotted. At higher altitudes (≥ 6000m), plots for Mach numbers below 0.4 have been omitted since those scenarios do not reflect feasible engine performance points.

Assuming a constant altitude, an increase in flight Mach number causes a linear increase in engine SFC as shown in figure 4-4, which is related to the reduction in propulsive efficiency. Also, SFC will improve with increase in altitude assuming a constant flight Mach number. At higher altitudes the ambient temperatures decreases (refer to figure 3-3) which leads to an improved thermal efficiency causing an improvement in SFC.

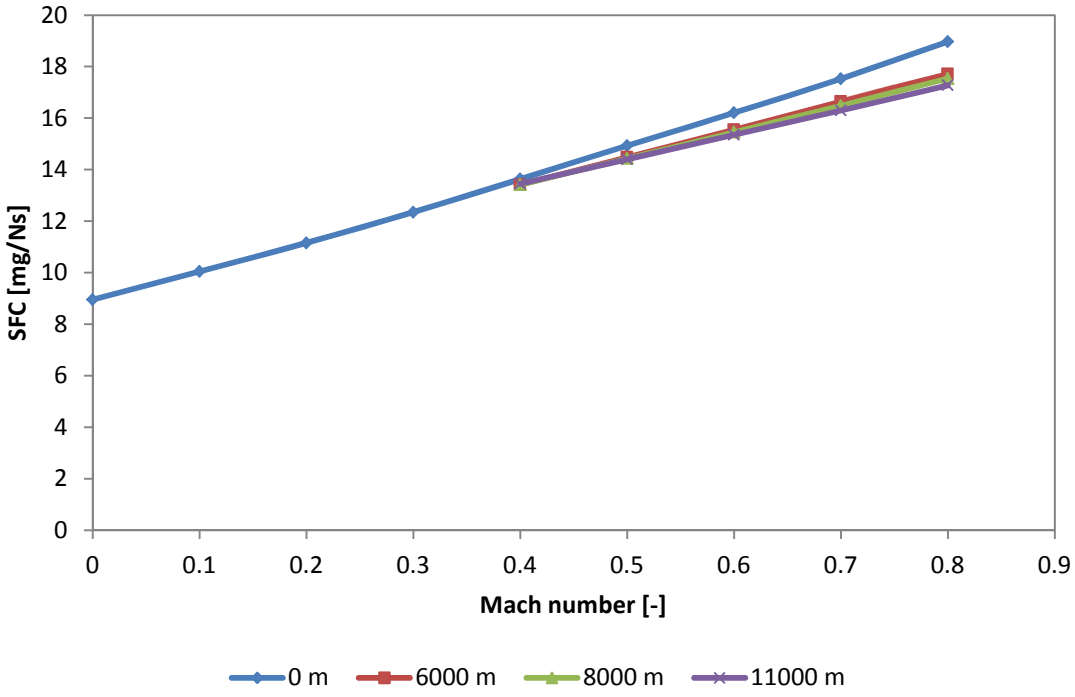

Figure 4-4: CU2STF-LT – SFC vs. Mach number at constant TET (1500K)

As illustrated in figure 4-5, an increase in flight Mach number at constant altitude reduces engine net thrust. The flight Mach number or velocity has three major effects on the engine net thrust performance. Firstly, an increase in velocity raises the incoming air momentum flow (momentum drag). Assuming a constant gross thrust, an increase in momentum drag leads to a net thrust decay. Secondly, an increase in velocity increases the exhaust nozzle pressure ratio and causes an inlet pressure rise,

called ram compression. The inlet pressure rise consequently causes an increase in air density and inlet mass flow leading to a net thrust increase. Thirdly, at higher velocity a temperature rise at the fan inlet occurs which is related to the isentropic relationship of static and total temperature. Assuming constant TET and shaft rotational speed, this causes a decrease in net thrust. For lower flight Mach numbers up to 0.3 the momentum drag is predominant while the influence of ram compression and inlet temperature rise will come into effect at Mach numbers above 0.3.

The altitude also affects the engine net thrust performance. As air density and pressure decrease with increasing altitude a reduction in engine mass flow and engine pressure ratio is observed. However, the lower ambient temperature at altitude leads to an increased ratio of TET and inlet temperature which positively affects the engine thrust and offsets the thrust decay at higher altitudes.

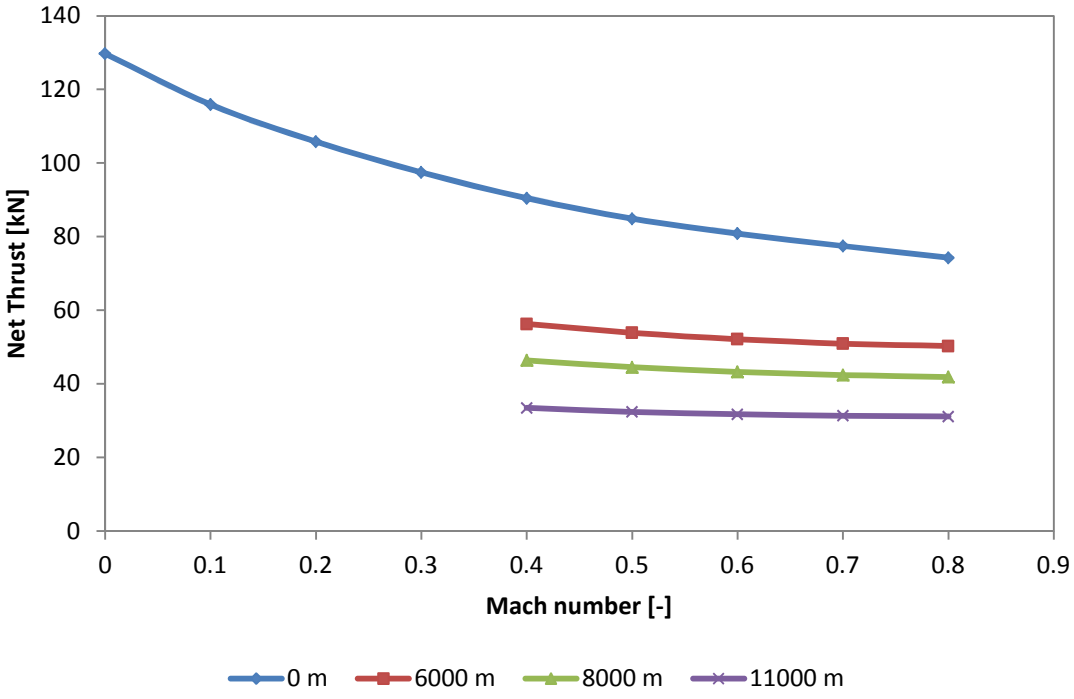

Figure 4-5: CU2STF-LT – Net thrust vs. Mach number at constant TET (1500K)

Figure 4-6 shows the set of curves obtained for the net thrust versus TET at different ambient temperatures ranging from ISA -30 to ISA +30 and figure 4-7 shows the curves for the SFC versus TET at the same ambient temperatures. Sea Level Static (SLS)

conditions with an altitude of 0 m and a Mach number of 0.0 apply to both analyses and the lower TET limit was kept at 1200K and the upper TET limit at 1800K, which is close to the take-off condition.

As TET increases, the thermal efficiency of the engine improves which consequently causes engine SFC to improve. At the same time, the propulsive efficiency of the engine degrades with increasing TET. The lowest points of the curves in figure 4-7 represent the highest overall engine efficiency and thus lowest SFC. A further increase in engine TET then causes a further degradation of propulsive efficiency which in turn exceeds the effects of increased thermal efficiency and leads to an increase in SFC. At constant engine TET, an increase in ambient temperature causes engine net thrust to decrease. On the other hand, at constant ambient temperature conditions, an increase in engine TET causes the net thrust to increase. Hotter ambient conditions require more work to be extracted from the compressor as illustrated in figure 4-3, where the inlet temperature conditions move from $T_{1,\ standard\ day}$ to $T_{1,\ hot\ day}$. However, since turbine work remains constant, the difference between turbine work and compressor work reduces and net thrust will decrease. This means, if engine TET is kept constant, the net thrust will drop. In order to compensate for the increased compressor work, the turbine has to produce more work and thus the engine TET has to be increased to maintain the same level of thrust.

Another effect that causes net thrust to drop with increasing ambient temperature conditions is related to the operating conditions of the compressor. The corrected rotational speed of the compressor, which is defined as speed N over root T, will decrease with hotter ambient temperatures when constant shaft speed is assumed. This results in the compressor operating at a lower compressor pressure ratio and lower corrected mass flow compared to standard ambient conditions.

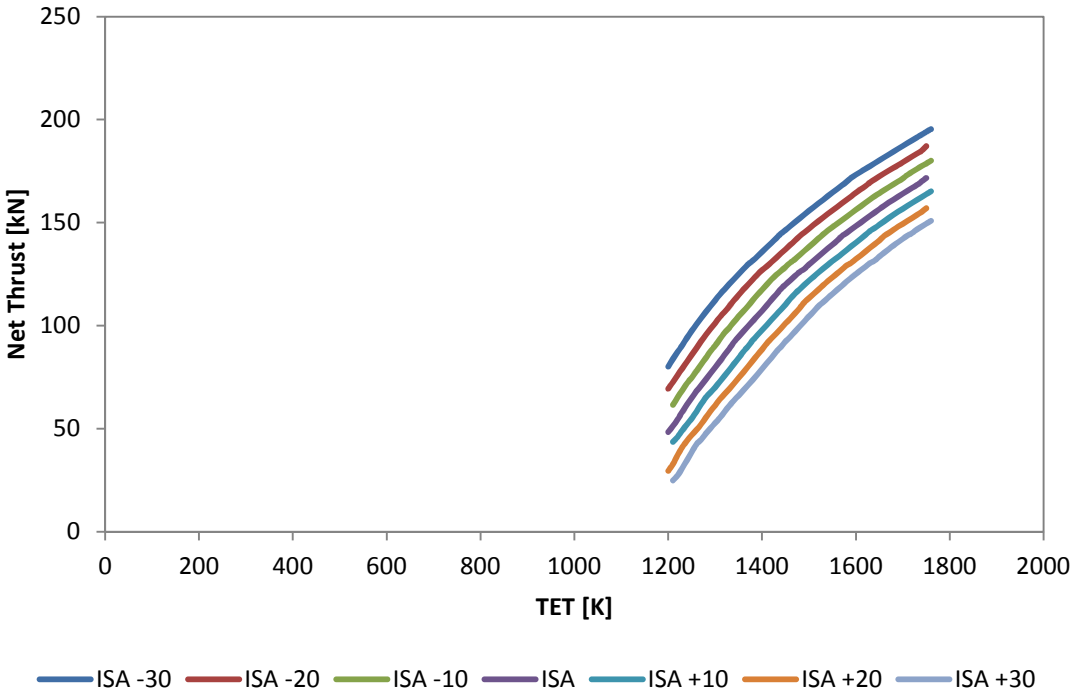

Figure 4-6: CU2STF-LT – Net thrust vs. TET at SLS conditions

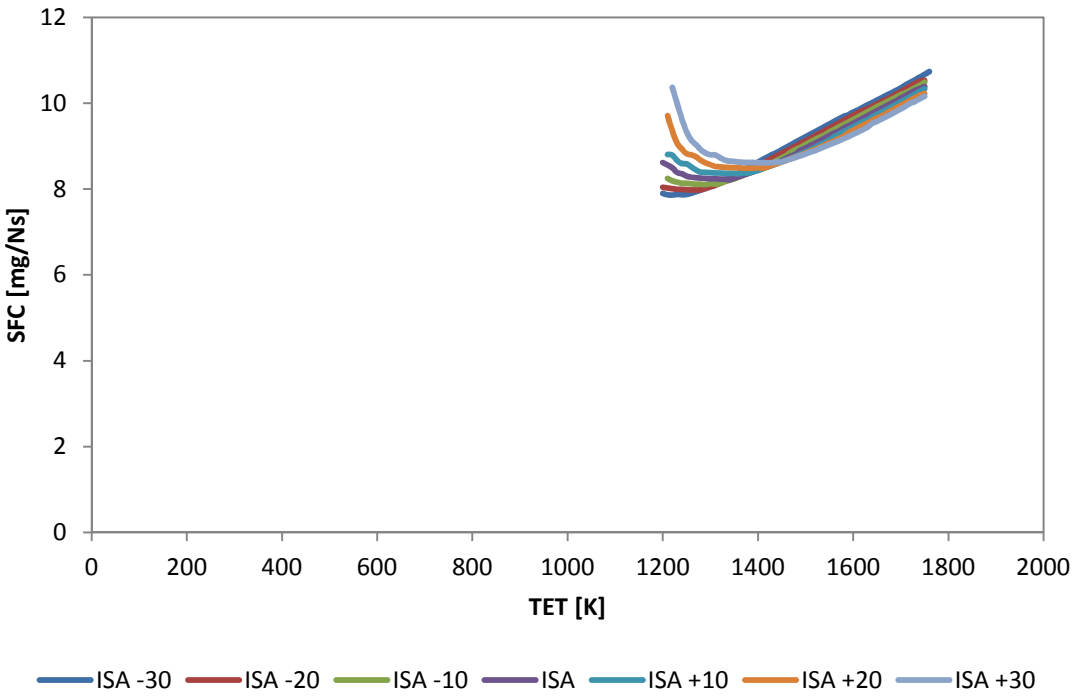

Figure 4-7: CU2STF-LT – SFC vs. TET at SLS conditions

Figures 4-8 to 4-11 show the same set of result plots for the medium thrust engine variant, namely CU2STF-MT. The results of the engine SFC performance correspond to the concurrent increase in TET which was necessary to achieve the desired increase in net thrust.

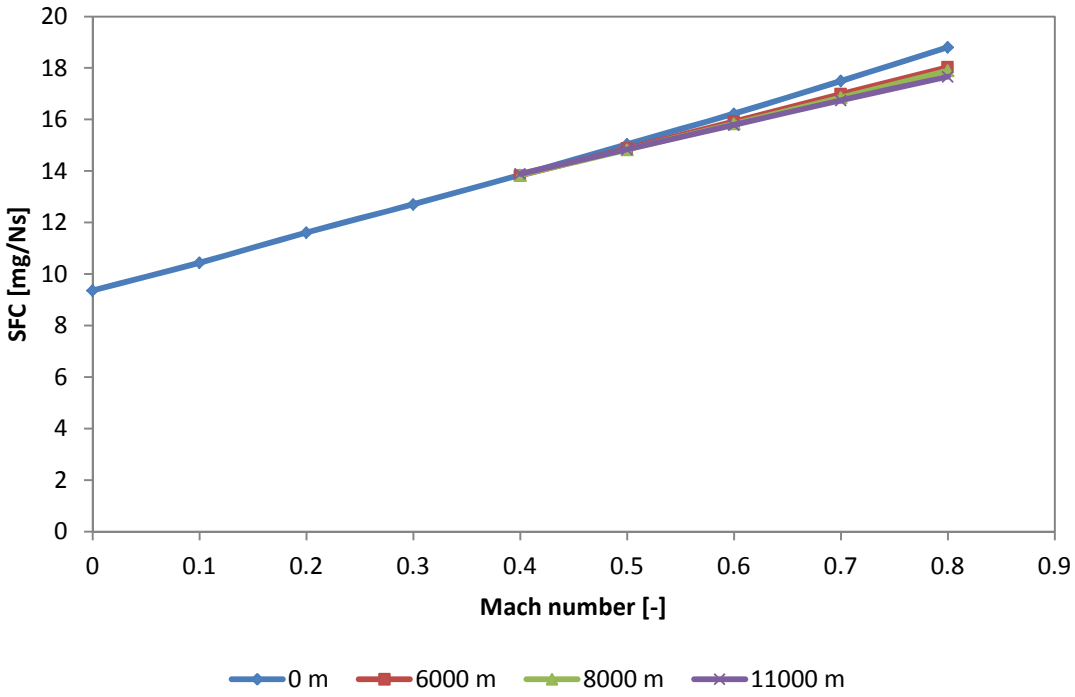

Figure 4-8: CU2STF-MT – SFC vs. Mach number at constant TET (1575K)

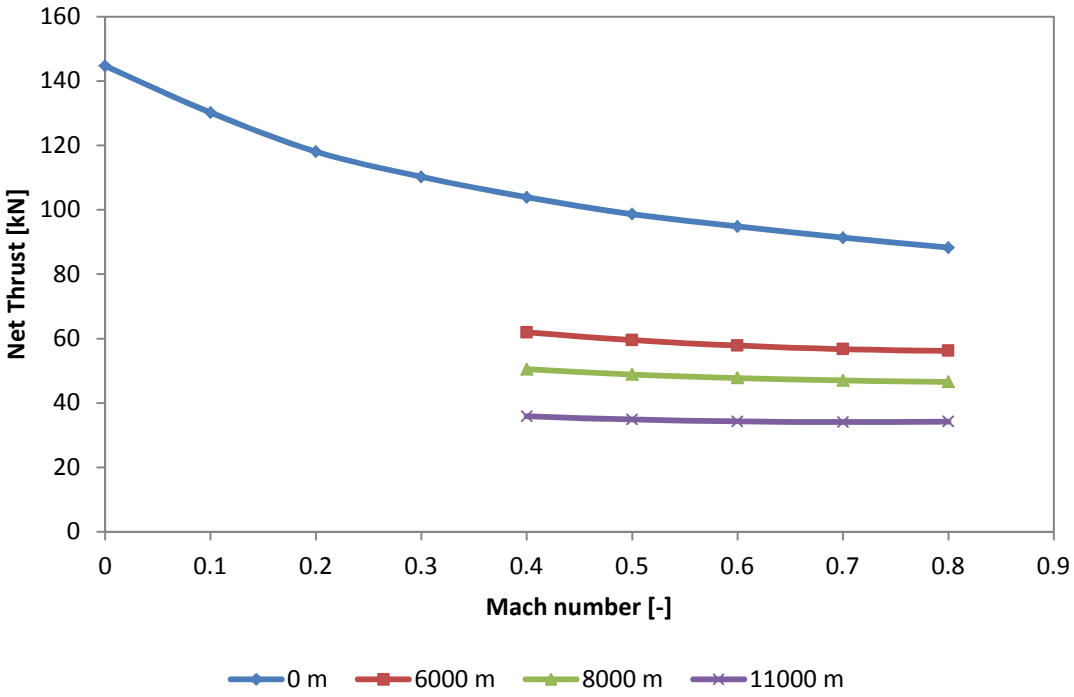

Figure 4-9: CU2STF-MT – Net thrust vs. Mach number at constant TET (1575K)

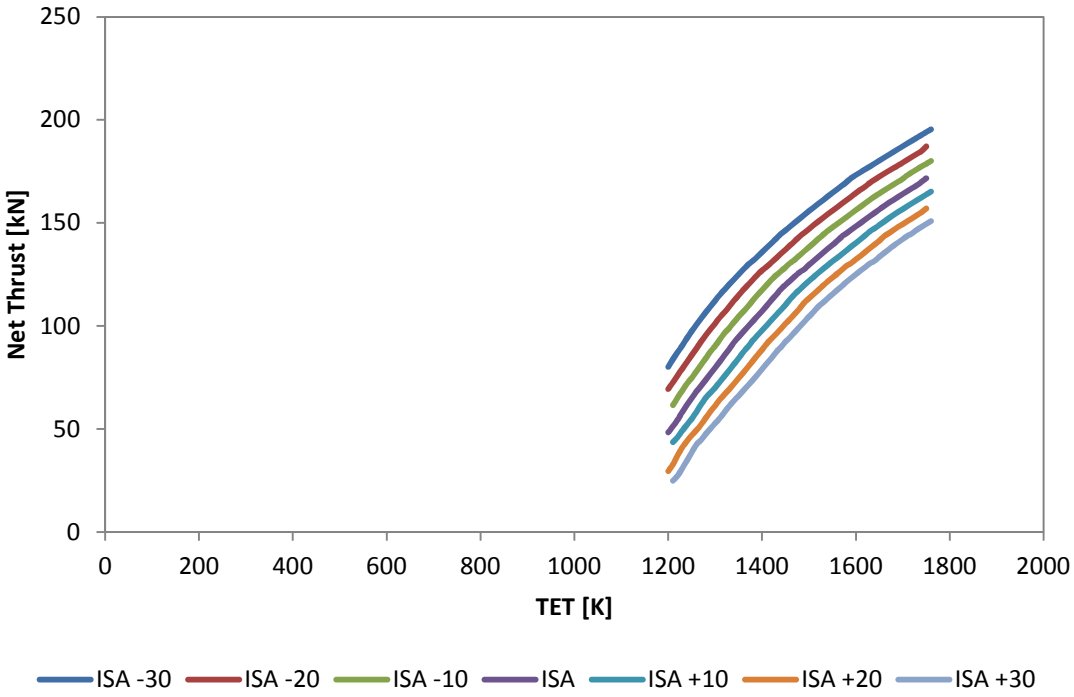

Figure 4-10: CU2STF-MT – Net thrust vs. TET at SLS conditions

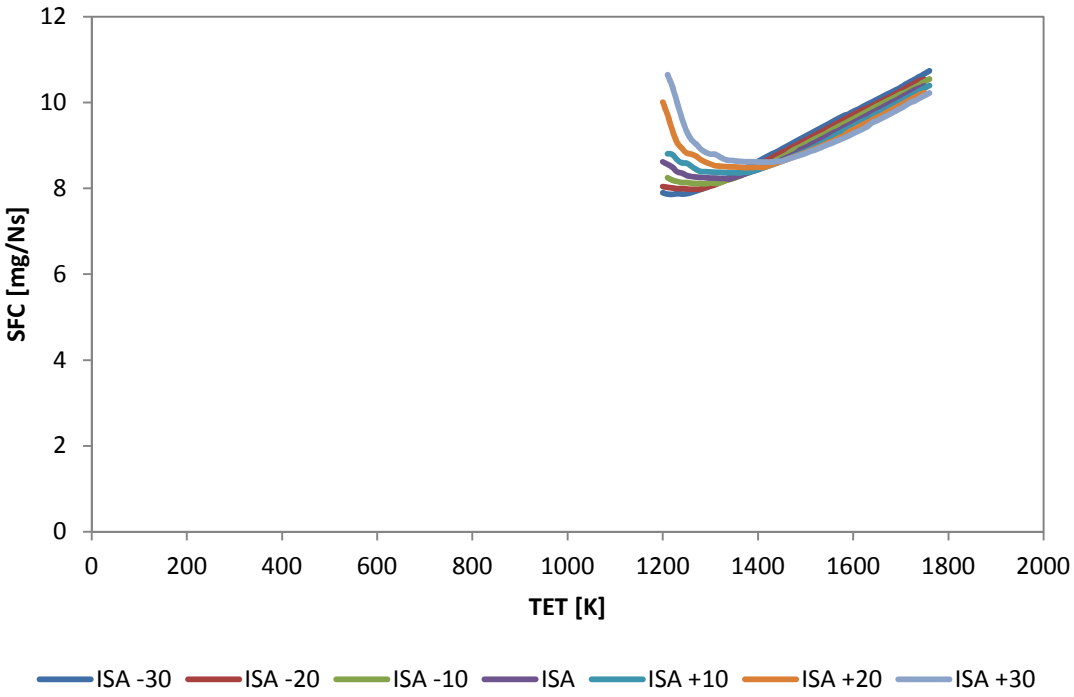

Figure 4-11: CU2STF-MT – SFC vs. TET at SLS conditions

Lastly, figures 4-12 to 4-15 show the result plots for the high thrust engine variant, namely CU2STF-HT. These results also follow the trends of the medium thrust engine results so that the further rise in engine TET leads to an increase of net thrust output and in parallel to a further increase of the engine SFC.

The off-design performance simulations for all three engine variants yielded in general the expected engine characteristics in terms of specific fuel consumption and net thrust, when variations in altitude, flight Mach number, ambient temperature and turbine entry temperature (TET) are implemented. References [41], [46] and [39] provide in-depth descriptions of the effects of various parameters, such as altitude, turbine entry temperature etc. on gas turbine performance. They also elaborate the typical trade-offs between thermal efficiency and propulsive efficiency for high bypass ratio turbofan engines.

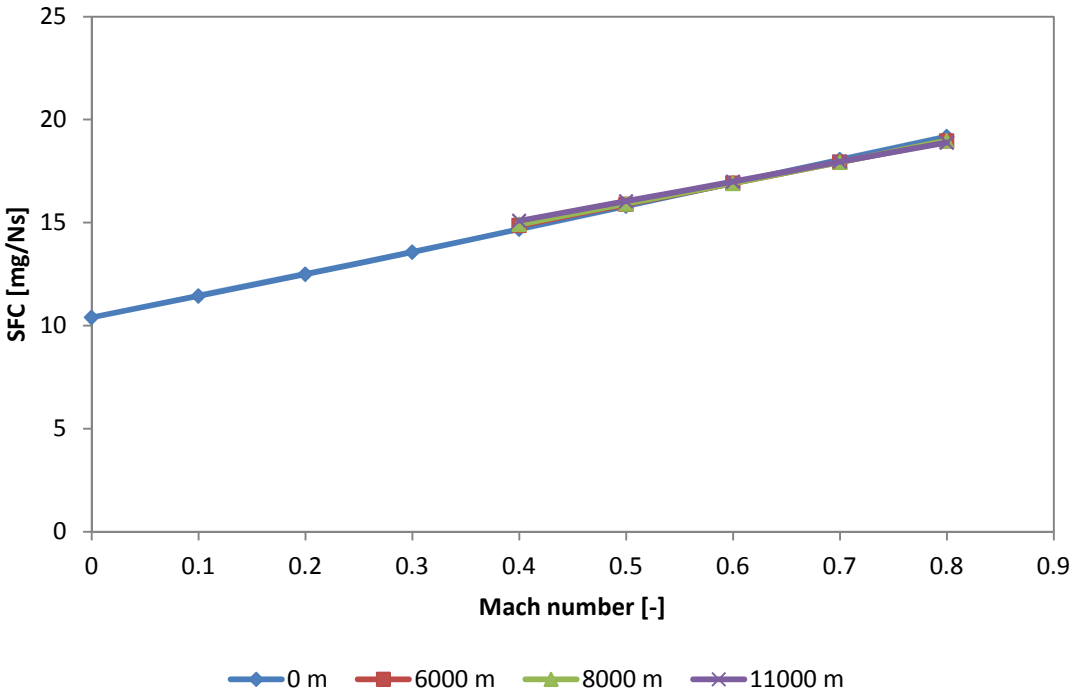

Figure 4-12: CU2STF-HT – SFC vs. Mach number at constant TET (1760K)

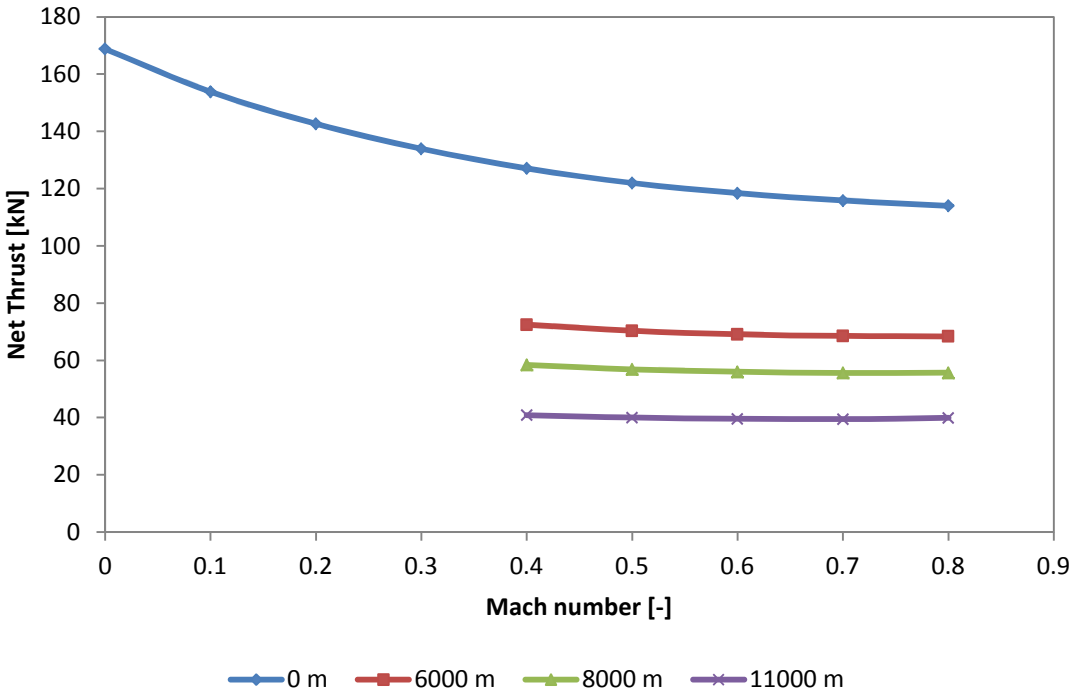

Figure 4-13: CU2STF-HT – Net thrust vs. Mach number at constant TET (1760K)

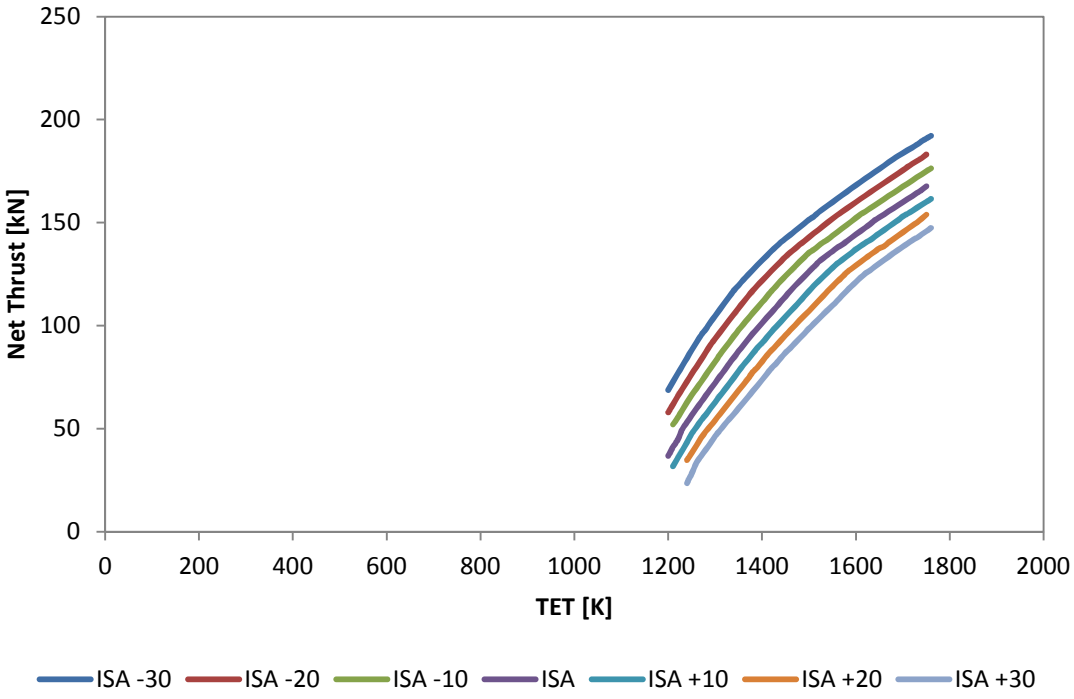

Figure 4-14: CU2STF-HT – Net thrust vs. TET at SLS conditions

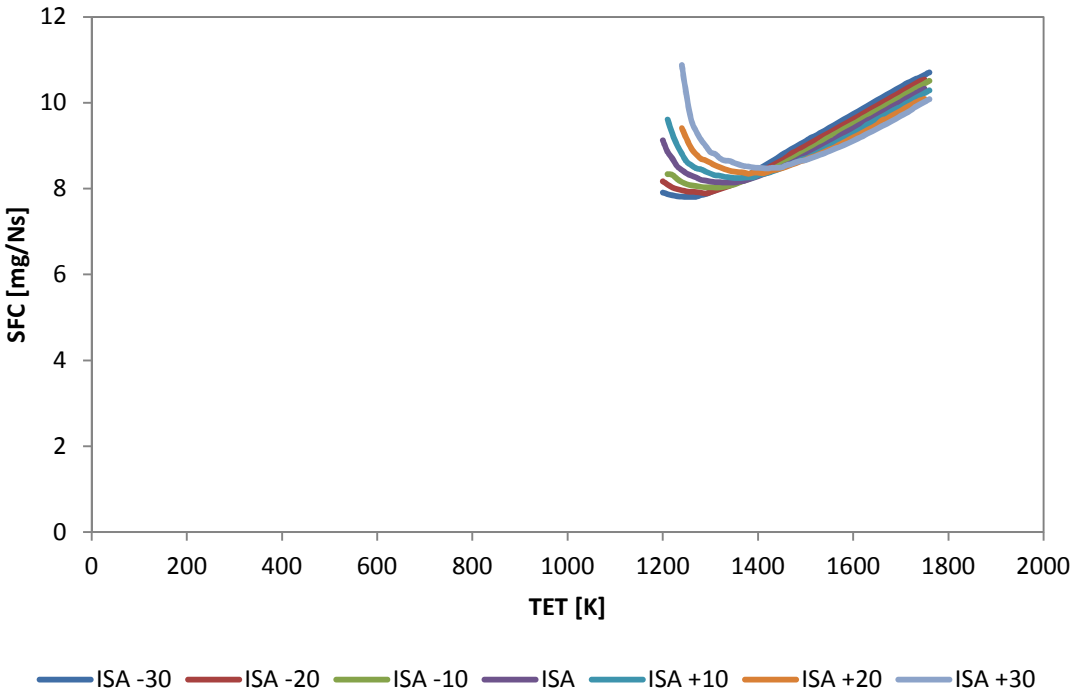

Figure 4-15: CU2STF-HT – SFC vs. TET at SLS conditions

Figures 4-16, 4-17 and 4-18 show the characteristic maps (including running line, surge line and design point) of the CU2STF-LT engine fan, Low Pressure Compressor (LPC) and High Pressure Compressor (HPC) at TOC power settings. The engine component running line can be obtained by simulating a change in engine fuel flow which in turn causes a change in TET, rotational speed and consequently results in a change in engine mass flow and a shift of the operating point. Figure 4-17 shows the distinctive running line of the LPC which approaches the surge line at lower engine power settings thus requiring flow adjustments through a handling bleed as previously described. Figure 4-18 shows the distinctive running line of the HPC with the operating points moving in parallel to the surge line. In addition, the running line of a degraded HPC (dashed line) is shown for reference. The engine degradation analysis will be explained in subsection 4.1.4 in more detail. Figures 4-19 to 4-24 show the same characteristic maps for the CU2STF-MT and CU2STF-HT engine variant respectively.

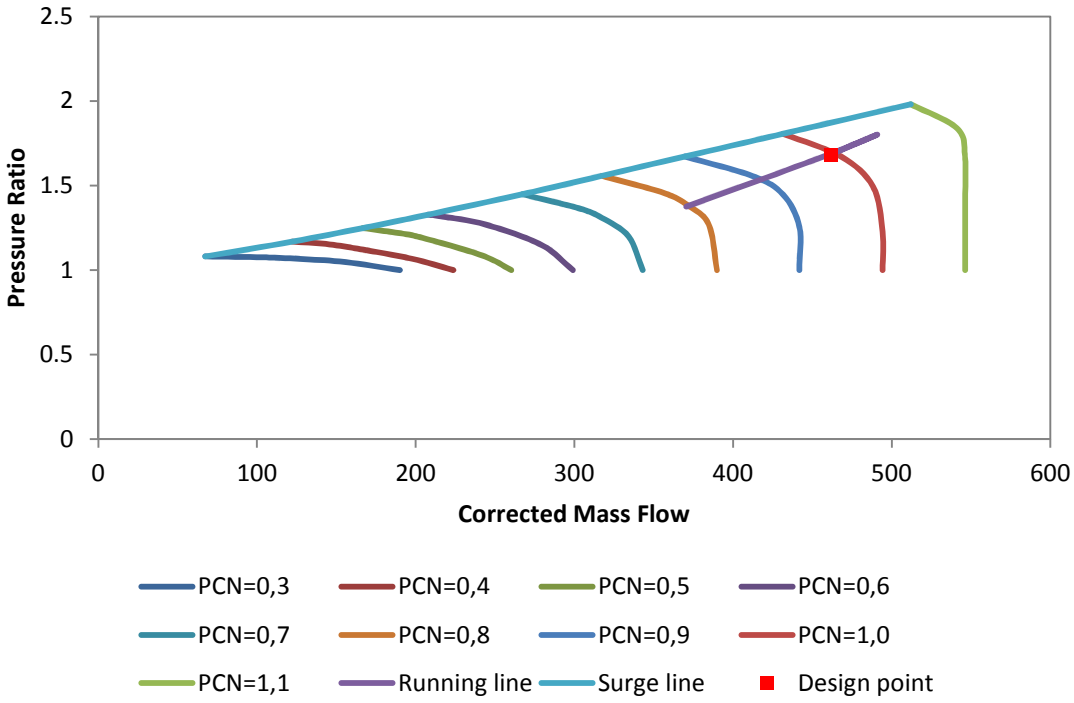

Figure 4-16: CU2STF-LT Fan map (running line at TOC)

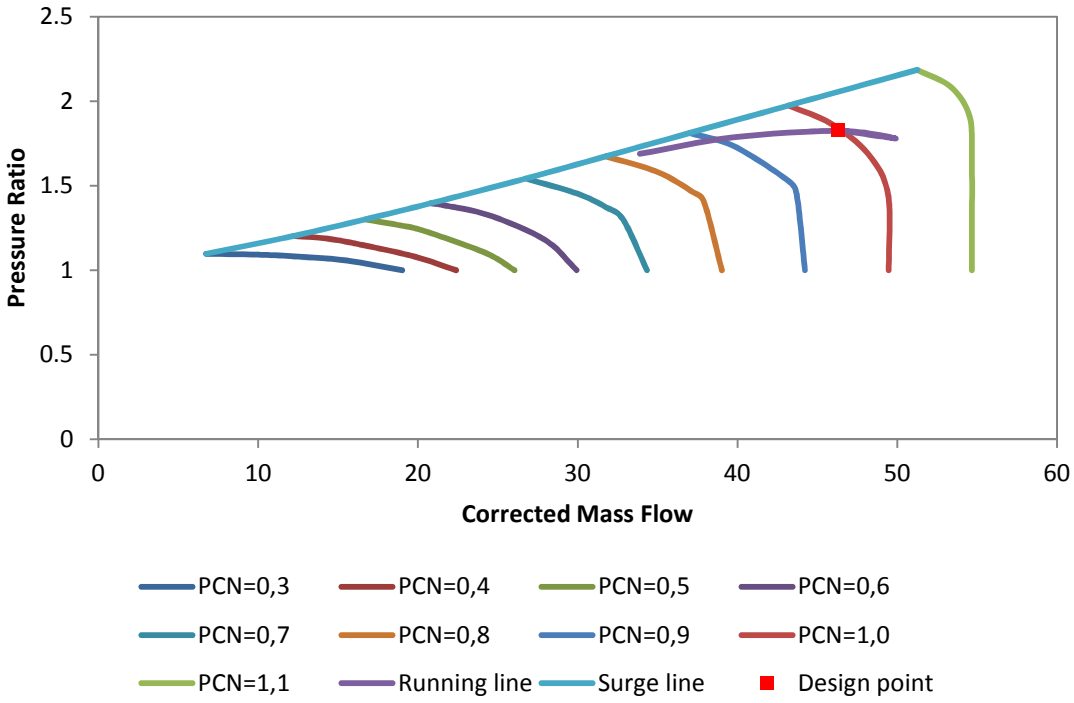

Figure 4-17: CU2STF-LT LPC map (running line at TOC)

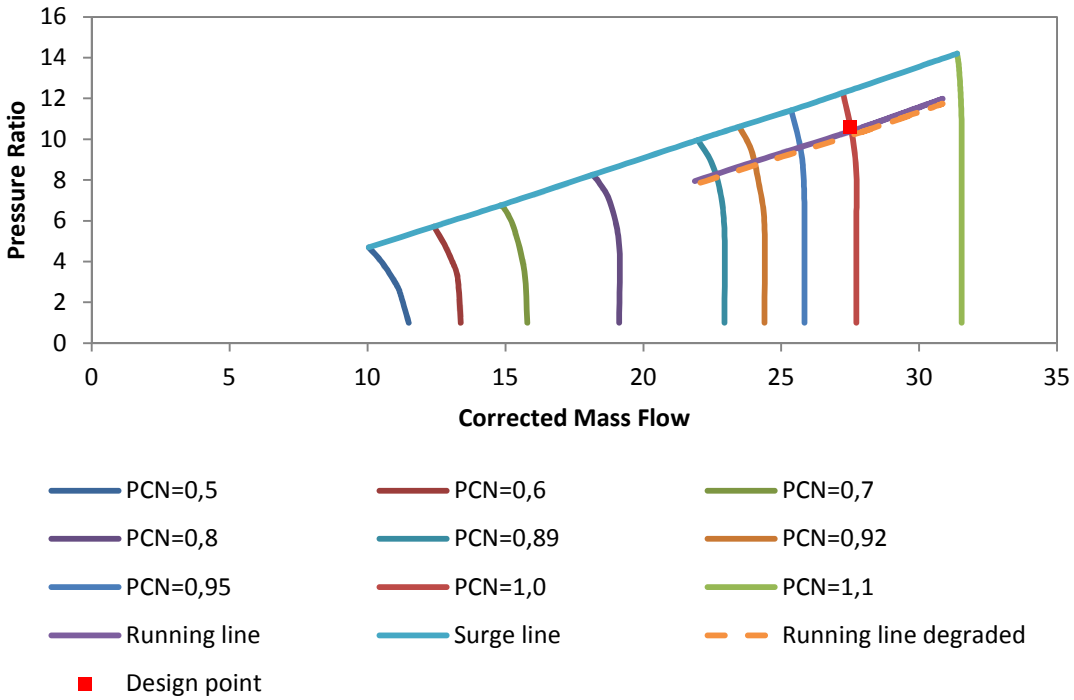

Figure 4-18: CU2STF-LT HPC map (running line at TOC)

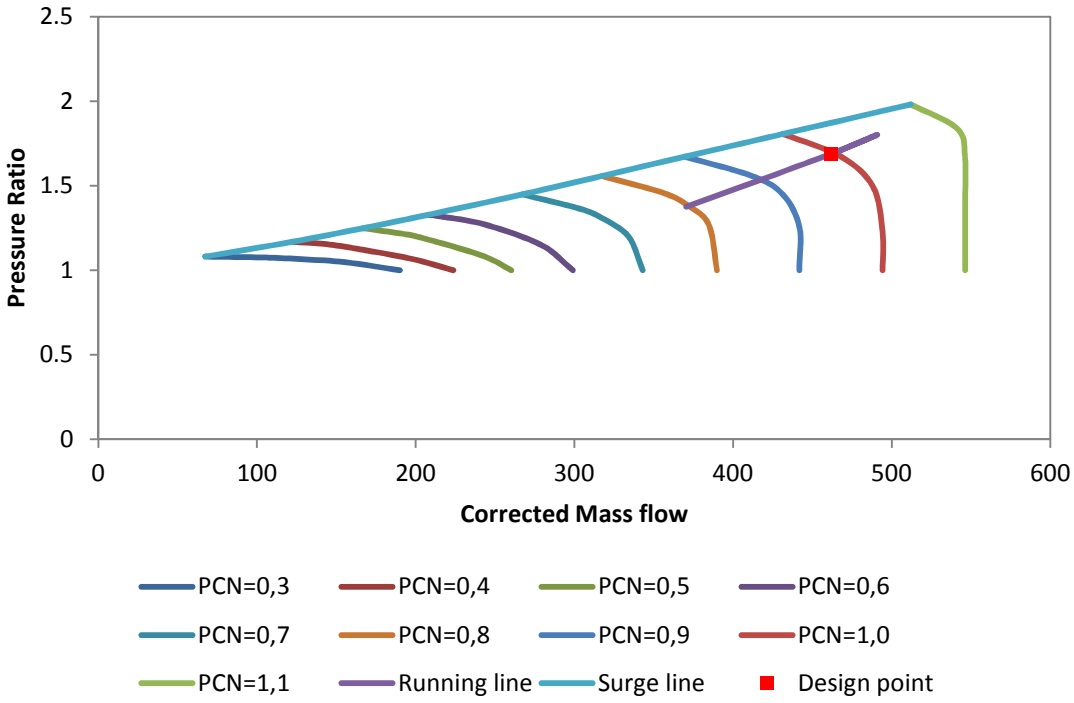

Figure 4-19: CU2STF-MT Fan map (running line at TOC)

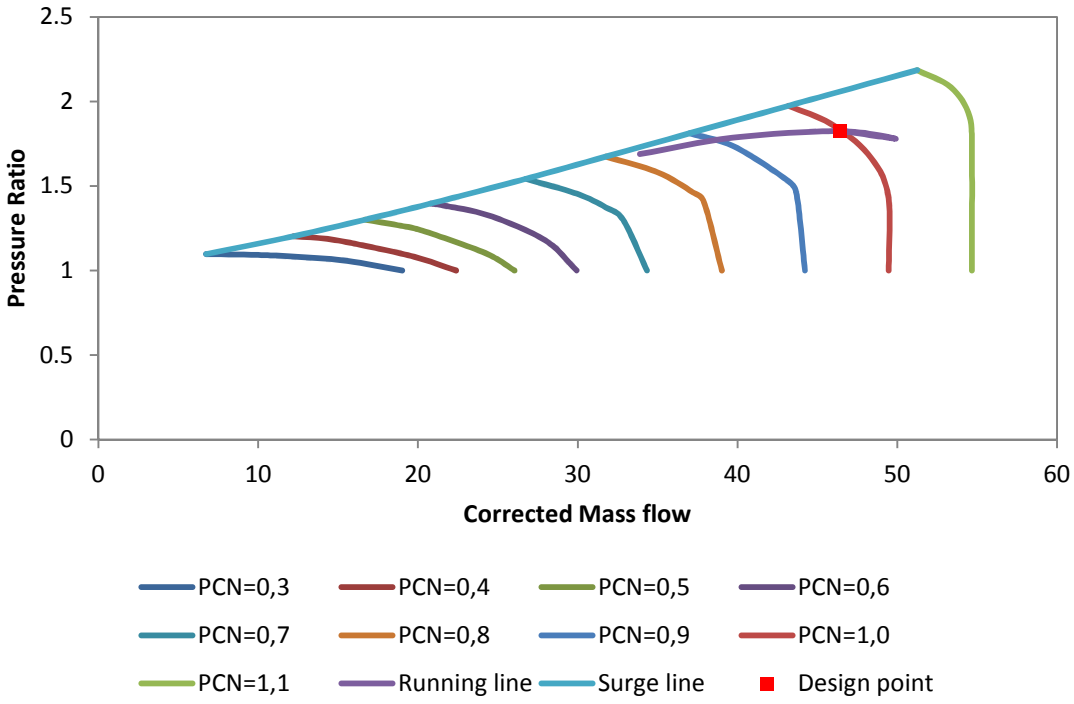

Figure 4-20: CU2STF-MT LPC map (running line at TOC)

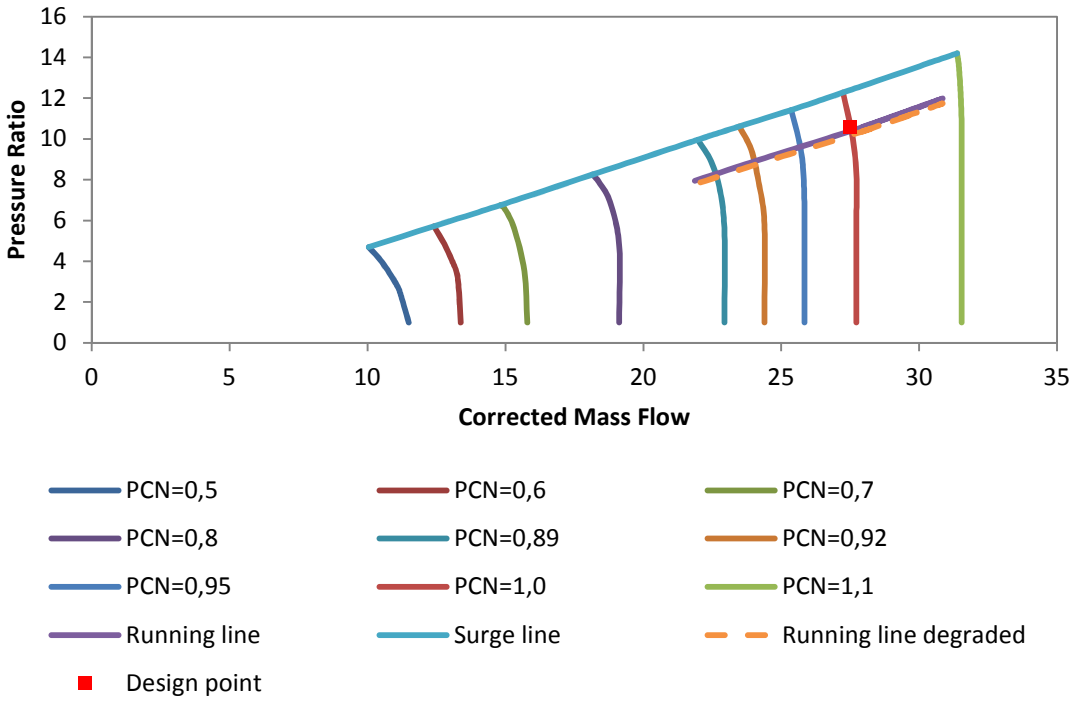

Figure 4-21: CU2STF-MT HPC map (running line at TOC)

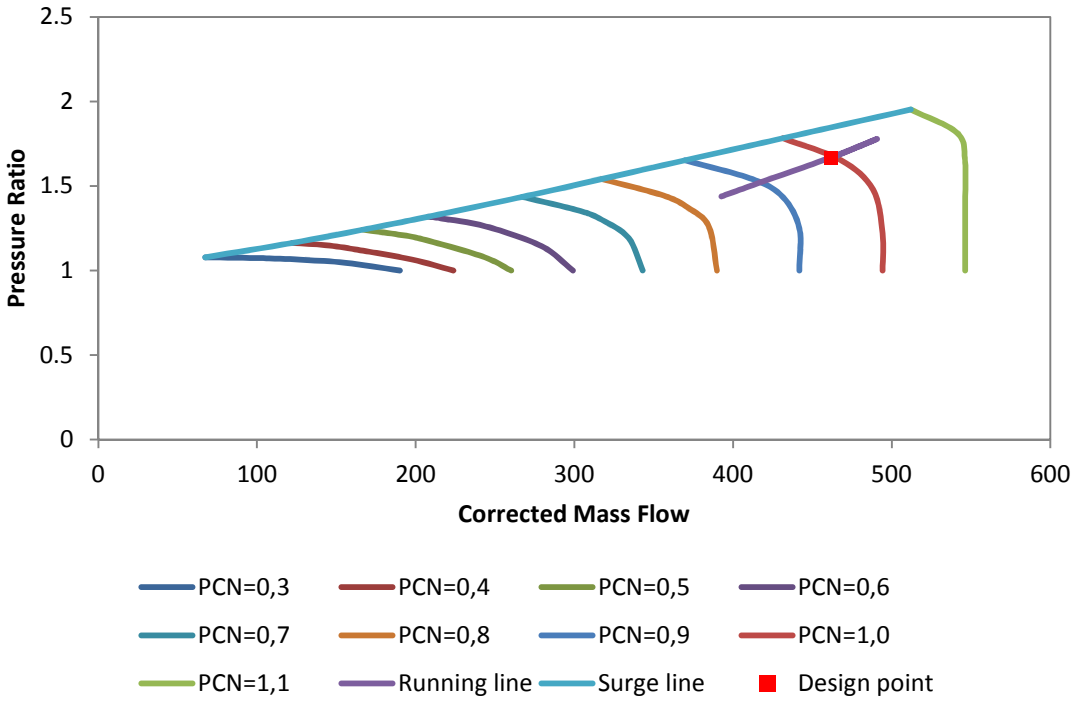

Figure 4-22: CU2STF-HT Fan map (running line at TOC)

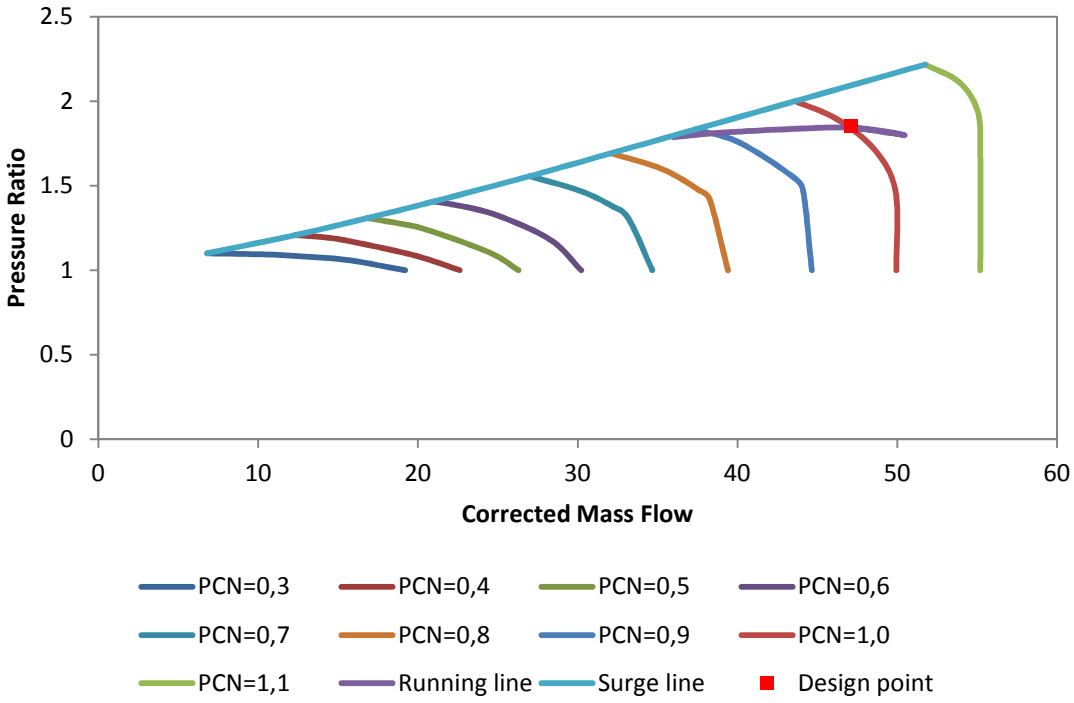

Figure 4-23: CU2STF-HT LPC map (running line at TOC)

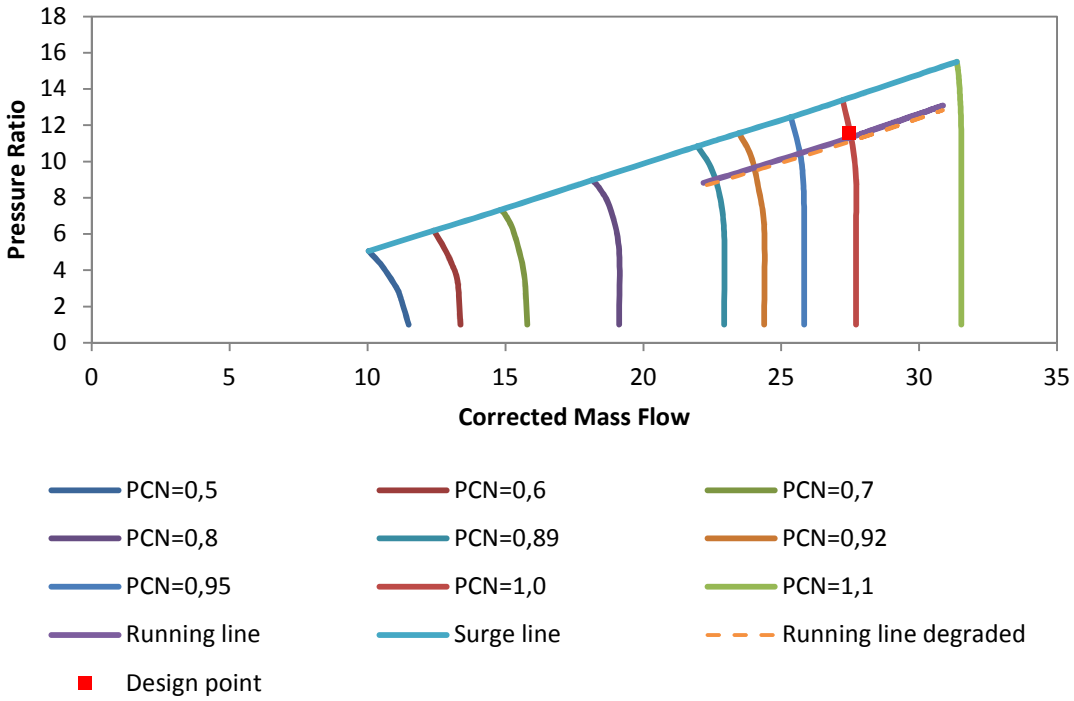

Figure 4-24: CU2STF-HT HPC map (running line at TOC)

It can also be noted that an increase in take-off thrust from the low thrust engine variant (104.5 kN T/O thrust) to the medium thrust engine variant (120.1 kN T/O thrust) requires a rise in turbine entry temperature (TET) of 5%. A further increase in thrust from the medium thrust engine variant to the highest thrust variant (146.8 kN T/O thrust) then requires a rise in TET of about 12%. Figure 4-25 shows the expected correlations between turbine and entry temperature (TET) and T/O thrust and between fuel flow and T/O thrust for all three engine variants.

However, it must be kept in mind that not only the TET was adjusted between the individual engine models but also changes to the pressure ratios of the Fan, the LPC and the HPC have been incorporated to match the engine design point and take-off conditions.

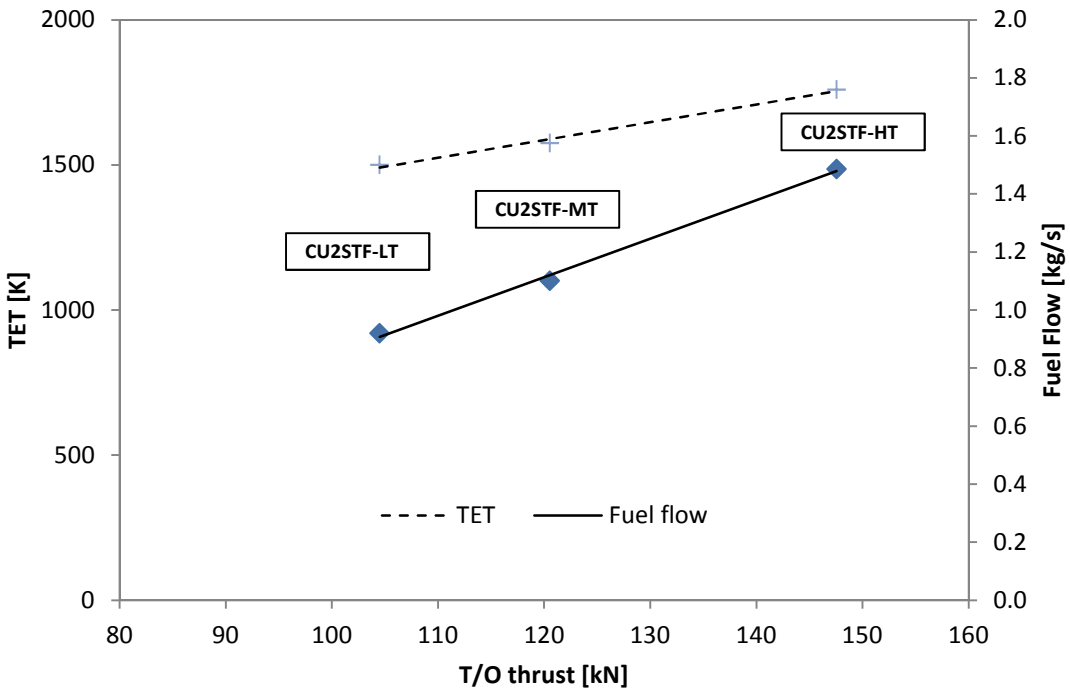

Figure 4-25: TET and Fuel Flow over T/O Thrust

4.1.4 Degraded Engine Performance

Based on the three created engine model variants, an additional degraded engine model has been implemented for each engine variant. To simulate the degraded engine performance in a simplified manner, specific engine component data has been arbitrarily changed in such a way that the engine performance characteristics will reflect those of a deteriorated engine. On the basis of the considerations made in section 2.4 and 2.5 the degradation was achieved by altering the following 4 engine component design parameters thus creating artificial engine performance deterioration:

1. High Pressure Compressor (HPC) Pressure Ratio
2. High Pressure Compressor (HPC) Efficiency
3. Combustion Efficiency
4. High Pressure Turbine (HPT) Efficiency

It must be noted that no adjustment of the flow capacity of the degraded components in relation to the design point values has been made which would cause a decrease in Corrected Mass Flow in turn. A decrease of the 4 above mentioned parameters due to degradation will cause the engine to be less efficient in producing the same amount of thrust than the clean baseline engine model would be. Lower efficiencies of the HPC, the Combustor and the HPT will require the turbine work to increase in order to compensate for the loss in compressor flow capacity and discharge pressure. Consequently, this is accompanied by an increase in engine fuel flow and specific fuel consumption. The increase in fuel flow then leads to an increase in TET.

Tables 4-5, 4-6 and 4-7 show the engine performance changes if a 2% degradation of the above mentioned engine component parameters is assumed. The design point TET for all three engine variants increases by more than 1.3% and the SFC increases by more than 4%. At take-off conditions the TET increases by at least 1.4% and the fuel flow increases by more than 4.4%. Figures 4-18, 4-21 and 4-24 in the previous section 4.1.2 also show the shift of the engine running line in the HPC map due to the degradation effects.

Table 4-5: CU2STF-LT degraded performance (2% degradation)

Engine Design Point Parameter degraded				
Parameter	**Degradation**	**Baseline**	**Degraded**	
HPC Pressure Ratio	-2%	10.59	10.37	
Combustion Efficiency	-2%	0.999	0.979	
HPT Efficiency	-2%	0.90	0.88	
HPC Efficiency	-2%	0.875	0.855	
Engine Model Design Point degraded				
Parameter	**CU Turbomatch**	**Degraded/Recovered**		**Delta [%]**
TOC thrust [N]	25075	25180		0.42%
TOC SFC [g/kN sec]	16.65	17.42		4.42%
TOC TET [K]	1345	1365		1.47%
Engine Model Take-Off degraded				
	CU Turbomatch	**Degraded/Recovered**		**Delta [%]**
T/O thrust [N]	104510	104430		-0.08%
T/O TET [K]	1500	1525		1.64%
T/O fuel flow [kg/s]	0.920	0.972		5.35%

Table 4-6: CU2STF-MT degraded performance (2% degradation)

Engine Design Point Parameter degraded				
Parameter	**Degradation**	**Baseline**	**Degraded**	
HPC Pressure Ratio	-2%	10.59	10.37	
Combustion Efficiency	-2%	0.999	0.979	
HPT Efficiency	-2%	0.90	0.88	
HPC Efficiency	-2%	0.875	0.855	
Engine Model Design Point degraded				
Parameter	**CU Turbomatch**	**Degraded/Recovered**		**Delta [%]**
TOC thrust [N]	25075	25180		0.42%
TOC SFC [g/kN s]	16.65	17.42		4.42%
TOC TET [K]	1345	1365		1.47%
Engine Model Take-Off degraded				
Parameter	**CU Turbomatch**	**Degraded/Recovered**		**Delta [%]**
T/O thrust [N]	120550	121050		0.41%
T/O TET [K]	1575	1605		1.87%
T/O fuel flow [kg/s]	1.101	1.169		5.82%

Table 4-7: CU2STF-HT degraded performance (2% degradation)

Engine Design Point Parameter degraded				
Parameter	**Degradation**	**Baseline**	**Degraded**	
HPC Pressure Ratio	-2%	11.53	11.30	
Combustion Efficiency	-2%	0.999	0.979	
HPT Efficiency	-2%	0.90	0.88	
HPC Efficiency	-2%	0.875	0.855	
Engine Model Design Point degraded				
Parameter	**CU Turbomatch**	**Degraded/Recovered**		**Delta [%]**
TOC thrust [N]	28254	28502		0.87%
TOC SFC [g/kN s]	16.91	17.68		4.36%
TOC TET [K]	1440	1460		1.37%
Engine Model Take-Off degraded				
Parameter	**CU Turbomatch**	**Degraded/Recovered**		**Delta [%]**
T/O thrust [N]	147570	147160		-0.28%
T/O TET [K]	1760	1785		1.40%
T/O fuel flow [kg/s]	1.486	1.555		4.44%

For figures 4-5 to 4-7, it must be noted that the net thrust values at TOC and T/O achieved after recovery of the degradation condition were matched as close as possible to the initial CU Turbomatch model values. It can be seen that, depending on the engine running point (TOC or T/O) and the engine variant, these matched net thrust values may be slightly lower or slightly higher than the initial values of the non-degraded engine model.

In figure 4-26 the engine TET is plotted over the net thrust range at take-off conditions (Mach number = 0). An increase in TET can be observed over the take-off thrust range for the degraded engine configuration compared to the clean configuration. Figure 4-27 shows the peak take-off TET for the clean, the degraded and the derated (15% take-off thrust reduction) engine configuration at ISA+30°C conditions. Thrust reduction reduces take-off TET by approximately 4% for the CU2STF-LT, by 5.7% for the CU2STF-MT and by about 7.9% for the CU2STF-HT.

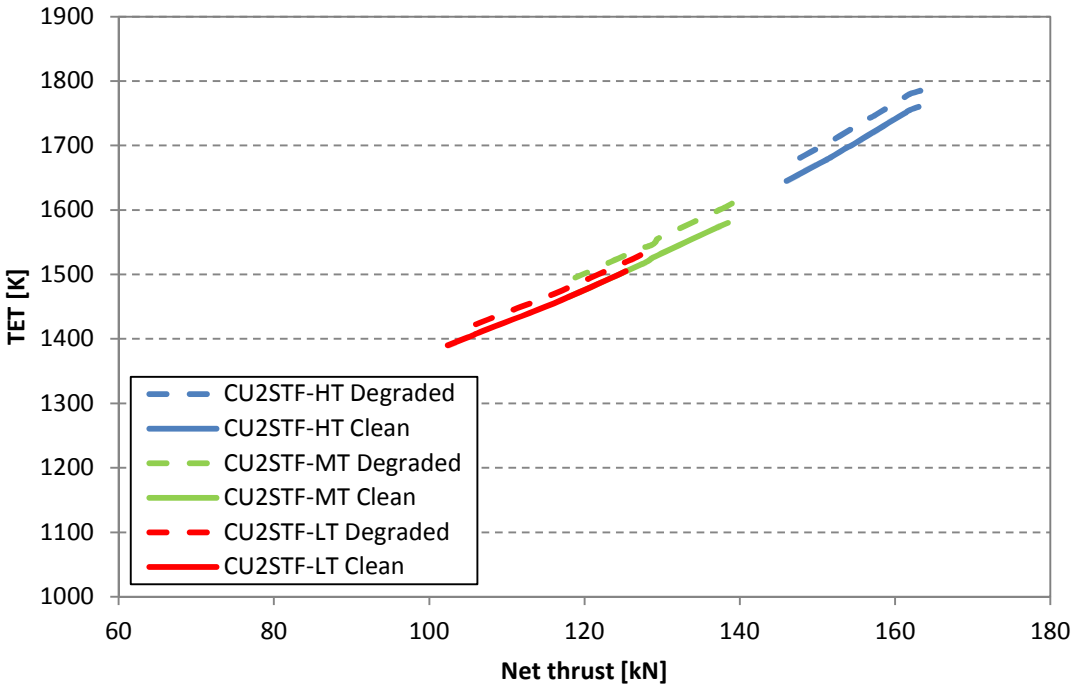

Figure 4-26: TET over net thrust at T/O conditions (Ma=0)

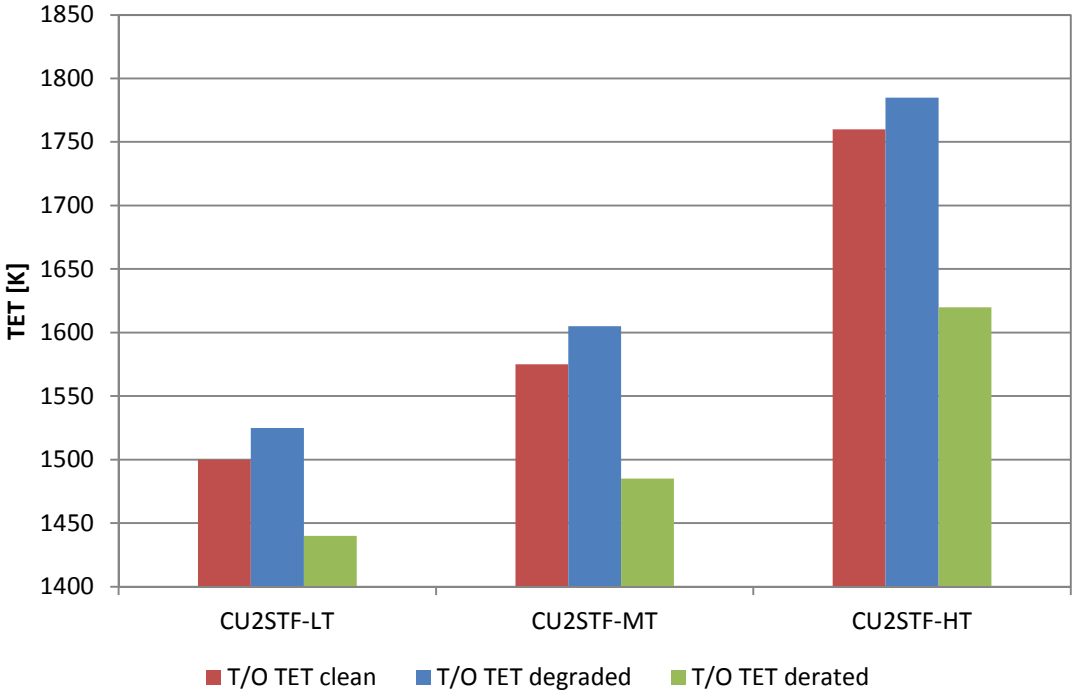

Figure 4-27: Engine T/O TET for clean, degraded and derated conditions

To estimate the engine in-service life in terms of flight cycles after which the above described degradation condition can be observed, the engine EGT margin (EGTM) may be used as performance indicator. Off-design performance analysis of the three engine variants revealed a nearly constant ratio of HP Turbine Entry Temperature to LP Turbine Exit Temperature over the engine thrust range with an approximate value of 1.4. This allows conversion of the engine TET to an approximate engine EGT value. According to reference [95] an average take-off EGTM deterioration of about 5-6°C per 1000 flight cycles is expected for the CFM56-5B series engine. Actual deterioration rates depend on engine thrust rating and utilisation.

The EGT increase between the clean configuration and the degraded configuration has been calculated for the three engine models as follows:

$$EGT_{degraded} - EGT_{clean} = EGTM\ loss + EGTM_{degraded,initial} \quad \textbf{(4-8)}$$

Assuming a degradation rate of 5°C EGTM per 1000 cycles for the CU2STF-LT engine variant, 5.5°C EGTM per 1000 cycles for the CU2STF-MT variant and 6°C EGTM per 1000 cycles for the CU2STF-HT variant, and assuming an initial EGTM degradation of 12°C, 12,5°C and 13°C respectively for the first 1000 cycles, the corresponding accumulated engine life in flight cycles can be estimated as shown in figure 4-28. Based on these assumptions, the degradation of CU2STF-LT variant would roughly equal 4600 flight cycles, the degradation of the CU2STF-MT variant would equal about 5000 flight cycles and the degradation of the CU2STF-HT would be equal to 4000 flight cycles. Since an equal 2 percent degradation scenario has been assumed for all three engine models, an accretion in total flight cycles from the highest thrust variant (CU2STF-HT) to the lowest thrust variant (CU2STF-LT) would have been expected. However, as illustrated in figure 4-28, it can be seen that the 2 percent degradation scenario equals with an in-service life of nearly 5000 flight cycles for medium thrust variant (CU2STF-MT). This is due to the fact that this engine model variant experienced the highest take-off TET increase (+30K) when degradation was induced causing the highest loss in EGTM. It must be noted that this approach only represents a rough estimation based on assumptions for initial EGTM degradation and per cycle based degradation as well

as a simplification of the temperature ratio between HP Turbine Entry Temperature to LP Turbine Exit Temperature.

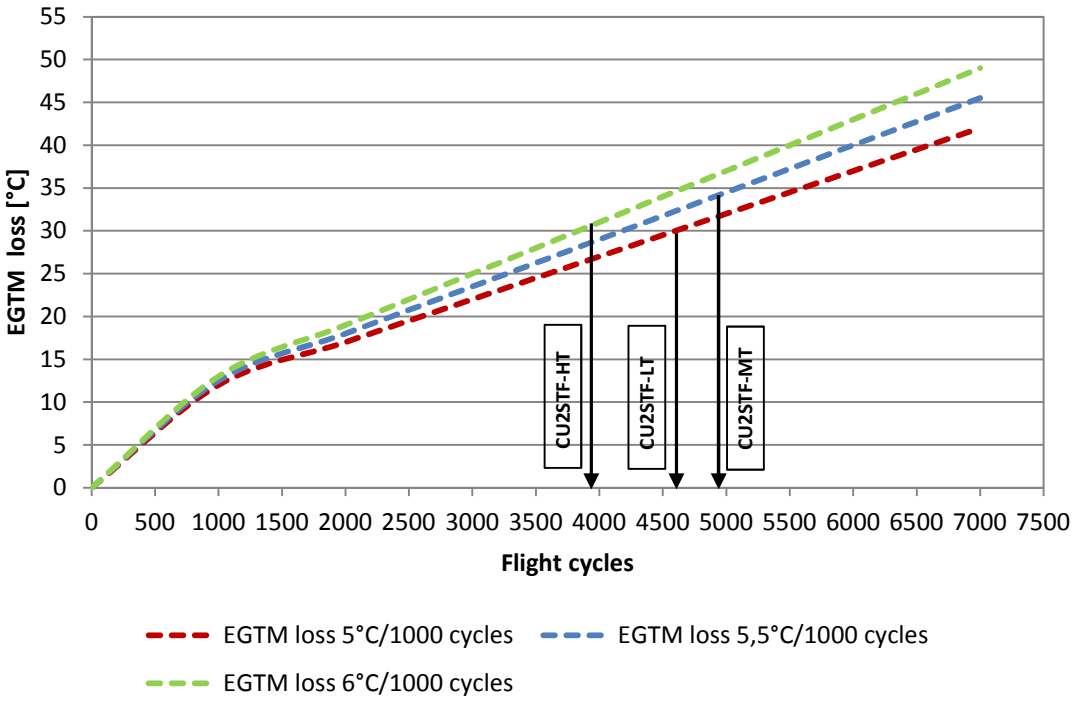

Figure 4-28: Take-off EGTM loss over engine flight cycles

4.1.5 Engine Model Verification

As initially stated, the above described engine model performance results were achieved by using the Cranfield University in-house code Turbomatch. Even though the engine performance calculations which were carried out yielded consistent results in terms of accuracy and comparability, some limitations must be considered when it comes to interpreting those engine performance calculations. It must be noted that the above created models only represent a basic engine design with certain simplifications. Especially since not all engine parameters are publicly available, some assumptions made, may still deviate from the original engine configuration. Also, dynamic engine off design performance scenarios and transient behaviour are not accounted for in this study. This is also due to the fact that engine features which exist in engines in operation such as variable stator vanes (VSV) or active bleed distribution were not integrated in the engine models. A comprehensive overview of engine control systems and their components in commercial turbofan applications can be found in reference [96]. It describes in depth all major engine control elements, their functions and the effect on engine operation.

4.2 Aircraft Performance Model (Hermes)

The aircraft configuration that is used throughout this study represents a narrow body single-aisle aircraft for use in short to medium range applications. The aircraft model has been created based on publicly available information and was adapted for the work carried out in this study. Three aircraft configurations were modelled, each configuration representing a different aircraft size and thus each one having a different maximum payload [97], [98], [99]. The models are designated as CUSA-S (Cranfield University Single Aisle Short), CUSA-M (Cranfield University Single Aisle Medium) and CUSA-L (Cranfield University Single Aisle Long). All three configurations encompass the same basic aircraft design like wing geometry, high lift systems and landing gear characteristics. Only the fuselage geometry, in this study the length, was altered to meet the three different model requirements. The model requirements are based on

the Airbus A320 aircraft series which is a common commercial aircraft available in different configurations.

The described aircraft model performance results were achieved by using the Cranfield University in-house code Hermes. This aircraft/engine performance model incorporates an aircraft aerodynamic and performance model and also connects with the Turbomatch engine performance model [100]. Figure 4-29 shows the basic structure of the Hermes input and output data flow. Hermes requires input from the engine model (engine performance input) as well as input from the aircraft model and its operational limits (aircraft model input and aircraft mission input). The two main output files contain the calculated aircraft performance (aircraft trajectory performance) including all major engine parameters throughout the trajectory.

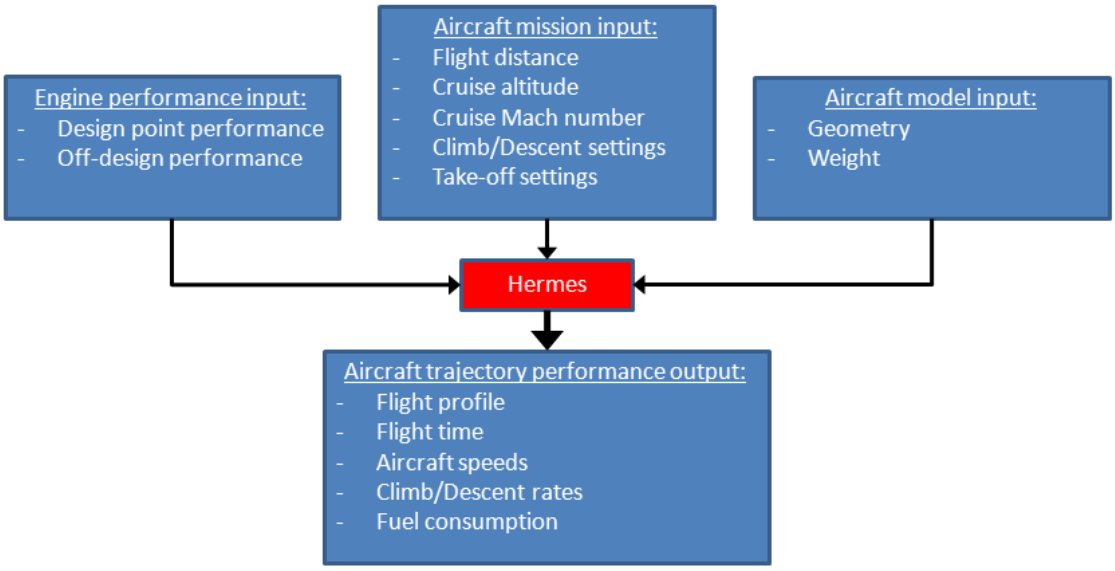

Figure 4-29: Hermes aircraft performance model (inputs and outputs)

The main inputs for the aircraft performance calculations are summarised below: (Refer also to tables 4-8, 4-9 and 4-10 in the next section)

- Engine performance data including: Design point and off-design performance (clean and degraded configuration).
- Aircraft mission data including: 17 climb segments, 11 descent segments, 1 fixed take-off segment and 86-285 cruise segments (depending on range).

- Aircraft model data including: aircraft geometry specifications and aircraft weight specifications.

The Hermes aircraft/engine model uses the following user specified information to calculate the flight path performance of the particular phase:

- Climb segments: Altitude, ISA temperature deviation, EAS, engine power
- Cruise segments: Altitude, ISA temperature deviation, Mach number
- Descent segments: ISA temperature deviation, TAS, engine power

The input specifications of the climb phase and descent phase differ due to the fact that Hermes internally calculates the descent altitudes by interpolating between the cruise altitude and the landing altitude. This means there is no provision to select a descent path based on specific altitudes. Aircraft speed and engine power settings can similarly be adjusted for climb and descent segments.

A simulation program that provides similar functionality to perform flight mission analysis is called Varmission and has been developed by DLR (Deutsches Zentrum für Luft -und Raumfahrt) Institute of Propulsion Technology. Another commercially available software suite to perform flight mission studies is called Pacelab Mission developed by PACE which offers comprehensive functionality for aircraft route and performance analyses. Also aircraft manufacturers such as Airbus or Boeing provide comprehensive analysis suites to airline operators based on their own aircraft models and flight test data.

4.2.1 Hermes Aircraft Model

The basic aircraft model structure of the CUSA model is depicted in figure 4-30. It is a single-aisle narrow body aircraft design. Each version, according to the length, reflects a different passenger capacity and thus a different aircraft OEW, maximum payload weight and maximum take-off weight. The passenger weight has been assumed with a mean value for all adults of 86kg according to a survey on standard passenger weights and baggage performed at 8 different airports in the European region in 2008 and 2009 [101].

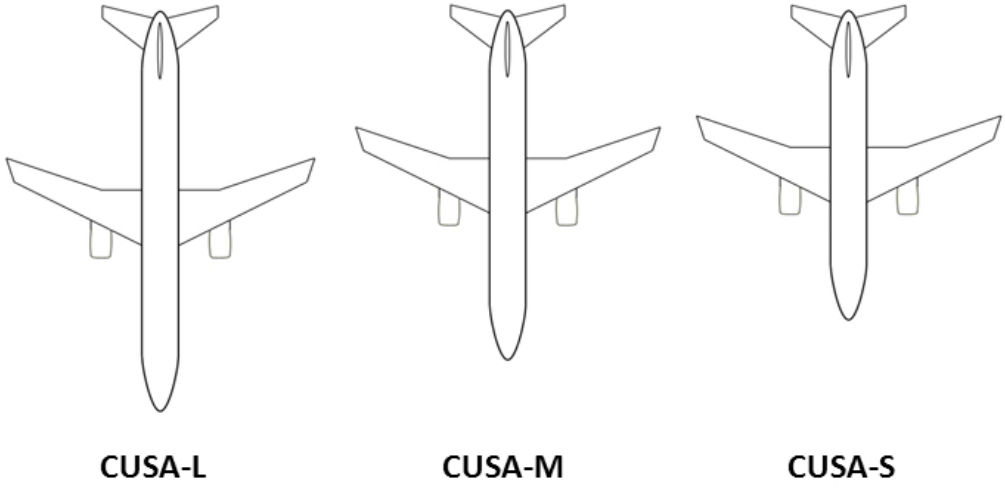

Figure 4-30: CUSA family schematic

The basic aircraft specifications for each CUSA model and its corresponding Airbus A320 family equivalent are listed in the following tables 4-8, 4-9 and 4-10. It must be noted that the aircraft OEW has been assumed less for all three models compared to the A320 aircraft specification.

Table 4-8: Aircraft specification comparison CUSA-S

Aircraft model specifications **Maximum Operation Mach Number: 0.82 Service Ceiling: 12000 m**			
	Unit	**Aircraft specification**	**CU Hermes**
Overall length	m	33.84	33.84
Fuselage width	m	3.95	4.05
Wing area	m^2	122.6	122.7
Wing aspect ratio	-	9.5	9.5
Tailplane area	m^2	31.0	31.0
Tailplane aspect ratio	-	5.0	5.0
Aircraft OEW	kg	40800.0	40000.0
Max. payload weight	kg	13200.0	10664.0
Max. T/O weight	kg	64000.0	64000.0
Max. range	km	6850	7765-
Number of engines	-	2	2
Typical seating	-	124	124

Table 4-9: Aircraft specification comparison CUSA-M

Aircraft model specifications Maximum Operation Mach Number: 0.82 Service Ceiling: 12000 m			
	Unit	**Aircraft specification**	**CU Hermes**
Overall length	m	37.57	37.57
Fuselage width	m	3.95	4.05
Wing area	m^2	122.6	122.7
Wing aspect ratio	-	9.5	9.5
Tailplane area	m^2	31.0	31.0
Tailplane aspect ratio	-	5.0	5.0
Aircraft OEW	kg	42600.0	41800.0
Max. payload weight	kg	16600.0	12900.0
Max. T/O weight	kg	73500.0	73500.0
Max. range	km	5900	7405-
Number of engines	-	2	2
Typical seating	-	150	150

Table 4-10: Aircraft specification comparison CUSA-L

Aircraft model specifications Maximum Operation Mach Number: 0.82 Service Ceiling: 12000 m			
	Unit	**Aircraft specification**	**CU Hermes**
Overall length	m	44.51	44.51
Fuselage width	m	3.95	4.05
Wing area	m^2	122.6	122.7
Wing aspect ratio	-	9.5	9.5
Tailplane area	m^2	31.0	31.0
Tailplane aspect ratio	-	5.0	5.0
Aircraft OEW	kg	48500.0	47800.0
Max. payload weight	kg	21200.0	15910.0
Max. T/O weight	kg	89000.0	89000.0
Max. range	km	5600	6800-
Number of engines	-	2	2
Typical seating	-	185	185

4.2.2 Aircraft Model Verification

To assess the performance characteristics of the adapted aircraft models a series of basic trajectory calculations with Hermes has been performed. In this way the maximum operational limits in terms of payload and range have been determined for each of the three aircraft variants. Based on the aircraft model specifications provided in the previous section Hermes calculates the maximum mission ranges depending on the selected payload and while taking into account aircraft fuel weight limitations.

Figure 4-31 shows the payload-range diagram for the CUSA-S aircraft variant. Three key points of the payload-range curve have been plotted in the diagram, each point representing a particular load configuration in terms of payload weight and fuel weight. (1) The maximum range with maximum take-off weight and maximum payload weight is designated as maximum payload range. (2) The maximum range with maximum take-off weight and maximum fuel weight is designated as maximum economic range. (3) The maximum range with no payload weight and maximum fuel weight is designated as maximum ferry range. Figure 4-32 shows the payload-range diagram for the CUSA-M aircraft variant in a similar fashion. The payload-range diagram for the CUSA-L aircraft variant is shown in figure 4-33. This aircraft variant does not have a particular maximum economic range, id est the maximum payload range and maximum economic range fall in the same point since the aircraft is only limited by the maximum fuel weight. In addition, all diagrams show the respective payload-range points for the two mission analysed in chapter 5.

The depicted payload-range diagrams have been plotted assuming the following conditions [102], [103], [104]:

- ISA+10°C conditions
- Cruise altitude of 10668 m
- Cruise Mach number of 0.76
- No diversion mission

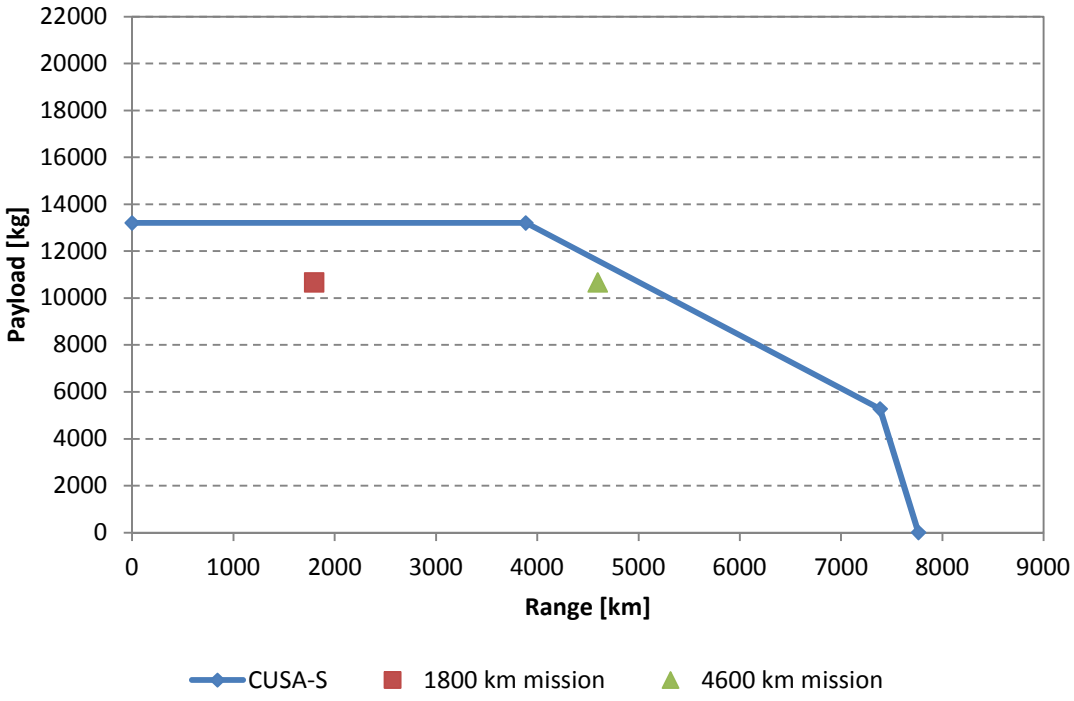

Figure 4-31: CUSA-S Payload-Range diagram

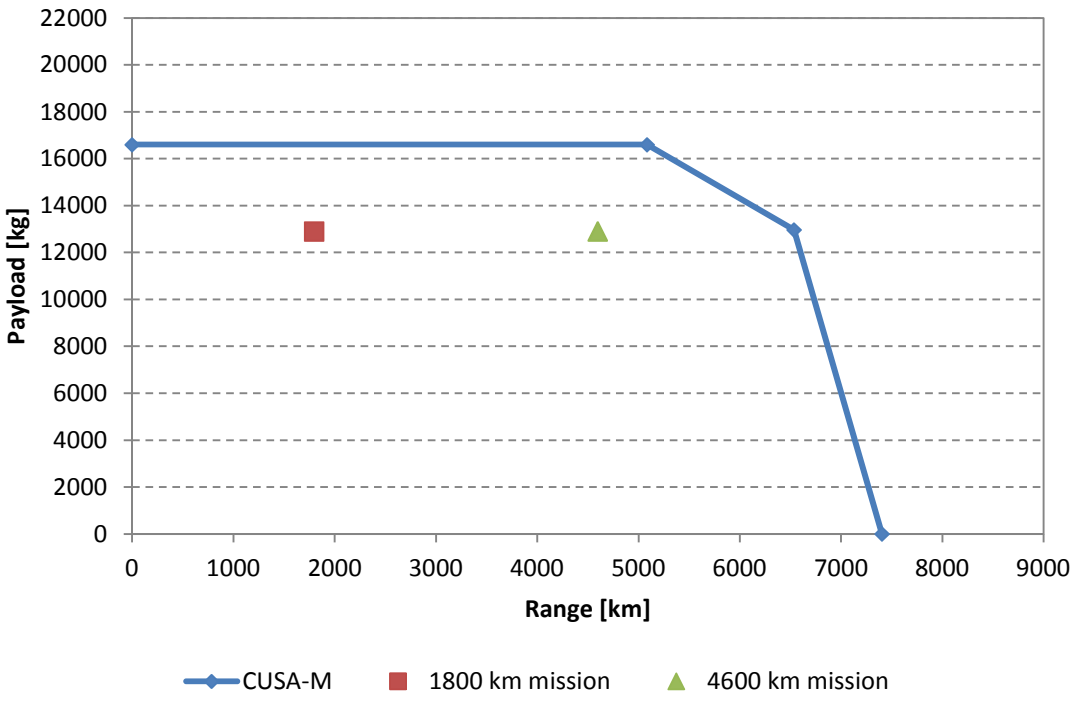

Figure 4-32: CUSA-M Payload-Range diagram

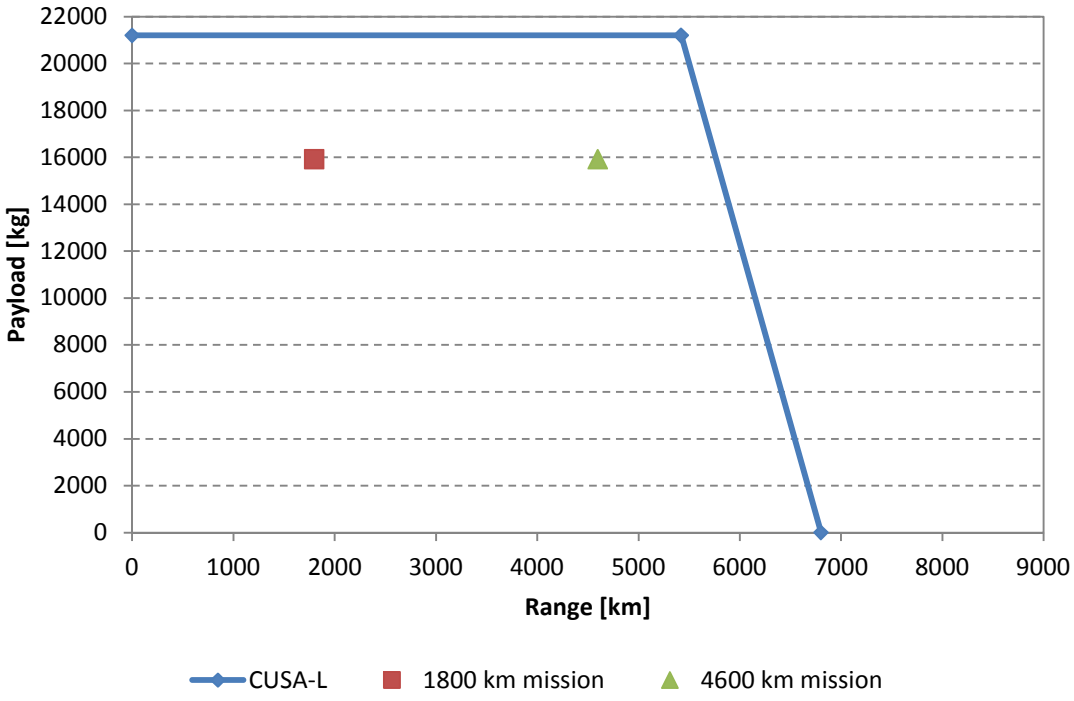

Figure 4-33: CUSA-L Payload-Range diagram

4.3 Emissions Predictions Model (Hephaestus/P3T3)

For the assessment of engine emissions during, id est pollutant emitted during the combustion process in the combustor, there are three common methods available to predict those emissions: The empirical correlation based method, the numerical simulation through CFD calculations, and calculations based on stirred reactor models (physics-based models) [105]. Empirical correlation based models are typically less demanding in terms of computational resources and they are generally suitable for existing fixed combustors where particular data is available. This means these models are adequate for predicting emissions, especially NO_x, when there pre-exists historical certification data for that specific engine type [106]. The more sophisticated and complex numerical and calculations based models are generally more computationally intensive because of their high level of detail in mapping a particular combustor design. This makes them especially suitable for new combustor designs for which no historical data points exist but detailed information like combustor geometries and

operating conditions are predetermined. For the purpose of aircraft trajectory analyses, where the engine and combustor design have been largely investigated in the past, an empirical correlation based model is expected to be satisfactory.

4.3.1 P3T3 Emissions Prediction Model

The aircraft and engine configurations described in the previous chapters which are used throughout this study were also integrated in an emissions performance model. This model is based on the Cranfield University in-house code HEPHAESTUS which provides the ability of emissions prediction calculations utilising the P3T3 Method. It comprises an empirical correlation-based approach to predict NO_x emissions at altitude using publicly available engine performance data from ground level testing. These calculations require sensitive engine component data such as compressor exit pressure (designated as P3) and temperature (designated as T3) as well as the fuel air ratio and the fuel flow both at altitude and at ground level. This data is taken from the engine performance models created using Turbomatch as described in sections 4.1-4.3 and fed into the emissions performance model. A summary of the P3T3 methodology is shown in figure 4-34. Compressor exit temperature at altitude is used for ground level correlation of EINOx. An EINOx altitude correction for the compressor exit pressure and FAR is performed. In addition, a humidity correction is included to account for the change in air properties at higher altitudes.

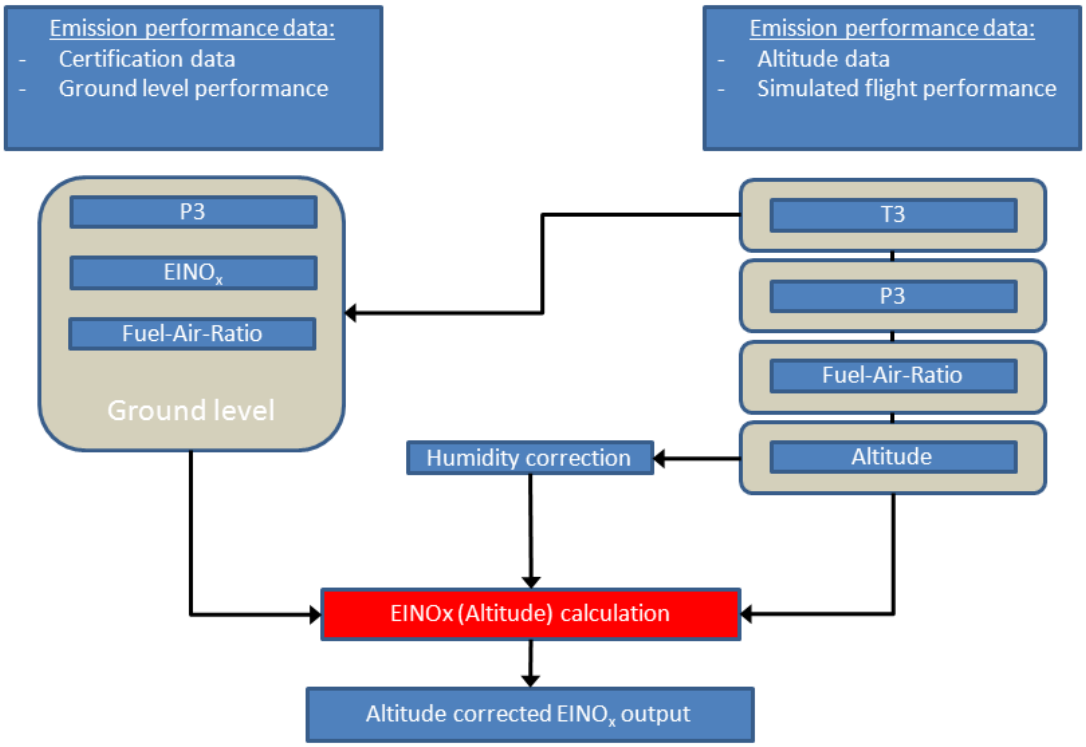

Figure 4-34: P3T3 methodology (adapted from Norman et al. [48])

Furthermore the emissions indices (EI) of the specific pollutant for each engine variant are required in order to correct them to the various flight conditions. The International Civil Aviation Organization (ICAO) hosts an exhaust emissions database of various production engines which incorporates information from certified engine tests provided by the engine manufacturers. This data is based on established emissions measurement procedures and compliance standards for gaseous pollutants. In order to characterise the operational conditions of an engine in terms of their emissions performance a standard Landing and Take-off Cycle (LTO Cycle) was defined. An excerpt of the emissions performance data for the CFM56-5B3/P engine type is shown in table 4-11. Similarly tables 4-12 and 4-13 show the same data for the CFM56-5B4/P and CFM56-5B6/P engine type respectively.

It should be noted that the LTO cycle only assesses the emissions below 915 m (3000 feet) and therefore may not be suitable for comparing the emissions of different engines in other flight modes, e.g. cruise.

Table 4-11: ICAO Database exhaust emissions CFM56-5B3/P

Mode	Power Setting [% T/O Thrust]	Time [min]	Fuel Flow [kg/s]	Emissions Indices [g/kg]		
				HC	CO	NO_x
Take-off	100	0.7	1.430	0.1	0.8	37.3
Climb out	85	2.2	1.141	0.2	0.9	28.5
Approach	30	4.0	0.366	0.5	1.7	11.2
Idle	7	26.0	0.115	3.5	19.2	4.7

Table 4-12: ICAO Database exhaust emissions CFM56-5B4/P

Mode	Power Setting [% T/O Thrust]	Time [min]	Fuel Flow [kg/s]	Emissions Indices [g/kg]		
				HC	CO	NO_x
Take-off	100	0.7	1.132	0.2	0.9	28.0
Climb out	85	2.2	0.935	0.2	0.9	23.2
Approach	30	4.0	0.312	0.5	2.3	10.0
Idle	7	26.0	0.104	4.6	23.4	4.3

Table 4-13: ICAO Database exhaust emissions CFM56-5B6/P

Mode	Power Setting [% T/O Thrust]	Time [min]	Fuel Flow [kg/s]	Emissions Indices [g/kg]		
				HC	CO	NO_x
Take-off	100	0.7	0.961	0.2	0.9	23.6
Climb out	85	2.2	0.799	0.2	1.0	19.6
Approach	30	4.0	0.275	0.6	2.9	9.2
Idle	7	26.0	0.097	5.5	27.7	4.0

The P3T3 model utilises both, engine model performance data as well as the ground level exhaust emissions data published by the engine manufacturers to establish the emissions indices at certain altitudes and flight speeds. The resulting total NO_x emissions in kilogram can then be calculated according formula 4-9:

For this study, only the emissions index (EI) for the NO_x emissions is of interest and other pollutants are not considered.

$$NO_x = (w_f \times Time) \times EINO_x \quad \textbf{(4-9)}$$

This is where w_f is the fuel flow given in kilogram per second, time is given in seconds and EINOx in gram/kilogram.

4.3.2 Emissions Model Verification

In order to verify the emissions performance of the three engine variants they have been matched and compared with existing equivalent engine models from the ICAO database. The Hephaestus tool has been used to calculate the emissions based on this ICAO data. The fuel flow at the four discrete power settings provided in the ICAO database for each engine variant (refer to table 4-11, 4-12, 4-13) has been used as target value to match the engine performance of the created engine models. Data from the previously performed engine off-design studies was used to find the respective fuel flow at the different power settings for each model by adjusting the TET. The corresponding values of burner inlet temperature (T3) and burner inlet pressure (P3) as well as the fuel/air ratio have then been used as input parameters for the emissions model. Figures 4-35, 4-36 and 4-37 show the fuel flow comparison of the ICAO data and the engine models at the different power settings (the four discrete power settings have been converted to the actual net thrust value given in kN). It can be noted from figures 4-35, 4-36 and 4-37 that the engine model results at T/O, climb, approach and idle power settings are generally following the trend of the ICAO data and can be considered acceptable for the purpose of this study. The results at idle power settings however have only limited validity. One reason for this behaviour arises from the limitations of the created engine models which did not return viable engine performance results at very low power settings. Figure A.1-1 in the appendix illustrates a comparison between the block fuel and block NO_x plotted over the payload conditions for the three aircraft variants as simulated in the following chapter 5.

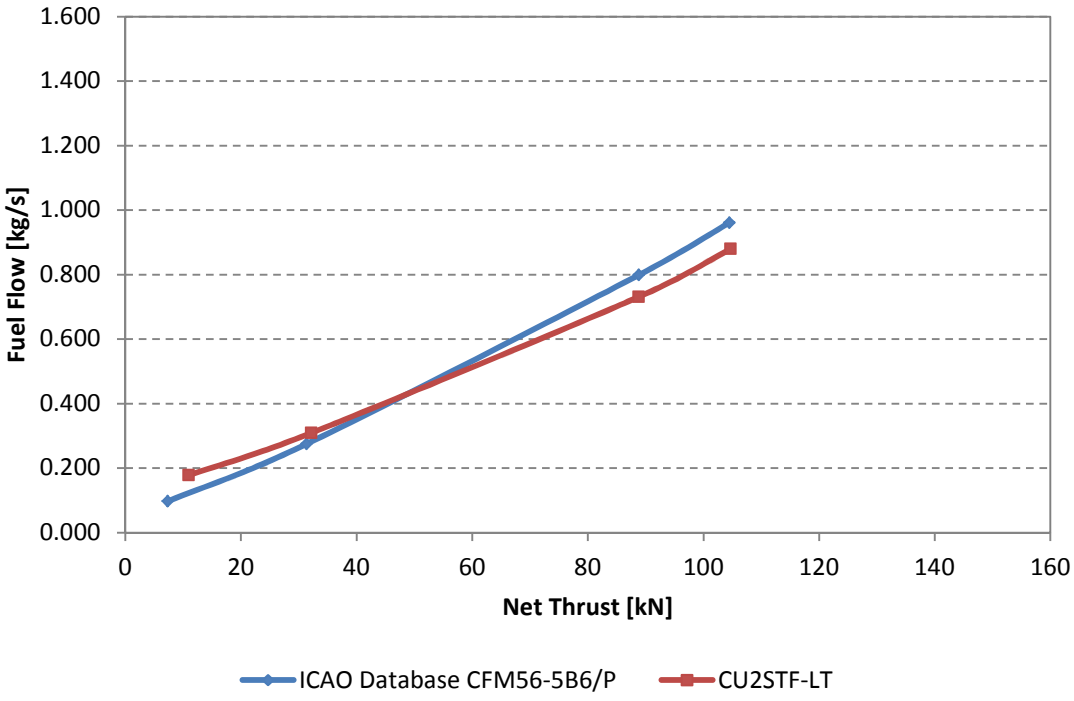

Figure 4-35: CU2STF-LT - Fuel Flow versus Net Thrust

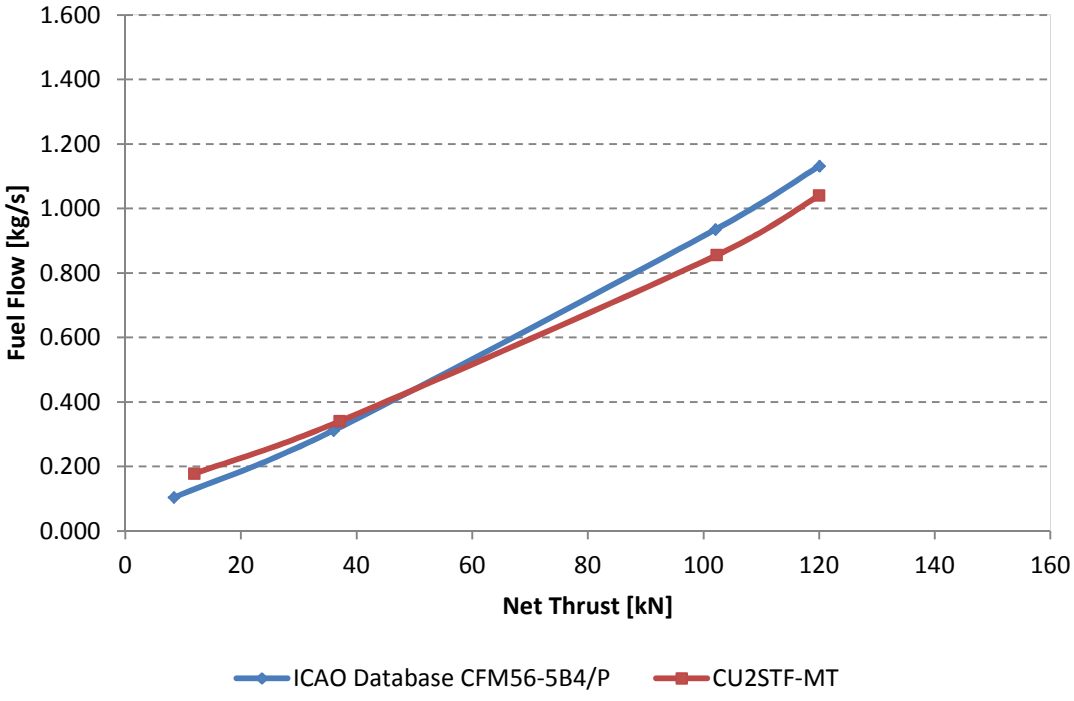

Figure 4-36: CU2STF-MT - Fuel Flow versus Net Thrust

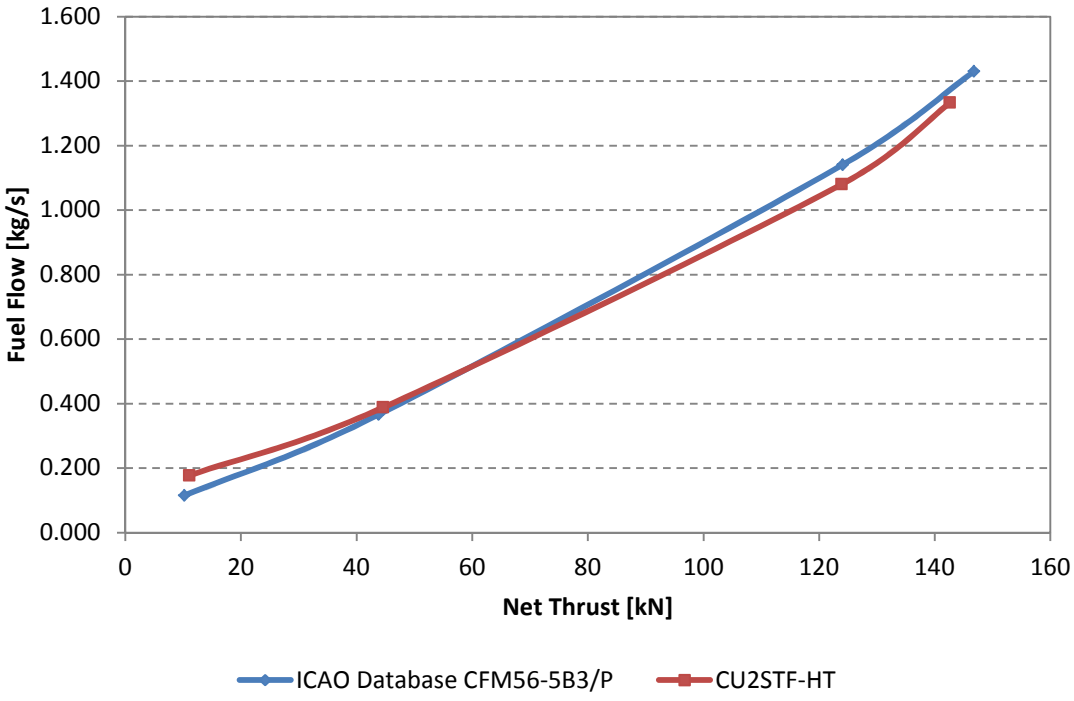

Figure 4-37: CU2STF-HT - Fuel Flow versus Net Thrust

4.4 Optimisation Framework

The framework for the aircraft trajectory optimisation case studies used in this work is comprised of the aircraft, engine and emissions models and an optimisation suite. The framework provides the interfaces between the individual models and the optimisation algorithm. Figure 4-38 shows a schematic diagram of the optimisation framework including the engine, aircraft and emissions model, the optimiser and the two optimisation scenarios (fuel vs. time and fuel vs. NO_x). Depending on the configuration loaded in the optimiser, the framework will run calculations to find results for either scenario 1 or scenario 2. The two different scenarios will be addressed in detail in the following sections 4.5.

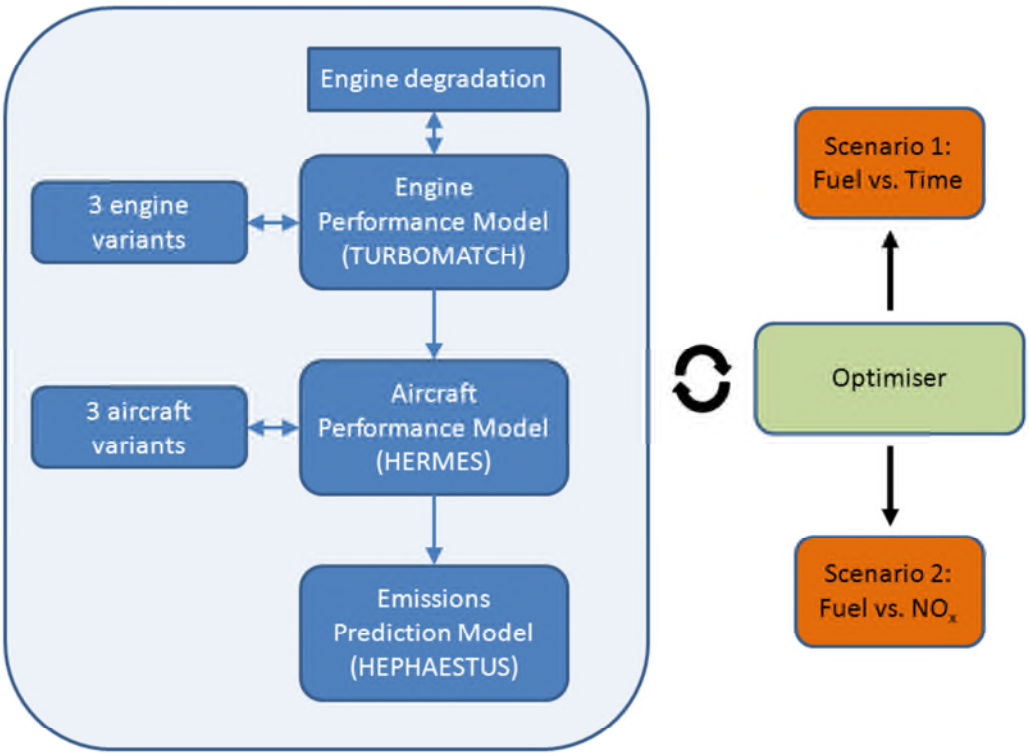

Figure 4-38: Optimisation framework

4.4.1 GATAC Optimisation Suite

As described in chapter 2 section 10, the GATAC optimisation suite utilises the genetic based optimiser called NSGAMO. This optimisation suite provides the functionality to perform multi-objective constrained optimisation calculations. The optimisation algorithm utilised within the GATAC suite has been collaboratively designed, implemented and tested by Airbus France and Cranfield University. It is written in the object oriented programming language JAVA and has been benchmarked and tested by Cranfield University for the use in the Clean Sky project [70]. The requirements, design concept and key features of the GATAC optimisation suite for aircraft flight trajectory optimisation have been evaluated and are presented in the paper in reference [107]. An overview of the framework structure is shown in figure 4-39.

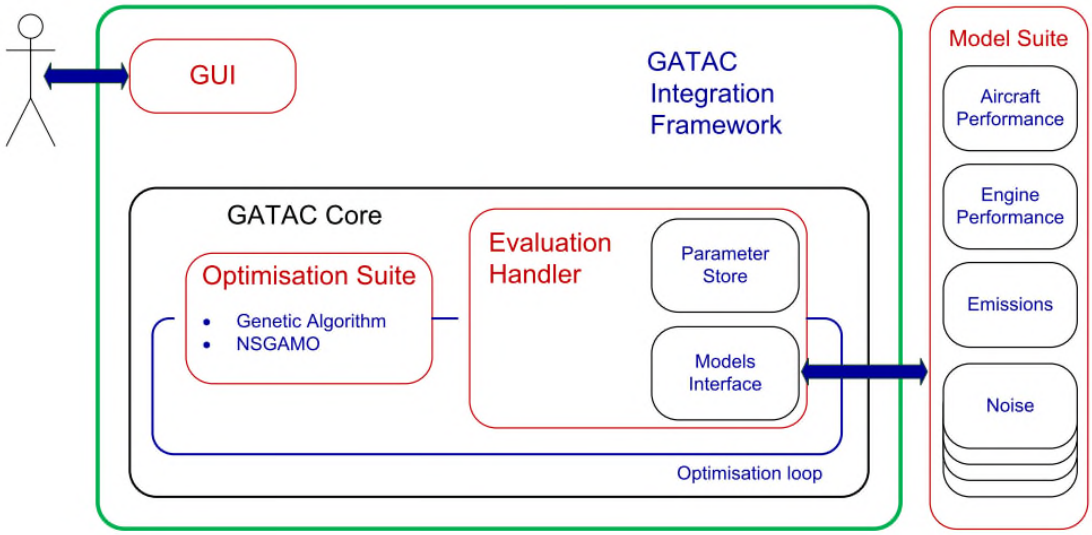

Figure 4-39: GATAC framework structure [71]

4.4.2 Optimisation Suite Verification

Several benchmark studies of the GATAC optimiser have been performed in the past to validate the suitability for multi-objective aircraft trajectory optimisation. In order to be able to verify the actual performance of a particular optimiser predefined test problems must be used where the true Pareto optimal front is known. The results of the optimiser to be benchmarked can then be compared to the known solutions.

Common test problems which have been used in the past were standard mathematical test functions according to Zitzler, Deb and Thiele, short ZDT functions [108]. Several different ZDT test functions have been established and are described in detail in reference [66]. The different ZDT functions aim at testing the ability of the optimiser to handle some or all of the below mentioned difficulties while delivering a diverse set of solutions within the range of the Pareto optimal front:

- Large number of decision variables
- Discontinuous Pareto optimal fronts
- Non-uniform density Pareto optimal fronts with few solutions

Two goals in multi-objective optimisation problems can be identified which define the performance of the optimiser. One goal is the convergence of the results to the Pareto optimal set and the other goal is to maintain diversity in solutions of the Pareto optimal set [a fast and elitist].Thus the diversity metric (Δ) and the convergence metric (γ) are used to measure and assess the ability of the optimiser to reach these goals handle the above described problems. The diversity metric provides a measure of the spread of obtained solutions with regards to the entire Pareto optimal region. A set of solutions which covers the complete Pareto optimal region is desirable for satisfactory results. The convergence metric provides a measure of how close the obtained solutions lie in relation to a known set of Pareto optimal solutions. In the referenced study, three test functions (ZDT1, ZDT3 and ZDT6) have been utilised to benchmark the GATAC optimiser used for this study. A summary of the ZDT test functions, adapted from [66] is given in table 4-14. As part of the described study the GATAC optimiser was also benchmarked against two other genetic optimisers namely Matlab NSGA-II and Matlab MOGA. A detailed description of the benchmark studies mentioned above can be found in reference [70].

For the purpose of this study only the main conclusions of the benchmark studies will be highlighted here to reinforce the suitability of the GATAC optimiser for aircraft trajectory optimisation studies. For all three ZDT test functions it was found that the GATAC optimiser was able to deliver very good convergence and diversity with respect

to the true Pareto optimal front [70]. It was also noted that, compared to the other two tested optimiser, the GATAC optimiser achieved the same or better results with a lesser number of evaluations.

Table 4-14:ZDT1, ZDT3 and ZDT6 test functions (adapted from Deb et al. [66])

Problem	n	Variables bounds	Objective functions	Optimal solution	Comments
ZDT1	30	[0,1]	$f_1(x) = x_1$ $f_2(x) = g(x)\left[1 - \sqrt{\frac{x_1}{g(x)}}\right]$ $g(x) = 1 + \frac{9(\sum_{i=2}^{n} x_i)}{(n-1)}$	$x \in [0,1]$ $x_i = 0$ $i = 2, \ldots, n$	Convex
ZDT3	30	[0,1]	$f_1(x) = x_1$ $f_2(x) = g(x)\left[1 - \sqrt{\frac{x_1}{g(x)}} - \frac{x_1}{g(x)}\sin(10\pi x_1)\right]$ $g(x) = 1 + \frac{9(\sum_{i=2}^{n} x_i)}{(n-1)}$	$x \in [0,1]$ $x_i = 0$ $i = 2, \ldots, n$	Convex, disconnected
ZDT6	10	[0,1]	$f_1(x) = 1 - \exp(-4x_1)\sin^6(6\pi x_1)$ $f_2(x) = g(x)\left[1 - \left(\frac{f_1(x)}{g(x)}\right)^2\right]$ $g(x) = 1 + 9\left[\frac{(\sum_{i=2}^{n} x_i)}{(n-1)}\right]^{0.25}$	$x \in [0,1]$ $x_i = 0$ $i = 2, \ldots, n$	Non-convex, non-uniformly spaced

4.5 Model Interaction

Two different framework setups have been used in this study to address two different optimisation scenarios. The first scenario aims at analysing the trajectory optimisation with regards to the two objectives, namely fuel and time. The second scenario looks at the optimisation of the two objectives fuel and NO_x.

Figure 4-40 shows the optimisation framework setup and its calculation sequence for the fuel-time scenario (scenario 1). The optimisation loop consists of the GATAC optimisation suite which includes the NSGAMO optimiser and the Hermes aircraft/engine performance model for the flight path calculations. After initialising the setup with a defined population the optimiser sends particular decision variable values to aircraft/engine performance model as input to calculate the flight trajectories. The optimiser then extracts the values for total fuel burned and total flight time from the calculated output and processes these results by applying genetic operations to identify suitable values for the next optimisation loop.

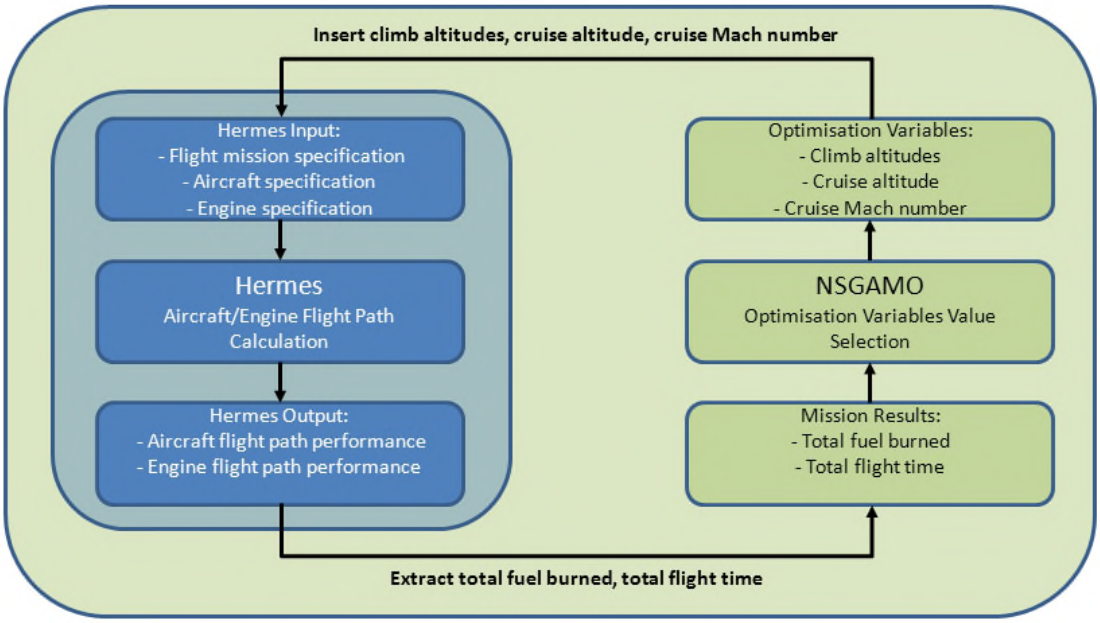

Figure 4-40: Scenario 1 - Fuel vs. Time

The same approach as previously described for the fuel-time scenario (scenario 1) applies to the fuel-NO_x scenario (scenario 2). Figure 4-41 shows the framework setup

for this second scenario. In addition to the NSGAMO optimiser and the aircraft/engine performance model, the Hephaestus emissions model (P3T3 method) is implemented in the framework. After the flight trajectory calculation (Hermes aircraft/engine flight path calculation), engine flight path performance data, namely HPC exit pressure and temperature and ambient pressure and temperature of the first cruise segment is extracted from the output and sent to the emissions model for calculation. It must be noted that this limitation compromises the accuracy of the NO_x calculations for the climb and descent phase. On the other, by applying this limitation, the computational time for each iteration is kept within acceptable limits. The optimiser then extracts the values for the amount of total NO_x emitted in addition to the amount of total fuel burned. These results are then used as optimisation input for the next optimisation loop.

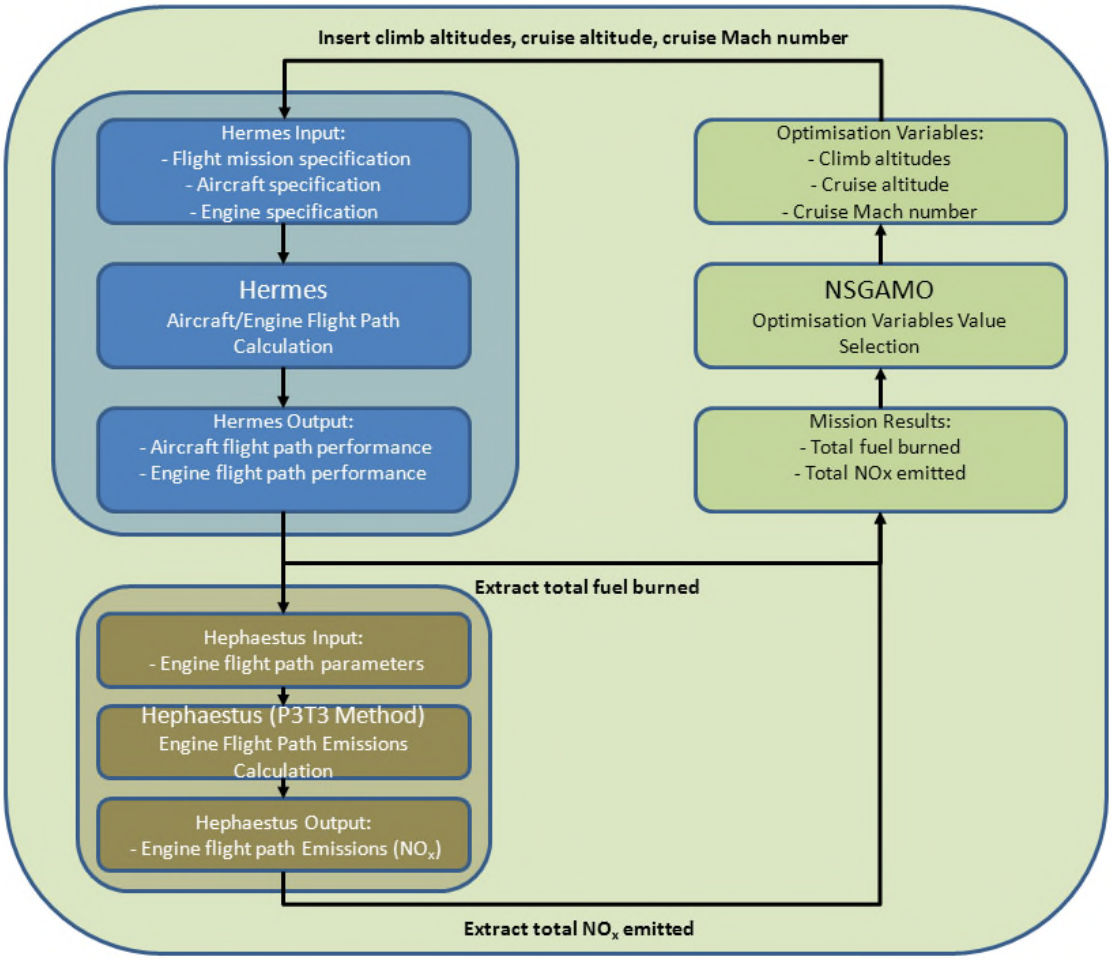

Figure 4-41: Scenario 2 - Fuel vs. NO_x

5 Aircraft Trajectory Analysis and Results

This chapter summarises the results of the basic trajectory analyses that have been conducted with the three different CUSA aircraft/engine configurations introduced in chapters 4.1 and 4.2, and their respective emissions models introduced in chapter 4.3. The trajectories analysed base on the aircraft trajectory definition made in chapter 3.1.3 and the assumptions and statements defined in chapter 3.2.

5.1 Summary of Analysed Scenarios

For the aircraft trajectory analyses two different flight distances have been selected which represent typical short-to-medium range flight missions. One 1800 km short range mission and one 4600 km medium range mission. The three aircraft variants with their respective engine variants have been used for the individual flight missions analysed. Each flight mission was completed with the engines in “clean” condition and with the engines in “degraded” condition. The engine degradation scenario is based on the assumptions introduced in chapter 4.1.2. The detailed “clean” engine condition and performance characteristics can be reviewed in chapter 4.1.3 and the detailed “degraded” engine condition and performance characteristics can be reviewed in chapter 4.1.4. For meaningful comparisons the duration of the different flight phases (take-off, climb, cruise, descent) for each flight mission and aircraft/engine configuration have been kept almost equal. This was achieved by adjusting the engine power settings for the climb and descent phase. The same adjustments were also made for each flight mission with the degraded engine configuration. The results are divided into two main sections: The first section covers the short range mission analysis in subchapters 5.2, 5.3 and 5.4. The second section covers the medium range mission analysis in subchapters 5.5, 5.6 and 5.7.

As an introduction to the results section, figure 5-1 and figure 5-2 show and overlay comparison between the real flight profile introduced in section 3.1.3 and the flight profile modelled with the Hermes aircraft performance code. The flight profiles, as well as the trend for fuel flow and EGT are in general agreement with the real flight data.

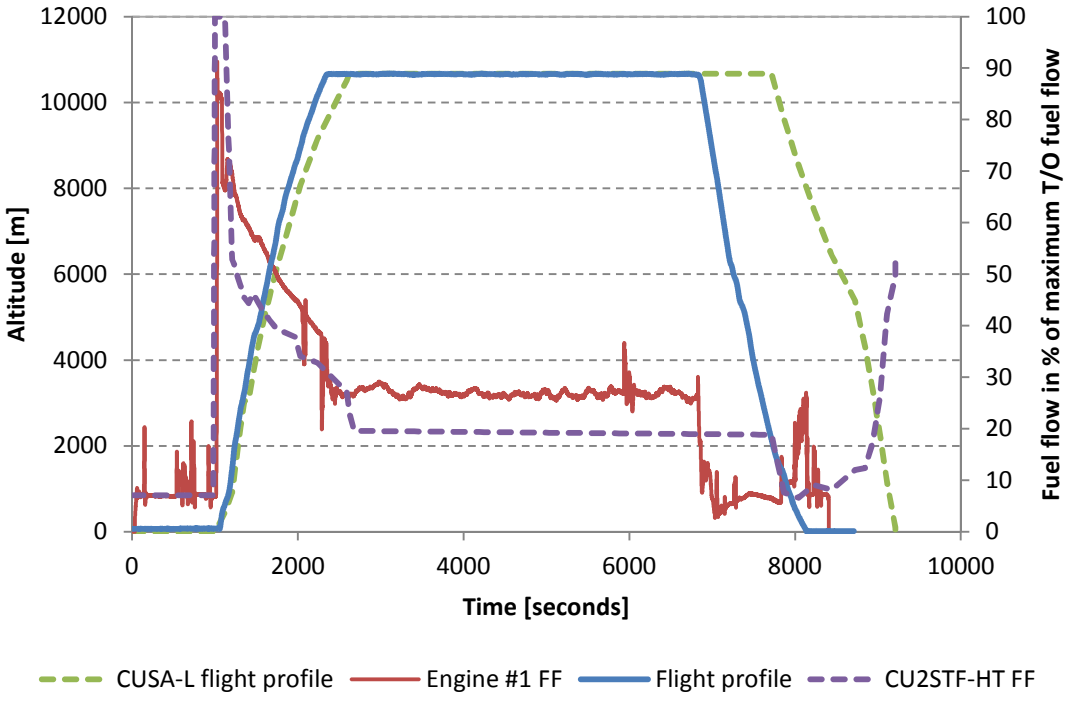

Figure 5-1: Real flight profile and engine FF vs. CUSA-L model

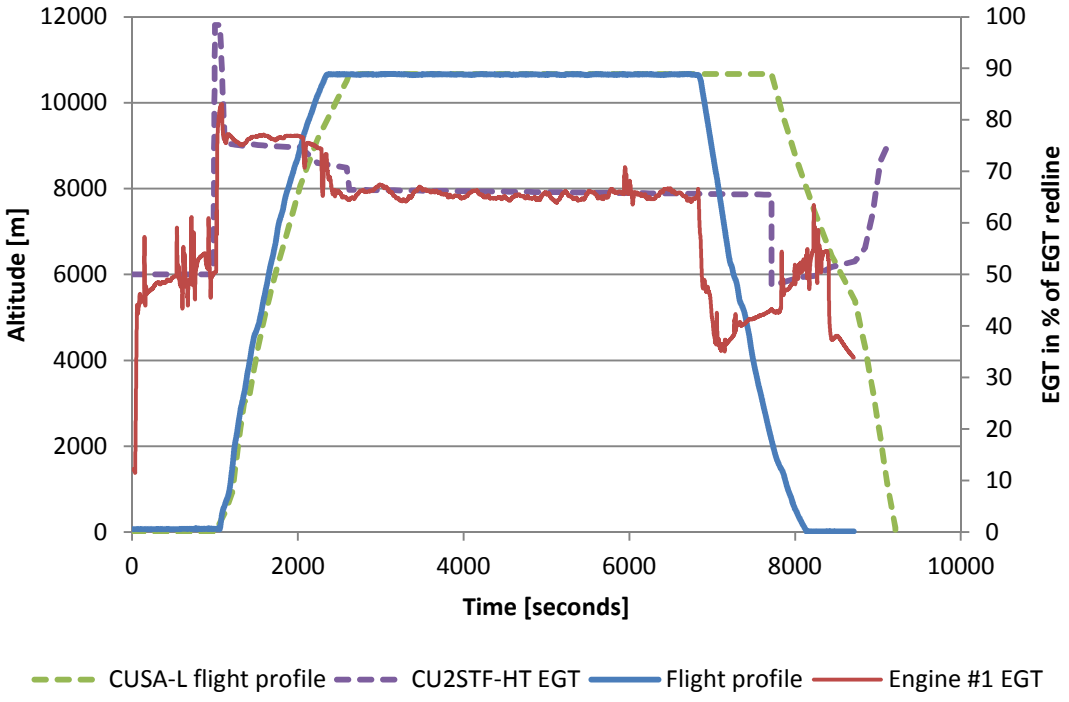

Figure 5-2: Real flight profile and engine EGT vs. CUSA-L model

5.2 Short Range Flight (Clean Engine)

The first case that is being looked at is the 1800 km short range flight mission with a clean engine configuration. This means the engine parameters correspond to the configurations as listed in tables 4-1, 4-2, 4-3 and 4-4 in chapter 4. All three aircraft variants CUSA-S, CUSA-M and CUSA-L with its respective engine variants CU2STF-LT, CU2STF-MT and CU2STF-HT performed the same flight mission.

5.2.1 General Description

The default settings of the 1800 km short range mission are summarised in table 5-1. The payload for each aircraft/engine configuration was set according to the maximum seating capacity assuming no luggage or other cargo. The values for cruise Mach number and cruise altitude were kept the same for all three aircraft variants. The achieved total flight time was also kept almost equal to permit direct comparisons of the flights.

Table 5-1: Short range mission characteristics (clean engine)

Mission	**1800 KM (clean engine)**		
Aircraft	**CUSA-S**	**CUSA-M**	**CUSA-L**
Engine	**CU2STF-LT**	**CU2STF-MT**	**CU2STF-HT**
Payload [kg]	10664	12900	15910
Cruise Mach number [-]	0.785		
Cruise altitude [m]	10668		
Flight duration [min]	133.6	133.7	133.9

5.2.2 Results

Figure 5-3 shows the calculated short range mission trajectory for the CUSA-S aircraft variant and the engine fuel flow trend throughout the flight. It can be seen that the trajectory flown is general in agreement with the real flight profile referenced in figure 3-6. The engine fuel flow trend at take-off, climb and cruise also follows a comparable pattern while the values during the descent phase deviate from the real trajectory to a larger extent. Engine fuel flow values and subsequently TET reach values equivalent to an engine power setting of about 85%. This is due to the fact that the engine power settings for the final segments of the descent have been selected to be at their

maximum permissible values. Figure 5-4 shows the engine TET trend along the flight path for the same aircraft variant following a corresponding pattern. It should be noted that for illustrative purposes the plot in figure 5-3 has been offset by 120 seconds before the take-off point. This allows adequate depiction of the peak fuel flow. This offset applies to all following plots where time in seconds is plotted on the horizontal coordinate axis.

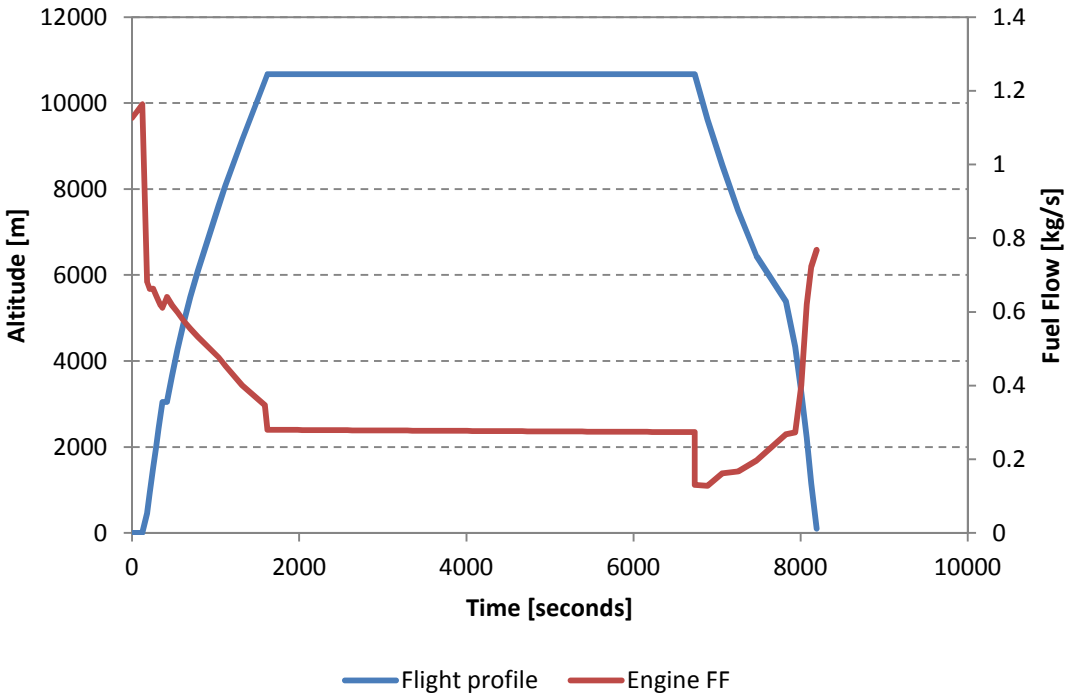

Figure 5-3: CUSA-S engine FF variation during flight (1800 km)

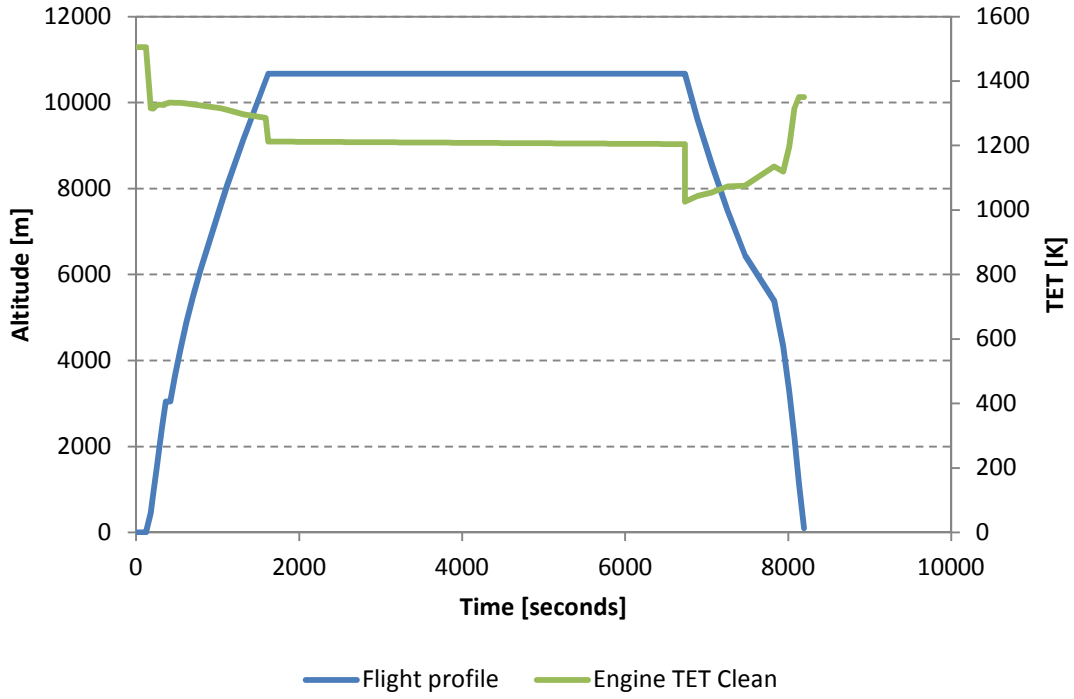

Figure 5-4: CUSA-S engine TET variation during flight (1800 km)

The results for the two other aircraft variants CUSA-M and CUSA-L can be found in appendix A.2.1. They follow the same pattern in all flight phases as the results of the CUSA-S while differences in peak values for fuel flow and TET can be observed due to the increased thrust requirements caused by the increased aircraft weight.

5.3 Short Range Flight (Degraded Engine)

The second case analysed is the 1800 km short range flight mission with a degraded engine configuration. This means the engine parameters correspond to the configurations as listed in tables 4-5, 4-6 and 4-7 in chapter 4. All three aircraft variants CUSA-S, CUSA-M and CUSA-L with its respective engine variants CU2STF-LT, CU2STF-MT and CU2STF-HT performed the same flight mission.

5.3.1 General Description

The default settings of the 1800 km short range mission with the degraded engines are listed in table 5-2 and follow the structure of the clean engine configuration as described in chapter 5.2.1.

Table 5-2: Short range mission characteristics (degraded engine)

Mission	1800 KM (degraded engine)		
Aircraft	**CUSA-S**	**CUSA-M**	**CUSA-L**
Engine	**CU2STF-LT**	**CU2STF-MT**	**CU2STF-HT**
Payload [kg]	10664	12900	15910
Cruise Mach number [-]	0,785		
Cruise altitude [m]	10668		
Flight duration [min]	133.7	133.7	133.8

5.3.2 Results

Figure 5-5 shows the take-off and climb profile of the CUSA-L aircraft and the corresponding engine TET in the clean and degraded configuration. The TET is kept nearly constant throughout the climb path while the delta between the clean and degraded engine is about 25K for the first 20 minutes of the climb and about 10K for the remaining 3 minutes. The TET is directly related to the selected engine power setting which is shown in figure 5-6 for the climb phase.

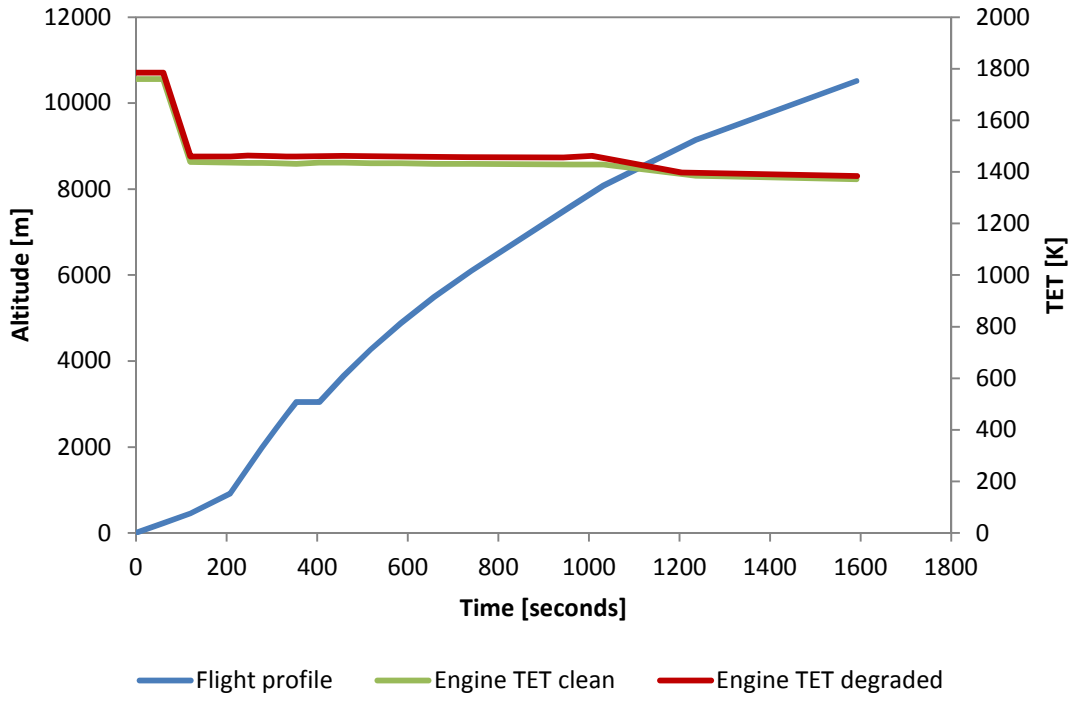

Figure 5-5: CUSA-L engine TET variation during climb

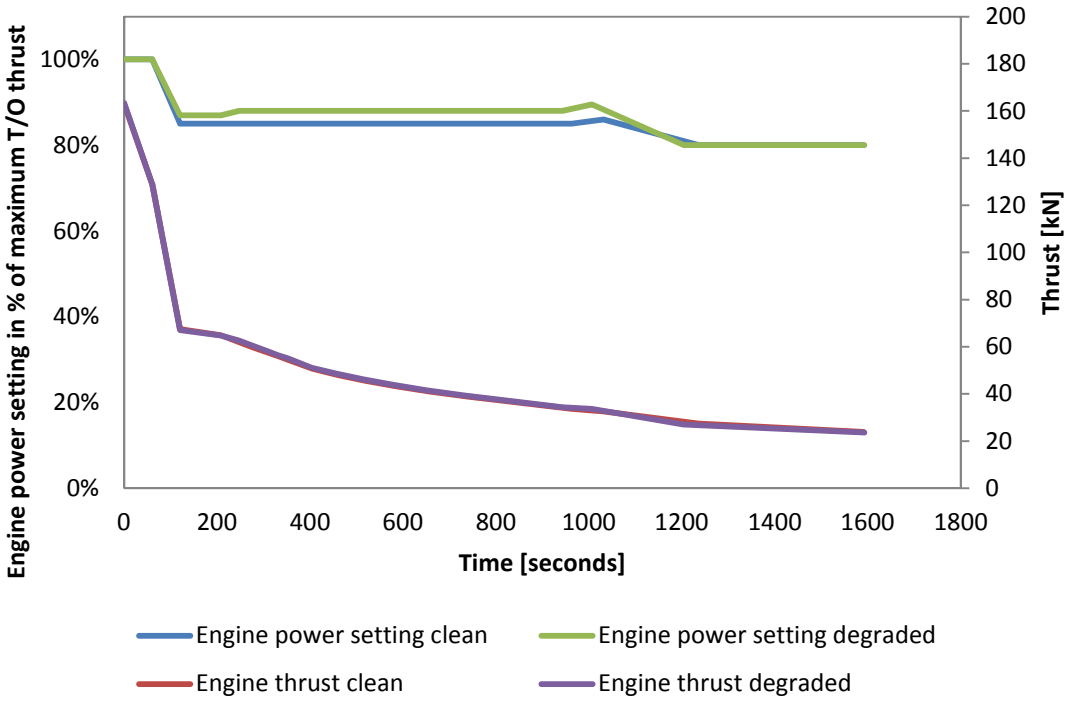

Figure 5-6: CUSA-L engine power setting and thrust during climb

In this figure, the engine power setting in percent of the maximum take-off thrust is plotted against the engine thrust for the clean and degraded engine configuration. In order to maintain an equivalent flight path (equivalent climb duration) for both configurations, the engine power setting for the degraded engine had to be increased to maintain the same thrust level for the climb as the clean engine configuration. It can also be noticed that the engine power setting for the last 3 minutes of the climb was not changed and remained at 80%. This is also in line with the TET trend shown in previous figure 5-5. Similar trends for TET and thrust levels can be observed for the CUSA-M and CUSA- S aircraft variants.

The increase in TET to maintain the thrust level translates into an increase in fuel burn and consequently causes the NO_x emissions to increase. Table 5-3 lists the percentage increase in fuel burn and NO_x emissions throughout the climb for the short range mission for all three aircraft variants. The CUSA-L aircraft with degraded engines will burn about 4.7% more fuel compared to the clean engine configuration. At the same time the NO_x emissions will increase by about 5.8%. The CUSA-M aircraft climb

performance shows a similar increase in fuel burn and NO_x emissions while the CUSA-S aircraft variant only exhibits a fuel burn increase of about 1.6% and a 0.9% increase in NO_x emissions.

Table 5-3: Climb fuel burn and NO_x emissions comparison (short range flight)

Climb	Fuel burned [kg]			NO_x emitted [kg]		
1800 km	**Clean**	**Degraded**	**Deviation [%]**	**Clean**	**Degraded**	**Deviation [%]**
CUSA-S	1571.2	1596.5	1.6%	25.1	25.3	0.9%
CUSA-M	1689.3	1779.6	5.1%	28.8	30.5	5.6%
CUSA-L	1895.3	1988.7	4.7%	33.8	35.9	5.8%

5.4 Short Range Results Comparison

The results for the short range flight mission scenarios with clean, degraded and derated engines are listed in tables 5-4, 5-5 and 5-6 for the three different aircraft variants. For the CUSA-S aircraft the increase in take-off fuel and take-off NO_x emissions due to engine degradation is approximately 3.6%. The increase in main block fuel is about 1.1% and the increase in total block NO_x emissions is about 0.4%. The introduction of a take-off thrust decrease (derate) reduces the take-off fuel burn by about 20% and reduces take-off NO_x emissions by about 33%. The main block fuel and total block NO_x emissions remain almost equal in the derated scenario. The results are summarised in in table 5-4 below.

Table 5-4: CUSA-S short range mission results

Mission	**1800 KM**		
Aircraft	**CUSA-S (CU2STF-LT engine)**		
Engine condition	**Clean**	**Degraded**	**Degraded + T/O derate**
Take-off fuel [kg]	135.1	140.2	112.6
Take-off NO_x [kg]	3.2	3.3	2.2
Main block fuel [kg]	5545.5	5608.0	5609.4
Total block NO_x [kg]	70.16	70.47	70.50

Correspondingly, for the CUSA-M aircraft the increase in take-off fuel and take-off NO_x emissions due to engine degradation is approximately 5.6%. The increase in main block fuel amounts to about 5.3% and the increase in total block NO_x emissions is about 5.7%. In this case the take-off thrust derate reduces take-off fuel burn by about 21% and reduces take-off NO_x emissions by nearly 35%. The main block fuel and total block NO_x emissions remain almost constant. The results are summarised in table 5-5 below.

Table 5-5: CUSA-M short range mission results

Mission	**1800 KM**		
Aircraft	**CUSA-M (CU2STF-MT engine)**		
Engine condition	**Clean**	**Degraded**	**Degraded + T/O derate**
Take-off fuel [kg]	156.8	166.2	131.1
Take-off NO_x [kg]	4.4	4.7	3.0
Main block fuel [kg]	5863.2	6189.4	6191.2
Total block NO_x [kg]	79.1	83.9	83.9

For the largest aircraft variant CUSA-L the increase in take-off fuel and take-off NO_x emissions due to engine degradation amount to 4.5%. The increase in main block fuel is about 4.9% and the increase in total block NO_x emissions is approximately 5.6%. The effect of take-off thrust reduction causes the take-off fuel burn to drop by almost 23% and causes take-off NO_x emissions to drop by about 41% compared to a full power take-off. The results are summarised in table 5-6 below.

Table 5-6: CUSA-L short range mission results

Mission	**1800 KM**		
Aircraft	**CUSA-L (CU2STF-HT engine)**		
Engine condition	**Clean**	**Degraded**	**Degraded + T/O derate**
Take-off fuel [kg]	202.9	212.6	164.2
Take-off NO_x [kg]	7.6	7.9	4.7
Main block fuel [kg]	6597.6	6934.9	6937.8
Total block NO_x [kg]	94.9	100.5	100.6

To highlight the fuel burn characteristic in the course of the total flight distance figures 5-7, 5-8 and 5-9 below compare the total fuel burn of the clean engine configuration with the degraded engine configuration for each aircraft variant. The negative effect of degradation accumulates with increasing cruise duration and leads to the characteristic fuel burned curves which progressively diverge over time. The effect is hardly noticeable for the CUSA-S aircraft variant but is pronounced for the largest aircraft variant CUSA-L as illustrated in figure 5-9. This is because the CUSA-S aircraft is the lightest variant, carries the least payload and thus has the lowest thrust requirements compared to the CUSA-M and CUSA-L variants. This in turn attenuates the effect of degradation on the engine performance which is reflected in the total fuel burn.

For the sake of completeness, TET variations throughout the total flight for the CUSA-L aircraft with clean and degraded engine configuration are shown in figure 5-10. Similar trends for TET variations can be observed for the CUSA-M and CUSA- S aircraft variants and detailed plots are listed in appendix A.2.1.

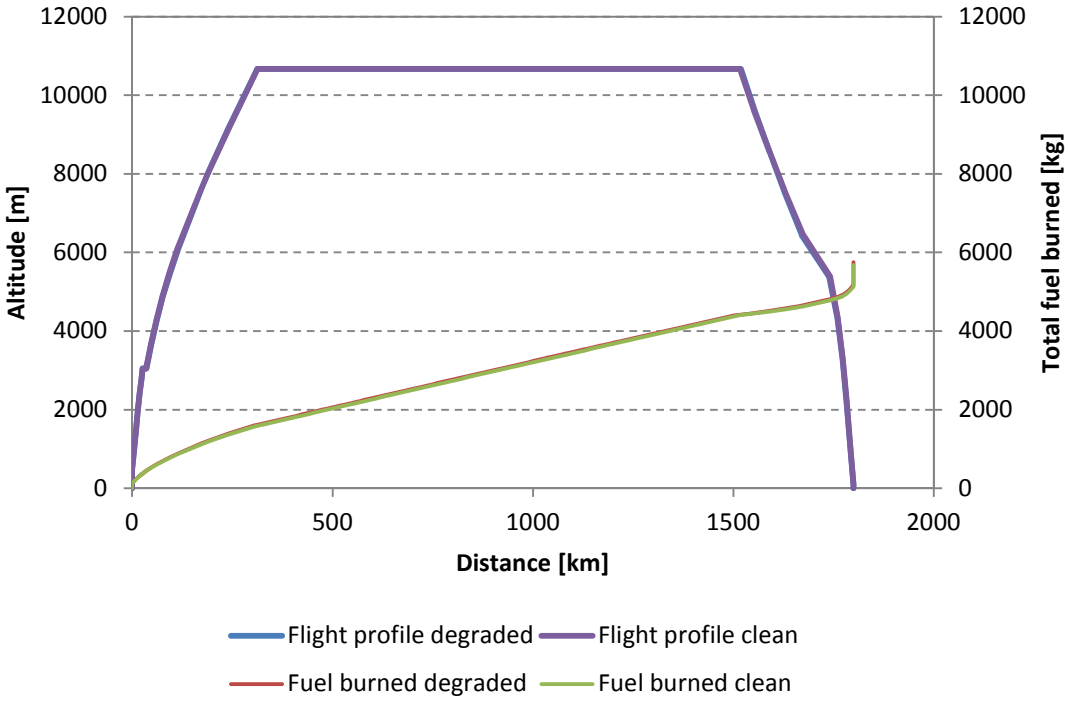

Figure 5-7: CUSA-S with CU2STF-LT

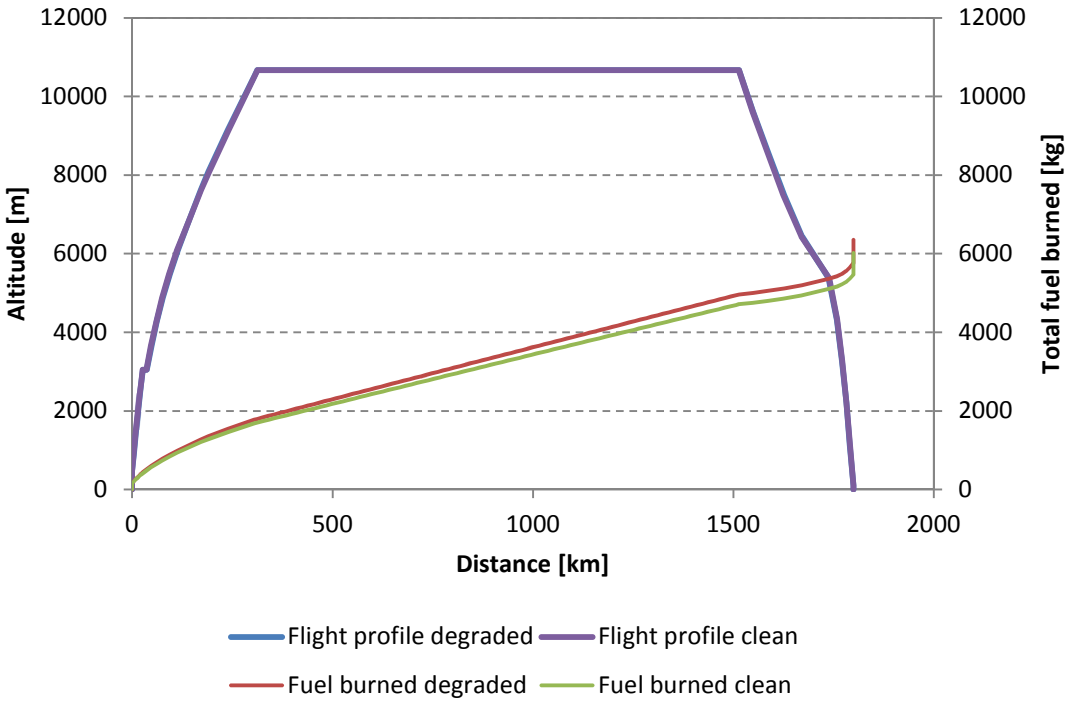

Figure 5-8: CUSA-M with CU2STF-MT

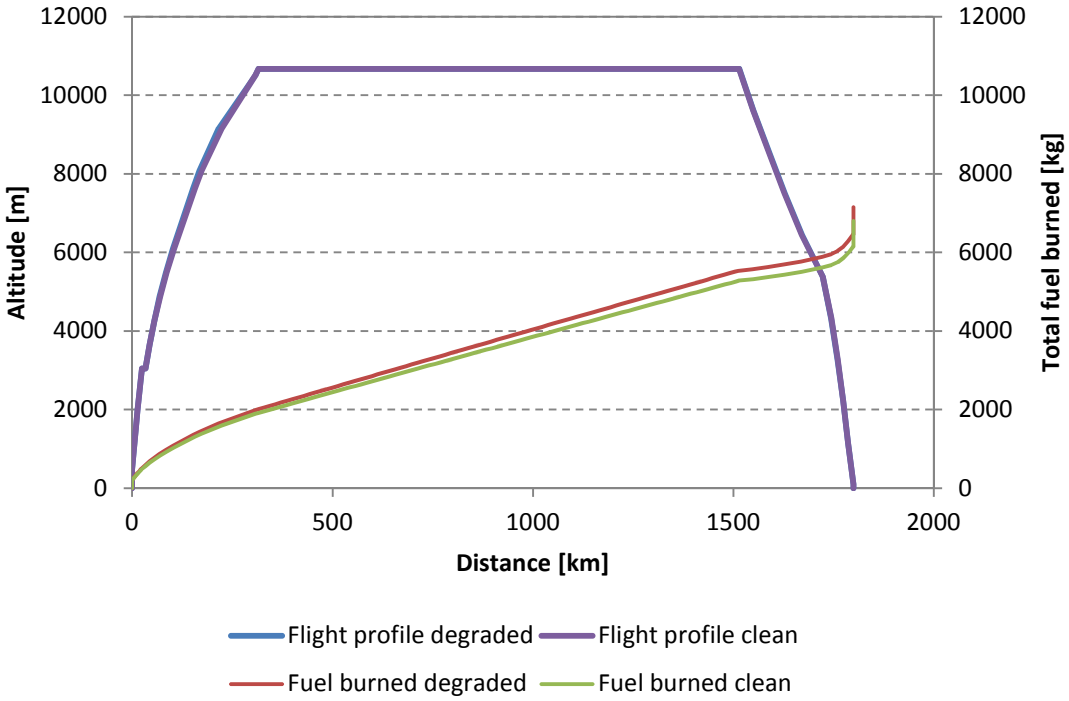

Figure 5-9: CUSA-L with CU2STF-HT

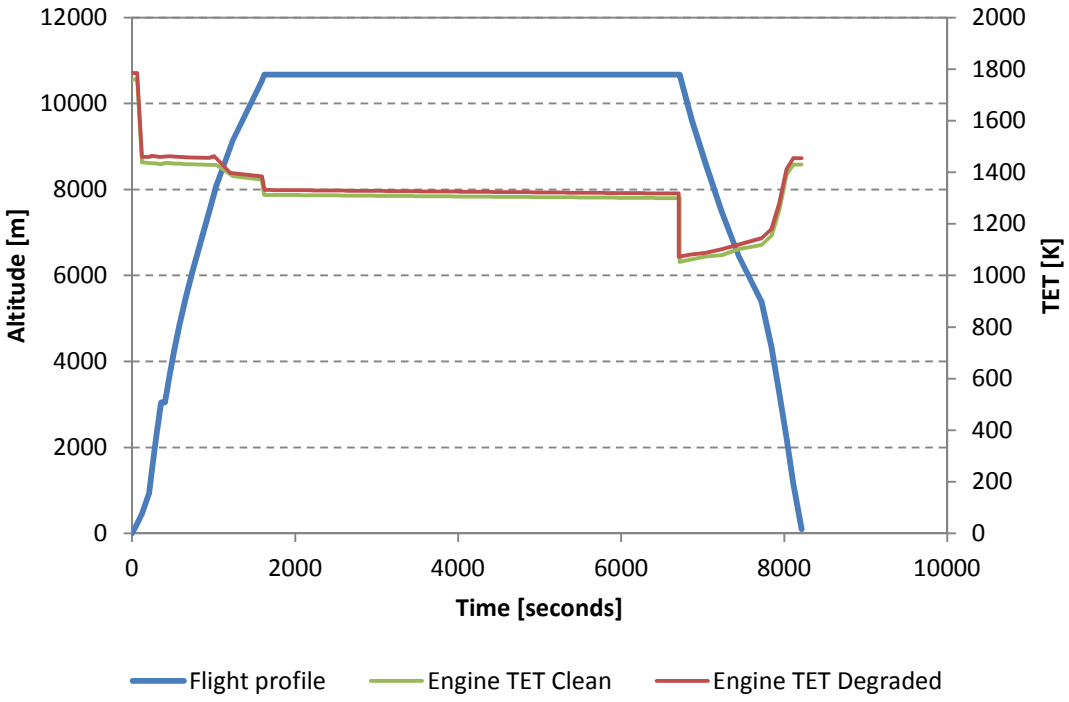

Figure 5-10: CUSA-L with CU2STF-HT engine (clean and degraded)

Table 5-7 illustrates the fuel economy, PFEE (Payload Fuel Energy Efficiency) and PEE (Payload Emissions Efficiency) comparison for the short range (1800 km) mission. The fuel economy is given as distance in kilometre per every megajoule of fuel energy used. The Payload Fuel Energy Efficiency is given as kilogram payload and kilometre travelled per every megajoule of fuel energy used. The Payload Emissions Efficiency is given as gram of NO_x emitted per kilogram payload and kilometre travelled. It can be observed that the fuel economy decreases with increasing aircraft size since only the distance travelled is taken into account. The PFEE however also accounts for the payload moved over the distance travelled and thus its value is increasing with aircraft size. In terms of emissions performance it can be seen that the amount of NO_x emitted decreases with aircraft size while engine degradation adversely affects NO_x emissions.

Table 5-7: Fuel Economy, PEE and PFEE comparison for the short range mission

Aircraft	Fuel Economy [km/MJ]	PFEE [kg*km/MJ]	PEE [g(NO_x)/kg/km]
CUSA-S (clean)	0.0077	82.41	3.66
CUSA-M (clean)	0.0073	94.29	3.41
CUSA-L (clean)	0.0065	103.35	3.31
CUSA-S (degraded)	0.0076	81.50	3.67
CUSA-M (degraded)	0.0069	89.32	3.61
CUSA-L (degraded)	0.0062	98.32	3.51

A direct comparison of the three aircraft variants in terms of total mission fuel burn and total NO_x emissions for the clean and degraded configuration is listed in table 5-8. For the CUSA-S aircraft, fuel burn increases by about 1.1% and NO_x emissions by 0.4%. The CUSA-M aircraft exhibits a fuel burn increase by about 5.3% and a NO_x emissions increase by about 5.7%. For the largest aircraft variant, CUSA-L, fuel burn increases by 4.9% and NO_x emissions rise by about 5.6%.

Table 5-8: Total fuel burn and NO_x emissions comparison (short range flight)

Total flight	Fuel burned [kg]			NO_x emitted [kg]		
1800 km	**Clean**	**Degraded**	**Deviation [%]**	**Clean**	**Degraded**	**Deviation [%]**
CUSA-S	5545.5	5608.0	1.1%	70.2	70.5	0.4%
CUSA-M	5863.2	6189.4	5.3%	79.1	83.9	5.7%
CUSA-L	6597.6	6934.9	4.9%	94.9	100.5	5.6%

Furthermore, an overview of the short mission take-off performance characteristics of each aircraft variant is shown in figures 5-11, 5-12 and 5-13. Figure 5-11 shows the take-off distance in kilometres required by each aircraft variant. There is only a negligible difference in take-off distance observed between the clean and degraded configuration, while the engine take-off derate shows to have a significant effect on the distance travelled. The take-off distance in this case then increases for all aircraft variants by about 12%.

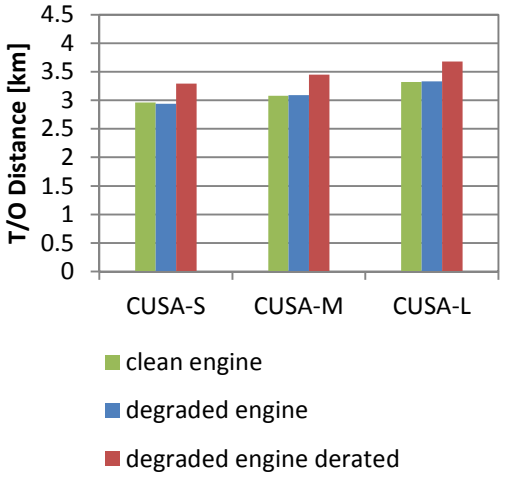

Figure 5-11: T/O distance comparison

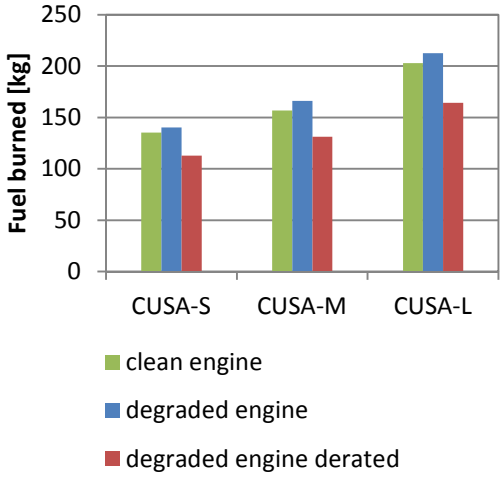

Figure 5-12: T/O fuel burn comparison

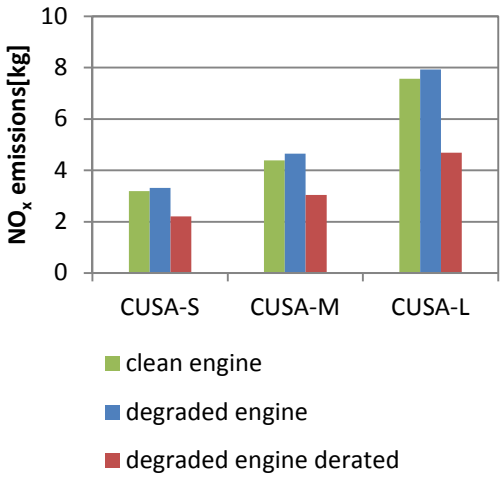

Figure 5-13: T/O NO_x emissions comparison

Finally, a comparison of the take-off fuel burn is illustrated in figure 5-12. As can be seen, engine degradation has an adverse effect on take-off fuel burn for all three aircraft variants. Fuel burn increases by about 3-6% depending on the specific aircraft variant. The introduction of a take-off thrust derate on the other hand significantly decreases take-off fuel burn. Fuel burn decreases by about 19-23% depending on the aircraft variant. Correspondingly, take-off NO_x emissions increase for the degraded configuration while the take-off thrust derate significantly reduces NO_x emissions. NO_x emissions decrease by 33-41% depending on the aircraft variant.

To conclude the short range mission comparisons, figures 5-14 and 5-15 show a direct comparison between the three aircraft variants and their fuel burn and NO_x emissions performance in the clean and degraded configuration.

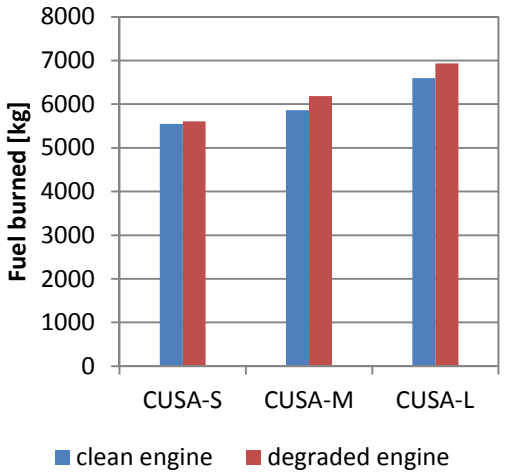

Figure 5-14: Fuel burned comparison

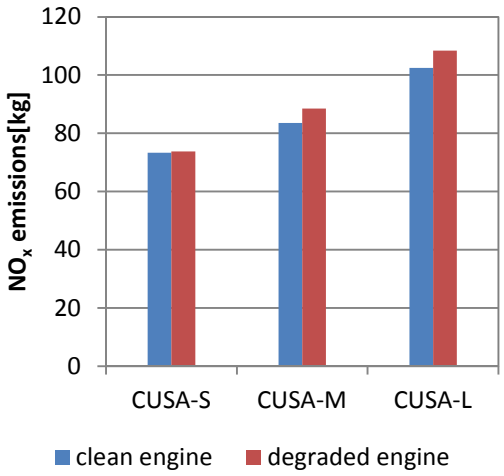

Figure 5-15: NO_x emissions comparison

5.5 Medium Range Flight (Clean Engine)

The third case as part of this analysis is the 4600 km medium range flight mission with a clean engine configuration. Again, all three aircraft variants CUSA-S, CUSA-M and CUSA-L with its respective engine variants CU2STF-LT, CU2STF-MT and CU2STF-HT performed the same flight mission.

5.5.1 General Description

A brief listing of the default settings of the 4600 km medium range mission with the clean engines is provided in table 5-8. It follows the same structure as the previous two scenarios.

Table 5-9: Medium range mission characteristics (clean engine)

Mission	**4600 km (clean engine)**		
Aircraft	**CUSA-S**	**CUSA-M**	**CUSA-L**
Payload [kg]	10664	12900	15910
Cruise Mach number [-]	0.785		
Cruise altitude [m]	10668		
Flight duration [min]	331.6	331.6	331.9

5.5.2 Results

Figure 5-14 shows the calculated medium range mission trajectory for the CUSA-L aircraft variant and the engine fuel flow trend throughout the flight. It can be seen that the trajectory flown follows the same basic trend as the short range mission profile shown in figure 5-1. The engine fuel flow trend at take-off, climb and cruise also follows a comparable pattern. Again, engine fuel flow values and subsequently TET during descent reach values equivalent to an engine power setting of about 85%. This is due to the fact that the engine power settings for the final segments of the descent have been selected to be at their maximum permissible values. Figure 5-2 shows the engine TET trend along the flight path for the same aircraft variant following a corresponding pattern.

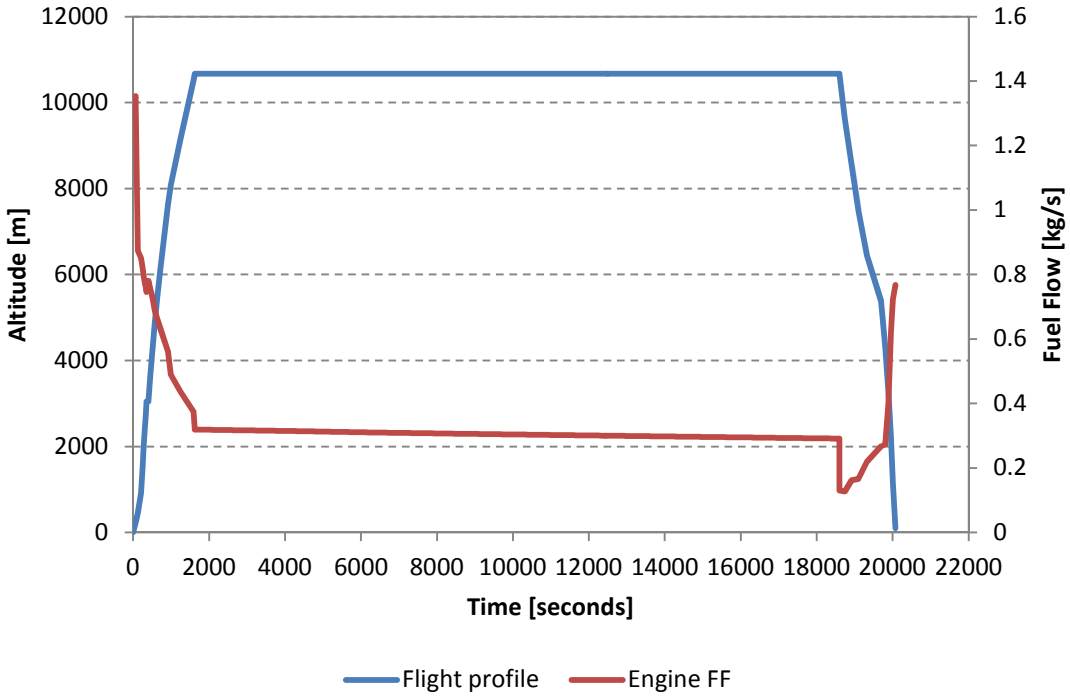

Figure 5-16: CUSA-L engine FF variation during flight (4600 km)

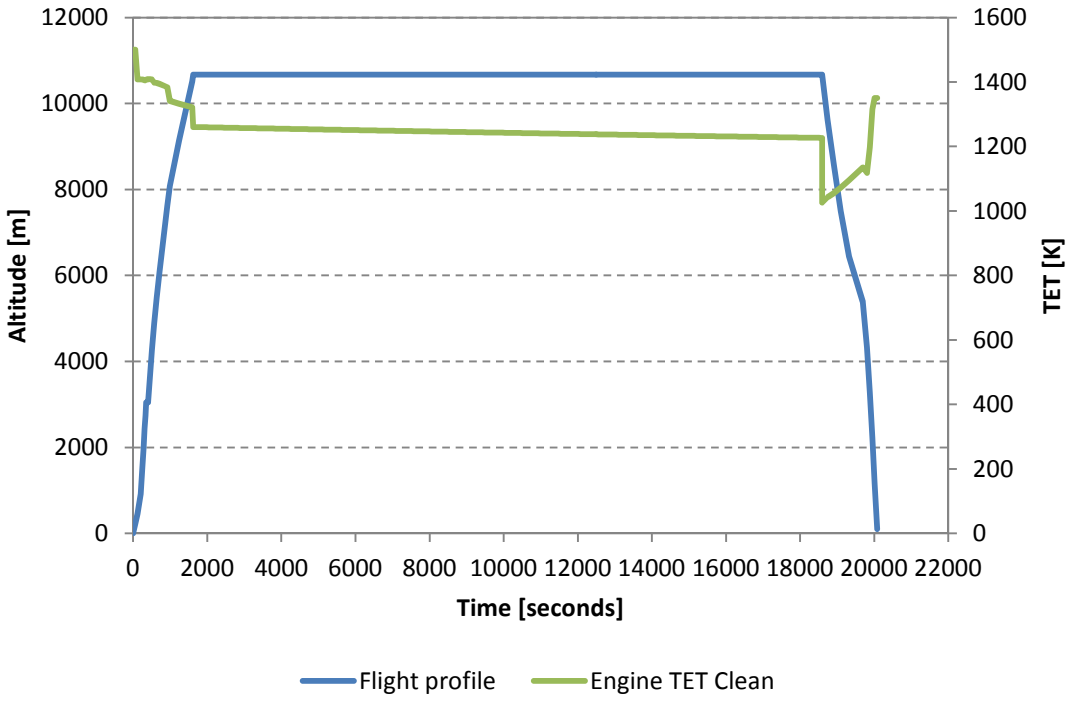

Figure 5-17: CUSA-L engine TET variation during flight (4600 km)

The results for the two other aircraft variants CUSA-S and CUSA-M can be found in appendix A.3.1. They follow the same pattern in all flight phases as the results of the CUSA-L while differences in peak values for fuel flow and TET can be observed due to the increased thrust requirements caused by the increased aircraft weight and the increase in initial fuel weight due to the longer mission range.

5.6 Medium Range Flight (Degraded Engine)

The fourth case evaluated is the 4600 km medium range flight mission with a degraded engine configuration. Again, all three aircraft variants CUSA-S, CUSA-M and CUSA-L with its respective engine variants CU2STF-LT, CU2STF-MT and CU2STF-HT performed the same flight mission.

5.6.1 General Description

The default settings of the 4600 km short range mission with the degraded engines are listed in table 5-10 and follow the structure of the clean engine configuration as described in chapter 5.5.1.

Table 5-10: Medium range mission characteristics (degraded engine)

Mission	**4600 km (degraded engine)**		
Aircraft	**CUSA-S**	**CUSA-M**	**CUSA-L**
Payload [kg]	10664	12900	15910
Cruise Mach number [-]	0.785		
Cruise altitude [m]	10668		
Flight duration [min]	331.5	331.5	332.0

5.6.2 Results

Figure 5-18 shows the take-off and climb profile of the CUSA-M aircraft and the corresponding engine TET in the clean and degraded configuration. The TET is kept nearly constant for the first part of the climb while the TET is then reduced during the second part of the climb. The difference in TET between the clean and degraded engine is about 35K for the first 12 minutes of the climb and about 20K for the remaining 11 minutes. The TET is directly related to the selected engine power setting which is shown in figure 5-19 for the climb phase.

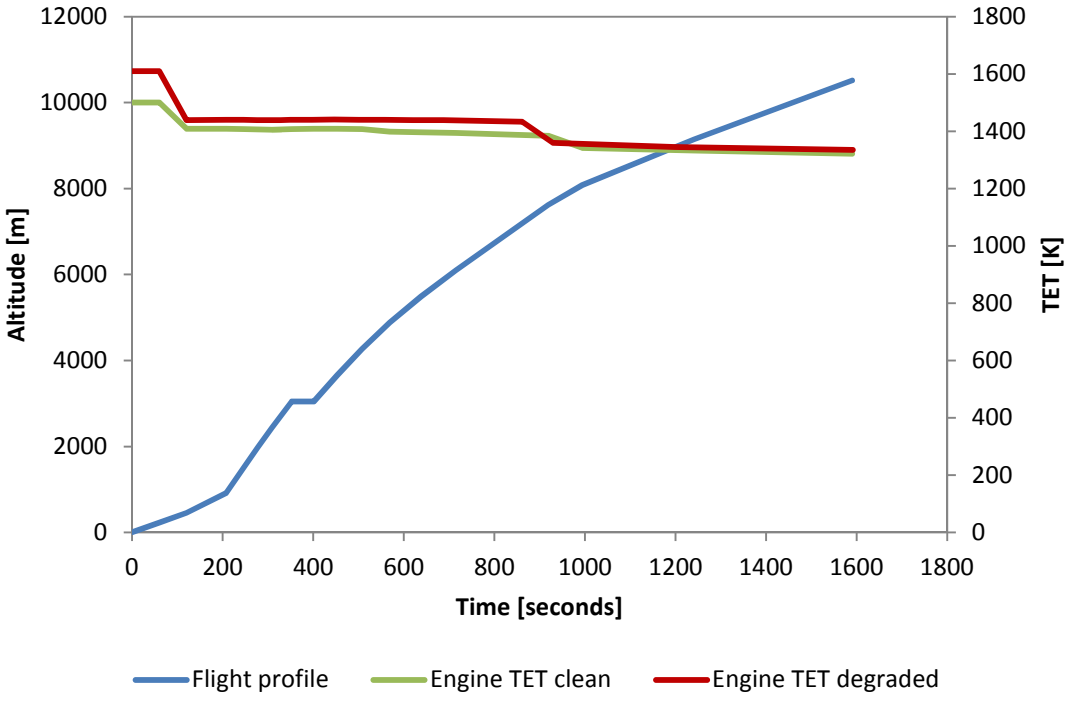

Figure 5-18: CUSA-M engine TET variation during climb

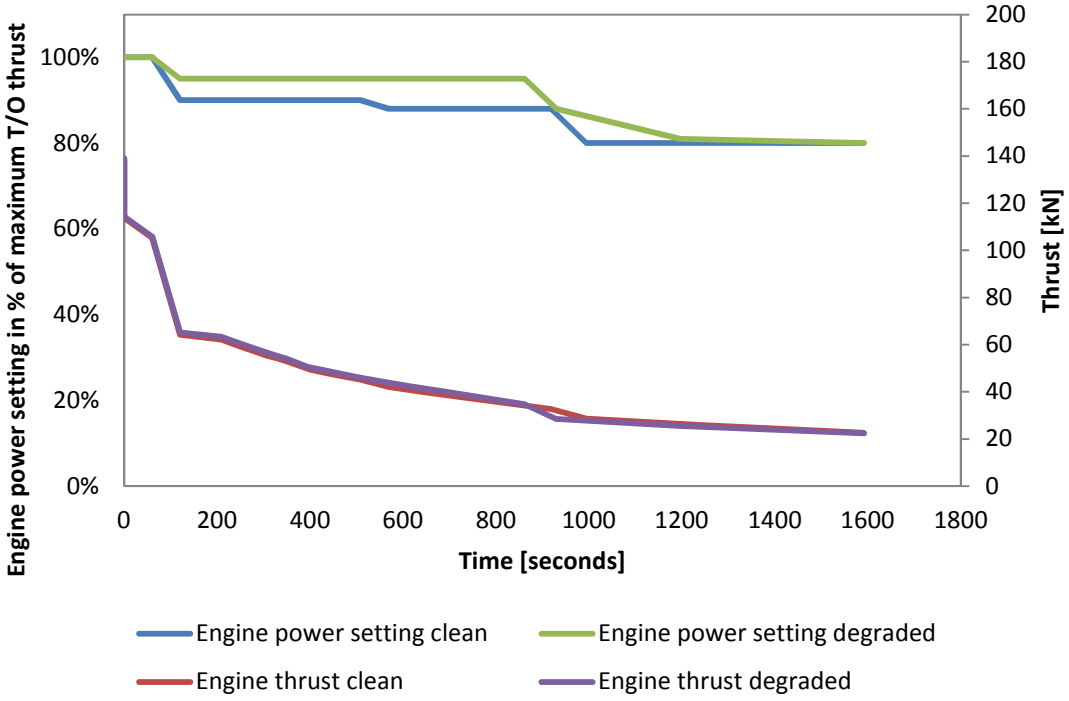

Figure 5-19: CUSA-M engine power setting and thrust during climb

In this figure, the engine power setting in percent of the maximum take-off thrust is plotted against the engine thrust for the clean and degraded engine configuration. In order to maintain an equivalent flight path (equivalent climb duration) for both configurations, the engine power setting for the degraded engine had to be increased to maintain the same thrust level for the climb as the clean engine configuration. It can also be noticed that the engine power setting for the last 11 minutes of the climb was changed to a lower setting of 80% later than for the clean engine. This is the reason for the small step in the engine thrust curve for the degraded engine. These results are also in line with the TET trend shown in previous figure 5-18. Similar trends for TET and thrust levels can be observed for the CUSA-M and CUSA- S aircraft variants.

The increase in TET to maintain the thrust level translates into an increase in fuel burn and consequently causes the NO_x emissions to increase. Table 5-11 lists the percentage increase in fuel burn and NO_x emissions throughout the climb for the medium range mission for all three aircraft variants. The CUSA-L aircraft with degraded engines will burn about 4.9% more fuel compared to the clean engine configuration. At the same time the NO_x emissions will increase by about 5.1%. The CUSA-M aircraft climb performance shows the highest increase in fuel burn of about 5.2% and NO_x emissions of about 6.8% while the CUSA-S aircraft variant only exhibits a fuel burn increase of about 1.6% and a 1.8% increase in NO_x emissions.

Table 5-11: Climb fuel burn and NO_x emissions comparison (medium range flight)

Climb	Fuel burned [kg]			NO_x emitted [kg]		
4600 km	**Clean**	**Degraded**	**Deviation [%]**	**Clean**	**Degraded**	**Deviation [%]**
CUSA-S	1658.3	1685.3	1.6%	28.3	28.9	1.8%
CUSA-M	1785.1	1882.2	5.2%	32.8	35.2	6.8%
CUSA-L	2037.6	2143.3	4.9%	39.6	41.7	5.1%

5.7 Medium Range Results Comparison

The results for the medium range flight mission scenarios with clean, degraded and derated engines are listed in tables 5-12, 5-13 and 5-14 for the three different aircraft variants. The increase in take-off fuel and take-off NO_x emissions due to engine degradation is equivalent to the percentage values presented for the short range mission. This is due to the fact that the take-off calculations are only approximated by the aircraft performance model (Hermes) and the take-off duration is fixed at 1 minute. The increase in main block fuel for the CUSA-S aircraft is about 0.7% and the increase in total block NO_x emissions is about 0.1%. The introduction of a take-off thrust decrease (derate) reduces the take-off fuel burn by about 20% and reduces take-off NO_x emissions by about 33% which is again equivalent to the short range mission values. The main block fuel and total block NO_x emissions remain almost equal in the derated scenario. The results are summarised in in table 5-12 below.

Table 5-12: CUSA-S medium range mission results

Mission	**4600 KM**		
Aircraft	**CUSA-S (CU2STF-LT engine)**		
Engine condition	**Clean**	**Degraded**	**Degraded + T/O derate**
Take-off fuel [kg]	135.1	140.2	112.6
Take-off NO_x [kg]	3.2	3.3	2.2
Main block fuel [kg]	12472.0	12560.6	12564.0
Total block NO_x [kg]	161.2	161.3	161.4

Correspondingly, for the CUSA-M aircraft the increase in take-off fuel and take-off NO_x emissions due to engine degradation is again equivalent to the values of the short range mission. The increase in main block fuel amounts to about 5.1% and the increase in total block NO_x emissions is about 5.9%. Again, the take-off thrust derate reduces take-off fuel burn by about 21% and reduces take-off NO_x emissions by nearly 35% which corresponds to the values of the short range mission. The main block fuel and total block NO_x emissions remain almost constant. The results are summarised in table 5-13 below.

Table 5-13: CUSA-M medium range mission results

Mission	4600 KM		
Aircraft	**CUSA-M (CU2STF-MT engine)**		
Engine condition	**Clean**	**Degraded**	**Degraded + T/O derate**
Take-off fuel [kg]	156.8	166.2	131.1
Take-off NO_x [kg]	4.4	4.7	3.0
Main block fuel [kg]	13288.1	14007.5	14012.0
Total block NO_x [kg]	183.6	195.0	195.1

For the largest aircraft variant CUSA-L the increase in take-off fuel and take-off NO_x emissions corresponds to the short range mission values. The increase in main block fuel is about 4.9% and the increase in total block NO_x emissions is approximately 5.6%. The effect of take-off thrust reduction causes the take-off fuel burn to drop by almost 23% and causes take-off NO_x emissions to drop by about 41% compared to a full power take-off, which again equals the values of the short range mission. The results are summarised in table 5-14 below.

Table 5-14: CUSA-L medium range mission results

Mission	4600 KM		
Aircraft	**CUSA-L (CU2STF-HT engine)**		
Engine condition	**Clean**	**Degraded**	**Degraded + T/O derate**
Take-off fuel [kg]	202.9	212.6	164.2
Take-off NO_x [kg]	7.6	7.9	4.7
Main block fuel [kg]	15067.0	15848.2	15855.9
Total block NO_x [kg]	221.5	234.7	234.9

To highlight the fuel burn characteristic in the course of the total flight distance figures 5-20, 5-21 and 5-22 compare the total fuel burn of the clean engine configuration with the degraded engine configuration for each aircraft variant. Similar to the results of the range mission, the negative effect of degradation accumulates with increasing cruise duration and leads to the characteristic fuel burned curves which progressively diverge over time. The effect is again hardly noticeable for the CUSA-S aircraft variant but is pronounced for the largest aircraft variant CUSA-L as illustrated in figure 5-22. This is because the CUSA-S aircraft is the lightest variant, carries the least payload and thus has the lowest thrust requirements compared to the CUSA-M and CUSA-L variants.

This in turn attenuates the effect of degradation on the engine performance which is reflected in the total fuel burn. In fact, due to the increased range, the effect of degradation on total mission fuel burn becomes less severe since relative time spent in the climb phase, where degradation has a more pronounced effect, becomes less.

For the sake of completeness, TET variations throughout the total flight for the CUSA-M aircraft with clean and degraded engine configuration are shown in figure 5-23. Similar trends for TET variations can be observed for the CUSA-M and CUSA- S aircraft variants and detailed plots are listed in appendix A.3.1.

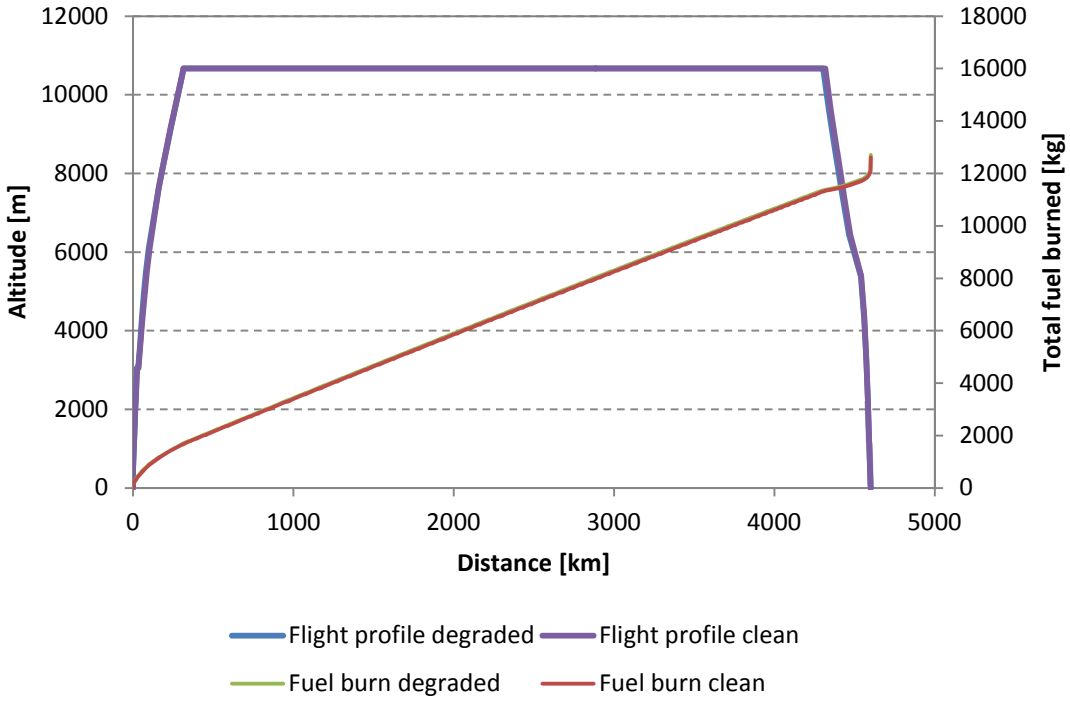

Figure 5-20: CUSA-S with CU2STF-LT

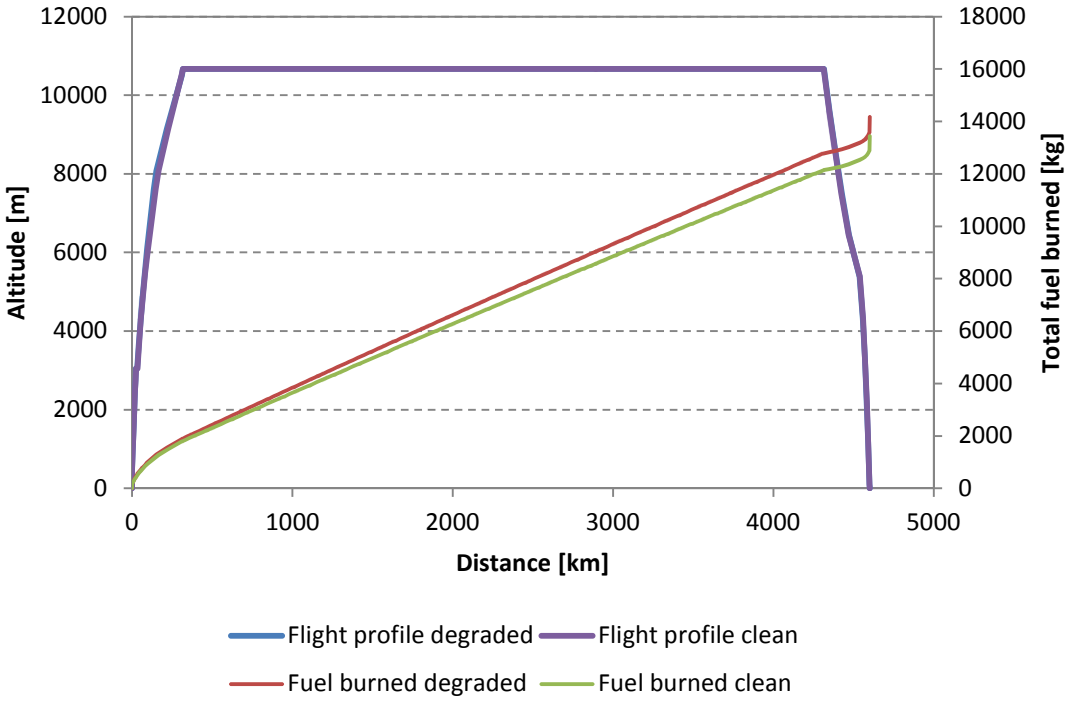

Figure 5-21: CUSA-M with CU2STF-MT

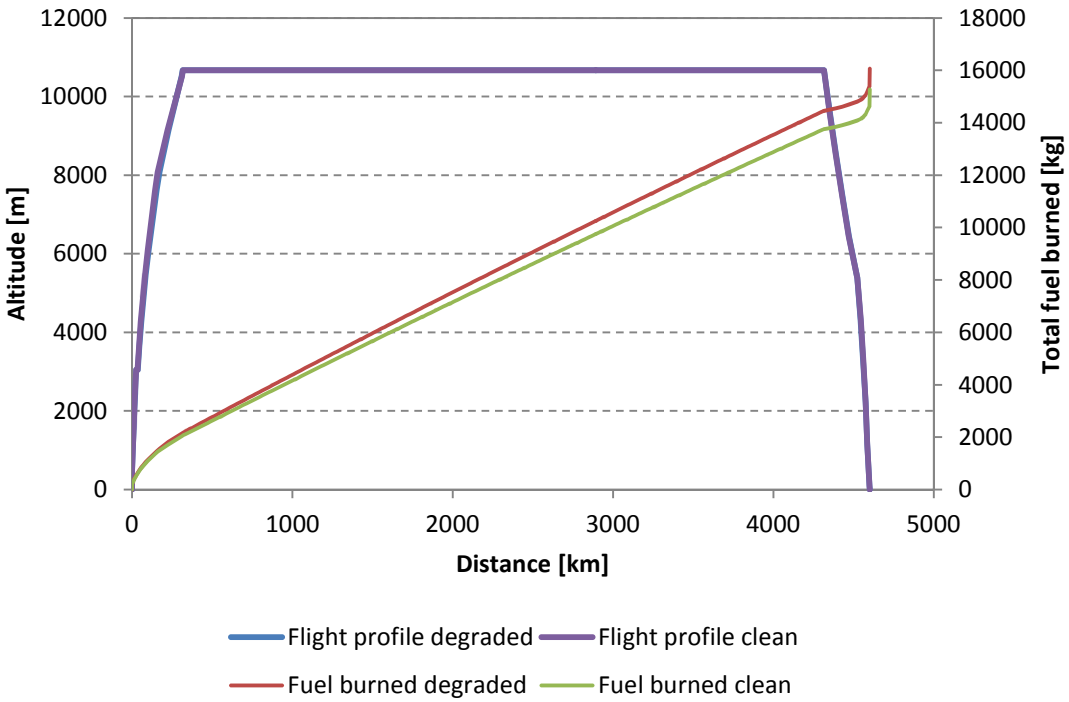

Figure 5-22: CUSA-L with CU2STF-HT

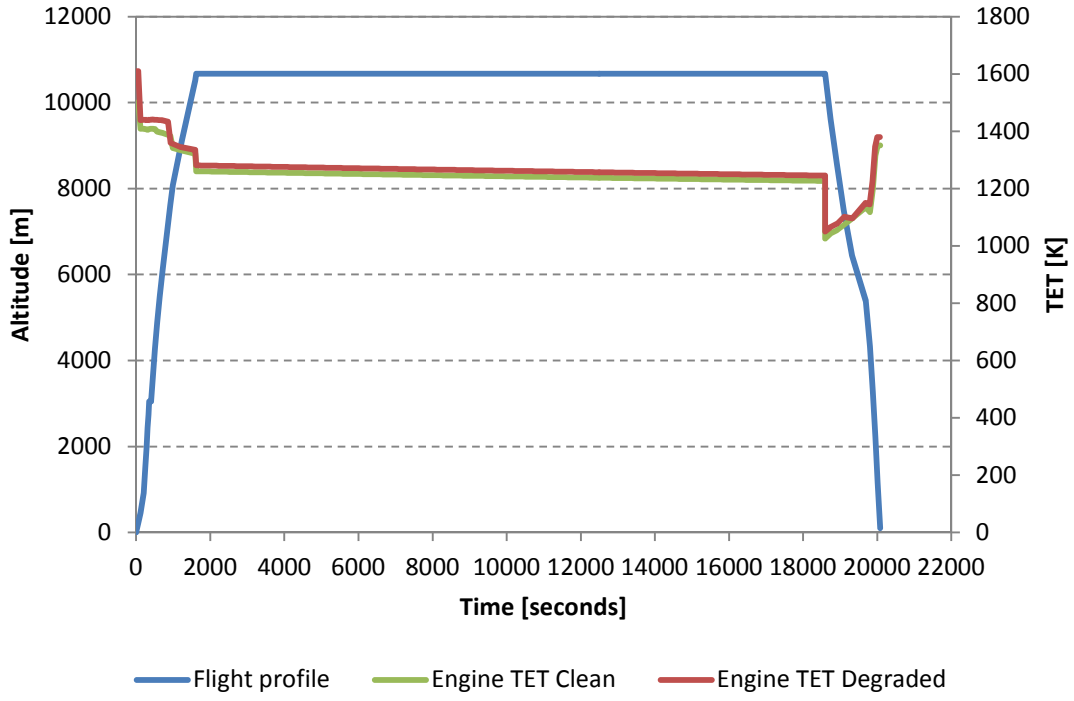

Figure 5-23: CUSA-M with CU2STF-MT engine (clean and degraded)

Table 5-15 illustrates the fuel economy, PFEE (Payload Fuel Energy Efficiency) and PEE (Payload Emissions Efficiency) comparison for the short range (4600 km) mission. The fuel economy is given as distance in kilometre per every megajoule of fuel energy used. The Payload Fuel Energy Efficiency is given as kilogram payload and kilometre travelled per every megajoule of fuel energy used. The Payload Emissions Efficiency is given as gram of NO_x emitted per kilogram payload and kilometre travelled. Similar to the short range mission results, it can be observed that the fuel economy is decreasing with increasing aircraft size since only the distance travelled is taken into account. The PFEE however also accounts for the payload moved over the distance travelled and thus its value is increasing with aircraft size. In terms of emissions performance it can be seen that the amount of NO_x emitted decreases only for the CUSA-M and CUSA-L aircraft variant. When comparing the absolute PEE values with the results of the short range mission it can be noted that the amount of NO_x emissions per kilogram and kilometre declines.

Table 5-15: Fuel Economy, PEE and PFEE comparison for the medium range mission

Aircraft	Fuel Economy [km/MJ]	PFEE [kg*km/MJ]	PEE [g NO_x/kg/km]
CUSA-S (clean)	0.0088	93.65	3.29
CUSA-M (clean)	0.0082	106.32	3.09
CUSA-L (clean)	0.0073	115.65	3.03
CUSA-S (degraded)	0.0087	92.99	3.29
CUSA-M (degraded)	0.0078	100.86	3.29
CUSA-L (degraded)	0.0069	109.95	3.21

A direct comparison of the three aircraft variants in terms of total mission fuel burn and total NO_x emissions for the clean and degraded configuration is listed in table 5-16. For the CUSA-S aircraft, fuel burn increases by about 0.7% and NO_x emissions by 0.1%. The CUSA-M aircraft exhibits a fuel burn increase by about 5.1% and a NO_x emissions increase by about 5.9%. For the largest aircraft variant, CUSA-L, fuel burn increases by 4.9% and NO_x emissions rise by about 5.6%.

Table 5-16: Fuel burn and NO_x emissions comparison (medium range flight)

Total flight	Fuel burned [kg]			NO_x emitted [kg]		
4600 km	**Clean**	**Degraded**	**Deviation [%]**	**Clean**	**Degraded**	**Deviation [%]**
CUSA-S	12472.0	12560.6	0.7%	161.2	161.3	0.1%
CUSA-M	13288.1	14007.5	5.1%	183.6	195.0	5.8%
CUSA-L	15067.0	15848.2	4.9%	221.5	234.7	5.6%

Furthermore, an overview of the medium mission take-off performance characteristics of each aircraft variant is shown in figures 5-24, 5-25 and 5-26. Figure 5-24 shows the take-off distance in kilometres required by each aircraft variant. The take-off distance remains almost equal when compared between the clean and degraded configuration, while the engine take-off derate shows to have a significant effect on the distance travelled. The take-off distance in this case then increases for all aircraft variants by about 14%.

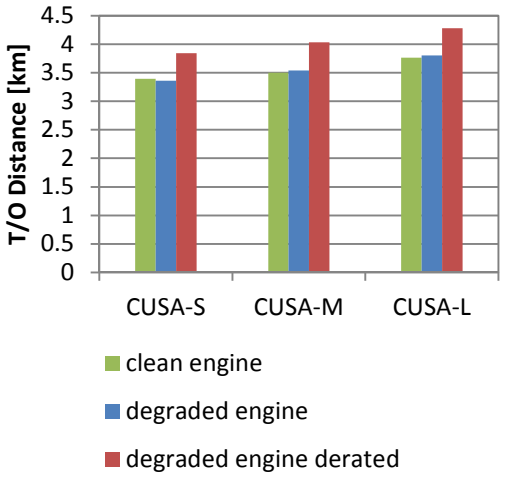

Figure 5-24: T/O distance comparison

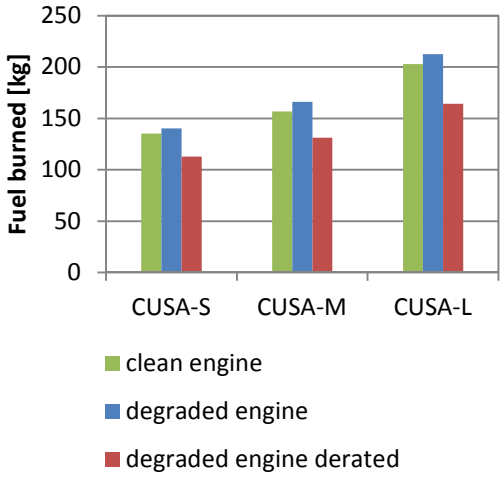

Figure 5-25: T/O fuel burn comparison

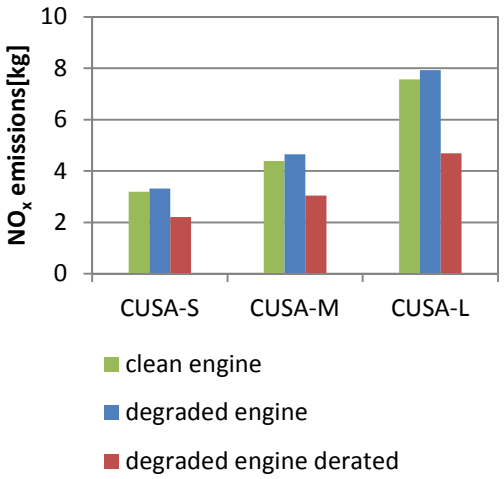

Figure 5-26: T/O NO_x emissions comparison

Finally, a comparison of the take-off fuel burn is illustrated in figure 5-25. As can be seen, engine degradation has an adverse effect on take-off fuel burn for all three aircraft variants. Fuel burn increases by about 3-6% depending on the specific aircraft variant. The introduction of a take-off thrust derate on the other hand significantly decreases take-off fuel burn. Fuel burn decreases by about 19-23% depending on the aircraft variant. Correspondingly, take-off NO_x emissions increase for the degraded configuration while the take-off thrust derate significantly reduces NO_x emissions. NO_x emissions decrease by 33-41% depending on the aircraft variant.

To conclude the medium range mission comparisons, figures 5-27 and 5-28 show a direct comparison between the three aircraft variants and their fuel burn and NO_x emissions performance in the clean and degraded configuration.

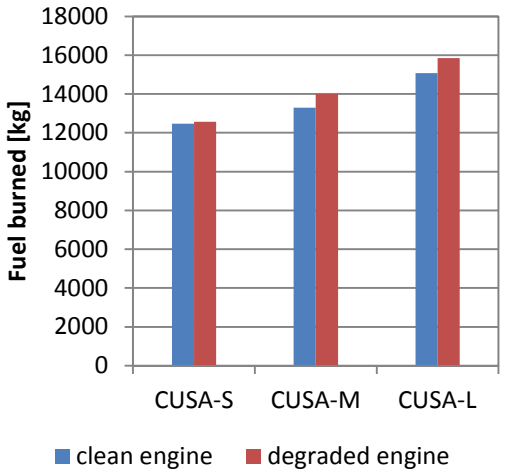

Figure 5-27: Fuel burned comparison

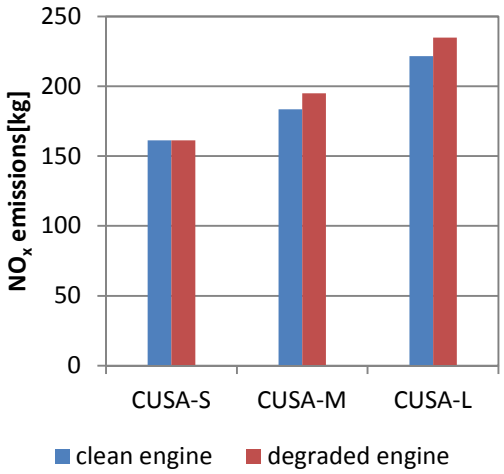

Figure 5-28: NO_x emissions comparison

6 Trajectory Optimisation Studies and Results

This chapter addresses the two-objective trajectory optimisation study which is based on the GATAC optimisation framework introduced in section 4.4. Two flight missions (short and medium range) of the CUSA-M aircraft have been considered for optimisation which base on the aircraft trajectories analysed in the previous chapter 5 and the assumptions and statements defined in section 3.2. The optimisation process and the framework are setup as described in section 4.5.

6.1 Summary of Case Studies

Two different scenarios have been analysed for each mission: Fuel vs. time and fuel vs. NO_x. Both scenarios aim at identifying flight mission trade-offs between total fuel burned and total flight time, and between total fuel burned and total NO_x emissions respectively. The optimisation variables, which represent explicit constraints of the optimisation problem, and their applicable boundaries, are listed in table 6-1.

Table 6-1: GATAC decision variables for climb and cruise

Decision variable	Lower bound	Upper bound
Altitude 1 [m]	457	1125
Altitude 2 [m]	1126	1792
Altitude 3 [m]	1793	2459
Altitude 4 [m]	2460	3126
Altitude 5 [m]	3127	3128
Altitude 6 [m]	3129	3130
Altitude 7 [m]	3131	3795
Altitude 8 [m]	3796	4462
Altitude 9 [m]	4463	5129
Altitude 10 [m]	5130	5796
Altitude 11 [m]	5797	6463
Altitude 12 [m]	6464	7130
Altitude 13 [m]	7131	7797
Altitude 14 [m]	7798	8464
Altitude 15 [m]	8465	9131
Altitude 16 [m]	9132	9999
Cruise altitude [m]	10059	11000

The array of each climb altitude has been set at 666 m from altitude 1 to altitude 15. For altitude 16 the array has been set at 867 m. The array of the final cruise altitude has been set between 10059 m and 11000 m. The 60 m gap between the last climb altitude and the minimum cruise altitude results from the adaption of the climb profile from the studies carried out in chapter 5. An additional variable (altitude 17) had been implemented into the optimisation framework but is not taken into account during the trajectory calculations. The maximum cruise altitude has been limited to 11000 m to stay well below critical altitudes at which outside temperatures and thus the speed of sound decrease to values low enough to affect subsonic aircraft operability. In addition, the off-design performance of engine models adapted for this study has only been validated up to an altitude of 11000 m. Furthermore, three different Mach number cases have been analysed (0.75, 0.80 and 0.85). Engine performance data has then been created once for each Mach number case as input for the optimiser. This setup ensures that feasible trajectories with a constant altitude increase are computed by the optimiser and it also takes into account the constraints of the utilised optimisation framework.

For the purpose of brevity, in this chapter, flights that were optimised to minimise the total amount of fuel burned for a given mission are denominated as minimum fuel flight and, correspondingly, flights that were optimised to minimise the total flight time of a given mission are denominated as minimum time flight.

6.2 Short Range Multi Objective Optimisation

The first scenario addresses the optimisation of the short range mission with regards to the two objectives, (1) total fuel burned and (2) total flight time. The second scenario then addresses the optimisation of the short range mission with regards to (1) total fuel burned and (2) total NO_x emissions generated.

6.2.1 General Description

The first case aims to optimise a short range (1800 km) aircraft mission in order to minimise total fuel burned or to minimise total flight time. This is achieved by altering

the aircraft climb profile (altitudes of 16 climb segments) and cruise altitude in such a way that either total fuel burned or total flight time becomes minimum. The optimisation is carried out three times at three different fixed Mach numbers (0.75, 0.80 and 0.85).

The second case then looks at the optimisation of the short range mission in order to minimise fuel burned or to minimise NO_x emissions. It uses the same methodology as has been deployed on the fuel vs. time optimisation case but only two different Mach numbers (0.75 and 0.85) are considered.

6.2.2 Fuel vs. Time Optimisation Results

Figure 6-1 shows the Pareto fronts for the short range mission of the CUSA-M aircraft performing the 1800 km mission at varying climb altitudes (altitude 1 to altitude 16 as listed in table 6-1), varying cruise altitudes (10059 m - 11000 m) and 3 different cruise Mach numbers (0.75, 0.80 and 0.85) and illustrates the influence on flight time and fuel burned. Each Pareto front comprises a set of non-dominated solutions which represents a trade-off between flight time and fuel burned. The shortest mission flight time (124.2 min) requires flying at the lowest possible altitude (10059 m) with the highest possible Mach number of 0.85. The lowest mission fuel burn (5587 kg) requires flying at the highest possible altitude (11000 m) with the lowest possible Mach number of 0.75. Increasing Mach number from 0.75 by 0.05 increments up to 0.85 reduces flight time by about 6 minutes per each increment. Figure 6-2 illustrates the corresponding flight profiles (climb, cruise and descent) and fuel burn curves for the minimum time and minimum fuel case. The solid green profile represents the minimum fuel trajectory and the dashed green line shows the corresponding fuel burn accumulation along the flight. The minimum time trajectory is plotted in red lines accordingly. It can be seen that the minimum fuel flight reaches its final cruise altitude after having travelled a shorter range than the minimum fuel flight. Since the final cruise altitude of the minimum fuel flight is higher than the cruise altitude of the minimum time flight, a higher climb gradient is recognised. Both flight profiles shown in figure 6-2 contain the information about the decision variables used by the GATAC

optimiser. The aircraft performance model (Hermes) uses the climb altitudes as inputs to calculate the individual range of the climb segments up to the cruise altitude. Since the distance travelled per segment may vary a listing of individual climb altitudes is not shown.

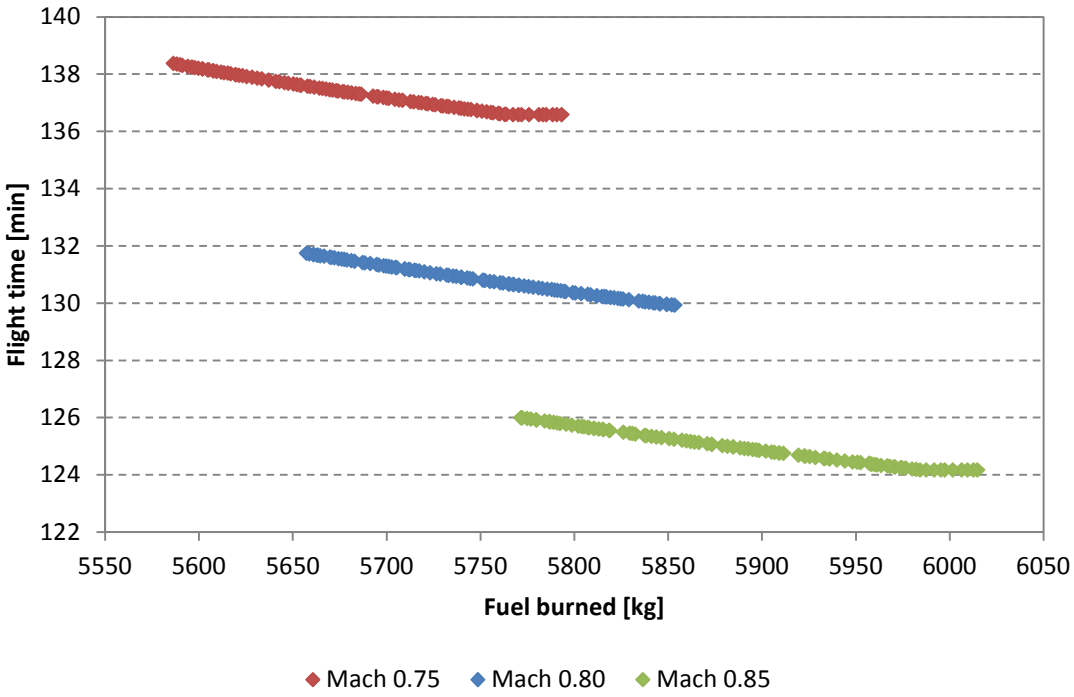

Figure 6-1: Fuel vs. time Pareto fronts for short range mission

Table 6-2 summarises the optimisation objective values (flight time and fuel burned) for the two extreme cases (minimum flight time and minimum fuel burned) as well as the resulting flight trajectory key performance points. In addition, it provides a comparison of those performance points to a reference flight which is based on the "non-optimised" trajectory analysed in previous chapter 5. To allow for a meaningful comparison, the power settings during all climb segments have been adjusted to maximum climb power settings as opposed to the predefined settings used in the "non-optimised" trajectory. Flight time is reduced by 6.7% for the minimum time flight at the expense of 4.4% increase in fuel burn. Fuel burned is reduced by 3.0% for the minimum fuel flight at the expense of a 4.0% increase in flight time. Both flights considered in relation to the reference flight. Moreover, the cruise duration for the

minimum time flight decreased by 7.8% and increased by 7.0% for the minimum fuel flight. Fuel consumption value till TOC for the minimum time flight increased by 1.2% while the same value decreased by 18.0% for the minimum fuel flight.

Table 6-2: Optimisation extreme solutions compared to reference flight (1800 km)

CUSA-M 1800 km	Reference flight	Minimum time flight	Delta [%]	Minimum fuel flight	Delta [%]
Fuel burned [kg]	5760.4	6014.7	4.4	5586.4	-3.0
Flight time [min]	133.1	124.2	-6.7	138.4	3.9
Cruise altitude [m]	10668.0	10059.0	-	10999.4	-
Cruise Mach [-]	0.785	0.850	-	0.750	-
Cruise duration [min]	96.7	89.2	-7.8	103.5	7.0
Fuel till TOC [kg]	1019.1	1031.0	1.2	836.3	-17.9
Fuel for cruise [kg]	3433.3	3691.6	7.5	3412.5	-0.6

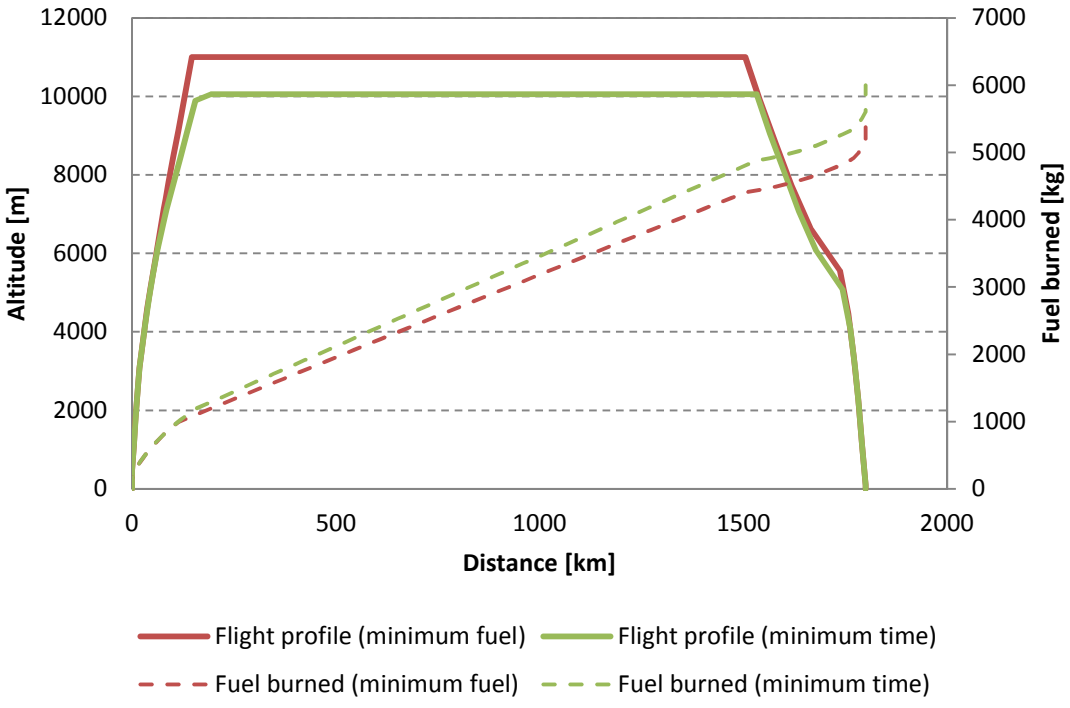

Figure 6-2: CUSA-M short range flight profile comparison (fuel vs. time)

In order for the optimiser to minimise either flight time or fuel burned, it selects the most suitable combination of decision variables (climb altitudes and cruise altitude) yielding a flight trajectory with an improvement in flight time or fuel burned. Since the bounds of the climb altitudes (altitude 1 to altitude 15) are kept relatively narrow and due to the fact that the individual calculated climb ranges vary to allow for reasonable climb profiles, the optimiser emphasises on the last climb altitude and the cruise altitude as crucial decision variables. The aircraft cruise altitude has a direct influence on the True Air Speed. At constant flight Mach number TAS increases with decreasing altitude due to an increase in speed of sound caused by an increment in ambient temperature ($TAS = M \cdot a$). This approach is illustrated in figure 6-1 where cruise altitude decreases from left to right for each of the three constant Mach number Pareto fronts. On the other hand, at constant altitude (constant speed of sound), an increase in flight Mach number causes an increase in TAS in the same manner. This approach is represented in figure 6-1 by each Mach number specific Pareto front which indicates a step change in flight time. Figure 6-3 illustrates the TAS variation during the climb profile and at initial cruise conditions. For the minimum fuel flight (solid orange line), the cruise Mach number (0.75) is reached earlier during the climb (at a lower altitude) and thus, TAS slightly decreases throughout the remaining climb as altitude still increases. The same process occurs for the minimum time flight (solid green line) only at a later point of the climb since the final cruise Mach number is higher (0.85).

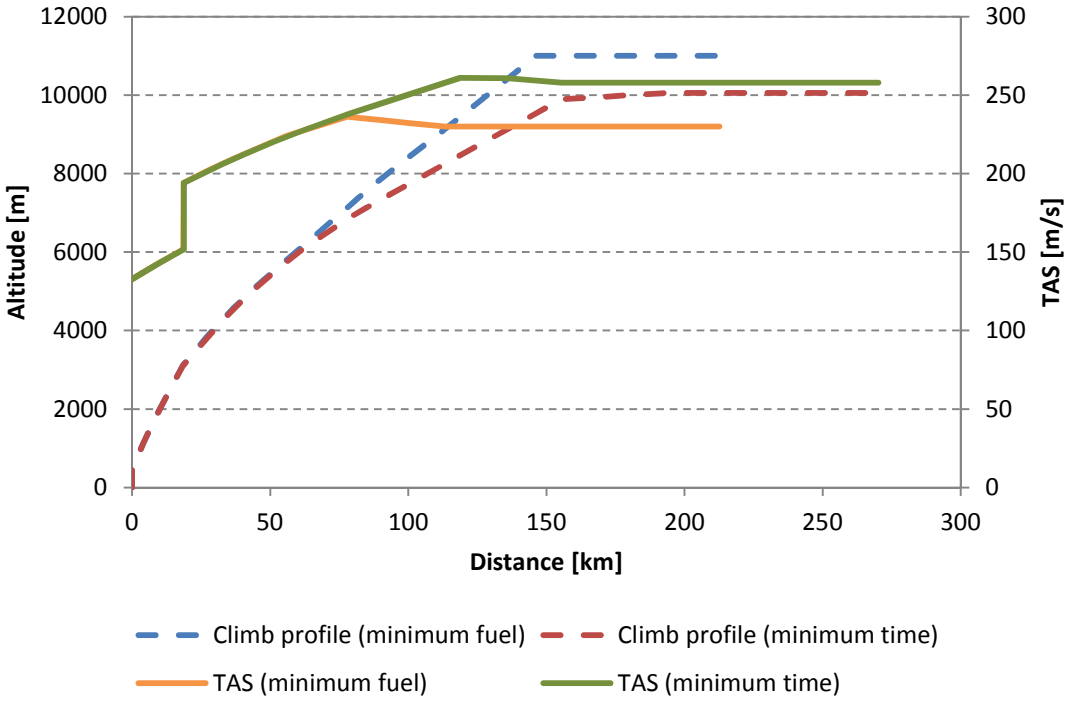

Figure 6-3: CUSA-M True Air Speed (TAS) variation during climb (short range)

Figure 6-4 furthermore shows that the initial climb phase for both trajectories is very similar due to the narrow bounds of the decision variables (climb altitudes) to be selected by the optimiser and the way the aircraft performance model (Hermes) computes a feasible climb profile. Following the TAS trends presented in figure 6-3, figure 6-4 illustrates the corresponding engine thrust trend of the two extreme climb profiles (minimum time and minimum fuel). Both figures also show a speed discontinuity (step change) during the climb phase which is related to a fixed increase in EAS from 250 to 320 knots as setup in the aircraft performance model.

In order to further highlight the results of the optimiser for the fuel versus time study, table 6-4 lists a comparison of three different short range flights selected from the three Pareto fronts (refer to figure 6-1) assuming a constant mission fuel burn value. It can be noted that overall flight time decreases with an increase in Mach number and an increase in cruise altitude. This means, for a fixed value of fuel burned and depending on the determinative objective of the individual flight mission, cruise altitude and cruise Mach number can be adjusted as suggested to reach this objective.

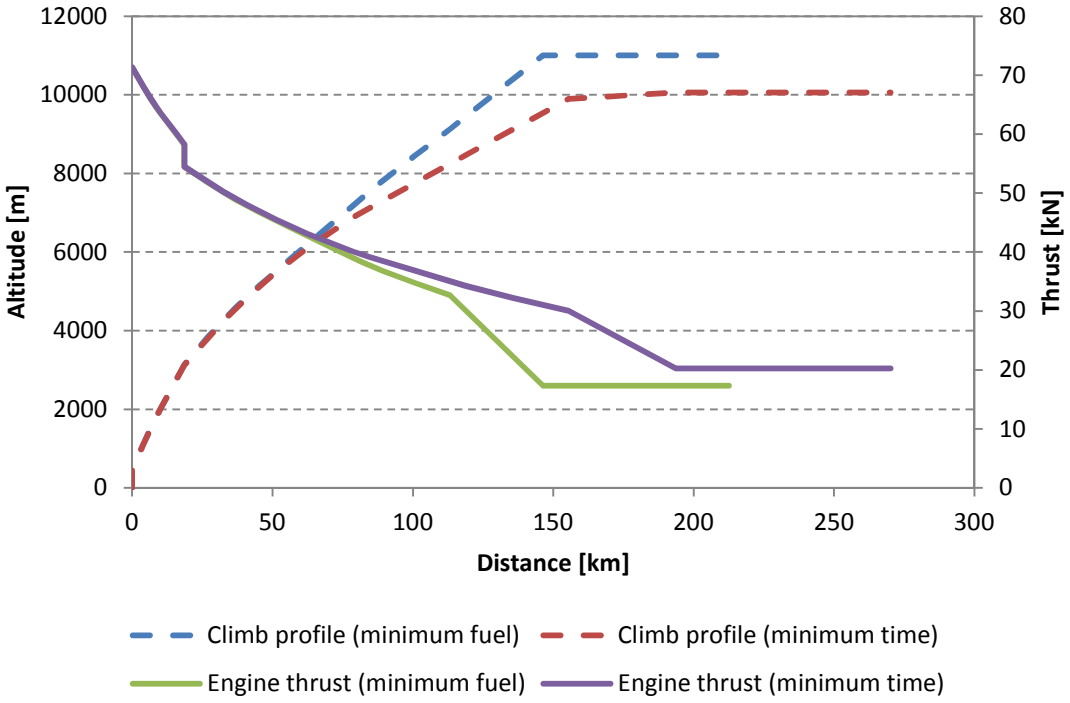

Figure 6-4: CUSA-M climb profile and engine thrust (short range)

Table 6-3: Flight comparison for fixed fuel burned value (short range)

CUSA-M 1800 km	Mach 0.75	Mach 0.80	Mach 0.85
Fuel burned [kg]	5770.2	5770.5	5771.7
Flight time [min]	136.6	130.6	126.0
Cruise altitude [m]	10059.0	10416.0	10999.6
Cruise duration [min]	103.9	96.7	89.9
Fuel till TOC [kg]	855.1	886.2	942.3
Fuel for cruise [kg]	3622.3	3573.9	3492.0

The analysis of the two single-objective extreme solutions (minimum time and minimum fuel burned) as well as the analysis of selected trajectories with fixed mission fuel burn revealed two techniques that were used to minimise the particular objective.

- The first technique, which is applied by the GATAC optimiser, involves the adjustment of the True Air Speed (TAS) by changing the cruise altitude.
- The second technique, which is based on predetermined inputs for the GATAC optimiser, involves the selection of specific cruise Mach numbers.

6.2.3 Fuel vs. NO_x Optimisation Results

Figures 6-5 and 6-6 show the optimiser output for the short range mission of the CUSA-M aircraft performing the 1800 km mission at varying climb altitudes (altitude 1 to altitude 16 as listed in table 6-1), varying cruise altitudes (10059 m - 11000 m) and 2 different cruise Mach numbers (0.75 and 0.85) with respect to fuel burned and NO_x emissions. In this case, each plot represents an optimal solution for the respective Mach number case. This means, the results of the optimiser converge towards one particular condition which indicates that both objectives (fuel burned and NO_x emissions) concur with each other. Differences in fuel burned for each solution is less than 0.1 kg and differences in NO_x emissions for each solution are less than 1 g. Since there is no trade-off between the two objectives, the optimiser does not find a set of non-dominated solutions. In both optimal cases, the optimiser selects the highest possible cruise altitude (11000 m) to achieve both, minimum fuel burn and minimum NO_x emissions for a given Mach number. As evaluated in the previous fuel vs. time optimisation study, minimum mission fuel burn is reached when flying at the highest possible altitude (11000 m) with the lowest possible cruise Mach number (0.75). Indeed, the same requirements apply to minimise NO_x emissions. The amount of NO_x emissions generated during the flight is directly related to the engine TET. Consequently, the mission flown at 0.75 Mach number will yield less NO_x emissions compared to the same mission flown at 0.85 Mach number. Since the values shown in figure 6-5 and 6-6 for fuel burned and NO_x emitted are based on a simplified calculation procedure using only the EINOx value of the initial cruise segment and fewer cruise increments to compute the total NO_x generated throughout the mission, the trajectory suggested by the GATAC optimiser has been reprocessed to establish the generated NO_x emissions for all flight phases using the respective EINOx values. The corrected values which account for these changes are listed in table 6-4.

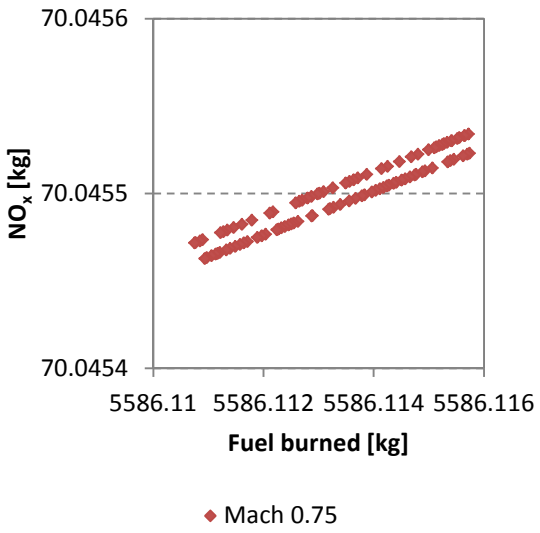

Figure 6-5: Fuel burned vs NO_x (0.75)

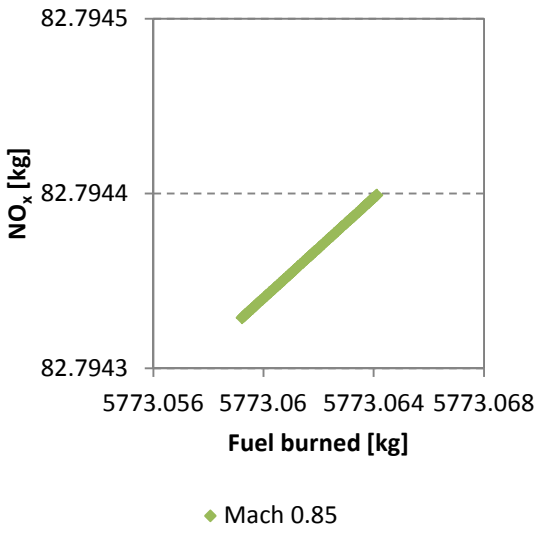

Figure 6-6: Fuel burned vs NO_x (0.85)

Table 6-4: Reprocessed fuel burned and NO_x values (short range)

1800 km	Mach 0.75	Mach 0.85
Fuel burned [kg]	5571.5	5756.6
NO_x emitted [kg]	73.1	83.1

6.3 Medium Range Multi Objective Optimisation

Equal to the short range optimisation cases, the first scenario of the medium range mission looks at the optimisation with regards to the two objectives, (1) total fuel burned and (2) total flight time while the second scenario then addresses the optimisation of the medium range mission with regards to (1) total fuel burned and (2) total NO_x emissions generated.

6.3.1 General Description

This case is similar to the previous short range cases, the difference being the increased flight distance. The flight distance is 4600 km. This second case aims to optimise a medium range aircraft trajectory in the same manner as the short range mission. This is again achieved by altering the aircraft climb profile (altitude of 16 climb segments) and cruise altitude in such a way that either total fuel burned or total flight

time becomes minimum. The optimisation is carried out three times at three different fixed Mach numbers (0.75, 0.80 and 0.85).

The second case then looks at the optimisation of the medium range mission in order to minimise fuel burned or to minimise NO_x emissions. It uses the same methodology as has been deployed on the short range fuel versus NO_x emissions optimisation study.

6.3.2 Fuel vs. Time Optimisation Results

Figure 6-6 shows the Pareto fronts for the short range mission of the CUSA-M aircraft performing the 4600 km mission at varying climb altitudes (altitude 1 to altitude 16 as listed in table 6-1), varying cruise altitudes (10059 m - 11000 m) and 3 different cruise Mach numbers (0.75, 0.80 and 0.85) and illustrates the influence on flight time and fuel burned. The results follow the same general trend as the Pareto fronts for the short range mission. Each Pareto front comprises a set of non-dominated solutions which represents a trade-off between flight time and fuel burned. The shortest mission flight time (305.9 min) requires flying at the lowest possible altitude (10059 m) with the highest possible Mach number of 0.85. The lowest mission fuel burn (13002 kg) requires flying at the highest possible altitude (11000) with the lowest possible Mach number of 0.75. Increasing Mach number from 0.75 by 0.05 increments up to 0.85 reduces flight time by about 22 minutes per each increment. Figure 6-7 illustrates the corresponding flight profiles (climb, cruise and descent) and fuel burn curves for the minimum time and minimum fuel case. The solid green profile represents the minimum fuel trajectory and the dashed green line shows the corresponding fuel burn accumulation along the flight. The minimum time trajectory is plotted in red lines accordingly. Both flight profiles shown in figure 6-7 contain the information about the decision variables used by the GATAC optimiser as previously described for the short range mission.

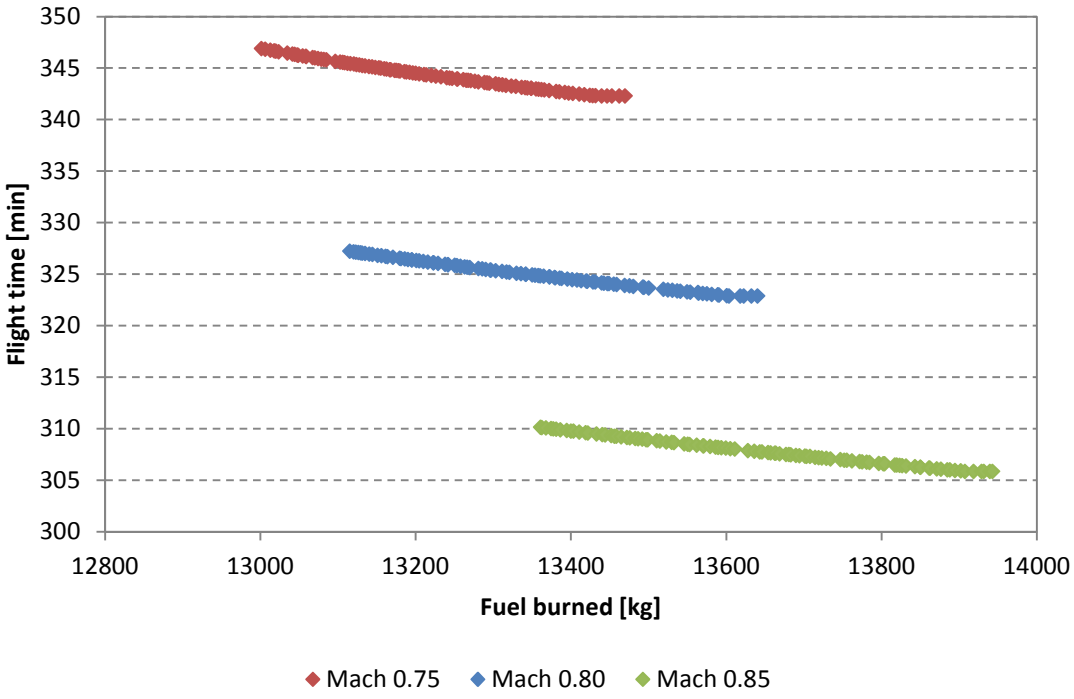

Figure 6-7: Fuel vs. time Pareto fronts for medium range mission

The optimisation objective values (flight time and fuel burned) for the two extreme points as well as the corresponding trajectory performance points are summarised in table 6-5 in the same fashion as for the short range mission. In addition, it provides a comparison of those performance points to a reference flight which is based on the "non-optimised" trajectory analysed in previous chapter 5. The reference flight is setup in the same manner as the reference flight introduced in the previous short range mission study. In this case, flight time is reduced by 7.7% for the minimum time flight at the expense of 5.7% increase in fuel burn. Fuel burned is reduced by 1.8% for the minimum fuel flight at the expense of a 4.7% increase in flight time. Both flights considered in relation to the reference flight. Furthermore, the cruise duration for the minimum time flight decreased by 8.3% and increased by 6.0% for the minimum fuel flight. Fuel consumption value till TOC for the minimum time flight increased by 2.5% while the same value decreased by 18.4% for the minimum fuel flight.

Table 6-5: Optimisation extreme solutions compared to reference flight (4600 km)

CUSA-M 4600 km	Reference flight	Minimum time flight	Delta [%]	Minimum fuel flight	Delta [%]
Fuel burned [kg]	13244.6	13943.0	5.3	13001.5	-1.8
Flight time [min]	331.5	305.9	-7.7	346.9	4.7
Cruise altitude [m]	10668.0	10059.0	-	10999.9	-
Cruise Mach [-]	0.785	0.850	-	0.750	-
Cruise duration [min]	293.0	268.6	-8.3	310.4	6.0
Fuel till TOC [kg]	1199.3	1229.0	2.5	978.3	-18.4
Fuel for cruise [kg]	10737.2	11385.4	6.0	10633.5	-1.0

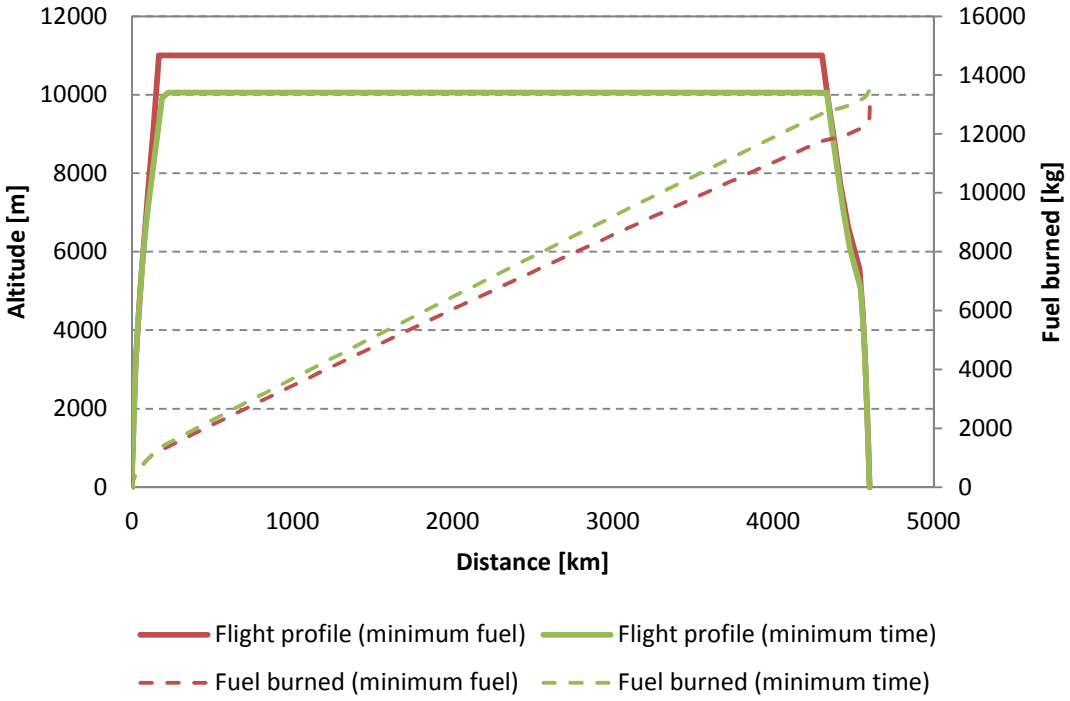

Figure 6-8: CUSA-M medium range flight profile comparison (fuel vs. time)

In this medium range case the optimiser follows the same strategy of optimising TAS by adjusting the climb and cruise altitudes, as described for the short range results. In order to minimise flight time the cruise altitude decreases progressively from the highest possible value (11000 m) to the lowest possible value (10059 m). Concurrently,

every step increment in Mach number (from 0.75 to 0.85) increases TAS during cruise and thus minimises flight time accordingly. The opposite effects take place if the objective of the optimisation is to minimise fuel burned. Figure 6-8 illustrates the TAS variation during the climb profile and at initial cruise conditions for the medium range flight. For the minimum fuel flight (solid orange line), the cruise Mach number (0.75) is reached earlier during the climb (at a lower altitude) and thus, TAS slightly decreases throughout the remaining climb as altitude still increases. The same process occurs for the minimum time flight (solid green line) only at a later point in the climb since the final cruise Mach number is higher (0.85). The final cruise altitude (10059 m) of the minimum time flight is reached later than in the minimum fuel case since the optimiser selects the final climb altitudes so as to prolong the climb duration at the lowest possible altitude.

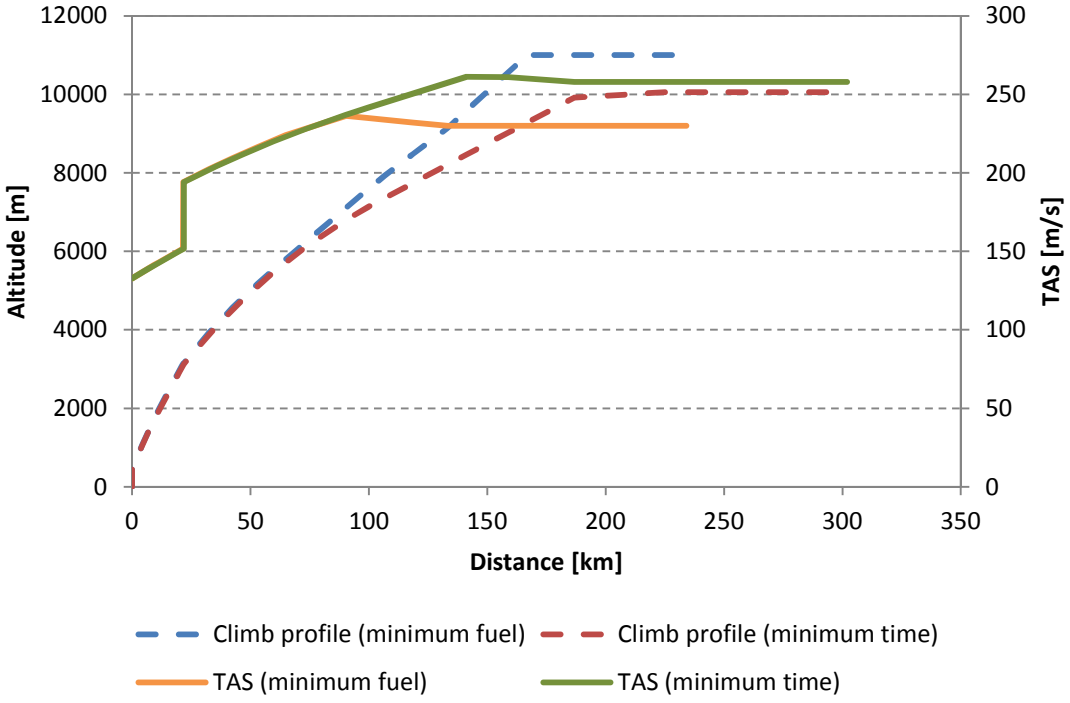

Figure 6-9: CUSA-M True Air Speed (TAS) variation during climb (medium range)

Figure 6-9 furthermore shows that the initial climb phase for both trajectories is very similar due to the narrow bounds of the decision variables (climb altitudes) to be selected by the optimiser and the way the aircraft performance model (Hermes)

computes a feasible climb profile. Figure 6-9 illustrates the corresponding engine thrust trend of the two extreme climb profiles (minimum time and minimum fuel). Both figures also show the same speed discontinuity (step change) during the climb phase that has been experienced in the short range mission and which is related to a fixed increase in EAS from 250 to 320 knots as setup in the aircraft performance model. Moreover, based on the lower cruise Mach number for the minimum fuel flight engine TET is decreased during that phase as well in comparison to the minimum time flight. Taking into account the results from the trajectory analysis performed in previous chapter 5, where engine degradation has been simulated, flying at slower Mach numbers and higher altitudes might alleviate engine degradation over time.

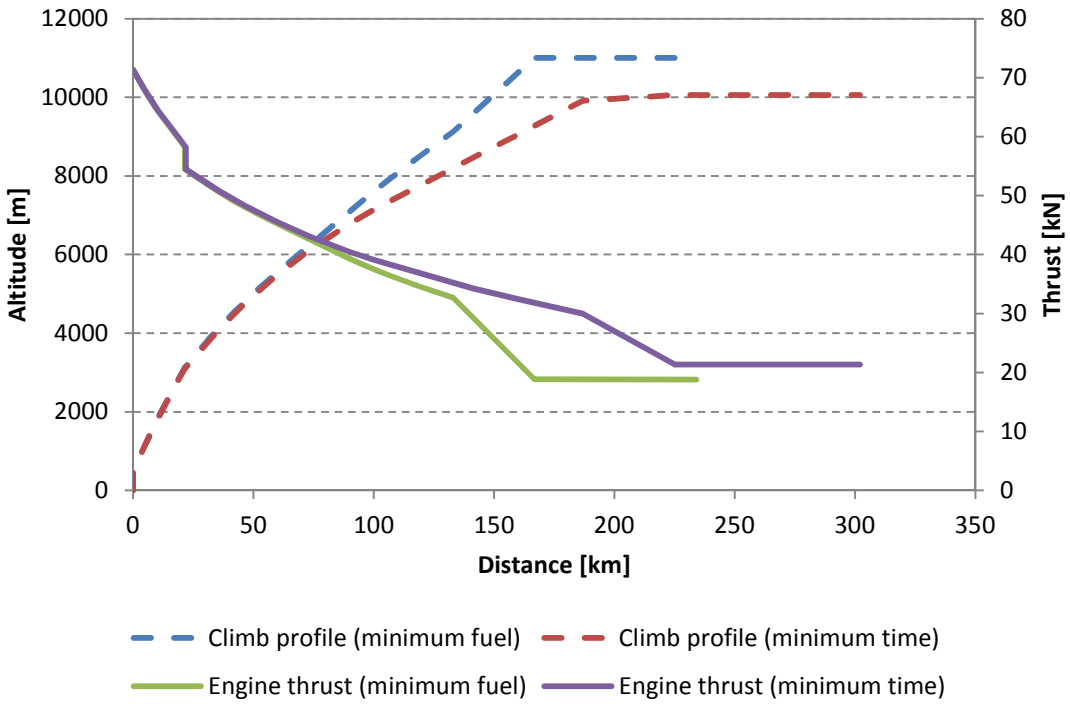

Figure 6-10: CUSA-M climb profile and engine thrust (medium range)

To also highlight the results of the optimiser for the medium range mission, table 6-6 lists a comparison of three different medium range flights selected from the three Pareto fronts (refer to figure 6-6) assuming a constant mission fuel burn value. It can be noted that overall flight time decreases with an increase in Mach number and an increase in cruise altitude. This means, for a fixed value of fuel burned and depending

on the determinative objective of the individual flight mission, cruise altitude and cruise Mach number can be adjusted as suggested to reach this objective.

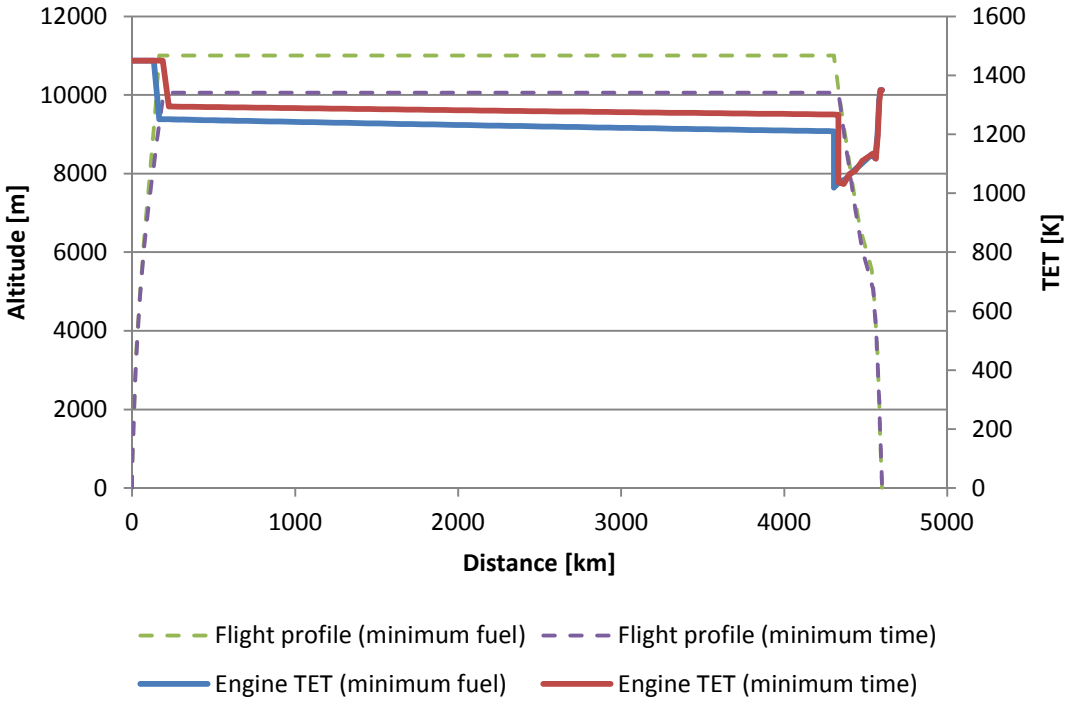

Figure 6-11: CUSA-M TET variation (medium range)

Table 6-6: Flight comparison for fixed fuel burned value (medium range)

CUSA-M 4600 km	Mach 0.75	Mach 0.80	Mach 0.85
Fuel burned [kg]	13362.0	13360.3	13360.7
Flight time [min]	342.9	324.8	310.1
Cruise altitude [m]	10181.5	10478.3	10999.9
Cruise duration [min]	308.5	289.0	272.1
Fuel till TOC [kg]	987.7	1041.0	1109.1
Fuel for cruise [kg]	11028.5	10960.9	10873.3

6.3.3 Fuel vs. NO_x Optimisation Results

Figures 6-11 and 6-12 show the optimiser output for CUSA-M aircraft performing the 4600 km mission at varying climb altitudes (altitude 1 to altitude 16 as listed in table 6-1), varying cruise altitudes (10059 m - 11000 m) and 2 different cruise Mach numbers (0.75 and 0.85) with respect to fuel burned and NO_x emissions generated. As in the previous case, each plot represents an optimal solution for the respective Mach number case. This means, the results of the optimiser converge towards one particular condition which indicates that both objectives (fuel burned and NO_x emissions) concur with each other. Again, differences in fuel burned for each solution is less than 0.1 kg and differences in NO_x emissions for each solution are less than 1 g. Since there is no trade-off between the two objectives, the optimiser does not find a set of non-dominated solutions. In both optimal cases, the optimiser selects the highest possible cruise altitude (11000 m) to achieve both, minimum fuel burn and minimum NO_x emissions for a given Mach number. The results for the medium range flight follow the same pattern as for the short range case as illustrated in figures 6-11 and 6-12 and have been reprocessed in the same way to correct the values of NO_x emissions and fuel burned. Correspondingly, the corrected values which account for these changes are listed in table 6-7.

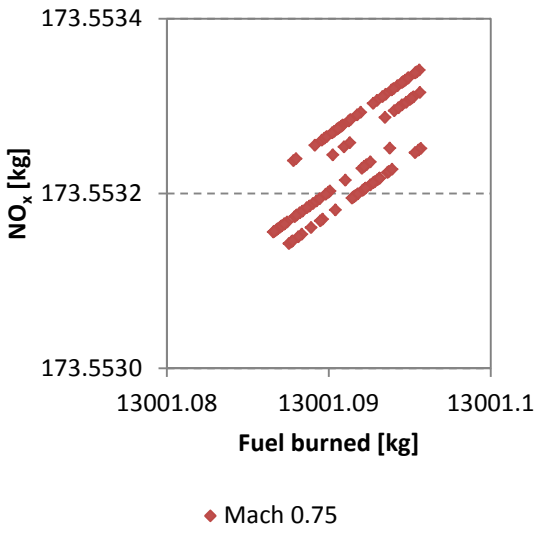

Figure 6-12: Fuel burned vs NO_x (0.75)

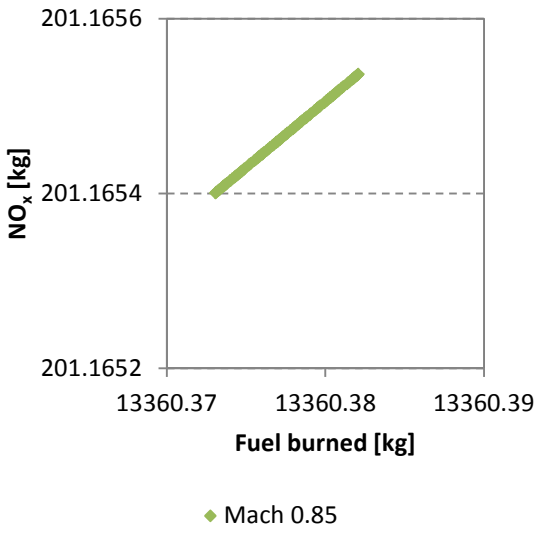

Figure 6-13: Fuel burned vs NO_x (0.85)

Table 6-7: Reprocessed fuel burned and NO_x values (short range)

4600 km	Mach 0.75	Mach 0.85
Fuel burned [kg]	12934.6	13304.7
NO_x emitted [kg]	170.6	196.4

7 Conclusions, Recommendations for Further Work and Outlook

This chapter summarises the main achievements and conclusions of the present research work and also addresses its limitations. Furthermore, some recommendations for future work are listed based on the results of this work.

7.1 Achievements

In the present research work, an analysis of aircraft trajectories with different aircraft/engine configurations has been conducted in order to verify and quantify their fuel burn and emissions performance. This has been achieved by adapting representative engine models, aircraft models and emissions predictions models to simulate commercial aircraft flight trajectories. All models have been compared to publicly available data in order to validate their suitability. Furthermore, the impact of engine degradation on the fuel burn and emissions has been investigated. In conjunction with the degradation analysis, the influence of derated take-offs has been considered as well. Two different flight missions, a short range mission (1800 km) and a medium range mission (4600 km) have been evaluated to estimate the values for mission fuel burn, NO_x emissions and flight time. The scenarios investigated included three different aircraft variants similar to the Airbus A320 family, and correspondingly three different engine variants similar to the CFM56-5B engine series. Moreover, an existing emissions predictions model based on correlations of ground level emission data has been customised for each engine variant.

Furthermore, a simple multi-disciplinary optimisation framework has been developed to perform aircraft trajectory optimisation studies. All models (engine model, aircraft model and emissions predictions model) have been integrated into this framework which then provided the capability to perform preliminary aircraft trajectory optimisation studies. Two different trajectory scenarios have been investigated which focus on the minimisation of fuel burned versus flight time and fuel burned versus NO_x emissions.

7.2 Conclusions

With regards to the aircraft trajectory analyses carried out at the initial part of the study it can be concluded that the effect of engine degradation on total mission fuel burn and emissions amplifies with flight distance and that it can considerably increase either of these values. Degradation affects the engine performance in all analysed flight phases (take-off, climb and cruise) and has its most adverse effect during take-off when engine TET is already elevated and reaches values which are close to operational limitations. The amounts of engine degradation (2% compressor, combustor and turbine degradation) simulated in this study were arbitrarily selected and thus cannot directly be correlated to a specific engine age. It can furthermore be inferred that a take-off thrust reduction of 15% (as a consequence of engine degradation) can significantly lower fuel burn and NO_x emissions during this flight phase while having only negligible negative impact on the total mission fuel burn and total mission NO_x emissions. The benefits achieved by reducing the maximum take-off power are consequently accompanied by a decrease in engine TET which in turn has a positive impact on engine life. Furthermore, it was observed that the amount of NO_x emissions per kilogram payload and kilometre decreases with aircraft size. This effect could in turn be considered by airline operators who utilise different aircraft variants of the same series in their fleets. Engines may then be swapped from larger aircraft variants (with higher thrust engine configurations) to smaller aircraft variants (with lower thrust configurations) to alleviate the effects of degradation on emissions.

The preliminary aircraft trajectory optimisation studies carried out as described in chapter 6 enabled the assessment of improved flight trajectories with the objective to minimise mission fuel burn, fight time or NO_x emissions generated. The deployment of a basic optimisation framework allowed the investigation of improved flight trajectories with regards to the selected optimisation of variables such as aircraft speed, aircraft climb altitudes and cruise altitude. The achieved results suggest that flight trajectories with reduced environmental impact (less fuel burned or less NO_x emitted) exist when compared to a “non-optimised” reference flight.

7.3 Limitations and Recommendations for Further Work

The results of the trajectory studies are subject to assumptions and limitations introduced in order to perform feasible and comparable analyses. The limitations imposed originate from various circumstances inherent to the simulation models and the optimisation framework respectively.

The aircraft performance model Hermes only employs a single fixed climb profile for the initial trajectory analyses which is based on a real example flight trajectory. Engine power settings for this climb profile are also fixed at predefined values. Take-off, landing and taxi phases are simulated in a simplified manner within the Hermes code and the resulting values should only be considered as reference points. In addition, the descent phase has been kept constant in terms of descent profile and power settings for all cases analysed.

The engine performance model Turbomatch provides many options to adapt various different engine designs and architectures to allow maximum simulation depth. For the purpose of this study, the adapted engine models have been developed with as many details as necessary to achieve a practical representation of the desired real engine variants. For example, no provision has been made for variable engine geometry or advanced bleed air control which may allow a more realistic engine simulation also in terms of transient engine performance. Thus, the engine performance model Turbomatch only yielded approximate results when simulating the engine off-design performance at very low power settings equivalent to idle conditions.

The emissions predictions model used in this study employs a correlations based approach (P3T3 method) to predict combustor NO_x emissions at different engine power settings. Other emissions such as CO or UHC have not been investigated as part of this study.

The current basic GATAC optimisation framework developed provides only capabilities to conduct preliminary optimisation studies since the setup requires refinement in

terms of input and output handling of the model parameters as well the amount of optimisation variables applied. In addition, the developed framework is subject to constraints inherent to the setup (model integration), as well as to the individual models and thus, the achieved optimisation results only represent a very limited range of possible solutions within the scope of the developed framework. In the current optimisation study, no provision for the speed con

Furthermore, parameter settings of the GATAC optimiser such as population size, creation rates or selection pressure have been kept equal for all cases analysed. Adjustment of these parameters for each optimisation scenario might improve the convergence of the results and reduce computational time.

The flight trajectory analyses carried out in the present work focused on certain aspects of an aircraft flight mission while other aspects have been excluded or neglected in order to create a manageable framework. For a more realistic representation of aircraft flight procedures and to increase and improve the validity of the simulation framework results, several recommendations for further work required are listed in the following:

- Extend the scope of the optimisation framework to include further models, such as noise models, weather models, lifing models and models for operational constraints such as air traffic management or particular airport restrictions.
- Investigate the implications of optimised trajectories on airlines' Direct Operating Costs (DOC) using a more all-encompassing approach, including factors like aircraft and engine maintenance costs, costs for flight operations and possible increased fuel prices and future emission taxes.
- Extend and improve the engine degradation model and scenarios to account for degradation of particular components and to investigate long-term effects.
- Extend the engine degradation model to account for flow capacity changes in the compressors and turbines (compressor and turbine fouling).

- Incorporate additional aircraft and engine models into the framework to investigate very short range and long range flight trajectories.
- Incorporate additional aircraft payload conditions which take into account a wider range of possible loading scenarios.
- Include all flight phases in the analyses and optimisation framework: Ground taxi-out, take-off, climb, cruise, descent, approach, landing, ground taxi-in. At the same time, extend the capability of the aircraft performance model to allow increased simulation accuracy for taxi, take-off and landing phases.
- Extend the emissions predictions model to allow modelling of different types of combustors (conventional or new design).
- Implement different emissions prediction models based on numerical simulations or physics based models.
- Include and quantify other pollutants, such as CO, UHC and soot.
- Allow optimisation of trajectory scenarios with more than two objectives (for example trade-offs between noise, NO_x emissions and fuel burn be particularly interesting in the LTO cycle).
- Investigate additional alternative multi-objective genetic algorithms.
- Adjust and refine the parameter settings of the GATAC optimiser for each optimisation scenario to improve the optimisation performance.
- Extend the type of optimisation variables to include the variation engine power settings during climb or the amount of take-off derate applied.
- Increase the number and/or combination of optimisation variables used for each optimisation scenario (fuel vs. time, fuel vs. NO_x).
- Investigate the possibility of incremental trajectory optimisation where flight phases are optimised individually to safe computing time and/or increase the fidelity of the results. Each flight phase could then be optimised with respect to the objectives which are of paramount importance in that particular phase (for example, noise during take-off and NO_x emissions during cruise).

- Implement the engine degradation model into the optimisation framework to investigate the effect on optimum trajectories with respect to fuel burned or NO_x emitted.

7.4 Outlook

A brief outlook on two important aspects of aircraft and engine operation is presented in this last section in order to highlight their importance for future developments and advancements in those fields. The first aspect deals with airline specific operational procedures and the second aspect focuses on engine health monitoring strategies.

7.4.1 Airline Operational Procedures

Many assumptions made throughout this study depend on custom airline procedures or operational restrictions imposed on airlines due to environmental constraints. Aircraft climb profiles or cruise altitudes are prescribed by local conditions of aerodromes and airspace controllers for example depending on aircraft speed and destination. Descent profiles are affected in the same way where certain flight paths have to be followed due to noise restrictions or traffic separation close to airports. An improvement of those procedures is investigated by one of the Clean Sky ITDs, the Systems for Green Operations (SGO). Three concepts are adopted for an overall optimisation of the aircraft and systems [20]. (1) Green Trajectories, including 3-dimensional flight paths and optimisation for minimum noise and emissions. (2) A Green Mission from start to finish, including management of climb, cruise and descent and multi-criteria optimisation (noise, emissions, fuel, time). (3) Smart Operations on Ground, including new ground procedures to reduce engine fuel consumption. The implementation of the before described mission optimisation systems will enable airlines to accurately predict complete flight missions in real-time and consequently assess their environmental impact.

With respect to engine operation and especially with respect to engine degradation one operational initiative which can significantly reduce the rate of engine degradation and in turn increase the engine on-wing life is regular engine gas path washing. Over time, dirt and other environmental pollutants accumulate in the engine air flow path and deposit on compressor blades and vanes. Washing of the engine compressor and airfoils can to some extent recover the engine performance by improving the surface finish of the blades and thus the aerodynamic contour which has a positive effect on

compressor efficiency. The work in reference [109] analyses the particular effects of engine washing on engine performance and in a second step identifies significant benefits of washing an engine at predetermined intervals.

7.4.2 Engine Health Management

As discussed in chapters 2.2, 2.3 and 2.4 of this study, engine performance degradation is continuously monitored to identify trend shifts or to detect faults ahead of time. This is usually achieved by analysing certain engine performance data points of every flight performed at a given day. Engine data such as temperatures, pressures and others are collected together with aircraft and atmospheric data to compute a smoothed engine performance trend. Normally these computations are carried out in retrospect, this means, when the aircraft has landed and data has been transmitted to centralised servers on ground. This means that these systems normally have inherent diagnostics latency. Due to the continuing advances in avionics, portions of the current on-ground monitoring activities and diagnostics data may be shifted to health management systems on-board the aircraft which would allow real-time monitoring of engine performance or early detection of faults. The paper in reference [110] describes this approach in detail and investigates an enhanced on-board model based GPHM (Gas Path Health Management) architecture.

Future Engine Health Management (EHM) Systems are expected to make propulsion system operation more intelligent, self-diagnostic, self-optimising and mission adaptable. Engine life cycle costs, fuel efficiency and reliability are major focus areas when new engine control and health management systems are investigated and are expected to have a significant potential to improve overall operational performance. The paper in reference [111] summarises specific engine health management technologies that are currently under development, which will enable efficient aircraft propulsion system operation. One common goal of those technologies is to operate an engine to achieve optimal performance while considering the actual engine condition and the current mission of the aircraft.

REFERENCES

1. **Tillmann, C. G, . et. al.** *Zusammenfassende Darstellung der Effizienzpotenziale bei Flugzeugen unter besonderer Berücksichtigung der aktuellen Triebwerkstechnik sowie der absehbaren mittelfristigen Entwicklungen.* FKZ UM 07 06 602/01 März 2008.

2. **Lee, D.S., et al.** *Aviation and global climate change in the 21st century.* Atmospheric Environment (2009).

3. **(EUROCONTROL), The European Organisation for the Safety of Air Navigation.** *Challenges of Air Transport 2030, Survey of experts' views, July 2009.*

4. **(EUROCONTROL), European Organisation for the Safety of Air Navigation.** *"Challenges of growth" environmental update study, January 2009.*

5. **Brasseur, G. P., et al.** *European Scientific Assessment of the Atmospheric Effects of Aircraft Emissions.* Atmospheric Environment Vol. 32, No. 13, pp. 2329—2418, 1998.

6. **(ICAO), International Civil Aviation Organization.** *ICAO Engine Emissions Databank.* http://www.caa.co.uk/default.aspx, (accessed 25th October, 2011).

7. **(CAEP), Committee on Aviation Environmental Protection.** *Correlation between LTO NOx and Cruise/Climb NOx .* Seventh Meeting, February 2007 .

8. **Mongia, H. C.** *On Continuous NOx Reduction of Aero-propulsion Engines.* 48th AIAA Aerospace Sciences Meeting Including the New Horizons Forum and Aerospace Exposition, Orlando, Florida, 2010.

9. **Hileman, J., I., et al.** *Payload Fuel Energy Efficiency as a Metric for Aviation Environmental Performance.* 26th International Congress of the Aeronautical Sciences, 2008.

10. **(CAEP), Committee On Aviation Environmental Protection (1).** *CAEP/7 Environmental Design Spsace (EDS) Progress.* Seventh Meeting, February 2007.

11. **(CAEP), Committee On Aviation Environmental Protection (2).** *CAEP/8 NOx Stringency Cost-Benefit Analysis Demonstration Using APMT-Impacts.* Eighth Meeting, February 2010.

12. **(PARTNER), Partnership for AiR Transporatation Noise and Emissions Reduction (1).** *About PARTNER.* http://web.mit.edu/aeroastro/partner/about/index.html (accessed 20th January, 2011).

13. **(PARTNER), Partnership for AiR Transporatation Noise and Emissions Reduction (3).** *Projects PARTNER.* http://web.mit.edu/aeroastro/partner/projects/index.html (accessed 20th January, 2011).

14. **Yutko, B., Hansman, R. J., Mozdzanowska, A., et. al.** *Assessment of CO2 Emission Metrics for a Commercial Aircraft Certification Requirement.* PARTNER Project 30 Interim Report, December 2010.

15. **(PARTNER), Partnership for AiR Transporatation Noise and Emissions Reduction (2).** *Aviation Environmental Portfolio Management Tool PARTNER.* http://web.mit.edu/aeroastro/partner/apmt/index.html (accessed 20th January, 2011).

16. **Personalities, Report of the Group of.** *European Aeronautics: A Vision for 2020, Meeting society's needs and winning global leadership.* January 2001.

17. **(ACARE), Advisory Council for Aeronautics Research in Europe.** *ACARE Strategic Research Agendas SRA-1 and SRA-2, ACARE SRA-2 Excecutive Summary.* http://www.acare4europe.org/documents/rarchive (accessed 31st Marchr, 2013).

18. **Addendum to the Strategic Research Agenda.** *Advisory Council for Aeronautics Research in Europe.* 2008.

19. **Donnerhack, Dr.-Ing. S.** *Beiträge der Flugtriebwerke zur Schadstoffreduktion im Luftverkehr.* Workshop "Flugverkehr und Luftqualität - Partikel- und Stickoxidemissionen" beim UBA Berlin, 14.06.2005.

20. **Clean Sky JTI Joint Technology Initiatve.** *CleanSky.* http://www.cleansky.eu, (accessed 20th January, 2011).

21. **Ogaji, S., Pilidis, P., Hales, R.** *TERA- A Tool for Aero-engine Modelling and Management.* 2nd World Congress on Engineering Asset Management and 4th International Conference On Condition Monitoring, 11-14th June 2007, Harrogate, UK.

22. **Celis, C., Long, R., Sethi, V., Zammit-Mangion, D.** *On Trajectory Optimization for Reducing the Impact of Commercial Aircraft Operations on the Environment.* ISABE-2009-1118.

23. **Zolata, H.** *Development of a Multi-Disciplinary Aircraft Trajectory Optimisation Simulation Framework.* MSc Thesis, School of Engineering, Cranfield University 2009, MK43 0AL, Bedfordshire, UK.

24. **Marzal Espi, R.** *Benchmarking and Testing of different Genetic Algorithms for Multi-Disciplinary Aircraft Trajectory Optimisation Studies.* MSc Thesis, School of Engineering, Cranfield University 2010, MK43 0AL, Bedfordshire, UK.

25. **Döpelheuer, A., Lecht, M.** *Influence of Engine Performance on Emission Characteristics.* German Aerospace Center, Institute of Propulsion Technology, Engine Systems, D-51147 Cologne, Germany.

26. **Bower, G. C., Kroo, I. M.** *Multi-Objective Aircraft Optimization for Minimum Cost and Emissions over Specific Route Networks: European Aeronautics.* 26th International Congress of the Aeronautical Sciences, Stanford University, Department of Aeronautics and Astronautics, 2008.

27. **Penner, J.E., Lister, D.H., Griggs, D.J., Dokken, D.J., McFarland, M.** *Aviation and the Global Atmosphere.* A Special Report of IPCC Working Groups I and III, 1999.

28. **AIRBUS Flight Operations Support & Line Assistance.** *Getting to grips with aircraft performance.* January 2002.

29. **Lawson, C. P.** *Aircraft Performance for Propulsion Systems Engineers.* Lecture Notes, Cranfield University, MK43 0AL, Bedfordshire, UK.

30. **Daggett, D. L.** *Water Misting and Injection of Commercial Aircraft Engines to REduce Airport NOx.* National Aeronatuics and Space Administration (NASA), Glenn Research Center, 2004, NASA/CR-2004-212957.

31. **(GAO), US General Accounting Office.** *Aviation And The Environment - Strategic Framework Needed to Address Challenges Posed by Aircraft Emissions.* Report to the Chairman, Subcommittee on Aviation, Committee on Transportation and Infrastructure, February 2003.

32. **(ICAO), International Civil Aviation Organization.** *Continuous Descent Operations (CDO) Manual.* Doc 9931, AN/476.

33. **(ICAO), International Civil Aviation Organization (1).** *Procedures for Air Navigation Services - Aircraft Operations - Flight Procedures - Volume I.* Fifth Edition, 2006.

34. **(ICAO), International Civil Aviation Organization (2).** *Procedures for Air Navigation Services - Aircraft Operations - Construction of Visual and Instrument Flight Procedures - Volume II.* Fifth Edition, 2006.

35. **(ICAO), International Civil Aviation Organization.** *Operational Opportunities to Minimize Fuel Use and Reduce Emissions.* February 2003.

36. **AIRBUS Flight Operations Support & Services.** *Getting to grips with A320 performance retention and fuel savings.* Issue 2, January 2008.

37. **Grieb, H.** *Projektierung von Turboflugtriebwerken.* Birkhäuser Verlag 2004 , Basel, Switzerland.

38. **Walsh, P.P., Fletcher, P.** *Gas Turbine Performance.* Second Edition, Blackwell Publishing, 2004, UK.

39. **Bräunling, W. J. G.** *Flugzeugtriebwerke.* Grundlagen, Aero-Thermodynamik, ideale und reale Kreisprozesse, Thermische Turbomaschinen, Komponenten, Emissionen und Systeme, 3., vollständig überarbeitete und erweiterte Auflage, Springer, Berlin, Heidelberg 2009.

40. **Wörrlein, K.** *Gasdynamische Probleme bei Flugantrieben.* Fachgebiet Gasturbinen und Flugantriebe, Technische Universität Darmstadt, 1. Auflage SS 2001.

41. **Pilidis, P., Palmer, J.P.** *Gas Turbine Theory and Performance.* MSc Lecture Notes, School of Engineering, Cranfield University 2008, MK43 0AL, Bedfordshire, UK.

42. **Baehr, H. D., Kabelac, S.** *Thermodynamik.* Springer Verlag Berlin, Heidelber 2012.

43. **ICF Consulting Group.** *Evaluation of Air Pollutant Emissions from Subsonic Commercial Jet Aircraft.* Engine Programs and Compliance Division, Office of Mobile Sources, U.S. Environmental Protection Agency, April 1999.

44. **Singh, R.** *Gas Turbine Combustors Volume 1.* School of Engineering, Cranfield University, October 2009, MK43 0AL, Bedfordshire, UK.

45. **Faber, J., Greenwood, D., Lee, D., et. al.** *Lower NOx at Higher Altitudes - Policies to Reduce the Climate Impact of Aviation NOx Emission .* Delft, CE Delft, October 2008.

46. **Saravanamuttoo, I., et al.** *Gas Turbine Theory.* Sixth edition 2009.

47. **Singh, R.** *Gas Turbine Combustors Volume 2.* School of Engineering, Cranfield University, 2009, MK43 0AL, Bedfordshire, UK.

48. **Norman, P. D., et al.** *Development of the technical basis for a New Emissions Parameter covering the whole AIRcraft operation: NEPAIR.* NEPAIR/WP4/WPR/01, September 2003.

49. **Lipowsky, H.** *Entwicklung und Demonstration eines integrierten Systems zur Zustandsüberwachung von Gasturbinen.* Institut für Luftfahrtantriebe der Universität Stuttgart, 2010.

50. **Li, Y. G.** *Performance-analysis-based gas turbine diagnostics: A review.* Proceedings of the Institution of Mechanical Engineers, Part A: Journal of Power and Energy, 2002.

51. **B. A., Roth, D. L., Doel, J. J., Cissell.** *Probabilistic Matching of Turbofan Engine Performance Models to Test Data.* GT2005-68201, Proceedings of ASME Turbo Expo 2005: Land Sea & Air.

52. **Gräter, Dipl.-Ing. F., Staudacher, Prof. Dr.-Ing. S., Weißschuh, Dr.-Ing. M.** *Probabilistische Beschreibung der Triebwerksalterung (Schwerpunkt Flugtriebwerke).* Institut für Luftfahrtantriebe, Universität Stuttgart, Oktober 2008.

53. **Kurz, R., Brun, K. (1).** *Degradation In Gas Turbine Systems.* Presented at the International Gas Turbine & Aeroengine Congress & Exhibition, Munich, Germany, 2000.

54. **Kurz, R., Brun, K. (2).** *Gas Turbine Tutorial - Maintenance and Operating Practices Effects on Degradation and Life.* Proceedings of the Thirty-Sixth Turbomachinery Symposium, 2007.

55. **Hamed, A., Tabakoff, W., Singh, D.** *Modeling of Compressor Performance Deterioration Due to Erosion.* International Journal of Rotating Machinery, 1998, Vol. 4, No. 4, pp. 243-248.

56. **Wensky, T., Winkler, L., Friedrichs, J.** *Environmental Influences On Engine Performance Degradation.* Proceedings of ASME Turbo Expo 2010: Power for Land, Sea and Air, Glasgow, UK, 2010.

57. **Cookson, R.A.** *Mechanical Design of Turbomachinery.* Thermal Power MSc Lecture Notes, Department of Propulsion and Power, School of Engineering, Cranfield University, MK43 0AL, Bedfordshire, UK.

58. **Suria, O.V.** *A flexible lifing model for gas turbines: Creep and low cycle fatigue appraoch.* MSc Thesis, School of Engineering, Cranfield University 2006, MK43 0AL, Bedfordshire, UK.

59. **Rao, S. S.** *Engineering Optimization - Theory and Practice.* Fourth Edition, 2009.

60. **Schwefel, H.-P.** *Numerical Optimization of Computer Models.* John Wiley & Sons, Ltd., Chichester, UK, 1981.

61. **Celis, C.** *Evaluation and Optimisation of Environmentally Friendly Aircraft Propulsion Systems.* PhD Thesis, School of Engineering, Cranfield University 2010, MK43 0AL, Bedfordshire, UK.

62. **Koumoutsakos, P., Freund, J., Parekh, D.** *Evolution strategies for parameter optimization in jet flow control.* Center for Turbulence Research, Proceedings of the Summer Program 1998.

63. **Charbonneau, P.** *An Introduction to Genetic Algorithms for Numerical Optimization.* National Center for Atmospheric Research, Boulder, Colorado, March 2002.

64. **Zitzler, E., Laumanns, M., Bleuler, S.** *A Tutorial on Evolutionary Multiobjective Optimization.* Swiss Federal Institute of Technology (ETH) Zurich, Computer Engineering and Networks Laboratory, Gloriastrasse 35, CH-8092 Zurich, Switzerland.

65. **Mitsuo, G., Runwei, C.** *Genetic Algorithms and Engineering Optimization.* First edition, December 28, 1999.

66. **Deb, K., et al.** *A Fast and Elitist Multiobjective Genetic Algorithm: NSGA-II, IEEE Transactions on Evolutionary Computation.* Vol.6, No.2, April 2002.

67. **Caramia, M., Dell'Olmo, P.** *Multi-Objective Management in Freight Logistics Increasing Capacity, Service Level and Safety with Optimization Algorithms.* Springer, 2008.

68. **Coello Coello, C. A., Lamont, G. B.** *An Iintroduction to Multi-Objective Evolutionary Alogorithms and Their Applications.*

69. **Van Veldhuizen, D.A., Lamont, G.B.** *Multiobjective Evolutionary Algorithm Research: A History and Analysis.* October 14, 1998, Graduate School of Engineering, Air Force Institute of Technology, Wright-Patterson AFB, USA.

70. **Pervier, H., Nalianda, D., Espi, R., Sethi, V. Pilidis, P., et. al.** *Application of Genetic Algorithm for Preliminary Trajectory Optimization.* SAE International, 2011-01-2594, 2011.

71. **Dimech, E., Chircop, K., Xuereb, M., Muscat, R.** *GATAC User Manual V2.* Clean Sky, Systems for Green Operations ITD, March 2011.

72. **Scheiderer, J.** *Angewandte Flugleistung, Eine Einführung in die operationelle Flugleistung vom Start bis zur Landung.* Springer, Berlin Heidelberg, 2008.

73. **NASA, National Aeronautics and Space Administartion.** *U.S. Standard Atmosphere. 1976.* NASA-TM-X-74335, U.S. Government Printing Office, Washington.

74. **AIRBUS Flight Operations Support & Line Assistance.** *Getting to grips with fuel economy.* Issue 4, October 2004.

75. **Clarke, J.-P., et al.** *Development, design, and flight test evaluation of a continuous descent approach procedure for nighttime operation at Louisville International Airport.* January 2006.

76. **Patterson, J., et. al.** *Analysis of Departure and Arrival Profiles Using Real-Time Aircraft Data.* Journal Of Aircraft, Vol. 46, No. 4, July – August 2009.

77. **Alam, S., Nguyen, M. H., Abbass, H. A., Lokan , C., et. al.** *A Dynamic Continous Descent Approach Methodology For Low Noise And Emission.* IEEE 2010.

78. **Torres, R., Chaptal, J., Bès, C., Hiriart-Urruty, J.-B.** *Optimal, Environmentally Friendly Departure Procedures for Civil Aircraft.* Journal Of Aircraft, Vol. 48, 2011.

79. **Trani, A.A.** *Aircraft Performance Calculations: Descent Analysis.* CEE 5614, Analysis of Air Transportation Systems, Virginia Tech, Air Transportation Systems Laboratory.

80. **Sammut, M.** *Multivariable Parameter Optimization Of Flight Trajectories.* Cranfield University, School of Engineering, August 2011 .

81. **Shakariyants, S. A., van Buijtenen, J. P., Visser, W. P. J., Tarasov, A. (1).** *A Multidisciplinary Aero-Engine Exhaust Emission Study.* Proceedings of GT 2006 ASME Turbo Expo 2006: Power for Land, Sea and Air, Barcelona, Spain, 2006.

82. **Shakariyants, S. A., van Buijtenen, J. P., Visser, W. P. J., Tarasov, A. (2).** *Generic Airplane And Aero-Engine Simulation Procedures For Exhaust Emission Studies.* Proceedings of GT2007 ASME Turbo Expo 2007: Power for Land, Sea and Air, Montreal, Canada, 2007.

83. **Filippone, A.** *Comprehensive analysis of transport aircraft flight performance.* Progress in Aerospace Sciences 44 (2008) 192–236.

84. **Mercer, C. R., Haller, W. J.** *Adaptive Engine Technologies for Aviation CO2 Emissions Reduction.* 42nd AIAA/ASME/SAE/ASEE Joint Propulsion Conference & Exhibit, Sacramento, California, 2006.

85. **Waldowski, A.** *Potenzialbewertung von Open-Rotor-Triebwerken.* Deutsches Zentrum für Luft- und Raumfahrt, Technische Universität Berlin, 2009.

86. **Najafi, E., Sethi, V., Celis, C.** *Preliminary Specification of the CUTSTF Engine Performance Model for Use in GATAC V1.* System for Green Operations (SGO) ITD, September 2009.

87. **CFM The Power of Flight.** *Engine Technology, CFM56-5B Series Turbofan Engines.* http://www.cfm56.com/products/cfm56-5b/cfm56-5b-technology, (accessed 20th October, 2011).

88. **The TURBOMATCH Theme.** *For Aero/Industrial Gas Turbine Engine Design Point/Off Design Performance Calculation.* Department of Power and Propulsion, October 1999, School of Engineering, Cranfield University, MK43 0AL, UK.

89. **Kurzke, J.** *The GasTurb Program.* http://www.gasturb.de, (accessed 15th August, 2012).

90. **NLR, Nationaal Lucht- en Ruimtevaartlaboratorium.** *Gas Turbine Simulation Program.* http://www.gspteam.com (accessed 15th August, 2012).

91. **Pachidis, V. A.** *Gas Turbine Performance Simulation.* Thermal Power MSc Course Notes, Department of Power Propulsion and Aerospace Engineering, School of Engineering, Cranfield University, MK43 0AL, Bedfordshire, UK.

92. **Pilidis, P., et al.** *Propulsion Systems Performance and Integration.* Lecture Notes Volume One, School of Engineering, Cranfield University 2008, MK43 0AL, Bedfordshire, UK.

93. **Matingly, J.D.** *Elements of Gas Turbine Propulsion.* International Editions 1996, McGraw-Hill, Singapore.

94. **Guha, A.** *Optimum Fan Pressure Ratio for Bypass Engines with Separate or Mixed Exhaust Streams.* University of Bristol, UK.

95. **Commerce, Aircraft.** *Aircraft Owner's & Operator's Guide: A320 Family.* Issue No. 44 • February/March 2006.

96. **Bauernfeind, K.** *Steuerung und Regelung der Turboflugtriebwerke.* Birkhäuser 1999, Berlin.

97. **AIRBUS, A320 Family (1).** *Dimensions & Key Data A319 Aircraft.* http://airbus.com/aircraftfamilies/passe-ngeraircraft/a320family/a319/specifications, (accessed 20th October, 2011).

98. **AIRBUS, A320 Family (2).** *Dimensions & Key Data A320 Aircraft.* http://airbus.com/aircraftfamilies/passe-ngeraircraft/a320family/a320/specifications, (accessed 20th October, 2011.

99. **AIRBUS, A320 Family (3).** *Dimensions & Key Data A321 Aircraft.* http://airbus.com/aircraftfamilies/passe-ngeraircraft/a320family/a321/specifications, (accessed 20th October, 2011).

100. **University, Cranfield.** *Hermes V5 & TmatchCalls V3 User Manual.* September 2009, School of Engineering, Cranfield University, MK43 0AL, Bedfordshire, UK.

101. **Berdowski, Z., et al.** *Survey on standard weights of passengers and baggage - Final report.* Reference EASA 2008.C.06/30800/R20090095/30800000/FBR/RLO , Zoetermeer, May 2009.

102. **AIRBUS, A319.** *Airplane Characteristics for Airport Planning, AIRBUS S.A.S.* Technical Data Support and Services, 31707 Blagnac Cedex, France, Revision May 01, 2011.

103. **AIRBUS, A320.** *Airplane Characteristics for Airport Planning, AIRBUS S.A.S.* Technical Data Support and Services, 31707 Blagnac Cedex, France, Revision May 01, 2011.

104. **AIRBUS, A321.** *Airplane Characteristics for Airport Planning, AIRBUS S.A.S.* Technical Data Support and Services, 31707 Blagnac Cedex, France, Revision May 01, 2011.

105. **Celis, C., Moss, B., Pilidis, P.** *Emissions Modelling for the Optimisation of Greener Aircraft Operations.* Proceedings of ASME Turbo Expo 2009, Power for Land, Sea and Air, Orlando, Florida, USA, GT2009-59211.

106. **Allaire, D. L.** *A Physics-Based Emissions Model for Aircraft Gas Turbine Combustors.* Massachusetts Institute Of Technology, May 2006.

107. **Chircop, K., Xuereb, M., Zammit-Mangio, D., Cachia, E.** *A Generic Framework for Multi-Parameter Optimization of Flight Trajectories.* 27th International Congress of the Aeronautical Sciences, 2010.

108. **Zitzler, E., Deb, K., Thiele, L.** *Comparison of Multiobjective Evolutionary Algorithms: Empirical Results.* Massachusetts Institute of Technology, 2000.

109. **Giesecke, D.** *On-Wing Compressor Washing Of A Short-Range Aircraft.* Cranfield University, School of Engineering, 2011.

110. **Simon, D. L.** *An Integrated Architecture for On-Board Aircraft Engine Performance Trend Monitoring and Gas Path Fault Diagnostics.* NASA/TM—2010-216358, Glenn Research Center, Cleveland, Ohio.

111. **Litt, J. S., et al.** *A Survey of Intelligent Control and Health Management Technologies for Aircraft Propulsion Systems.* NASA/TM-2005-213622, Glenn Research Center, Cleveland, Ohio.

APPENDICES

A.1 CUSA-S, CUSA-M, CUSA-L Block fuel and Block NO_x

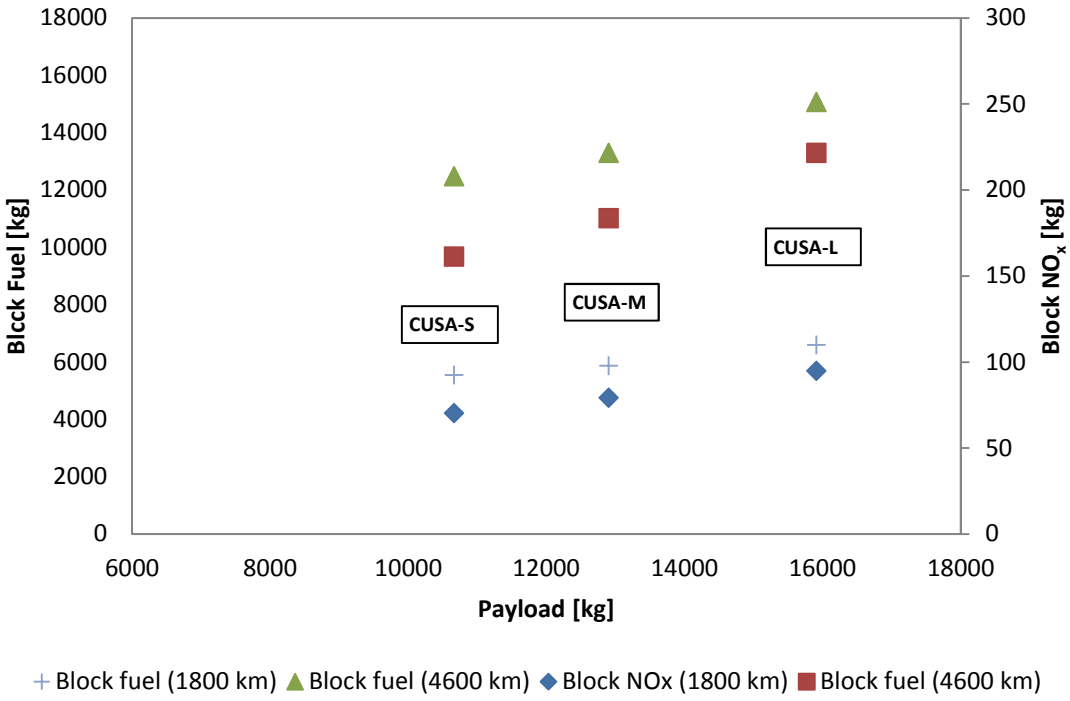

Figure A.1-1: Block Fuel and Block NO_x over Payload

A.2 Trajectory plots for 1800 km mission

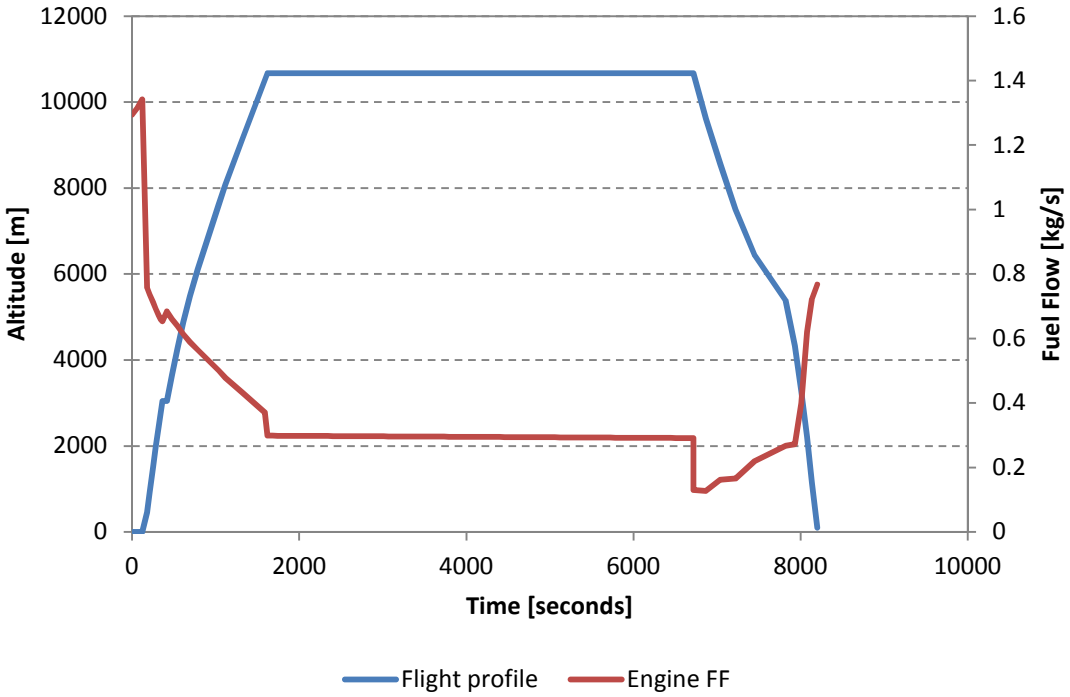

Figure A.2-1: CUSA-M engine FF variation during flight (1800 km)

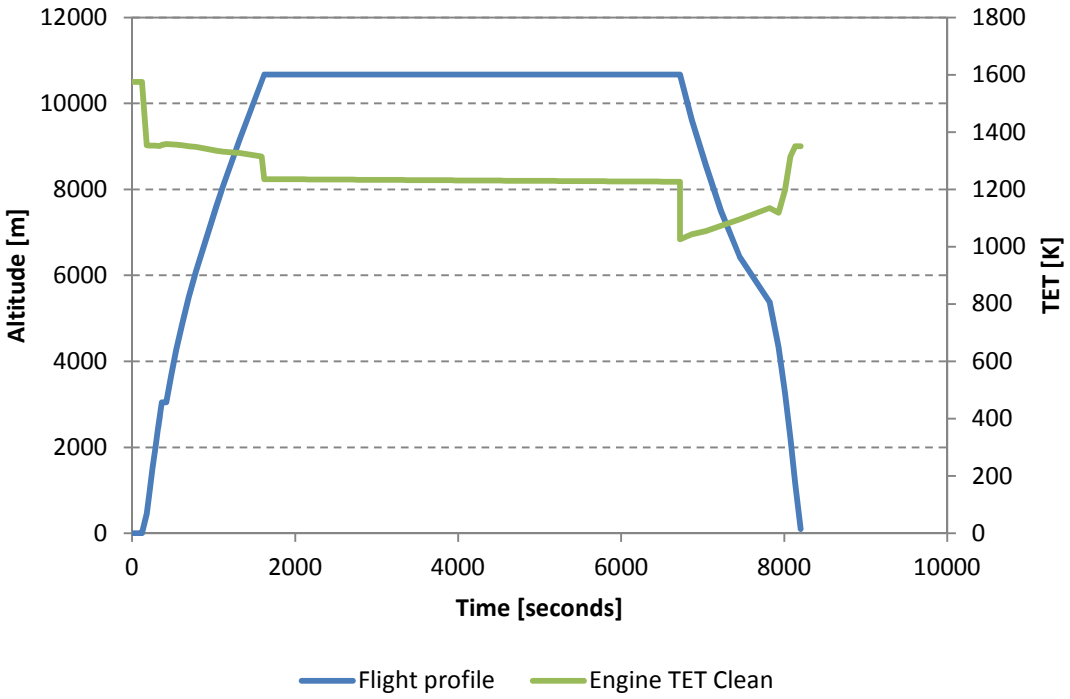

Figure A.2-2: CUSA-M engine TET variation during flight (1800 km)

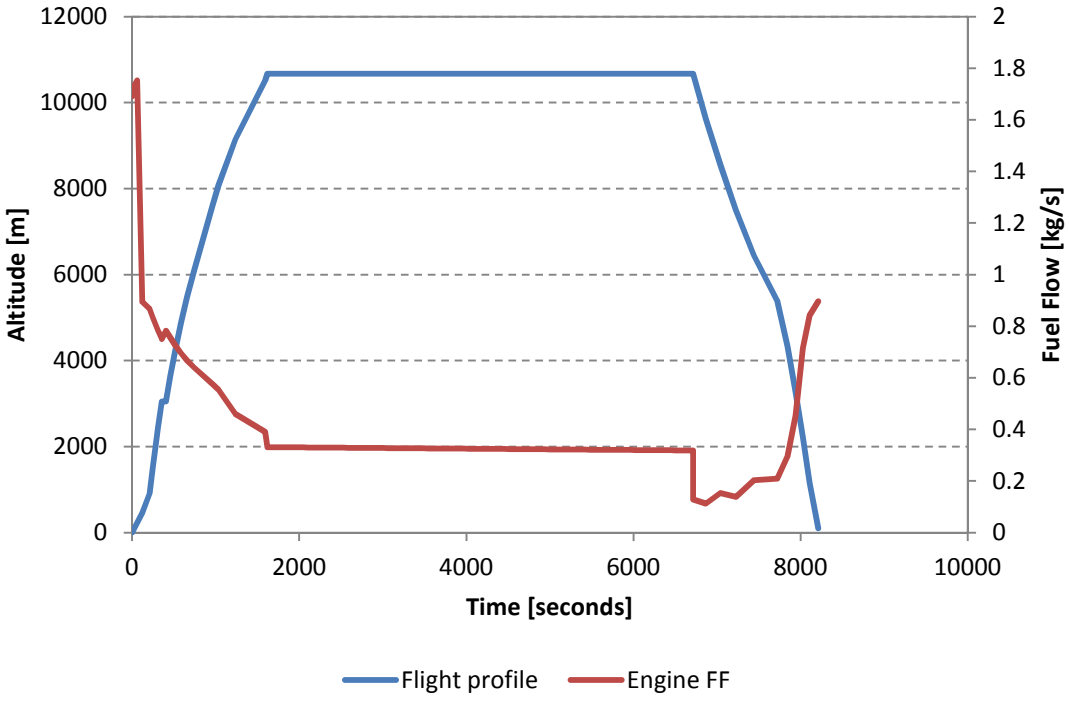

Figure A.2-3: CUSA-L engine FF variation during flight (1800 km)

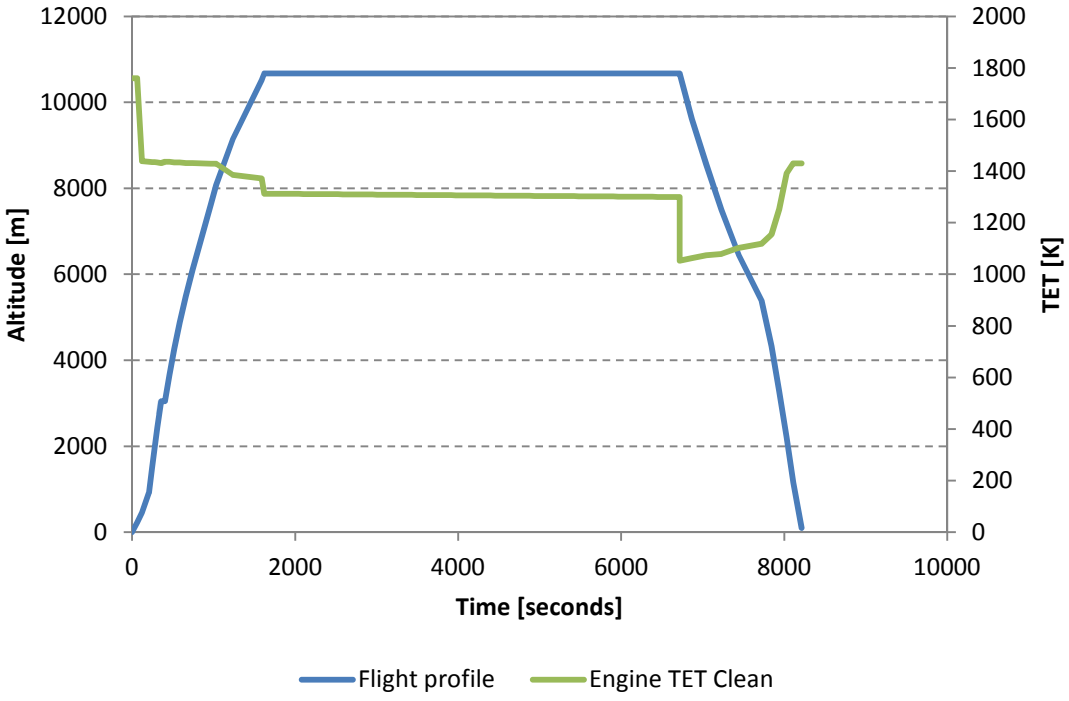

Figure A.2-4: CUSA-L engine TET variation during flight (1800 km)

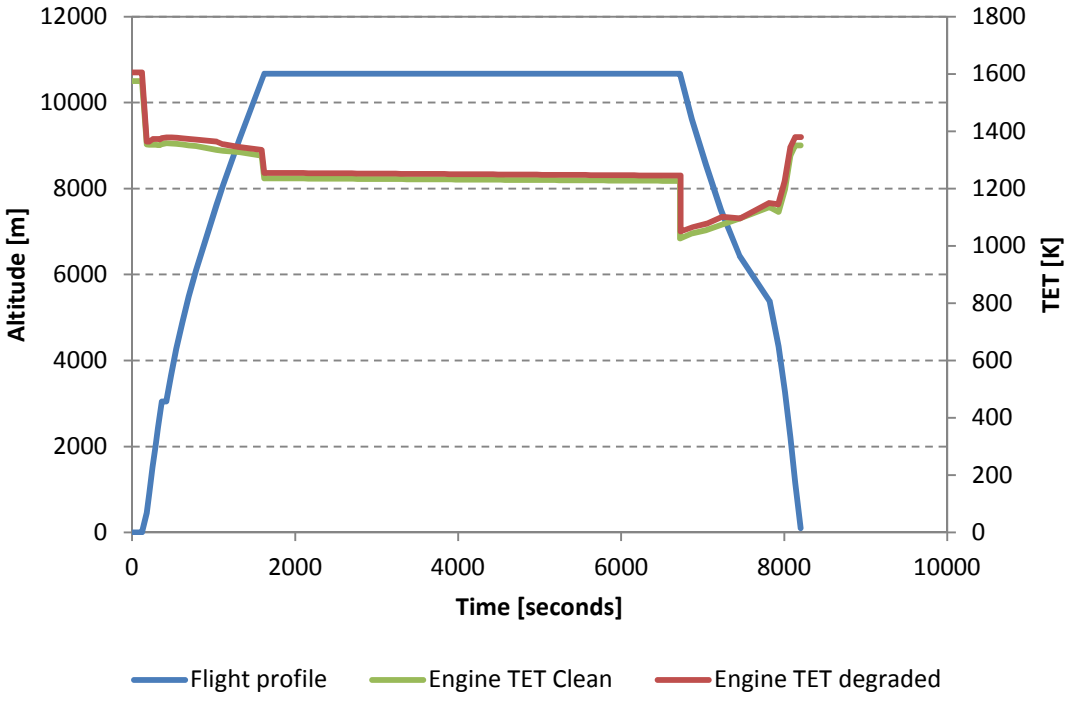

Figure A.2-5: CUSA-M engine TET variation during flight (1800 km)

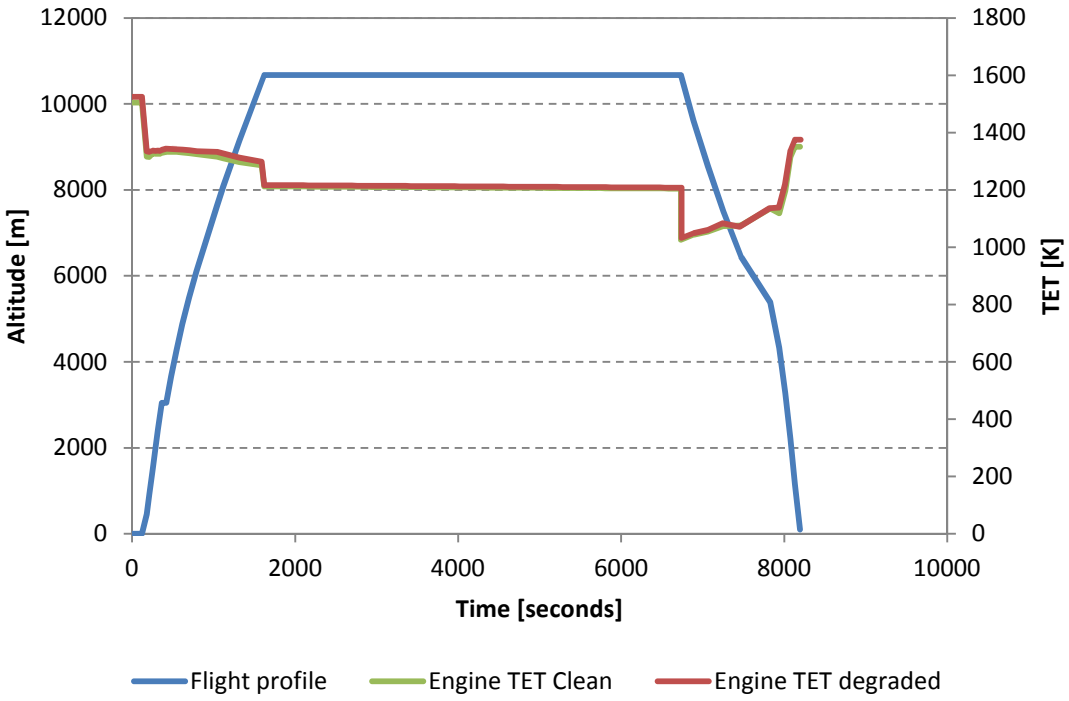

Figure A.2-6: CUSA-S engine TET variation during flight (1800 km)

A.3 Trajectory plots for 4600 km mission

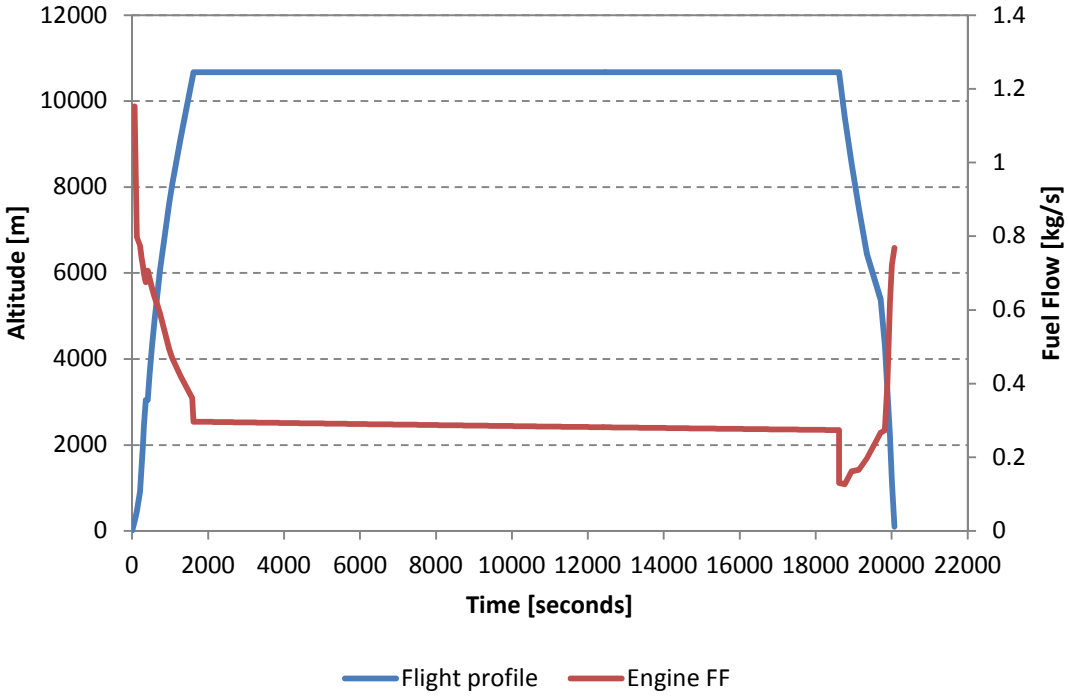

Figure A.3-1: CUSA-S engine FF variation during flight (4600 km)

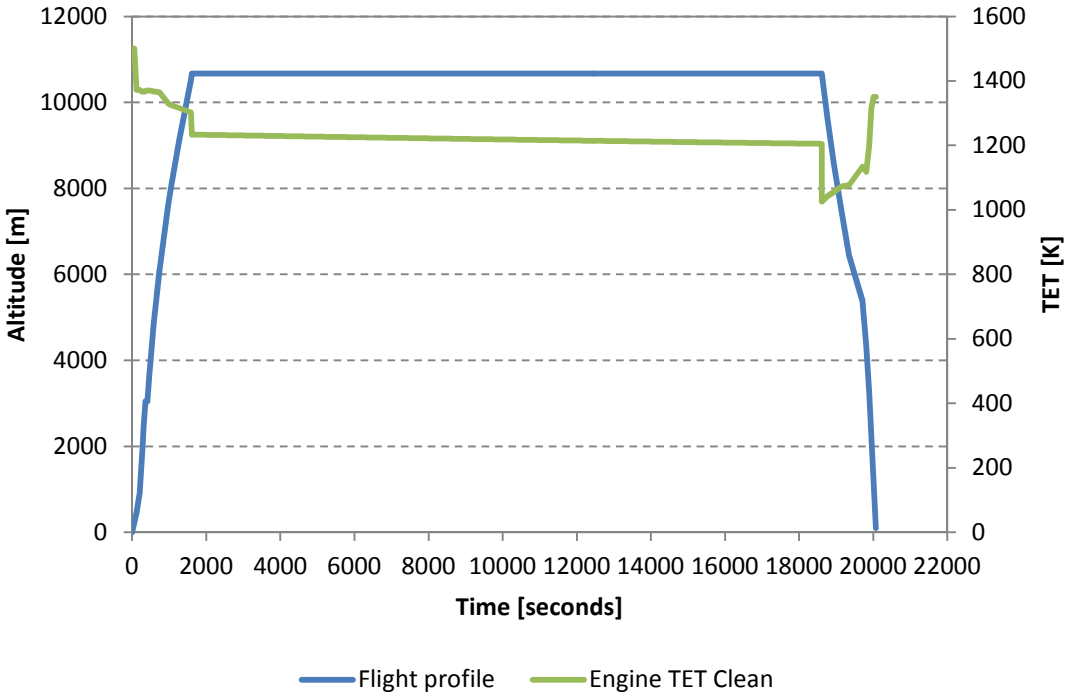

Figure A.3-2: CUSA-S engine TET variation during flight (4600 km)

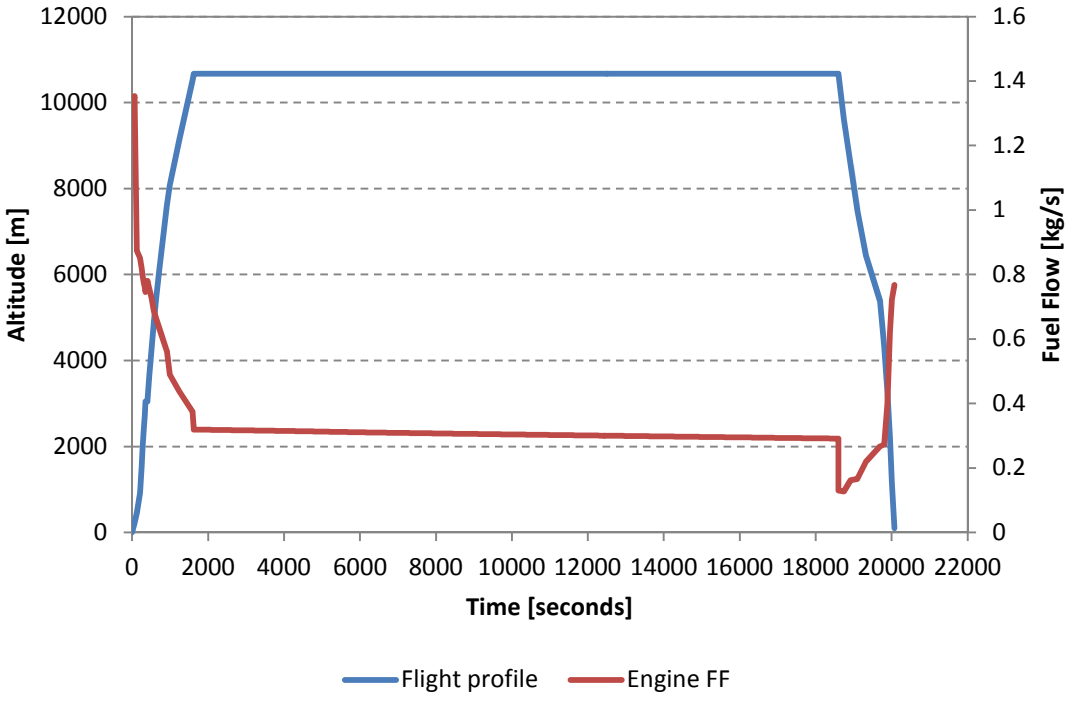

Figure A.3-3: CUSA-M engine FF variation during flight (4600 km)

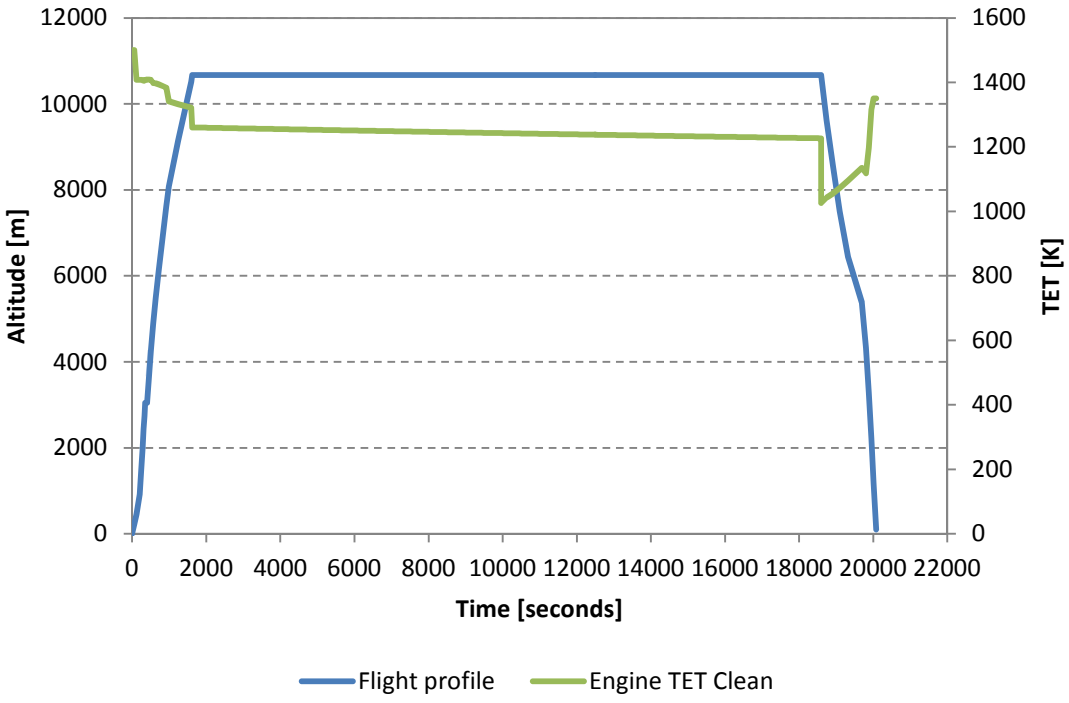

Figure A.3-4: CUSA-M engine TET variation during flight (4600 km)

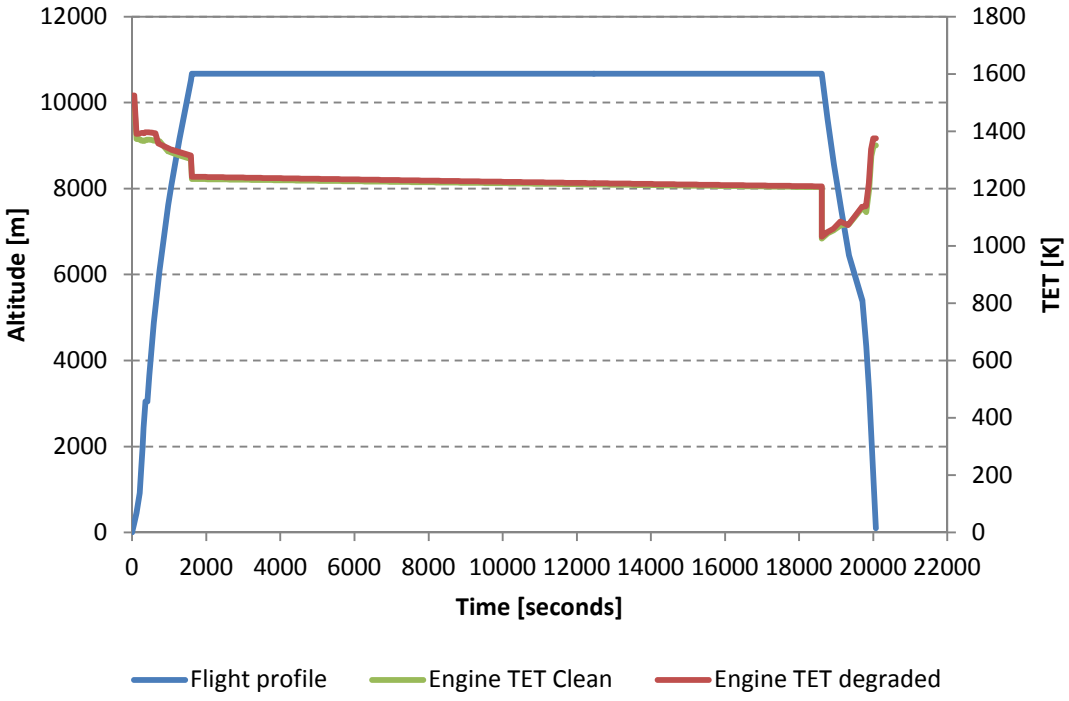

Figure A.3-5: CUSA-S engine TET variation during flight (4600 km)

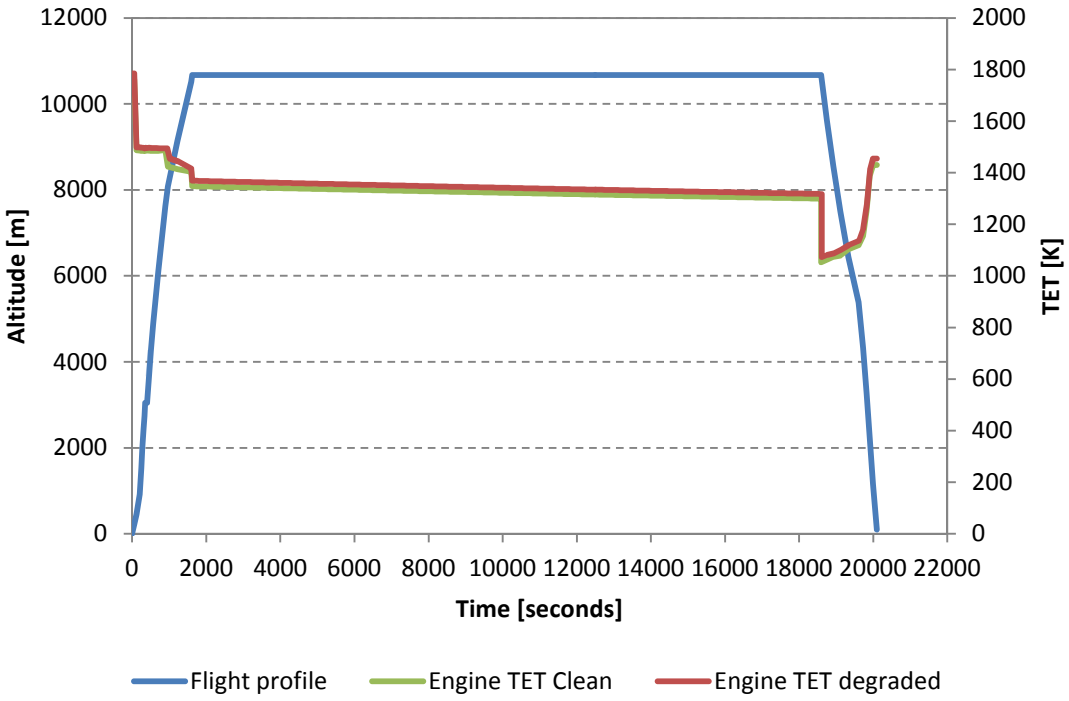

Figure A.3-6: CUSA-L engine TET variation during flight (4600 km)